G proteins transducing receptor-mediated inhibition of the M-type K^+ current in rat cultured sympathetic neurones.

A thesis submitted for the Doctorate of Philosophy
University of London

by

Susan Jones

Department of Pharmacology
University College London
Gower street
London WC1E 6BT

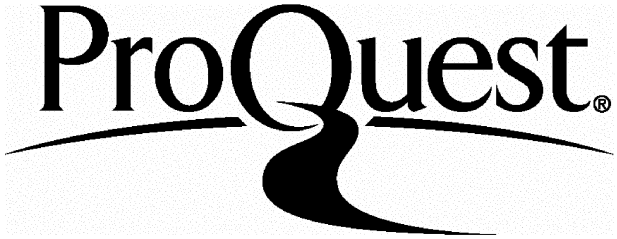

Abstract.

In rat sympathetic neurones, the M-type K^+ current ($I_{K(M)}$) can be inhibited *via* receptors that couple to G proteins. This thesis describes the identification of these G proteins.

The perforated patch voltage-clamp method was used to record $I_{K(M)}$ from rat cultured superior cervical ganglion (SCG) neurones. $I_{K(M)}$ inhibition by the muscarinic receptor agonist, oxotremorine-M (oxo-M; EC_{50} 204 nM), and the peptide hormone, bradykinin (BK; EC_{50} 0.95 nM), was recorded. To identify G proteins transducing $I_{K(M)}$ inhibition, anti-G_α protein (C-terminal sequence) antibodies were used.

Microinjection of anti-$G_{\alpha q/11}$ antibody caused a significant but variable reduction of $I_{K(M)}$ inhibition by 300 nM oxo-M; microinjection of anti-$G_{\alpha o}$ antibody had no effect on the response to oxo-M. The effect of the anti-$G_{\alpha q/11}$ antibody was surmountable on increasing the concentration of oxo-M, suggesting a spare G protein capacity. To ascertain whether $G_{\alpha q}$, $G_{\alpha 11}$, or both transduce muscarinic $I_{K(M)}$ inhibition, antisense DNA sequences were used. Although initial results suggested a significant role for $G_{\alpha 11}$, these experiments were not reproducible.

BK potently inhibited $I_{K(M)}$ in SCG neurones, and this effect of BK was also reduced by anti-$G_{\alpha q/11}$ (but not anti-$G_{\alpha o}$) antibody, suggesting that BK receptors and muscarinic receptors use a common or closely related mechanism to inhibit $I_{K(M)}$. However, there were differences in the response to the two agonists: the response to BK was slower in onset and offset, generally showed less recovery than the response to oxo-M, and the effect of high concentrations of BK, but not oxo-M, was susceptible to tachyphylaxis. Additionally, the effect of anti-$G_{\alpha q/11}$ antibody on $I_{K(M)}$ inhibition by BK was not as variable as the effect on the response to oxo-M.

It is concluded that muscarinic and BK receptors can couple to the same or highly homologous G proteins ($G_{\alpha q/11}$) to inhibit $I_{K(M)}$. The different characteristics of the responses to the two agonists are discussed.

Contents.

(Contents continued).

Page

(Contents continued).

(Contents continued).

Page

(Contents continued).

Page

List of Figures.

(List of Figures continued).

(List of Figures continued).

List of Tables.

List of Abbreviations.

ACh	Acetylcholine.
A/ GDP	Adenosine/ Guanosine diphosphate.
A/ Gpp(NH)p	5'-Adenylyl/ Guanylylimidodiphosphate.
A/ GTPγS	Adenosine/ Guanosine 5'-O-(3-thio)triphosphate.
A/ G/ UTP	Adenosine/ Guanosine/ Uridine triphosphate.
BAPTA	1,2-bis(2-aminophenoxy)ethane N, N, N', N'-tetraacetic acid.
BK	Bradykinin.
B_x	Bradykinin receptor subtype.
cA/ cGMP	cyclic Adenosine/ Guanosine monophosphate.
DAG	Diacylglycerol.
DRG	Dorsal root ganglion.
EGTA	Ethyleneglycol-bis-(β-aminoethyl ether)-N, N, N', N'-tetraacetic acid.
E/IPSP	Excitatory/ inhibitory postsynaptic potential.
EPSC	Excitatory postsynaptic current.
FITC	Fluorescein isothiocyanate.
GABA	γ-aminobutyric acid.
GDPβS	Guanosine 5'-O-(2-thio)diphosphate.
G protein	GTP-binding protein.
HEPES	N-[2-hydroxyethyl] piperazine-N'-[2-ethanesulphonic acid]
I_M	M-current; a potassium current with characteristic properties, including sensitivity to inhibition by muscarine, first described in bullfrog sympathetic ganglion neurones.
$I_{K(M)}$	M-type current; potassium currents having similar properties to I_M (including muscarine sensitivity), which were subsequently described in other tissues including mammalian peripheral and central neurones.
IP_3	Inositol 1,4,5-trisphosphate.

(List of Abbreviations continued).

K^+/ Na^+/ Ca^{2+}/ Mg^{2+}/ Ba^{2+}/ Cl^-	Potassium/ sodium/ calcium/ magnesium/ barium/ chloride ion.
LHRH	Leutenizing hormone-releasing hormone.
M_x	Pharmacologically defined muscarinic receptor subtype.
mx	Cloned muscarinic receptor subtype.
Oxo-M	Oxotremorine methiodide.
SCG	Superior cervical ganglion.
PTX	Pertussis toxin.
PLA_2	Phospholipase A_2.
PLC	Phospholipase C.
PKC	Protein kinase C.

Contributors.

Dr. M. P. Caulfield contributed half of the experimental data (and analysis) during the series of experiments using antisense oligodeoxynucleotides, as these experiments were carried out as a paired, "blind" design. Dr. Caulfield also contributed about 50% of the data using anti-GFAP and anti-$G_{\alpha q/11}$ antibodies during the first series of antibody-microinjection experiments, while I was learning this method with him. All G protein antibodies were raised by Dr. G. Milligan and his colleagues at the University of Glasgow. Antisense sequences were designed by Dr. N. J. Buckley. Most tissue culture, and the photography of SCG neurones was carried out by Y. Vallis.

Acknowledgments.

The work in this thesis started on the inspiration of Dr. Malcolm Caulfield, who established the method for injecting antibodies into SCG neurones to identify G proteins regulating Ca^{2+} current inhibition, and then had the idea of trying the same approach with M-currents. It was a pleasure for me to work in collaboration with Malcolm on the initial series of experiments using G protein antibodies, and experiments with antisense DNA. The remaining experiments described in this thesis were carried out by myself, but Malcolm has contributed enormously to this work through his advice, encouragement and friendship, and by constructively criticizing this thesis for me. I am grateful to Professor David Brown for his supervision and support, and the opportunity to work in his lab. I would also like to thank Drs. Steve Marsh, Jon Robbins, Alex Selyanko and Joan Sim for their helpful comments on various sections of this thesis, and for their help and advice over the last three years. I am particularly grateful to Dr. Heather Cambridge for reading Chapter 5 and advising me on bradykinin-related research. I thank Dr. Noel Buckley and all of his group for their enthusiasm and encouragement in the last year, and for the benefit of their expertise in the field of molecular biology. Yvonne Vallis has helped me considerably by patiently teaching me tissue culture and immunostaining methods, and by providing me with excellent cell cultures. Brenda Browning has also been helpful with tissue culture support. I am grateful to Dr. Graeme Milligan for raising the G protein antibodies and providing advice on their use. I would also like to thank Professor Don Jenkinson for his support over the last three years.

My family and friends have also contributed to this thesis through their love and support. In particular, I thank Robin Cloues, Justine Harvey, Jo Leal, Michele and Ian Scott, Patrick Shaw and Clare Yellowley for their friendship and continual faith in my abilities, and J. Antonio Lamas, for his friendship and support in the last few months. I am indebted to my father and my brother, Mark for always being there, and to my mother, who made this possible for me.

During my Ph.D. I was supported by a studentship from the Medical Research Council.

CHAPTER 1:

Introduction.

Many neurotransmitters and hormones influence excitable cells by modulating ion channels. Neurotransmitters and hormones exert their effects on ion channels, and hence on neuronal excitability, *via* two main super-families of receptors: (1) ligand-gated ion channel receptors, in which the ion channel is an integral part of the receptor complex, mediate fast changes in ion channel activity and cell excitability; (2) receptors that couple to GTP-binding proteins (G proteins) produce slower, modulatory effects on ion channels, notably voltage-dependent K^+, Ca^{2+} and Cl^- channels. The work described in this thesis is concerned with a voltage-dependent K^+ current, named the M-type K^+ current, which is found in peripheral and central neurones and can be modulated by neurotransmitters and hormones acting at G protein-coupled receptors. A variation of the whole-cell patch-clamp method was used to investigate the G protein(s) transducing inhibition of this K^+ current mediated by receptors for the neurotransmitter, acetylcholine, and the local hormone, bradykinin, in peripheral autonomic ganglion neurones. Because K^+ conductances are instrumental in controlling the excitability of neurones, understanding the mechanisms by which neurotransmitters and hormones modulate K^+ currents is a key step towards understanding how they can modulate neuronal excitability. In this general introduction the properties of the M-type K^+ current, and the role of G proteins in the modulation of this K^+ current, will be considered. The current status of G protein structure, function and diversity will first be discussed.

1.1. G proteins.

1.1.1. Structure, function and diversity.

These subjects have been well reviewed by Ross (1992), among others. G proteins are so-called because of their ability to bind guanine nucleotides. They are heterotrimers, composed of $\alpha\beta\gamma$ subunits, and it is the α-subunit that has nucleotide binding properties. The exchange of GTP for GDP on the α-subunit switches the G protein to an active state. In addition to a nucleotide binding site, α-subunits also possess intrinsic GTPase activity, causing hydrolysis of GTP to GDP, which therefore limits the activity of the G protein. This is a very simplistic view of the cycle of G protein activity; interaction of G proteins with agonist-occupied receptors influences

this process. When the G protein is not interacting with activated receptor, the hydrolysis of GTP (by GTPase) is much faster than nucleotide exchange, and the inactive GDP-bound form predominates. The release of GDP is the rate limiting step, and receptor-G protein interaction accelerates this exchange so that the active GTP-bound form predominates. Concurrent with nucleotide exchange, the affinity of the receptor-G protein interaction is thought to be reduced, allowing the active G protein α-subunit to find its effector, and the receptor to find further GDP-bound G protein. Association of the α-subunit with the βγ-subunit is apparently necessary for efficient nucleotide exchange (Weiss *et al.*, 1988), and the affinity of the α-βγ interaction decreases upon nucleotide exchange, suggesting that the subunits dissociate when GTP is bound. However, active but undissociated G_α subunits have been described, indicating that physical dissociation is not essential for G protein activation (reviewed by Clapham and Neer, 1993). In the scheme of G protein cycling (modified from Ross, 1992) shown in Box 1 below, it is assumed that βγ does dissociate from α upon nucleotide exchange.

Box 1

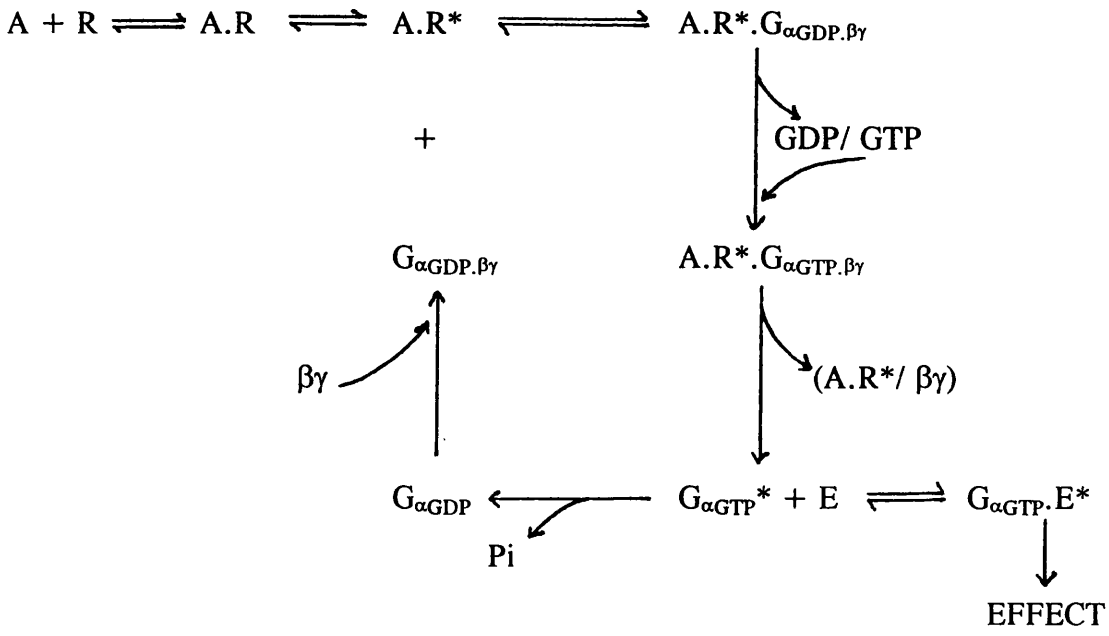

A = Agonist; R = Receptor; G = G protein; E= Effector; * denotes active forms

Many studies using G protein toxins, antibodies and genetic mutations have attempted to clarify which structural features of the G protein control key functions (Weiss *et al.*, 1988 for review). Such work suggests that the C-terminal region of the α-subunit is the site for G protein-receptor interaction, and that the N-terminal region may be the site for interaction with the βγ-subunit.

For many years, the properties of the α-subunit, coupled with the striking diversity of these proteins (see below), consolidated the view that it was the functional component of G proteins, with the closely associated βγ-subunit taking a subsidiary role: this view is now changing. Structural diversity (see below) as well as evidence for distinct functional roles for βγ-subunits are now increasingly being described. Initially, the primary function of the βγ was considered to be that of an anchor for the α-subunit. G proteins are membrane-associated, and βγ-subunits appear to stabilize α-subunits at the membrane (and in receptor-G protein interactions, enhancing nucleotide exchange). Additionally, βγ-subunits re-associate with α-subunits after the hydrolysis of GTP, thus aiding inactivation of the G protein. However, diversity of β- and γ-subunits indicates that they may also confer signalling specificity, and may act as regulators themselves. The first proposal that βγ could interact with effectors came with the finding that, like α-subunits, βγ could activate the atrial K^+ conductance normally activated by acetylcholine (ACh), $I_{K(ACh)}$ (Logothetis *et al.*, 1987). Although this was a matter of controversy for some years (Brown and Birnbaumer, 1990), the cloning of the underlying channel for $I_{K(ACh)}$ has revealed that co-expression of the channel with βγ-, and not α-subunits in *Xenopus* oocytes leads to activation of $I_{K(ACh)}$, and application of βγ-subunits, but not α-subunits, increases channel activity in excised patches (Reuveny *et al.*, 1994). βγ-subunits have also been shown to activate phospholipase A_2 (PLA_2), either activate or inhibit different isoforms of adenylyl cyclase, activate certain isoforms of phospholipase C (PLC) and inhibit voltage-gated Ca^{2+} currents (reviewed by Clapham and Neer, 1993).

On the subject of G protein diversity, this is now known to be conferred by all three subunit components. The α-subunit family is highly homologous, and the

structural similarities made cloning an essential step for identifying specific members. There are at least 18 different α-subunits (Hepler and Gilman, 1992), which may be grouped into classes according to either structural or functional similarities. Simon *et al.* (1991) and Hepler and Gilman (1992) have described 4 main structurally-related classes: G_s, G_i (including G_i, G_o, G_t and G_z), G_q and G_{12} (see Table of G protein α-subunits). The βγ-subunits comprise at least 4 β and 6 γ proteins. All of the β-subunits are ubiquitously distributed and are highly homologous, while the γ-subunits are less homologous and have distinct patterns of distribution (Hepler and Gilman, 1992). βγ-subunits exist as tightly bound complexes and cannot be isolated separately unless denaturing conditions are used (Ross, 1992). The same βγ-subunits can be used by different α-subunits (Hepler and Gilman, 1992), but with different affinity (Simon *et al.*, 1991). Because of the remarkable diversity of G proteins, there has been enormous interest in developing tools to investigate the specific functions of different G protein subunits.

Table of G protein α-subunits (modified from Hepler and Gilman, 1992).

Family	α-subunit members	Toxin	Distribution	Effectors (examples)
G_s	$G_{\alpha s}$ (2 subtypes) G_{olf}	CTX CTX	ubiquitous ubiquitous	both ↑ adenylyl cyclase.
G_i	$G_{\alpha i}$ (3 subtypes) $G_{\alpha o}$ (2 subtypes) $G_{\alpha t}$ (2 subtypes) $G_{\alpha z}$	PTX PTX PTX/CTX	ubiquitous neuronal/other retinal neuronal	↓ adenylyl cyclase ion channels ↑ cGMP PDE ?
G_q	$G_{\alpha q}$ $G_{\alpha 11}$ $G_{\alpha 14}$ $G_{\alpha 15}$ $G_{\alpha 16}$		ubiquitous ubiquitous lung/liver/kidney B cells T cells	both ↑PLCβ ↑ PLCβ ? ↑ PLCβ
G_{12}	$G_{\alpha 12}$ $G_{\alpha 13}$		ubiquitous ubiquitous	? ?

1.1.2. Techniques for studying function.

The involvement of G proteins in receptor-mediated cellular effects is readily demonstrated using guanine nucleotides or poorly-hydrolyzable guanine nucleotide analogues (Milligan, 1988; Ross, 1992). GTP and GTP analogues are commonly used to activate G proteins independently of the receptor, particularly analogues such as GTPγS and Gpp(NH)p, which are more resistant to hydrolysis and therefore move the G protein equilibrium towards the activated (GTP-bound) state. Conversely, the GDP analogue GDPβS can sometimes (but not always) be used to inactivate the G protein in the GDP-bound state. Furthermore, certain G protein classes can be identified based on their sensitivity to particular bacterial toxins (Dolphin, 1987; Milligan, 1988). For example, cholera toxin (CTX) catalyses the transfer of an ADP-ribose group from nicotinamide adenine dinucleotide to an arginine residue in the α-subunits of G_t and G_s, leading to permanent activation of these G proteins, while pertussis toxin (PTX) catalyses the same transfer but to a cysteine residue of the α-subunits of G_t, G_i and G_o which inactivates these G proteins by preventing receptor-G protein coupling (Milligan, 1988). These toxins have been useful not only in identifying the class of G protein mediating specific responses to neurotransmitters and hormones (for example, "PTX-sensitive" *versus* "PTX-insensitive" G proteins), but also in structure/ function determinations: the fact that the cysteine residue target for PTX is located 4 amino acids from the C-terminus of the α-subunit is one line of evidence for this region being the site of receptor-G protein interaction (Weiss *et al.*, 1988). However, a number of G protein α-subunits are sensitive and some are insensitive to both toxins, and so while the toxins have a general use in identifying G protein classes, more selective tools are necessary in order to discriminate more precisely the role of different α-subunits in signal transduction. Reconstitution experiments, in which purified G protein subunits are used to mimic the effect of the agonist, were instrumental in identifying G protein subunits regulating the atrial K^+ current ($I_{K(ACh)}$; see Brown and Birnbaumer, 1990 for review), and have also been employed in studies on neurones (reviewed by Brown, 1990). However, reconstitution experiments only reproduce the effect, they do not confirm that a given subunit is the endogenous regulator. Methods for removing a G protein from signal transduction pathways, either by functionally blocking its action

(using anti-G protein antibodies), or by preventing its expression (using G protein antisense oligodeoxynucleotide sequences), are increasingly popular in studies of G protein function.

Anti-G protein antibodies.

These can be used both to localize specific G protein subunits to specific tissues, or regions within a tissue, and to functionally remove a specific G protein from a signalling pathway. The earliest studies with G protein antibodies were concerned with G_t, G_s, G_i and G_o, as these were the earliest to be cloned (for reviews, see Milligan, 1988; Spiegel *et al.*, 1990). In intact cells, anti-G protein antibodies have been used to block a number of functional, G protein-mediated responses. In snail neurones, anti-$G_{\alpha o}$ antibody blocked inhibition of voltage-gated Ca^{2+} current by dopamine (Harris-Warrick *et al.*, 1988). Similar effects of anti-$G_{\alpha o}$ antibody (but not anti-$G_{\alpha i}$ antibody) have since been reported in neuroblastoma x glioma hybrid (NG108-15) cells (reduction of noradrenaline-inhibition of voltage-gated Ca^{2+} current; McFadzean *et al.*, 1989), in sensory neurones (reduction of $GABA_B$ receptor-mediated inhibition of N-type voltage-gated Ca^{2+} current (Menon-Johansson *et al.*, 1993), and μ-opioid-inhibition of voltage-gated Ca^{2+} current (Moises *et al.*, 1994)), and in sympathetic neurones (reduction of noradrenaline-inhibition of voltage-gated Ca^{2+} current; Caulfield *et al.*, 1993). In pituitary neurones, anti-G protein antibodies were used to show that dopamine D_2 receptors activate K^+ currents *via* $G_{\alpha i3}$ and inhibit voltage-gated Ca^{2+} currents *via* $G_{\alpha o}$ (Lledo *et al.*, 1992). With the cloning of different PTX-insensitive G proteins (see below), antibodies have since been developed to probe their function. Gutowski *et al.*, 1991 used an antibody raised against the C-terminal decapeptide sequence common to $G_{\alpha q}$ and $G_{\alpha 11}$ to demonstrate a role for either or both of these G proteins in phospholipase C activation by hormone receptors in membrane preparations from two cell lines and rat liver. Subsequently, this antibody was included in patch pipettes for electrophysiological recordings from NG108-15 cells to show that the PTX-insensitive G protein transducing bradykinin (BK)-activation of a Ca^{2+}-dependent K^+ current was $G_{\alpha q}$, $G_{\alpha 11}$ or both; BK-inhibition of the voltage-gated Ca^{2+} current was *via* another PTX-insensitive G protein (Wilk-Blaszczak *et al.*, 1994).

Antibodies have proved extremely useful tools in G protein research, but they also have limitations. The high homology of G protein subunits, particularly the C-terminal sequences of certain α-subunits, makes it difficult to develop antibodies that specifically recognize a single G protein. The solution to this problem may come from the adoption of antisense DNA and RNA methods, which are now being used with considerable success.

Anti-G protein antisense nucleic acid.

Antisense sequences to either RNA or DNA can be used to selectively suppress expression of a particular protein encoded by the target nucleic acid (Hélène and Toulmé, 1990). Generally, short DNA sequences (oligodeoxynucleotides, ODNs; <30 nucleotides) have been useful in G protein research. Increasing the length increases specificity and affinity, but also increases susceptibility to degradation. Details of ODN uptake, distribution within cells and the sites of ODN action are still debatable, and the subject for continuing research: recent ideas on these subjects have been reviewed by Hélène and Toulmé, 1990, Akhtar and Juliano, 1992 and Wahlestedt, 1994. Because of the sensitivity of ODNs to hydrolysis by nucleases, they are often modified by replacing a non-bridging oxygen atom of the phosphodiester with, for example, sulphur (to form a phosphorothioate-modified ODN). Modified ODNs can also be taken up into cells and act in the same way as unmodified ODNs, but possible toxic and non-specific effects must be carefully monitored (Wahlestedt, 1994). ODNs can be introduced into cells by incubation (*via* receptor-mediated, adsorptive or fluid-phase endocytosis: Akhta and Juliano, 1992), by microinjection (see below), by transfection, or by cell-permeabilization (for example, see Barry *et al.*, 1993). *In vivo*, osmotic minipumps have been used to continuously perfuse ODNs to a region (Wahlestedt, 1994). It is hoped that, in addition to their potential as research tools, ODNs may also provide new therapeutic approaches (Stein and Cheng, 1993).

In pharmacological research, two significant papers describing the use of ODNs appeared in 1991. Listerud *et al.* (1991) used ODNs to the subunits of the nicotinic ACh receptor expressed in sympathetic neurones to show that the α3 subunit was critical in determining the expression of functional receptors, and the α7 subunit also

appeared to be functionally important. However, the first application of antisense techniques to G protein function came from Kleuss *et al.* in a series of three papers (Kleuss *et al.*, 1991; 1992; 1993), in which ODNs against specific αo, β and γ subunits (injected into the nuclei of GH_3 pituitary cells) highlighted a very specific coupling pattern for muscarinic ACh receptor (αo1β1γ4 being the critical subunits) and somatostatin receptor (αo2β3γ3) mediated inhibition of voltage-gated Ca^{2+} current. G protein ODNs have since been used successfully in dorsal root ganglion neurones to reduce $GABA_B$ receptor-mediated inhibition of voltage-gated Ca^{2+} current (microinjection of G_{α_o} but not G_{α_i} ODN: Campbell *et al.*, 1993), in CNS neurones, to reduce muscarinic receptor-mediated inhibition of delayed rectifier K^+ current (incubation with $G_{\alpha 11}$, but not G_{α_q} ODN: ffrench-Mullen *et al.*, 1994), and in Xenopus oocytes, to inhibit bombesin receptor-mediated activation of the Ca^{2+}-dependent Cl^- current (microinjection of G_{α_q}, but not $G_{\alpha 11}$ ODN: Shapira *et al.*, 1994).

These tools for probing G protein function have contributed to the present knowledge concerning which G protein α-subunits regulate particular effectors, or second messengers, in cell signalling.

1.1.3. Target effectors.

Some, but not all, of the G protein α-subunit diversity can be explained in terms of their function. The naming of the α-subunits can indicate this: for example, G_s and G_i stimulate and inhibit adenylyl cyclase activity respectively (regulating levels of cAMP and hence cAMP-dependent kinase, which phosphorylates proteins such as ion channels). Stimulation of adenylyl cyclase by G_s and activation of cGMP phosphodiesterase (PDE) by transducin (G_t) were the first well-studied examples of G protein-effector interaction, and have been widely reviewed (for example, Ross, 1992; Kennedy, 1992): they are not discussed further here. G_i, in addition to inhibiting adenylyl cyclase, is also thought to couple "directly" to ion channels, such as the atrial K^+ channel underlying $I_{K(ACh)}$ (see Brown and Birnbaumer, 1990 for review). In neuronal cells, G_o also appears capable of "direct" coupling to ion channels (see Brown,1990 for review). However, this thesis is concerned with receptor-modulation

of a K^+ conductance *via* a PTX-insensitive G protein, namely a member of the G_q and/or G_{12} classes of G proteins (based on the classification of Simon *et al.*, 1991). Therefore, it is the effector targets for these G proteins which will be considered here.

In 1990, Strathmann and Simon cloned two novel (and highly homologous) G protein α-subunits. These differed from the other known α-subunits in several respects; notably, they lacked the target cysteine residue for PTX-catalyzed ADP-ribosylation, and were not modified by PTX. In the same year, Pang and Sternweis purified PTX-insensitive G proteins from rat brain, and Taylor *et al.* purified a protein from bovine liver which activated PLC in a GTPγS-dependent manner. Subsequently, further PTX-insensitive G protein α-subunits have been identified, giving a total of eight. Of the G_q class, $G_{\alpha q}$ and $G_{\alpha 11}$ are widely distributed, while $G_{\alpha 14}$ is found primarily in epithelial cells (for example, in the lung, liver and kidney), and $G_{\alpha 15}$ and $G_{\alpha 16}$ are found in B and T immune cells respectively; in the G_{12} class, both $G_{\alpha 12}$ and $G_{\alpha 13}$ are widely distributed; in the G_i class, $G_{\alpha z}$ is also PTX-insensitive and is found mainly in neurones (Simon *et al.*, 1991; see Table of G protein α-subunits).

A series of publications established $G_{\alpha q}$ and $G_{\alpha 11}$ as the hitherto unidentified "G_p": the G protein responsible for coupling receptors to PLC, which catalyses the hydrolysis of membrane phosphatidylinositol 4,5-bisphosphate to inositol phosphates (including inositol 1,4,5-trisphosphate, IP_3, which releases Ca^{2+} from intracellular stores) and diacylglycerol (DAG, which in turn activates protein kinase C, PKC; see Kennedy, 1992 for review). Ca^{2+} can directly regulate ion channels, as well as enzymes such as kinases (see above); PKC, like cAMP-dependent kinase, can phosphorylate proteins. Thus, activators of PLC can generate a spectrum of second messengers. Three families of PLC have been identified (PLCβ, γ, δ), with further families predicted; the PLCβ family, of which there are three subtypes (1-3), is regulated by G proteins (Cockcroft and Thomas, 1992). Taylor *et al.* (1991) used a G protein purified from liver (Taylor *et al.*, 1990), and related to the G_q class, to stimulate the PLCβ1, but not PLCγ1 or PLCδ1 isoforms of PLC. When αq, α11, α14 or α16 were expressed in Cos-7 cells, and the membranes of these cells were

reconstituted with PLCβ isozymes, all of these α-subunits stimulated PLCβ1, although αq and α11 were the most efficient, while α16 most efficiently stimulated PLCβ2, with αq and α11 causing less stimulation (Lee *et al.*, 1992) indicating that the structural diversity of this class could have a functional purpose. Expression of $G_{\alpha q}$ and $G_{\alpha 11}$, but not $G_{\alpha z}$, $G_{\alpha o}$ and $G_{\alpha t}$ in Cos-7 cells supported formation of [^{3}H]-inositol phosphates, with higher levels of stimulation when $G_{\alpha q}$ and $G_{\alpha 11}$ were co-transfected with PLCβ1 (Wu *et al.*, 1992). Employing G protein antibodies, Aragay *et al.* (1992) reduced activation of PLC (measured by increased [^{3}H]-IP_3 production) by thyrotropin releasing hormone (TRH) in GH_3 pituitary cells with anti-$G_{\alpha q/11}$ antibody, but not with antibodies to other G protein C-terminal sequences. G protein antibodies were also used by Gutowski *et al.* (1991) to block hormonal stimulation of inositol phosphate turnover (as an index of PLC activation) in three cell types. In reconstitution experiments, $G_{\alpha q}$ and $G_{\alpha 11}$ were equally effective in transducing TRH receptor-activation of PLC (Aragay *et al.*, 1992). Berstein *et al.* (1992) reconstituted m1 receptors with $G_{\alpha q/11}$ and purified PLCβ1 in lipid vesicles and observed receptor-activated, GTPγS-dependent stimulation of PLC. The use of G protein antibodies to demonstrate a role for these G protein subunits in transducing activation of a Ca^{2+}-dependent K^+ current in NG108-15 cells, which is thought to occur via the PLC-IP_3-Ca^{2+} pathway (Wilk-Blaszczak *et al.*, 1994), was described above. $G_{\alpha q}$ and $G_{\alpha 11}$ do not always regulate the same effector in the same manner. For example, Lipinsky *et al.* (1992) co-expressed $G_{\alpha q}$ or $G_{\alpha 11}$ with TRH receptors in *Xenopus* oocytes: while α11 potentiated the response to TRH (activation of a Ca^{2+}-dependent Cl^- current), αq inhibited this response. Shapira *et al.* (1994) found that αq antisense but not α11 antisense could inhibit the Cl^- current activated by neuromedin B in Xenopus oocytes; ffrench-Mullen *et al.* (1994) found the converse was true for muscarinic inhibition of delayed rectifier current in hypothalamic neurones.

Clearly, there is some diversity in the choice of effector for the different PTX-insensitive G proteins. Whether there are further effectors for these G proteins, including ion channels themselves, remains to be determined. Thus, neurotransmitter

and hormone receptors may couple to a number of PTX-insensitive G proteins, and activate several isoforms of PLC, in order to modulate cellular activity.

1.2. M-currents and their modulation.

The K^+ channel family represents a diverse group of voltage-dependent ion channels, and some can be modulated by neurotransmitters (Hille, 1992). By activating K^+ conductances, neurotransmitters and hormones can decrease cell excitability; conversely, inhibition of K^+ channels leads to increases in cell excitation. Examples of neuronal K^+ currents that are susceptible to neurotransmitter effects include delayed rectifier K^+ currents (I_K) (ffrench-Mullen *et al.*, 1994), inward rectifier K^+ currents ($I_{K(IR)}$) (reviewed by North, 1989) and calcium-dependent K^+ currents ($I_{K(Ca)}$) (for example, Pennefather *et al.*, 1985; Malenka *et al.*, 1986). This thesis is concerned with the M-type K^+ current (I_M or $I_{K(M)}$), whose inhibition by neurotransmitters is known to involve a G protein. In this section, the properties of this current and its modulation by neurotransmitters *via* G protein-dependent pathways will be discussed.

1.2.1. Properties of M-type K^+ currents ($I_{K(M)}$).

Bullfrog sympathetic ganglion neurones.

Slow, non-nicotinic, atropine-sensitive changes in potential of autonomic ganglion neurone membranes were described as early as the 1940s and 1950s, with inhibitory (I) and excitatory (E) effects being noted, and attributed to a postsynaptic source (see Libet, 1970 for review). These slow postsynaptic potentials (PSPs) were characterized by a long delay (around 100 ms) and duration (> 10 s) compared with the fast EPSP, and required repetitive preganglionic stimulation to reach their maximum amplitude. Furthermore, unlike the fast EPSP, the slow PSPs were not accompanied by a detectable increase in conductance, and in fact an associated increase in membrane resistance had been reported in frog ganglion cells; additionally, the slow EPSP was enhanced at depolarized potentials (the converse of the fast EPSP). It was predicted that released neurotransmitter (ACh), in addition to evoking a fast EPSP by interaction with nicotinic receptors, could also interact with muscarinic receptors to produce a slow EPSP *via* a direct action, and a slow IPSP *via* an action on adrenergic interneurones

(Libet, 1970). The ionic mechanisms underlying these slow membrane effects, and the reason for the slow action, were not understood up until the 1970s, and the possible involvement of an active transport process was considered. However, in 1970 Weight and Votava demonstrated that the slow EPSP in frog ganglion neurones was generated by a decrease in a resting K^+ conductance. Finally, a novel K^+ current was described in frog ganglion neurones, which was suppressed by muscarinic receptor activation (Brown and Adams, 1980); this K^+ current was named the M-current (I_M), and was proposed to be the main target for muscarinic receptor-mediated excitatory effects.

In bullfrog sympathetic neurones, I_M is a voltage- and time-dependent, non-inactivating K^+ current which is kinetically and pharmacologically distinct from other K^+ currents in these cells (Adams *et al.*, 1982a; Adams *et al.*; 1982b); the threshold for activation of I_M was -60 mV, and at increasingly depolarized potentials I_M contributed outward rectification to the steady-state current, with conductance reaching half-activation at around -35 mV and maximum at between -20 and 0 mV. The time constants of the time-dependent I_M activation and deactivation current relaxations showed voltage-dependence, accelerating with increasing hyperpolarization from the half-activation potential. I_M was proposed to have a "clamping" effect on the membrane at potentials subthreshold to excitation. I_M was inhibited by muscarine (EC_{50} around 3 μM), leutenizing hormone-releasing hormone (LHRH; 1 to 5 μM), uridine triphosphate (50 to 100 μM) and Ba^{2+} ions (1 to 4 mM): none of these agents (at these concentrations) had appreciable effects on the other K^+ currents in these cells. Their effect on I_M was characterized by a decrease in the standing outward current at potentials where I_M was pre-activated, a decrease in the amplitude of the slow I_M deactivation currents during hyperpolarizing voltage steps, a decrease in membrane conductance (at potentials where I_M was activated) and a decrease in the outward rectification of the steady-state current-voltage relationship, with no effect on the kinetics or voltage-dependence of I_M. Adams *et al.* (1982b) proposed that inhibition of I_M by ganglion transmitters (ACh and LHRH) would facilitate the response to excitatory synaptic inputs. Evidence that I_M could be inhibited by synaptically-released ACh came from Adams and Brown (1982), when they demonstrated a decrease in I_M amplitude in response to a voltage step applied during the slow excitatory postsynaptic

current (EPSC) evoked by repetitive preganglionic stimulation. EPSCs decreased in amplitude with hyperpolarization and reduced the outward rectification of the steady-state current-voltage relationship. Interestingly, although repetitive stimuli were used to augment the slow EPSC, a slow EPS*P* could be evoked by a single stimulus. This was also found by Jones (1985) in a comprehensive study of the effects of muscarine, peptides and nerve stimulation on I_M in these cells. Jones also described an additional inward current, resulting not from I_M inhibition, in response to muscarine, peptides and EPSCs. Both effects were proposed to contribute to the slow EPSP.

Rat sympathetic neurones.

K^+ conductances with the characteristic properties of I_M have since been demonstrated in mammalian sympathetic neurones (including from rats), other peripheral neurones and neurones from several brain regions (see below). The properties of the M-type K^+ current ($I_{K(M)}$) in rat sympathetic neurones in the intact superior cervical ganglion (SCG) and in dissociated, cultured SCG neurones are described in more detail in Chapter 3. Essentially, properties of $I_{K(M)}$ in rat sympathetic neurones were similar to those described in bullfrog neurones (Constanti and Brown, 1981): muscarinic receptor- and peptide (angiotensin II) receptor-mediated inhibition of $I_{K(M)}$ was also described in this study. As in bullfrog ganglia, preganglionic stimulation caused a muscarinic receptor-mediated suppression of $I_{K(M)}$ (Brown and Selyanko, 1985b), and an additional outward current evoked by muscarine (attributed principally to inhibition of an inward Cl^- conductance) was also described (Brown and Selyanko, 1985a; Brown and Selyanko, 1985b). The single channel currents underlying the macroscopic $I_{K(M)}$ have been characterized in cell attached and excised patches from rat sympathetic neurones, in terms of their kinetics, voltage-dependence and sensitivity to pharmacological agents (Selyanko *et al.*, 1992; Stansfeld *et al.*, 1993; Selyanko and Brown, 1993). Persistent M-channel activity in cell-attached patches increased with the same voltage-sensitivity to depolarization as whole-cell currents, with the channel currents reversing at a membrane potential of around -80 mV. Activation and deactivation of channel currents in cell-attached patches also exhibited the time-dependence characteristic of $I_{K(M)}$ (Selyanko *et al.*, 1992), although this time-dependence was lost during recordings from excised patches, and a slow

inactivation of the channels was described (Stansfeld *et al.*, 1993). Multiple conductance levels were detected in cell-attached and excised patches. Muscarine could inhibit M-channel activity in cell-attached patches when applied to the bath solution (Selyanko *et al.*, 1992), and the effect of muscarine was to decrease the frequency of channel opening (Selyanko and Brown, 1993). Muscarine did not inhibit channel activity in cell-attached patches when included in the patch pipette (Selyanko *et al.*, 1992) or in excised, outside-out patches when applied to the bath (Stansfeld *et al.*, 1993).

CNS neurones.

K^+ currents exhibiting many of the properties of I_M have been demonstrated in various CNS neuronal types including guinea pig hippocampal CA1 pyramidal cells (Halliwell and Adams, 1982), pyramidal cells from guinea pig olfactory cortex (Constanti and Galvan, 1983) and from the rat basolateral amygdala (Womble and Moises, 1992). In addition to being inhibited by muscarine, $I_{K(M)}$ in hippocampal neurones also has the interesting property of being augmented by somatostatin (Jacquin *et al.*, 1988). Using co-cultures of cells from the medial septum and the hippocampus, Gähwiler and Brown (1985) showed that septal cholinergic innervation of the hippocampus could be reproduced *in vitro*, and that a train of stimuli to septal neurones generated a slow, cholinergic EPSC associated with a decrease in a membrane conductance which shares many of the properties of $I_{K(M)}$. Thus, inhibition of $I_{K(M)}$ by synaptically released ACh also seems to be a possible mechanism for the slow EPSP in CNS neurones.

1.2.2. Pharmacology of $I_{K(M)}$ inhibition in rat sympathetic neurones.

Five muscarinic receptor genes have been identified, enabling detailed studies of the distribution and function of muscarinic receptor subtypes; cloned receptors m1 to m4 correspond to the pharmacologically defined M_1 to M_4 receptors, while the cloned m5 receptor presently has no pharmacological correlate (Hulme *et al.*, 1990; Caulfield, 1993 for reviews). In rat sympathetic neurones, the muscarinic receptor subtype mediating $I_{K(M)}$ inhibition has been well characterized. Sympathetic neurones express mRNA encoding the subtypes m1 to m4 (Dr. N. J. Buckley, personal communication),

although immunoprecipitation studies using selective muscarinic receptor antibodies have only identified m1, m2 and m4 receptors (reviewed by Caulfield, 1993). Pharmacological studies on dissociated SCG neurones suggests that the M_1 subtype mediates $I_{K(M)}$ inhibition (Marrion *et al.*, 1989; Bernheim *et al.*, 1992), which is consistent with the finding that M_1 receptors also mediate muscarinic receptor-induced ganglion depolarization (Brown *et al.*, 1980; Field and Newberry, 1989). This also agrees partially with findings in NG108-15 cells transfected with DNA encoding the different muscarinic receptor subtypes (m1 to m4), where m1 and m3 (but not m2 and m4) receptors couple to inhibit $I_{K(M)}$ (Fukuda *et al.*, 1988; Robbins *et al.*, 1991). The absence of reports of M_3-mediated inhibition of $I_{K(M)}$ in sympathetic ganglia may reflect very low (or no) expression of this subtype in ganglia (see above, studies with muscarinic receptor antibodies). Muscarinic receptors have the characteristic structure of the family of receptors which couple to G proteins, and interestingly the biochemical coupling preferences of the subtypes show a similar pattern to the coupling to ion channels: m1, m3 and m5 receptors preferentially couple to PTX-insensitive G proteins to activate PLC (while m2 and m4 receptors couple to PTX-sensitive G proteins to inhibit adenylyl cyclase; see Caulfield, 1993 for review). In cultures of rat SCG cells, mRNA encoding the PTX-insensitive G proteins, $G_{\alpha q}$ and $G_{\alpha 11}$ (in addition to the PTX-sensitive G proteins $G_{\alpha o1\text{-}2}$ and $G_{\alpha i1\text{-}3}$) has been detected (Dr. N. J. Buckley, personal communication). Immunostaining has revealed strong bands for $G_{\alpha q}$ and $G_{\alpha 11}$ (and $G_{\alpha o1}$ and $G_{\alpha i2}$, but only weak bands for $G_{\alpha o2}$ and $G_{\alpha i1}$; Caulfield *et al.*, 1994). The presence of other G proteins in SCG cells, including other PTX-insensitive G proteins, has not been determined. Moreover, it is not known whether the principal SCG neurones express different levels (or a different range) of G proteins to the background cells. However, at least two PTX-insensitive G proteins may be available to transduce M_1 receptor-mediated $I_{K(M)}$ inhibition in sympathetic neurones.

The slow kinetics of the atropine-sensitive EPSP in sympathetic and some CNS neurones can now be understood in light of the transduction mechanism for $I_{K(M)}$ inhibition: receptor-mediated inhibition of $I_{K(M)}$ proceeds *via* G protein activation, and possibly involves the generation of a diffusible second messenger, although intracellular events subsequent to G protein activation have remained elusive or ambiguous in

neurones. Known information regarding the identity of the G proteins and putative intracellular signalling systems in transducing inhibition of $I_{K(M)}$ by neurotransmitter and hormone receptors is discussed below.

1.2.3. Transduction mechanism for $I_{K(M)}$ inhibition.

The involvement of a G protein in transducing inhibition of $I_{K(M)}$ by receptors for muscarine and peptides has been demonstrated in frog (Pfaffinger, 1988, reviewed by Bosma *et al.*, 1990) and rat (Brown *et al.*, 1989) sympathetic neurones using G protein activators and poorly hydrolyzable analogues of GTP and GDP. The effects of these analogues on $I_{K(M)}$ inhibition by muscarine, LHRH, UTP or substance P in frog sympathetic neurones were similar, indicating that receptors for all of these agonists use a mechanism that involves a G protein (Lopez and Adams, 1989). Interestingly, GDPβS has been demonstrated to cause a partial, but not a complete block of the agonist-inhibition in both preparations. The G protein transducing this response is not susceptible to ADP-ribosylation by pertussis toxin, which suggests it is a member of one of the classes of G proteins that lack the target cysteine residue (G_q, G_{12} or G_z: Simon *et al.*, 1991). Although evidence from cell-attached patch recordings of single M-channel activity in rat (Selyanko *et al.*, 1992) and frog (Marrion, 1993) sympathetic neurones indicates that a diffusible messenger mediates agonist-inhibition of $I_{K(M)}$, the identity of this putative second messenger remains elusive (and therefore, the possibility that the G_α subunit fulfills this role cannot yet be excluded). Early experiments discounted a role for cyclic nucleotides and phosphorylation or dephosphorylation reactions (Brown and Adams, 1987; Brown *et al.*, 1989; Bosma *et al.*, 1990), although a poorly hydrolyzable analogue of ATP can increase "rundown" of I_M in frog sympathetic neurones (Pfaffinger, 1988; Chen and Smith, 1992) without affecting I_M inhibition (Chen and Smith, 1992).

Because receptors that couple to inhibit $I_{K(M)}$ can often also activate PLC (for example, certain muscarinic receptor subtypes: Fukuda *et al.*, 1988), and because PLC is also activated *via* a PTX-insensitive G protein, products of PLC activation have occupied a favourable position as potential candidates for the diffusible messenger (see Brown, 1988a). Activation of PLC induces two biochemical pathways (see above)

generating IP_3, Ca^{2+}, DAG and PKC. In sympathetic neurones it is the latter, DAG-PKC pathway that initially enjoyed popularity. Thus, in frog sympathetic neurones, the phorbol ester, phorbol dibutyrate (PDBu), which activates PKC, had a similar effect to muscarine on I_M, reducing the time-dependent deactivation and activation relaxations and reducing the outward rectification of the steady-state current voltage relationship across the I_M activation range; additionally, down-regulation of PKC by a long-term exposure to PDBu made the cells refractory to muscarine (Brown and Adams, 1987). However, unlike the effect of muscarine, the effect of PDBu was incomplete and irreversible (Brown and Adams, 1987). A similar result was described with respect to phorbol esters and the response to peptides (Bosma and Hille, 1989): PKC activators caused a partial suppression of I_M, and the residual current could still be inhibited by peptides. Moreover, although compounds that inhibit PKC (staurosporine, H7 and the more selective peptide inhibitor, PKC(19-36)) inhibited the effect of the PKC activators, they did not affect inhibition of I_M by the peptides substance P and LHRH (Bosma and Hille, 1989). A lack of effect of PKC(19-31) and H7 on the muscarinic inhibition of I_M was reported by Marrion (1994), although staurosporine did inhibit the response to muscarine, and all three inhibitors reduced the effect of phorbol esters on I_M. The data suggest that agonists inhibit I_M by a PKC-independent pathway, although such a pathway has not yet been identified. Similar conclusions can be drawn from experiments on rat sympathetic neurones: although phorbol esters can inhibit $I_{K(M)}$ (Brown *et al.*, 1989), indirect evidence from studies of muscarinic- and phorbol ester-evoked depolarizations of rat ganglia suggest that the muscarinic depolarization response does not involve PKC activation (Grove *et al.*, 1990).

The alternative branch of the PLC pathway has also received much attention, particularly the possible role of Ca^{2+} in $I_{K(M)}$ regulation and inhibition. That IP_3 itself is the trigger for $I_{K(M)}$ inhibition in sympathetic neurones appears unlikely: although muscarinic receptors in the rat (Bone *et al.*, 1984; Patterson and Volle, 1984; Horwitz *et al.*, 1985) and muscarinic and peptide receptors in the frog (Pfaffinger *et al.*, 1988) can increase the production of inositol phosphates in whole ganglia (and are therefore clearly capable of activating PLC), inclusion of IP_3 in the pipette during whole-cell recording from frog neurones had no effect on I_M or its inhibition by agonists

(Pfaffinger *et al.*, 1988), and both ionophoretic intracellular injection, and inclusion in the patch pipette of IP_3 had no effect on $I_{K(M)}$ in rat neurones (Brown *et al.*, 1989). The role of Ca^{2+} is more controversial and intriguing. Pfaffinger *et al.* (1988) reported that although agonists that inhibit I_M also evoke small Ca^{2+} transients (measured with the Ca^{2+}-sensitive dye fura-2) in frog neurones, these two events are not related. However, Kirkwood *et al.* (1991) reported contrary results to Pfaffinger *et al.* and suggested that in fact inhibition of I_M does involve an increase in intracellular Ca^{2+}. One possible explanation for these apparent discrepancies is that Ca^{2+} does regulate $I_{K(M)}$, but is very sensitive to the recording conditions used and the agents used to study its involvement. Thus, Marrion *et al.* (1991) used "caged" Ca^{2+} in combination with Ca^{2+} imaging to correlate very rapid changes in intracellular Ca^{2+} (to different intracellular concentrations, and for different durations) with effects on I_M in frog neurones, and showed that different changes in Ca^{2+} could differentially affect I_M, the inhibition of I_M, and the I_M "over-recovery" phenomenon. Similar findings have been reported by Ping Yu *et al.* (1994). In rat sympathetic neurones, agonists that inhibit $I_{K(M)}$ did not evoke detectable changes in intracellular Ca^{2+} (measured with fura-2); however, tightly buffering the intracellular Ca^{2+} with 10 mM BAPTA reduced the inhibition of $I_{K(M)}$ by agonists (Beech *et al.*, 1991). The authors proposed that a minimum Ca^{2+} concentration is required for inhibition, although the inhibition was not itself mediated by an increased level of Ca^{2+}. One note of caution is that generally, Ca^{2+} sensitive dyes such as fura-2 are not used to monitor changes in Ca^{2+} in specific regions of the cell, so any regional changes in Ca^{2+} that may occur (for example, in the proximity of the plasma membrane) would perhaps be lost in the averaged measurement from the whole cell. It is possible that Ca^{2+} does have an important role in regulating M-channels and may also be significant in $I_{K(M)}$ inhibition: more sophisticated Ca^{2+} imaging techniques and methods for raising intracellular Ca^{2+} in a "physiological" manner may be required to clarify this.

In central neurones, the situation appears to be the converse to that in sympathetic neurones, with IP_3 being the most popular candidate for mediating $I_{K(M)}$ inhibition. Dutar and Nicoll (1988) used the hippocampal slice preparation to show that carbamylcholine and oxotremorine-M acted as full agonists and oxotremorine,

pilocarpine and arecoline acted as partial agonists in inhibiting $I_{K(M)}$. Interestingly, this profile coincided with that for inositol phosphate turn over in preparations of nerve endings and slices from guinea pig cerebral cortex (Fisher *et al.*, 1983; Fisher *et al.*, 1984). However, as the latter observation was made by a different group using a different CNS preparation, some caution must be exercised in laying emphasis on this point, particularly in view of the dangers in classifying receptor subtypes mediating responses on the basis of agonist potency, which may represent differences in the number of receptors, the number of transducers (for example, G proteins) and the receptor-transducer coupling efficiency between different tissues. However, in support of the IP_3 hypothesis (but not as conclusive evidence for it), intracellular injection of IP_3 did mimic the $I_{K(M)}$ inhibition. Interestingly, increasing the Ca^{2+} buffering capacity of the cell by introducing Ca^{2+} chelators did not affect the $I_{K(M)}$ inhibition, although it did inhibit the Ca^{2+}-dependent afterhyperpolarization (AHP) current. However, as the chelators were introduced *via* a high resistance microelectrode, the success of this experiment is questionable: the effect on the AHP current may simply reflect a higher Ca^{2+}-sensitivity than that of $I_{K(M)}$. Previous experiments had ruled out the involvement of PKC in $I_{K(M)}$ inhibition (Malenka *et al.*, 1986), although this pathway may mediate inhibition of the Ca^{2+}-dependent AHP. Further, carefully controlled experiments investigating G protein and second messenger involvement in inhibition of $I_{K(M)}$ by neurotransmitters in CNS neurones would be of interest.

The difficulties associated with identifying the putative second messenger mediating $I_{K(M)}$ inhibition is perhaps exemplified by the comprehensive study of Robbins *et al.*, (1993) using the neuronal cell line, NG108-15 cells. These model neurones are useful for biochemical and electrophysiological studies as they express a range of voltage-dependent ion channels (Brown *et al.*, 1993 for review) and biochemical responses. The cells are robust, facilitating intracellular manipulations during electrophysiological recordings. Furthermore, it has been possible to transfect these cells with DNA encoding specific muscarinic receptor subtypes (although they do express an endogenous m4 receptor). M-type K^+ currents in NG108-15 cells can be inhibited by ACh in cells transfected with m1 or m3 but not m2 and m4 receptor DNA (Fukuda *et al.*, 1988; Robbins *et al.*, 1991). Robbins *et al.* (1993) tested for the

involvement of most known second messenger system in mediating ACh-inhibition of $I_{K(M)}$ in m1-transfected cells, including products of PLC activation, phosphorylation and dephosphorylation reactions, products of PLA_2 activation and the nitric oxide-cGMP pathway, with no conclusive evidence for any of these, or even a combination of pathways, in mediating this response. As in sympathetic neurones, there was evidence for the involvement of a PTX-insensitive G protein. However, in non-transfected NG108-15 cells, there is some information about the coupling of BK receptors to $I_{K(M)}$: thus, phorbol esters mimic the inhibition of $I_{K(M)}$ by BK (Higashida and Brown, 1986), and down regulation of PKC using phorbol esters decreases the effect of BK; however, inhibitors of PKC do not affect the response to BK (Schäfer *et al.*, 1991). There is some evidence that fatty acids (including arachidonic acid and its metabolites) can inhibit $I_{K(M)}$ (Béhé *et al.*, 1992), and this effect may involve PKC activation (Schmitt and Meves, 1993).

1.3. Statement of purpose.

The aim of the experiments presented in this thesis was to identify the PTX-insensitive G protein transducing $I_{K(M)}$ inhibition in rat sympathetic neurones. The first priority was to establish a method for recording stable $I_{K(M)}$ deactivation currents and agonist effects which were reproducible and reversible (Chapter 3). Using this method, anti-G protein antibodies and antisense DNA were used to identify G proteins transducing muscarinic inhibition of $I_{K(M)}$, and therefore provide new information about this modulatory pathway (Chapter 4). Subsequently, inhibition of $I_{K(M)}$ by the local peptide hormone, bradykinin (BK) was characterized (Chapter 5).

CHAPTER 2:

Methods.

2.1. Tissue Culture.

Dissociation and culture of rat SCG cells.

Sympathetic neurones from rat superior cervical ganglia (SCG) were cultured using a similar protocol to that outlined by Owen *et al.* (1990). SCG were removed from Sprague-Dawley rats (15-19 day old, killed by CO_2 asphyxiation) into Leibovitz L15 medium, cleaned of connective tissue, desheathed and cut into four pieces. After washing twice in HBSS, cells were dissociated by incubation with collagenase (390 units/ ml of HBSS plus 6 mg/ ml bovine serum albumin, BSA) for 15 minutes and, after two washes, trypsin (type XII-S; 10,000 units/ ml HBSS plus 6 mg/ ml BSA) for 30 minutes, followed by trituration (in incubation medium) with a fire-polished Pasteur pipette. The dissociated cells were suspended in L15 medium, centrifuged (900 revolutions per minute, 3 minutes), and resuspended in incubation medium. The cell suspension (200 µl volumes) was transferred to the laminin-coated centre of 35 mm diameter plastic dishes, and the cells were allowed to adhere to the laminin overnight in an incubator (37 °C, 95% O_2/ 5% CO_2). Cells used on the first day in culture were not fed, but cells used after more than one day in culture were fed on the day after plating, with approximately 2 ml of incubation medium, and maintained in the incubator.

Solutions.

HBSS: Hank's Balanced Salt Solution (containing no Ca^{2+} and no Mg^{2+}, with 10 mM HEPES added).

Incubation medium: contains Leibovitz L15 medium, fetal calf serum (10%), glucose (32 mM), penicillin (50 units/ ml), streptomycin (50 µg/ ml), L-glutamine (2 mM), bicarbonate (24 mM) and nerve growth factor (50 ng/ ml).

2.2. Electrophysiology.

2.2.1. Voltage-clamp procedure.

Dishes of cells were transferred to an inverted microscope (Nikon TMS) and superfused by gravity with a modified bicarbonate-buffered Krebs' solution (composition given below). All experiments were performed at room temperature (20-

26 °C). Voltage-clamp experiments were carried out using single patch pipettes to achieve the whole-cell or perforated patch recording configuration (Hamill *et al.*, 1981; Horn and Marty, 1988; Rae *et al.*, 1991). Patch pipettes were pulled from thin-walled, filamented glass (Clark Electromedical) using either a Flaming/ Brown programmable horizontal puller (Sutter) or a List vertical puller. To minimize pipette/ bath capacitance, pipettes were coated near the tip with Sylgard; pipette tips were then fire-polished (using a Narishige microforge) to enhance giga-seal formation, giving resistances of 4-7 M Ω (for whole-cell experiments) or 2-5 M Ω (for perforated patch experiments). Patch pipettes were back-filled with one of the intracellular solutions detailed below. For perforated patch recordings using the pore-forming antibiotic agents nystatin or amphotericin B, patch pipettes were first front-filled with antibiotic-free intracellular solution (by dipping for 20-60 seconds), which allowed time for seal formation before permeabilization began. Patch pipettes were then fitted onto a Ag wire coated with AgCl, connected to an Axoclamp 2A amplifier (Axon instruments).

Pipettes were positioned above cells in the extracellular solution. The voltage difference across the pipette was set to zero in bridge mode; the reference electrode was a KCl/ agar bridge connected to a pool of 3 M KCl which was in turn connected to ground. This was checked again at the end of the experiment to monitor any drift in the voltage detected across the pipette: the voltage offset at the end of the experiment was subtracted from the cell membrane potentials recorded. While in bridge mode, the pipette voltage in response to a current injection (0.1 nA, 20 ms duration every 100 ms) was continuously monitored using an oscilloscope (Tektronix). The voltage (V) drop across the tip of the pipette during current (I) passing was compensated prior to seal formation using the bridge balance; this provided an estimate of pipette resistance (R) from Ohm's Law ($V = I.R$). The pipette was gently touched on to the cell using a Narishige hydraulic manipulator. Contact was monitored (using the oscilloscope) by a voltage drop in response to the injection of current, due to the increase in resistance. A high resistance seal (of at least 1 GΩ) was formed between the pipette and the membrane by the application of gentle suction. Seal formation was monitored by the increasing voltage deflection in response to the current injection. For whole-cell recordings, the whole-cell configuration was achieved by applying a short increase in

suction to break the cell membrane under the patch pipette, and monitored by a sudden decrease in the voltage deflection, to achieve access resistances of 10-15 MΩ. For perforated patch recordings, the pore-forming agent used in the pipette was allowed to permeabilize the cell membrane under the patch pipette (monitored by the slowly decreasing voltage deflection), usually in 5-10 minutes, to access resistances of 30-40 MΩ (nystatin) or 20-30 MΩ (amphotericin B). During the experiment there was usually a further decrease in access resistance of around 10 MΩ when using either agent.

Neurones were voltage-clamped in discontinuous single electrode voltage-clamp mode (Finkel and Redman, 1984). The duty cycle had a 30% period of current passing (the amplitude being related to the difference between the recorded voltage and the command voltage, according to the gain), and the sampling frequency was set so that the voltage response across the electrode had decayed prior to voltage sampling (this was monitored using a second oscilloscope). Typically, the sampling frequency was 5-7 kHz for whole-cell recordings and 3-5 kHz for perforated patch recordings. To establish optimum voltage-clamp conditions, electrode capacitance (monitored from the electrode voltage response throughout a duty cycle) was first optimally compensated (sampling frequency was then adjusted at this stage). A 10 mV (hyperpolarizing) step was then applied (20 ms, every 100 ms), and the gain (for the current-passing circuit) was increased until the voltage response was square, with no overshoot. Phase was adjusted if it offered improvement to the voltage response, and the antialias filter was increased to reduce noise on the voltage and current signals without altering the settling characteristics during the duty cycle.

SCG membrane resistance (R_m), calculated from the current response to a 1s, 10 mV voltage step from the zero current potential (in voltage clamp) using Ohm's Law ($V = I.R$), was 350 ± 30 MΩ ($n = 11$ cells). Membrane capacitance (C_m) was estimated from the slow membrane time constant (τ_m), determined from a fit of a two exponential function to the decay of the capacitance current during a -10 mV step from

the zero current potential in voltage-clamp mode ($\tau_m = R_m.C_m$). Average membrane capacitance was 92 ± 11 pF (n = 11).

2.2.2. Solutions.

Modified Krebs' solution: NaCl, 120 mM; KCl, 3 mM; $CaCl_2$, 2.5 mM; $MgCl_2$, 1.2 mM; $NaHCO_3$, 22.6 mM; HEPES, 5 mM; D-glucose, 11.1 mM; tetrodotoxin, 0.5 μM; pH 7.4 approximately, when bubbled with 95% O_2/ 5% CO_2. Osmolarity was between 270-290 mOsm. In some experiments the [KCl] was increased to 15 mM. The flow rate was 7 ml/ minute when using the local perfusion system, and 13 ml/ minute when using the distant perfusion system in conjunction with the U-tube-like device (see below).

K acetate-/ K gluconate-based whole-cell intracellular solution: Potassium acetate (or potassium gluconate) 80 mM; KCl, 30 mM; $MgCl_2$, 3 mM; HEPES, 40 mM; EGTA, 3 mM (estimated Ca^{2+} concentration is less than 1 nM*). For some experiments, ATP and GTP (Mg^{2+} salts) were added to give a final concentration of 2 mM ATP and 0.5 mM GTP.

*Using the Ca^{2+}-sensitive dye, indo-1, the basal Ca^{2+} concentration in the Krebs' solution has been estimated to be up to 10 μM: addition of 3 mM EGTA buffers this basal Ca^{2+} concentration to almost zero (Dr. S. J. Marsh, personal communication).

Intracellular solution for perforated patch recordings: nystatin or amphotericin B were suspended in dimethyl sulphoxide (0.5% and 0.2% respectively) by sonication, freshly each day, and then diluted to a final concentration of 0.25 mg/ ml nystatin or 50 μg/ ml amphotericin B in a K acetate-based solution similar to above, but containing no EGTA, ATP or GTP.

All intracellular solutions were adjusted to around pH 7.2 with a 10 M solution of KOH, and to between 270 and 280 mOsm using 1 M solutions of K acetate or K gluconate, giving a total intracellular [K^+] of 125 mM. When using the K acetate-based solution (and accounting for the ionic activity of K acetate), the equilibrium potential for K^+ ions (calculated from the Nernst equation) was -94 mV in 3 mM

extracellular [K^+] and -53 mV in 15 mM extracellular [K^+]; the equilibrium potential for Cl^- ions was -33 mV.

The liquid junction potential between the intracellular and extracellular solutions was estimated from the method of Neher (1992). Using the KCl reference electrode, the pipette voltage was zeroed with intracellular solution in the pipette and in the bath. The bath was then superfused with the extracellular Krebs' solution. Using the K gluconate intracellular solution, a liquid junction potential of -7 mV was measured (outside with respect to inside). Using the K acetate solution, a liquid junction potential of -6 mV was measured on superfusing Krebs' solution containing 3 mM KCl, and -5 mV on superfusing Krebs' solution containing 15 mM KCl. These values have not been subtracted from measurements of membrane potential.

2.2.3. $I_{K(M)}$ recordings: voltage protocols.

When SCG neurones are depolarized, a standing outward current develops, which is predominantly due to activation of the M-type K^+ current ($I_{K(M)}$) between -70 and -20 mV (Constanti and Brown, 1981). Because $I_{K(M)}$ does not inactivate, it is convenient to voltage-clamp cells at depolarized potentials to activate $I_{K(M)}$, and then elicit $I_{K(M)}$ deactivation currents by applying hyperpolarizing voltage steps, thus allowing measurement of $I_{K(M)}$ deactivation currents in the absence of contaminating currents (such as the A-type K^+ current and voltage-dependent Na^+ and Ca^{2+} currents: Marrion *et al.*, 1987) seen when depolarizing steps are applied to re-activate $I_{K(M)}$. Therefore, the voltage protocol used to study $I_{K(M)}$ and the modulation of $I_{K(M)}$ by agonists was to depolarize the cell membrane to a holding potential (V_H) between -20 and -30 mV to activate $I_{K(M)}$, and then apply 1 s, -30 mV voltage steps to deactivate $I_{K(M)}$. Original M-current recordings indicated that the deactivation currents followed a single exponential time course in bullfrog (Adams *et al.*, 1982a) and rat (Constanti and Brown, 1981) sympathetic neurones, although subsequent studies have indicated that a better fit of the deactivation current can sometimes be obtained using a two exponential function, particularly at membrane potentials more hyperpolarized than -50 mV (rat sympathetic neurones: Owen *et al.*, 1990; Stansfeld *et al.*, 1993). In the experiments outlined in this thesis, $I_{K(M)}$ deactivations at around -55 mV could be best fit with a two

exponential function, representing a component of $I_{K(M)}$ that deactivates with a time constant of around 60 ms (contributing 40% - 70% of the total deactivation), and a component that deactivates with a (variable) time constant of several hundred milliseconds (time constant values, under different experimental conditions, are given throughout the thesis): these values accord with the estimates of Stansfeld *et al.*, 1993 (whole-cell recording from rat cultured SCG neurones; 67 ± 5 ms and 277 ± 38 ms, n = 34). Similar time constant values were obtained for $I_{K(M)}$ deactivation recordings from replated SCG cells, which have very few processes (47 ± 7 ms (contributing 45%-80%) and 356 ± 62 ms, n = 5; Dr. J. A. Lamas, personal communication), suggesting that the (variable) slow component of the deactivation current is not a consequence of poor space clamp due to process outgrowth, which occurs when SCG cells are left in culture for more than one day. Figure 2.1. shows an example current record during a typical $I_{K(M)}$ deactivation voltage protocol (throughout this thesis, voltage protocols are omitted for space, but the voltage step recorded at the pipette was generally >90% of the -30 mV step). The cell membrane was voltage-clamped to -26 mV, then stepped for one second to -56 mV. The instantaneous current step at the start of the voltage step represents "leak" current and current through M-channels open at the holding potential. The slow, current relaxation (arrow) is the $I_{K(M)}$ deactivation current as the M channels slowly close in response to the voltage step. At the end of the voltage step, when the membrane potential is stepped back to -26 mV, the same (but opposite) sequence of events is seen: the instantaneous current is smaller because more M channels are closed at -56 mV and therefore the instantaneous current is mostly "leak" current. Voltage steps to potentials more positive than -20 mV caused activation of the delayed rectifier K^+ current; voltage steps to potentials more negative than -60 mV led to activation of the transient A-type K^+ current on the step back to the depolarized potential. Current through voltage-dependent Na^+ channels was blocked with 0.5 μM tetrodotoxin. $I_{K(M)}$ was recorded in all SCG neurones tested, including all neurones treated with anti-G protein antibodies and antisense DNA, and was always sensitive to inhibition by agonists. In occasional cultures (<5%), $I_{K(M)}$ deactivations elicited by the voltage protocol described above were less than 100 pA in amplitude: data from these neurones were not included in the analysis as the error in calculating $I_{K(M)}$ inhibition was considered likely to be large.

To study the current-voltage relationship of both $I_{K(M)}$ and membrane steady-state current, the cell membrane was again voltage-clamped at between -20 and -30 mV, and 1 s hyperpolarizing steps in increments of 10 mV were applied. To study the effect of agonists on $I_{K(M)}$ at different membrane potentials, current was measured in response to voltage ramps (in the hyperpolarizing direction) across the activation range for $I_{K(M)}$ (ramp speed, -10 mV/ s). When current-voltage relationships were studied, CsCl (1 mM) was added to the extracellular solution to reduce inwardly rectifying K^+ current at hyperpolarized membrane potentials.

2.2.4. Agonist application.

This thesis describes the effect of two agonists on $I_{K(M)}$: the muscarinic receptor agonist, oxotremorine-M (oxo-M) and the local peptide hormone, bradykinin (BK). In the figures illustrating the effect of agonists on $I_{K(M)}$, current traces recorded in control solution are designated "c", in the presence of agonist, "d" (drug), and after washing out the agonist, "w". Most of the experiments with oxo-M utilized a local agonist application system which was positioned approximately 5 mm away from the cell. The agonist had to be applied to the extracellular solution and so there was a delay in onset while the agonist equilibrated throughout the system. During experiments using BK as an agonist, cells in a given dish gave variable responses to BK when using the existing system. Therefore, it was necessary to use an agonist application system which minimized the exposure of cells to the peptide. For all of the experiments with BK described in this thesis, a device similar to a "U-tube" was used to apply the BK. The device consisted of two glass tubes of fine diameter (50 μm), and silanized to minimize peptide binding to the glass, closely associated. Agonists were continuously superfused *via* one tube and removed by vacuum *via* the other, until the vacuum was manually switched off and the agonist allowed to superfuse the cell. The device was positioned approximately 1 mm away from the cell, and kept above the meniscus until prior to agonist application. After obtaining control $I_{K(M)}$ deactivation records, the device was lowered into the bath, and a further control recording made, before applying the agonist. Applying the normal extracellular solution *via* this device had no effect on $I_{K(M)}$ deactivation relaxations. The advantage of this system was that it minimized exposure of other cells in the dish to BK (due to the continued superfusion of normal

extracellular solution through a distant system), and it also provided a more rapid method of agonist application and enabled comparisons between the rate of response to the two agonists, oxo-M and BK, to be made. The device was calibrated using 45 mM KCl in the extracellular solution to set E_K to around -25 mV, and measuring the delay in onset and the rate of development of zero current after switching to this high K^+ solution (Figure 2.2.; V_H -23 mV). From four determinations in one cell, the onset latency was 2.2 ± 0.2 s, the half-time to zero current was 1.9 ± 0.4 s, and the full time to zero current was 5.9 ± 0.6 s. The latency in offset of the high K^+ effect, on switching back to normal Krebs' solution after around 30 s, was 7.0 ± 0.4 s, and the full time to reversal of the effect was 26.0 ± 1.3 s.

In experiments to compare $I_{K(M)}$ inhibition in response to maximally effective concentrations of the two agonists, concentrations of 3 μM oxo-M and 10 nM BK were used. There was no significant difference between the responses to 3 μM and 10 μM oxo-M, or between the responses to 10 nM and 30 nM BK. In experiments to study the effect of G protein antibodies on muscarinic receptor-mediated $I_{K(M)}$ inhibition, a test concentration of 300 nM oxo-M was used, as this concentration produces a submaximal inhibition, and this position on the linear part of the ($\log_{10}$) concentration-response curve should be sensitive to any change in receptor-G protein coupling. To investigate the G proteins mediating inhibition of $I_{K(M)}$ by BK, a test concentration of 1 nM BK was used. This concentration is close to the EC_{50} for this response, and therefore was also expected to be sensitive to changes in receptor-G protein coupling efficiency; additionally, at this concentration, no tachyphylaxis of the response was observed (see Chapter 5). In the series of experiments on antibody-injected cells, responses to BK from the same dish were measured alternately from cells injected with control agents (anti-G_{α_o} antibody or peptide: see below) and test (anti-$G_{\alpha_{q/11}}$) antibody.

2.2.5. Data acquisition and analysis.

Voltage protocols were generated, and data were acquired (through an analogue-to-digital interface) using pClamp 5.1 Clampex software on a Zenith PC-486. Current records were filtered at 100 to 300 Hz, and then amplified *via* a pen recorder (Gould)

before acquisition. The amplitude of $I_{K(M)}$ deactivations during voltage steps was measured by eye using pClamp 5.1 Clampan "cursor measurement" as illustrated by the dashed lines in Figure 2.1. Throughout the thesis, the term "$I_{K(M)}$ amplitude" refers to the amplitude of the deactivation current elicited by the voltage command protocol described above, and "holding current" refers to the absolute current measured at the membrane potential to which cells were voltage-clamped (also measured by eye in Clampan). Measurements of steady-state current refer to absolute current at the end of 1 s hyperpolarizing, incremental 10 mV steps to generate current-voltage relationships. All $I_{K(M)}$ deactivation current time constants were measured using pClamp 5.1 Clampfit. The delay of onset and rate of development of agonist inhibition of $I_{K(M)}$ were measured using pClamp 6 Clampfit software. Inhibition of $I_{K(M)}$ by agonists is defined as the reduction in the amplitude of the $I_{K(M)}$ deactivation current during the voltage step, and is expressed throughout as a percentage of control current amplitude. Recovery from inhibition is defined as the amount of inhibited $I_{K(M)}$ deactivation current that returns after washing out the agonist, that is $(I_{wash} - I_{agonist})/(I_{control} - I_{agonist})$, and is also expressed as a percentage.

2.3. G protein antisense oligodeoxynucleotides.

For experiments investigating the effect of G protein antisense oligodeoxynucleotides (ODNs), SCG neurones were incubated with ODNs for 3-35 hours. Cells were maintained in 200 µl volumes throughout the incubation time. ODNs were stored at -20 °C in 2 µl aliquots (2 mM) and were made to a final concentration of 20 µM in 200 µl of SCG medium. The normal SCG medium was replaced with the ODN-containing medium on the day after plating. The following ODNs were used:

485a (anti-$G_{\alpha q}$): CTACACGGTCCAAGTCAT

605a (anti-$G_{\alpha 11}$): GGTGGGCAGGTAGCCTAC

499a (anti-$G_{\alpha 11}$): GTAGCCATCTGTGGCGAT

All ODNs were phosphorothioate-modified (pODNs). Experiments utilizing ODNs were carried out in collaboration with Dr. M. P. Caulfield (in paired experiments, using coded dishes, so that both the experiments and the analysis were performed "blind"), with a 50% contribution from each to the experimental data.

2.4. G protein antibodies.

2.4.1. Antibody injections.

Anti-G protein antisera were raised by Dr. G. Milligan, in New Zealand white rabbits using synthetic peptides conjugated to keyhole limpet haemocyanin (Goldsmith *et al.*, 1987). Synthetic peptides corresponded to the following:

Anti-$G_{\alpha o}$ antiserum (OC2): C-terminal decapeptide sequence of the α-subunit of G_o, ANNLRGCGLY. OC2 recognizes $G_{\alpha o1}$ and $G_{\alpha o2}$, but not $G_{\alpha i}$ isoforms (Georgoussi *et al.*, 1993).

Anti-$G_{\alpha q/11}$ antiserum (CQ1 and CQ2, from different rabbits): C-terminal decapeptide sequence common to the α-subunits of $G_{\alpha q}$ and $G_{\alpha 11}$, QLNLKEYNLV. CQ2 shows no cross-reactivity with synthetic peptides representing C-terminal sequences of $G_{\alpha i}$ isoforms, $G_{\alpha o}$ isoforms or $G_{\alpha z}$ (Mitchell *et al.*, 1991).

Antisera were stored at -20 °C in 20 µl aliquots. Dr. Milligan also supplied the synthetic decapeptide against which anti-$G_{\alpha q/11}$ antibodies were raised: this was used to preabsorb the antibody in some experiments (1 µg/ ml). SCG cells for antiserum injections were plated on dishes marked on the underside with 1 mm^2 grids (to facilitate localization of injected cells), and superfused with Krebs' solution containing tetrodotoxin. Because the perforated patch recording method was adopted in these studies, antisera could not diffuse into cells from the patch pipette, and so antisera were introduced to the cell interior by microinjection. High resistance electrodes (40-80 MΩ when filled with antiserum) were pulled from thin walled, filamented glass using the Flaming/ Brown horizontal puller, then back-filled with 5 µl of undiluted antiserum, and positioned just above cells. The electrode was manoeuvered gently onto the

surface of the cell using the Narishige manipulator, and penetration of the cell membrane was achieved using the "clear" option on the amplifier to pass a brief, large hyperpolarizing current (-60 nA). Successful impalement was monitored by a standing negative potential in bridge mode (around -30 mV with antiserum-filled electrodes). Antiserum was then expelled into the cell by the application of gentle pressure to a 10 ml syringe connected to the electrode holder. If the injection was successful, a slight swelling of the cell was apparent. The electrode was withdrawn from the cell using the micromanipulator, a mark in the laminin was made close to the injected cell, and the position of the cell was noted. Nearly all cells survived this procedure (>90%). Cells injected with antiserum were left for approximately 2 hours before commencing recordings.

2.4.2. Verification of antibody injections.

Post-recording immunostaining.

In an initial series of experiments, verification of successful injection was carried out after $I_{K(M)}$ recordings. Cells were superfused with ice-cold phosphate-buffered saline (0.1 M, containing 4% BSA: PBS/ BSA), then permeabilized and fixed in 5% acetic acid in ethanol (15 minutes, -20 °C). After washing three times in PBS/ BSA, the cells were incubated with fluorescein isothiocyanate-labelled sheep anti-rabbit antibody (1:100 solution in PBS/ BSA, 30 minutes, room temperature). Unbound second layer antibody was then removed (three washes with PBS/ BSA), and the cells mounted in Citifluor under a glass coverslip, ready for identification of injected cells under a fluorescence microscope. The series of experiments utilizing this verification method were carried out in collaboration with Dr. M.P. Caulfield, and so approximately 50% of the experimental data using the anti-GFAP and the anti-$G_{\alpha q/11}$ antibodies were contributed by each.

Co-injection with FITC-dextran.

In a second series of injections, antisera were co-injected with a 0.1% solution of high MW dextran (MW: 10 kD) tagged with fluorescein isothiocyanate. Injections were either carried out on a Nikon Diaphot 300 fluorescence microscope, to monitor

the success of the injection on-line, or immediately after a series of injections (and prior to electrophysiological recordings).

2.5. Data presentation.

All figures were prepared using Sigmaplot 5 software (Jandel). Example $I_{K(M)}$ deactivation relaxation records (average of three traces unless otherwise stated) and current recorded in response to voltage ramps were imported from Clampfit. Concentration-response parameters were estimated from non-linear, least squares iterative curve fitting using the function $y = m.10^{n.\log(A)} / (10^{n.\log(A)} + 10^{n.\log(K)})$, where y = percent inhibition of $I_{K(M)}$, m = maximum response, A = [agonist], n = Hill coefficient, and K = EC_{50}; with weight ($1/SEM^2$) for the bradykinin data, as the curve was fit to mean values from a number of different experiments (see Chapter 5). The logarithmic form of the logistic equation was used because estimates of EC_{50} values are distributed normally on a logarithmic rather than an arithmetic scale (Fleming *et al.*, 1972), and so the use of logarithms of concentration parameters in fitting procedures has been recommended (Hulme and Birdsall, 1992).

2.6. Statistics.

Data are expressed throughout as mean ± standard error of the mean (SEM), unless otherwise indicated. All statistical analyses were performed using Graph Pad Instat2 software. For data from a number of treatment groups, analysis of variance was carried out, and post-tests were performed only if the variation among the groups was greater than expected by chance: individual statistical tests are indicated in the text. For comparisons between two groups of data, paired or unpaired t-tests were used, as appropriate to the experimental design. For data which did not exhibit Gaussian distribution for all test groups, a non-parametric analysis was used (details in text).

2.7. Materials.

All standard laboratory chemicals for making physiological solutions were purchased from BDH Limited. Tissue culture reagents were purchased from Sigma. Nystatin and amphotericin B were also purchased from Sigma. Oxotremorine methiodide was purchased from RBI, and bradykinin from Bachem. Pertussis toxin was purchased from Porton Products. G protein antibodies were provided by Dr. G. Milligan, University of Glasgow; anti-GFAP antibody was purchased from Sigma, and sheep anti-rabbit antibody (labelled with fluorescein) was purchased from Serotec. Antisense and sense oligodeoxynucleotides were provided by Dr. N. J. Buckley. Fluorescein-labelled dextran was purchased from Molecular Probes.

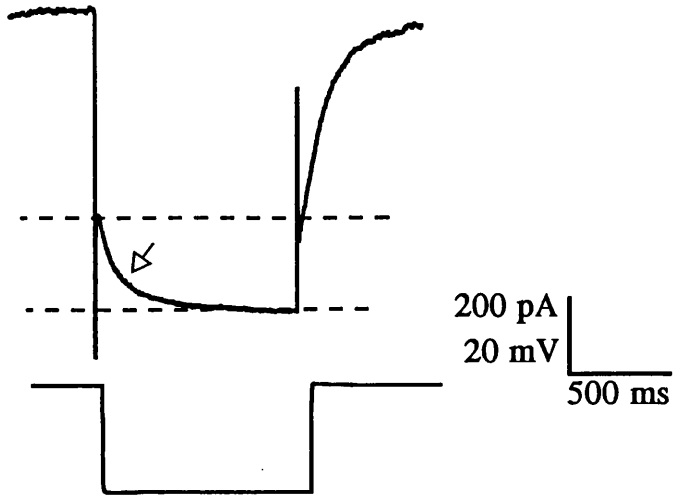

Figure 2.1. Measurement of $I_{K(M)}$ deactivation relaxation amplitude during a 1s voltage step from -26 mV to -56 mV.

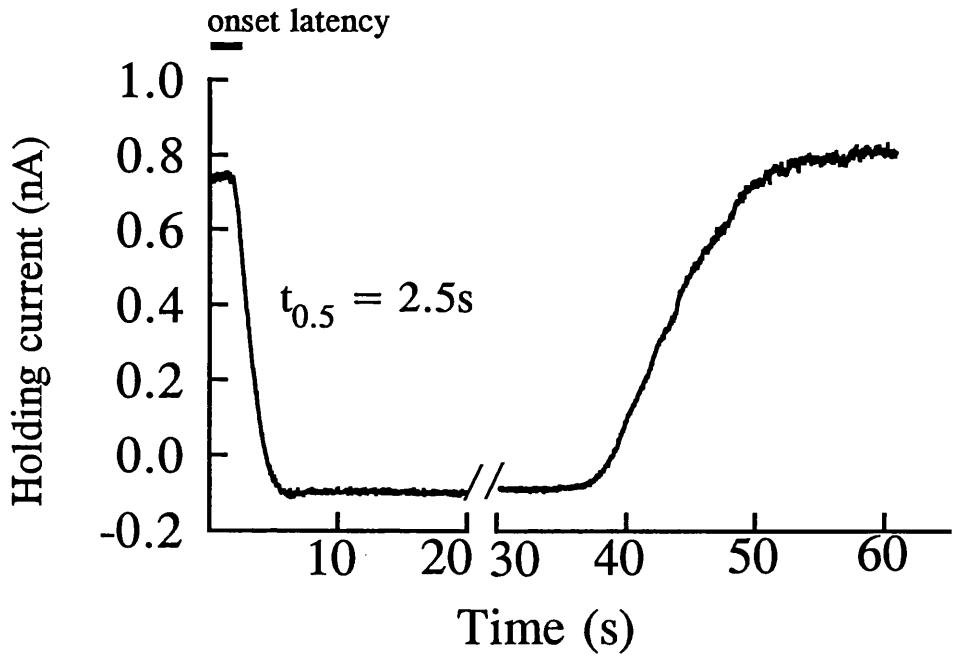

Figure 2.2. Onset/ offset of shift in E_K on changing $[K^+]_{ec}$ (t_0 and t_{30} s) indicated by the change in current.

CHAPTER 3:

Use of the perforated patch method to record $I_{K(M)}$: a comparison with conventional whole-cell recording.

3.1. INTRODUCTION.

Most of the experiments presented in this thesis were carried out using the perforated patch technique to record whole-cell M-type K^+ currents ($I_{K(M)}$) from cultured sympathetic neurones from the rat SCG. In this introduction, some of the advantages and disadvantages of the conventional whole-cell recording technique will be discussed, along with various remedies to overcome the disadvantages. The properties of $I_{K(M)}$ in rat sympathetic neurones, recorded using conventional whole-cell patch-clamp or microelectrode voltage-clamp methods will also be described.

3.1.1. The whole-cell patch-clamp recording method.

3.1.1.1. Conventional whole-cell recording methods.

The introduction of the "patch-clamp" recording technique (Neher and Sakmann, 1976) first enabled single channel currents to be detected, but in addition to this breakthrough in ion channel research the technique also offered new opportunities for studying whole-cell currents under voltage-clamp conditions. The technique presented certain advantages over traditional microelectrode recording, and has been particularly useful for recording from small cells previously unavailable for microelectrode impalement. The advantages offered by the refined whole-cell patch-clamp recording technique include improved resolution of the signal due to "giga-seal" formation between patch pipette and cell membrane (Sigworth and Neher, 1980; Hamill *et al.*, 1981) and the lower resistance pathway between the cell and the patch pipette, the mechanical stability conferred by the "giga-seal", and the avoidance of potential cell damage due to impalement (Horn and Korn, 1992). The large-diameter (around 1 μm) patch pipette tip which provides a low-resistance electrical pathway into the cell can also be exploited when studying the effects of the cytoplasmic environment on ionic conductances by introducing an artificial intracellular medium *via* diffusion from the pipette solution.

This latter phenomenon can become a hindrance when studying certain ion channels. It appears that the exchange of intracellular components between the cytoplasm and the pipette solution by diffusion can have adverse effects on ion channels and on the processes participating in their regulation by neurotransmitters. Thus, a common problem of conventional whole-cell recording is "rundown" (a decrease in current amplitude), as well as loss of responses to neurotransmitters and hormones: this has been encountered in studies of voltage- and ligand-gated ionic conductances (reviewed by Horn and Korn, 1992; Kay, 1992).

A variety of precautions have been adopted in order to limit rundown and restore receptor-activated responses, including reductions in pipette tip diameter to slow diffusion between the pipette solution and the cytoplasm, and alterations in the pipette solution (for example, the choice of major anion appears to be critical for certain conductances), including the addition of supplements such as ATP and GTP (Horn and Korn, 1992; Kay, 1992).

3.1.1.2. Perforated patch recording methods.

An increasingly popular alternative to conventional whole-cell recording is the perforated patch method. This was first accomplished using ATP (Lindau and Fernandez, 1986) which, however, had a limited application because of the resulting high access resistance (200 to 5000 MΩ). The introduction of the pore-forming antibiotics nystatin (Horn and Marty, 1988) and amphotericin B (Rae *et al.*, 1991) has made the technique more widely available for studies of ionic conductances. Either of these agents can be included in the patch pipette and, after forming a giga-seal, the antibiotics partition into the membrane under the patch pipette and form channels that are permeable to monovalent cations and anions (mainly Na^+, K^+, and Cl^-), but are apparently impermeable to high molecular weight and multivalent charged species. Perforated patch recording offers the advantage of minimum perturbation of the intracellular environment, allowing the intracellular composition of multivalent ions and large molecules such as enzymes to be maintained. The compromise of using this technique is the slightly higher access resistance compared with whole-cell recording,

and the inability to manipulate the intracellular composition, for example with drugs that modify intracellular enzyme activity.

3.1.2. Properties of $I_{K(M)}$ in rat sympathetic neurones.

3.1.2.1. $I_{K(M)}$ in rat sympathetic ganglia (intact).

The M-current is a time- and voltage-dependent, non-inactivating K^+ current, first described in bullfrog sympathetic ganglion neurones (Brown and Adams, 1980). Subsequently, a K^+ current with very similar properties to the M-current in bullfrog neurones was described in sympathetic neurones of the rat superior cervical ganglion (Constanti and Brown, 1981). The M-type K^+ current ($I_{K(M)}$) in the intact SCG from the rat activated at -70 mV (slightly more negative than the activation threshold for M-current in bullfrog neurones, although this may be attributed to the higher temperature at which experiments on rat SCG neurones were carried out: Brown, 1988b), contributed an increasing outward current between -70 and -20 mV, had a half-activation at around -45 mV (also slightly more hyperpolarized than in bullfrog neurones), and showed no time-dependent inactivation. The reversal potential for $I_{K(M)}$ in rat sympathetic ganglion neurones, determined from deactivation currents during hyperpolarizing steps from a potential at which $I_{K(M)}$ was pre-activated, was around -80 mV, and was sensitive to the extracellular K^+ concentration. Furthermore, $I_{K(M)}$ could be inhibited by muscarinic receptor activation, with 10 μM muscarine causing a 90% suppression of the current. Peptide-inhibition of $I_{K(M)}$ was also described, although not with LHRH, which inhibits M-current in bullfrog neurones, but with angiotensin II. With the advent of the patch-clamp technique, the potential to study mechanisms of $I_{K(M)}$ modulation in sympathetic neurones arose. To facilitate patch-clamp studies, it became convenient to dissociate sympathetic ganglion neurones.

3.1.2.2. $I_{K(M)}$ in rat sympathetic neurones (cultured).

Properties of $I_{K(M)}$.

Since the original observations by Constanti and Brown in the intact SCG, $I_{K(M)}$ and inhibition of the current by muscarine has also been demonstrated in dissociated, cultured SCG neurones using both microelectrodes (Marrion *et al.*, 1989) and single

patch electrodes (Marrion *et al.*, 1987; Brown *et al.*, 1989) to study $I_{K(M)}$ under voltage-clamp conditions. In cultured sympathetic neurones, properties of $I_{K(M)}$ resembled those reported in the intact ganglion: the activation threshold for $I_{K(M)}$ was -70 mV, and the reversal potential for $I_{K(M)}$ deactivation currents was around -80 mV (Marrion *et al.*, 1989). The rate of $I_{K(M)}$ deactivation increased as the hyperpolarizing step from -40 mV was increased. When using microelectrodes to record $I_{K(M)}$, Marrion *et al.* (1989) did not report $I_{K(M)}$ "rundown". However, in experiments using the whole-cell recording method, Marrion *et al.* (1987) did remark on the decline in amplitude of $I_{K(M)}$ deactivation relaxations; Brown *et al.* (1989) found that this could be reduced by lowering the pH of the intracellular solution, making it feasible to study the involvement of G proteins and intracellular messengers in mediating $I_{K(M)}$ inhibition.

Characteristics of $I_{K(M)}$ inhibition.

Marrion *et al.* (1989) reported inhibition of $I_{K(M)}$ in response to a number of muscarinic receptor agonists, including muscarine. However, muscarine only produced a maximum inhibition of $I_{K(M)}$ of around 60%, in contrast to the 90% inhibition reported by Constanti and Brown (1981) in intact SCG: in this respect, it is interesting that Constanti and Brown conducted their experiments at 29 °C, while Marrion *et al.* conducted theirs at 20-23 °C. Marrion *et al.* also commented on the very long recovery time (> 20 minutes) required following agonist-inhibition of the current. The muscarinic agonist, oxotremorine methiodide (oxo-M) was used by Bernheim *et al.* (1992) to inhibit $I_{K(M)}$. Oxo-M inhibited $I_{K(M)}$ with an EC_{50} of 300 nM, with 10 μM oxo-M causing a maximum inhibition of 93%. The original observation of Constanti and Brown (1981) that angiotensin II could also inhibit $I_{K(M)}$ in the intact SCG has also been confirmed in rat cultured SCG neurones using whole-cell recording (Shapiro *et al.*, 1994).

3.1.2.3. $I_{K(M)}$ recorded using the perforated patch method.

Selyanko *et al.* (1992) first described $I_{K(M)}$ recorded using the perforated patch recording method. Using this technique, $I_{K(M)}$ appeared to exhibit the expected properties of this current, in terms of reversal potential, sensitivity to extracellular potassium, and inhibition by muscarine. Thus, it might be expected that perforated

patch recording would provide a useful technique for recording $I_{K(M)}$ with minimum disturbance to the cell interior, overcoming problems of "rundown", while at the same time maintaining the characteristic properties of this current to allow comparisons with other studies investigating mechanisms of modulation of $I_{K(M)}$.

3.1.3. Statement of purpose.

Initial attempts to record $I_{K(M)}$ in rat cultured sympathetic neurones using the conventional whole-cell voltage-clamp method revealed that it was difficult to maintain stable recordings using standard potassium acetate- or potassium gluconate-based solutions. Inclusion of ATP and GTP in the intracellular solutions contributed no substantial improvement to the stability of $I_{K(M)}$ recordings. The purpose of the experiments described in this chapter was to determine whether the perforated patch method offered any significant improvement in $I_{K(M)}$ recordings from rat SCG neurones, and to compare the properties of $I_{K(M)}$ recorded using the two methods to ensure that $I_{K(M)}$ recorded with the perforated patch method exhibited similar properties to those previously reported using intracellular and whole-cell recordings.

3.2. RESULTS.

3.2.1. Different characteristics of whole-cell and perforated patch $I_{K(M)}$ deactivation recordings.

3.2.1.1. "Run-down" of $I_{K(M)}$ deactivations.

Figure 1 shows example $I_{K(M)}$ deactivation relaxations recorded using either conventional whole-cell or perforated patch methods. For whole-cell recordings, intracellular solutions based on two different major anions were used: potassium acetate (Figure 1A) or potassium gluconate (Figure 1C). Both solutions were also tested after inclusion of ATP (2 mM) and GTP (0.5 mM) (Figures 1B and 1D respectively). Records shown are those made at the start of the experiment and after 10 minutes of recording. In all whole-cell experiments, the amplitude of $I_{K(M)}$ after 10 minutes of recording is much reduced, as can be seen from the decrease in the standing outward current at the holding potential and the smaller amplitude of the deactivation relaxation during the voltage step. In comparison, during experiments using the pore-forming antibiotics, nystatin or amphotericin B, to achieve the perforated patch configuration (Figure 1E and Figure 1F, respectively) the amplitude of $I_{K(M)}$ at the holding potential and the deactivation relaxation during the voltage step remain relatively constant during the 10 minute recording period. In the records shown in Figure 1 (E and F), there was a slight decline in $I_{K(M)}$ amplitude, which can be seen more clearly from the decrease in outward current at the holding potential than from the deactivation current during the voltage step, where the driving force for K^+ ions is less. Combined data from 3-6 cells, using the two methods, are shown for a 10 minute recording period (Figure 2), illustrating the change in amplitude of the $I_{K(M)}$ deactivation relaxation over this time course. $I_{K(M)}$ deactivation amplitude has been normalized to the amplitude at the start of the experiment. There is a dramatic decrease in $I_{K(M)}$ deactivation amplitude in all experiments utilizing the whole-cell method, with the amplitude of the relaxation being reduced to between 30-40% after 10 minutes. $I_{K(M)}$ deactivations recorded using the perforated patch method show only about a 15% decrease in amplitude over the same time period.

$I_{K(M)}$ is a non-inactivating current; in the present experiments, the decline in amplitude of $I_{K(M)}$ deactivation relaxations did not require continued activation of the current, as this phenomenon was observed when, after obtaining three control $I_{K(M)}$ deactivation records (1s, -30 mV steps from around -25 mV) at the start of the experiment, the membrane potential was set close to the zero current potential for 5 minutes. Three more $I_{K(M)}$ deactivation records were then obtained at time 5 minutes, and then the membrane potential was again set to the zero current potential. After a further 5 minutes, three $I_{K(M)}$ deactivation records were obtained. Using this protocol, the amplitude of the $I_{K(M)}$ deactivation relaxations at time 0, 5 and 10 minutes was 138 $\pm$ 2.5 pA, 93 $\pm$ 10.7 pA and 60 $\pm$ 10.8 pA respectively (n = 4 cells, K acetate + ATP/ GTP-based intracellular solution). This approximates to the 60% loss of $I_{K(M)}$ in whole-cell recordings described in Figure 2. Thus, the rundown of $I_{K(M)}$ cannot be explained by an anomalous process of voltage-dependent inactivation under the present whole-cell $I_{K(M)}$ recording conditions that has not previously been observed. The underlying cause of the loss of $I_{K(M)}$ over time when using the conventional whole-cell recording method has not been investigated further as a part of this thesis.

3.2.1.2. Recovery of $I_{K(M)}$ after agonist-inhibition.

Following inhibition of $I_{K(M)}$ with the muscarinic receptor agonist, oxo-M, deactivation currents recorded using the perforated patch method more closely returned to control amplitude than whole-cell currents after washing out the agonist. Figure 3A shows a recording from one cell made using the conventional whole-cell method with a K acetate (+ ATP/ GTP)-based intracellular solution. The amplitude of $I_{K(M)}$ deactivation relaxations recorded during the first minute of the experiment show evidence of decline. When the cell is superfused with 3 μM oxo-M (a maximally effective concentration: see Chapter 2), there is a decrease in the amplitude of $I_{K(M)}$ deactivations. After washing out the agonist, only a very small component of the inhibited $I_{K(M)}$ was recovered, much less than that expected even accounting for the loss of basal current with this recording method. Figure 3B shows a similar experiment carried out during a perforated patch recording. In this experiment, stable control current measurements were obtained, then application of 3 μM oxo-M produced inhibition of $I_{K(M)}$. When the agonist was washed out, there was an almost complete

recovery of the $I_{K(M)}$ deactivation relaxations within approximately 60 s. A summary of the recovery of agonist-inhibited current using the two methods is shown in Figure 4. Recovery is defined as the amount of inhibited deactivation relaxation that is recovered after washing out the agonist, that is $(I_{wash} - I_{agonist}) / (I_{control} - I_{agonist})$, expressed as percent. Recovery of $I_{K(M)}$ in perforated patch recordings following exposure to either a submaximally (300 nM) or maximally effective (3 μM) concentration of oxo-M was around 70% in each case; in conventional whole-cell recordings, recovery from either concentration of agonist was around 30%.

3.2.2. Similar characteristics of whole-cell and perforated patch $I_{K(M)}$ deactivation recordings.

3.2.2.1. $I_{K(M)}$ deactivation amplitude and time constant.

The kinetics of $I_{K(M)}$ deactivations during the voltage step were not different between whole-cell and perforated patch methods. $I_{K(M)}$ deactivation relaxations recorded using the voltage protocol outlined in Chapter 2 (1s, -30 mV steps from around -25 mV) were best-fit with a two exponential function, and measurements of the fast and slow time constants (τ) recorded using each intracellular solution are given in Table 1. There was no significant difference in the time constants of either fast or slow components of $I_{K(M)}$ deactivations, or the contribution of each component to the total deactivation current, recorded using whole-cell or perforated patch methods. Also shown in Table 1 are measurements of initial and end-of experiment $I_{K(M)}$ deactivation amplitudes. The amplitude of $I_{K(M)}$ deactivation relaxations at the start of recordings when using a K acetate-based intracellular solution was significantly different to the amplitude of relaxations recorded using perforated patch ($p < 0.05$), which may reflect a very rapid decline of $I_{K(M)}$ amplitude when using the K acetate solution. The amplitudes of $I_{K(M)}$ deactivation relaxations recorded with the other intracellular solutions were not significantly different to perforated patch recordings. Zero current potentials (determined at the end of the experiment with each recording solution) are also shown in Table 1. There is a significant difference in the values recorded with K acetate + ATP/ GTP and K gluconate and ATP/ GTP ($p < 0.05$) but no difference between perforated patch and whole-cell recordings, indicating that the waning of $I_{K(M)}$

deactivation amplitude was probably not due to a decline in the health of the cells when using the whole-cell recording method.

3.2.2.2. Voltage- and $[K^+]_{ec}$-dependence of $I_{K(M)}$.

Virtually identical steady-state current-voltage relationships were obtained from whole-cell and perforated patch recordings. Figure 5 shows a steady-state current-voltage relationship recorded using the whole-cell method (K acetate + ATP/ GTP intracellular solution). A family of currents generated by 1 s, incremental -10 mV steps from -10 mV to -93 mV (V_H -18 mV) were recorded in normal extracellular solution containing 3 mM KCl, after superfusing the cell with extracellular solution containing 15 mM KCl (Figure 5A) and then again after reverting to 3 mM KCl extracellular solution. The current at the end of the 1s voltage step was plotted against membrane potential (Figure 5B). The estimated null potential for steady-state current in 3 mM external K^+ (determined from three whole-cell recordings) was -59 ± 2.1 mV (n =3); for $I_{K(M)}$ deactivation relaxations, the reversal potential was -74 ± 2.3 mV (n = 3). In 15 mM K^+, the estimated null potential for steady-state current was -46 ± 2.7 mV (n = 3); for $I_{K(M)}$ deactivation relaxations, the reversal potential was -51 ± 2.1 (n = 3). Therefore the shift on changing from 3 mM to 15 mM extracellular K^+ was approximately 13 mV for steady-state current and 23 mV for $I_{K(M)}$ deactivation relaxations. Figure 6 shows the result of a similar experiment, but recorded using the perforated patch (amphotericin B) method. Current traces were generated from 1 s, incremental -10 mV steps from -11 mV to -91 mV (V_H -18 mV) in 3 mM, 15 mM and then 3 mM extracellular KCl. The estimated null potential in 3 mM K^+ for steady-state current was -61 ± 4.2 mV (n = 3) and the reversal potential for $I_{K(M)}$ deactivation relaxations was -76 ± 3.3 mV (n = 3); in 15 mM K^+, the null potential for steady-state current shifted (by approximately 14 mV) to -47 ± 1.5 mV, and for $I_{K(M)}$ deactivation relaxations (by approximately 28 mV) to -48 ± 3.6 mV (n = 3), which are similar to the shifts seen in the whole-cell recordings.

3.2.2.3. Agonist-inhibition of $I_{K(M)}$.

The effect of the muscarinic agonist, oxo-M, was almost identical when using the two recording methods. Because of the poor recovery of inhibited $I_{K(M)}$ when using the whole-cell method (Figures 3 and 4), it was not possible to obtain a full concentration-response curve with this recording configuration. Therefore, inhibition of $I_{K(M)}$ in response to single applications of two concentrations of oxo-M (300 nM and 3 μM) was measured. This data is summarized in Figure 7. The responses to each concentration are identical when using either recording method, indicating that there is no shift in the concentration-response curve when using the perforated patch method.

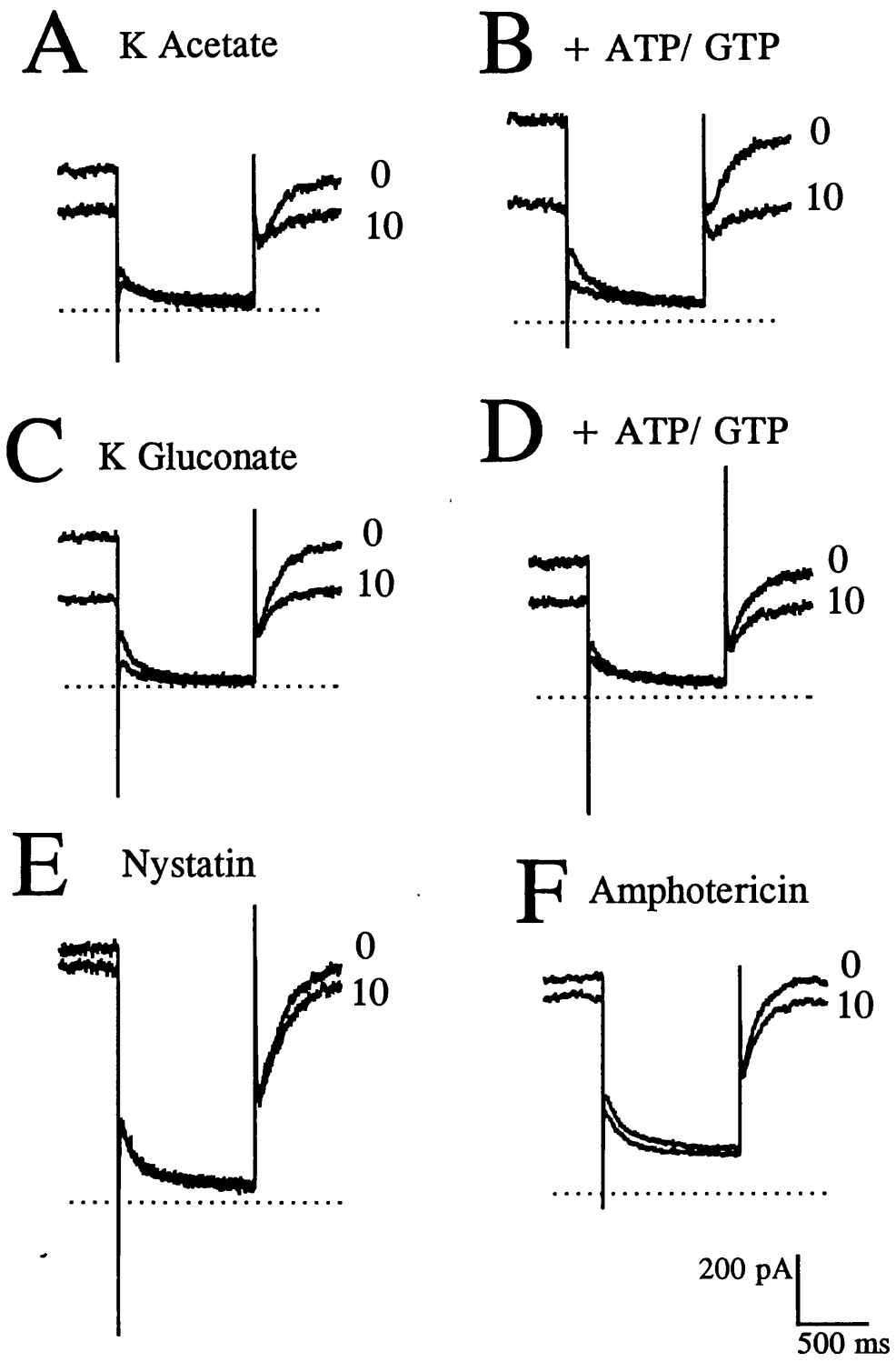

Figure 1. $I_{K(M)}$ deactivation relaxations recorded using different intracellular solutions. Example $I_{K(M)}$ deactivation records (-30 mV step, as described in Chapter 2, from V_H, in parentheses) made at the start of the experiment (0) and then after 10 minutes of recording (10) using different intracellular solutions: A. K acetate-based solution (V_H -25 mV), B. K acetate solution with ATP and GTP (V_H -20 mV), C. K gluconate based solution (V_H -20 mV), D. K gluconate solution with ATP and GTP (V_H -21 mV), and for perforated patch E. nystatin solution (V_H -31 mV) and F. amphotericin solution (V_H -21 mV). The dotted lines indicate the zero current level, and the scale bar applies to all records.

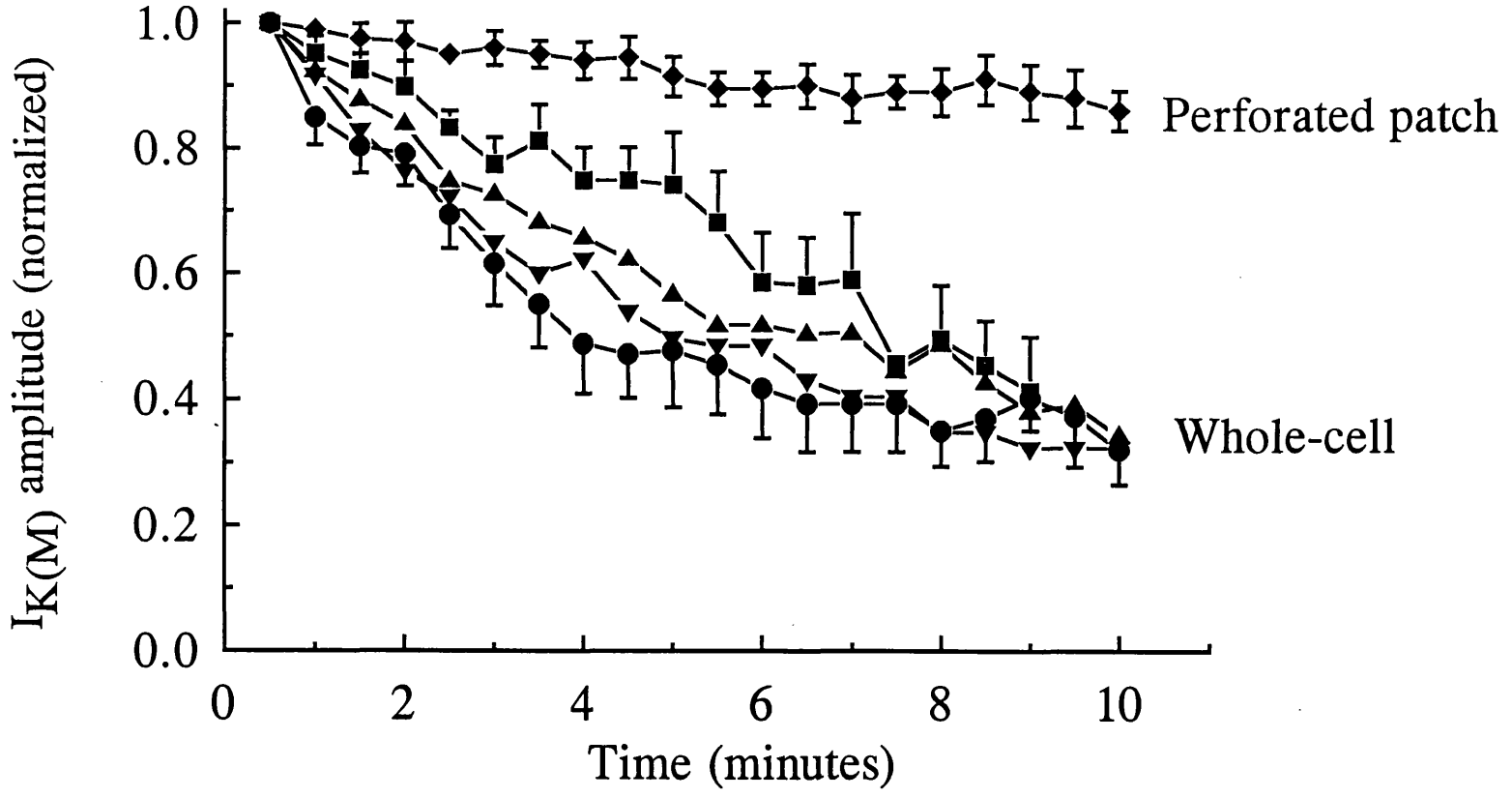

Figure 2. Stability of $I_{K(M)}$ recordings over time using whole-cell or perforated patch recording methods.
Graph showing amplitude of $I_{K(M)}$ deactivation relaxations (measured as described in Chapter 2, and normalized to the amplitude at the start of the experiment, data points represent mean ± SEM) over a 10 minute recording period using different intracellular solutions: perforated patch (nystatin or amphotericin, diamond, n = 6) or whole-cell using K acetate solution (circle, n = 3-6), K acetate plus ATP/ GTP (square, n = 3-4), K gluconate solution (downward triangle, n = 3-4) and K gluconate plus ATP/ GTP (upward triangle, n = 3-4). Some overlapping error bars have been removed for clarity.

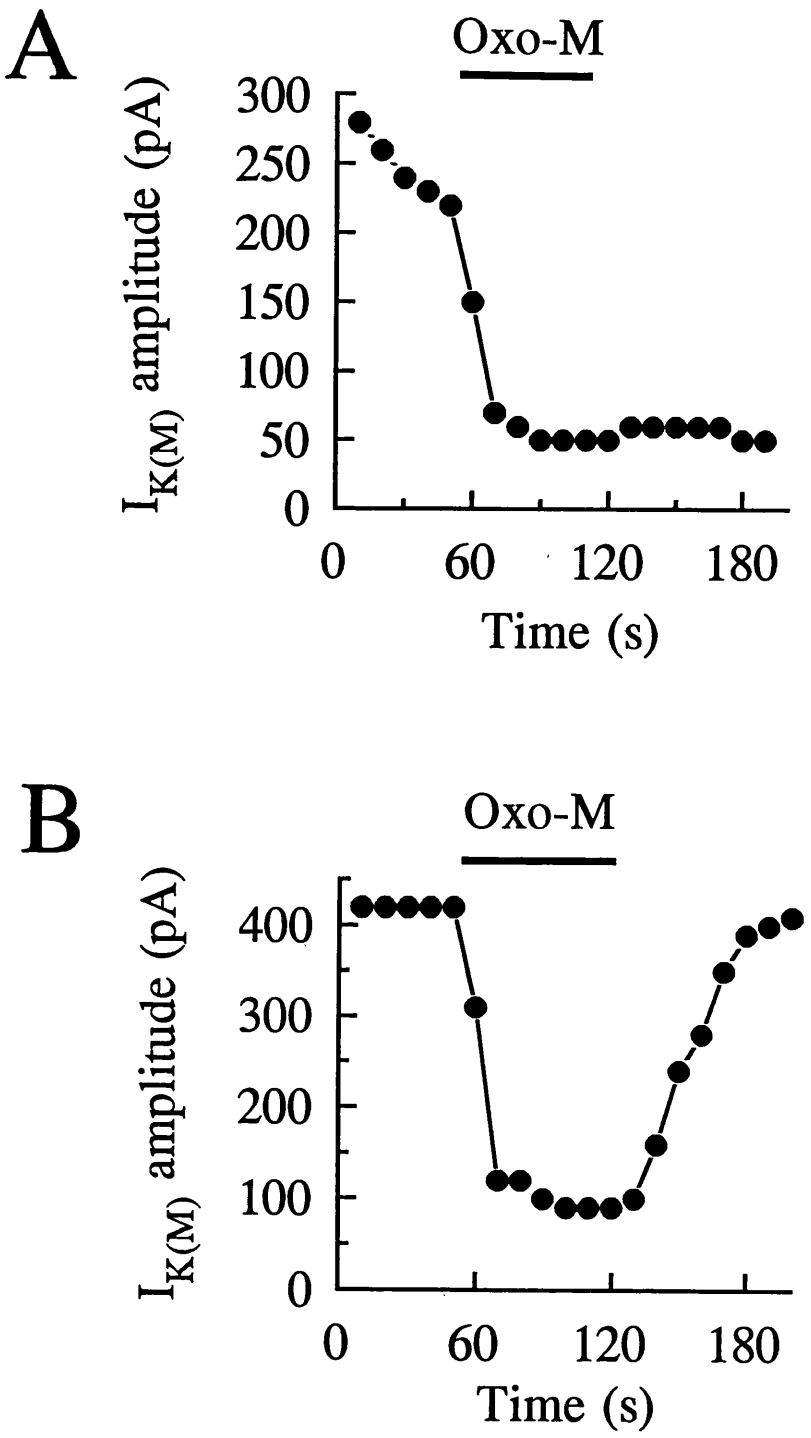

Figure 3. Recovery of oxotremorine-M-inhibited $I_{K(M)}$ using whole-cell or perforated patch methods. A. Graph of $I_{K(M)}$ deactivation relaxation amplitude (pA) against time (s) recorded using the whole-cell method with K acetate (+ ATP/ GTP)-based intracellular solution. $I_{K(M)}$ deactivations were measured every 10 s (1 s, -30 mV step from V_H -24 mV). The cell was superfused with 3μM oxo-M as indicated by the bar (78% inhibition, 5% recovery). B. A similar graph from a recording made using the perforated patch method (same culture as the cell in A). Amplitude of $I_{K(M)}$ deactivation relaxations were measured every 10 s (1 s, -30 mV step from V_H -26 mV). Superfusion with 3 μM oxo-M (bar) caused a 79% inhibition, and the recovery from inhibition was 97%. Inhibition and recovery from inhibition of $I_{K(M)}$ were measured as described in Chapter 2.

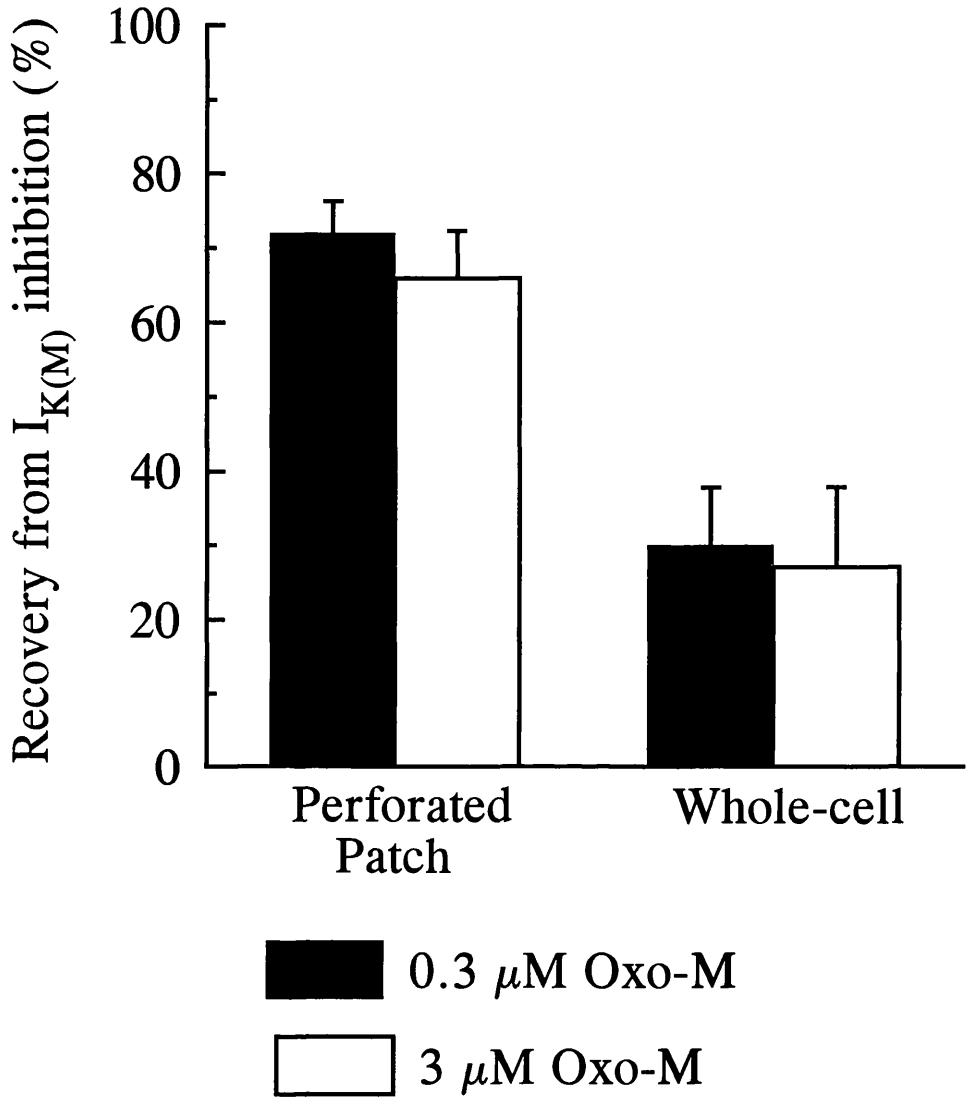

Figure 4. Bar graph showing recovery (%, mean ± SEM, measured as described in Chapter 2) of $I_{K(M)}$ deactivation relaxations inhibited by 300 nM (solid bars) or 3 μM (open bars) oxo-M when using perforated patch (nystatin; n = 17 and 9 respectively) or whole-cell (K acetate + ATP/ GTP; n = 7 and 6 respectively) recording methods.

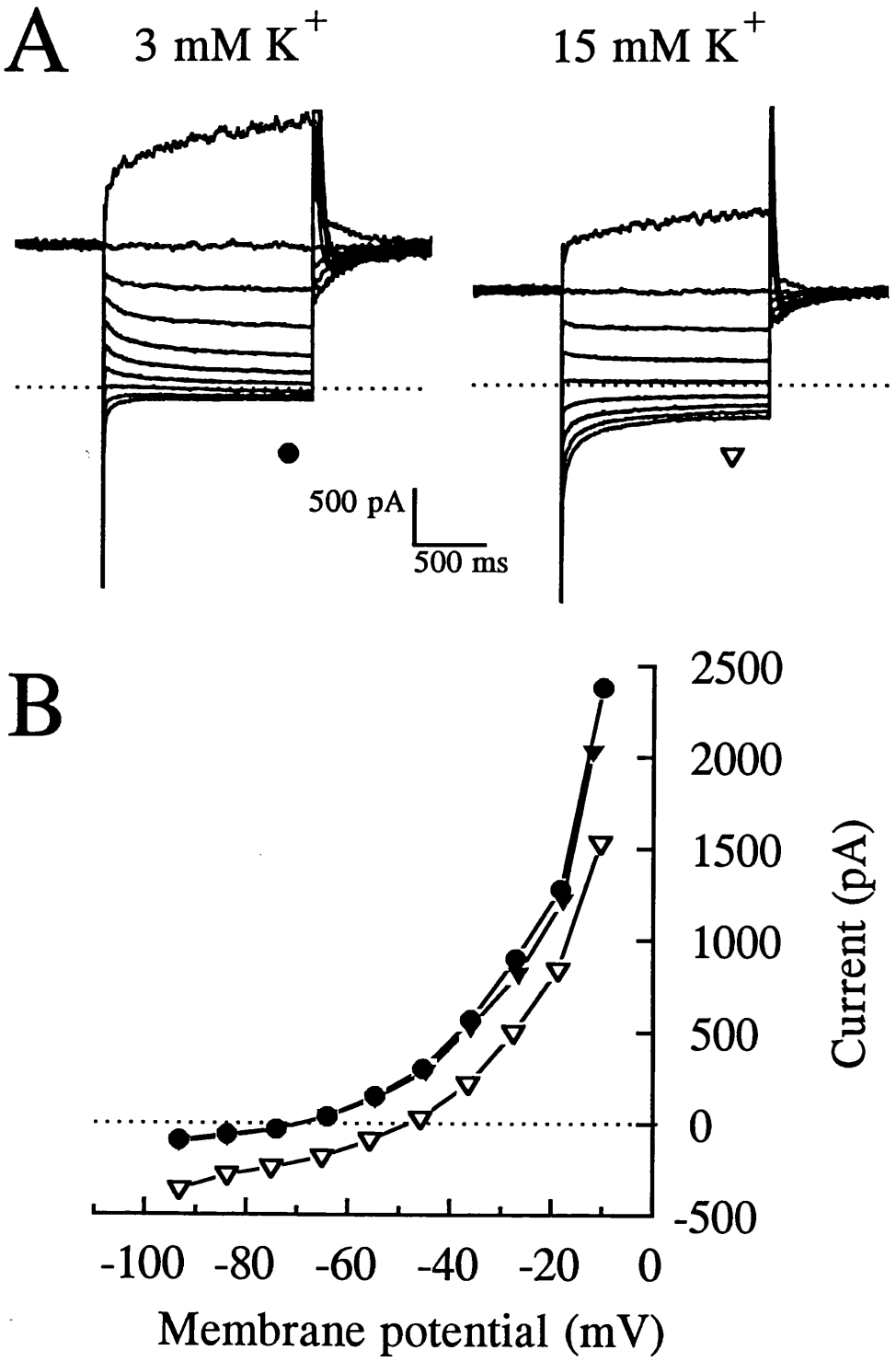

Figure 5. Steady-state current-voltage relationship (whole-cell recording).
A. Current records obtained from one cell during 1 s, incremental -10 mV steps from -10 mV to -93 mV every 15 s (V_H -18 mV) with 3 mM or 15 mM extracellular KCl. The dotted lines represent the zero current level, and the scale bar applies to both sets of records. In the records made in 3 mM KCl, the positive-going capacity transients are off of the current scale. B. Graph of steady-state current (pA) against membrane potential (mV) measured from the records in A in the presence of extracellular KCl concentrations of 3 mM (filled circles), 15 mM (open triangles), then back to 3 mM (filled triangles).

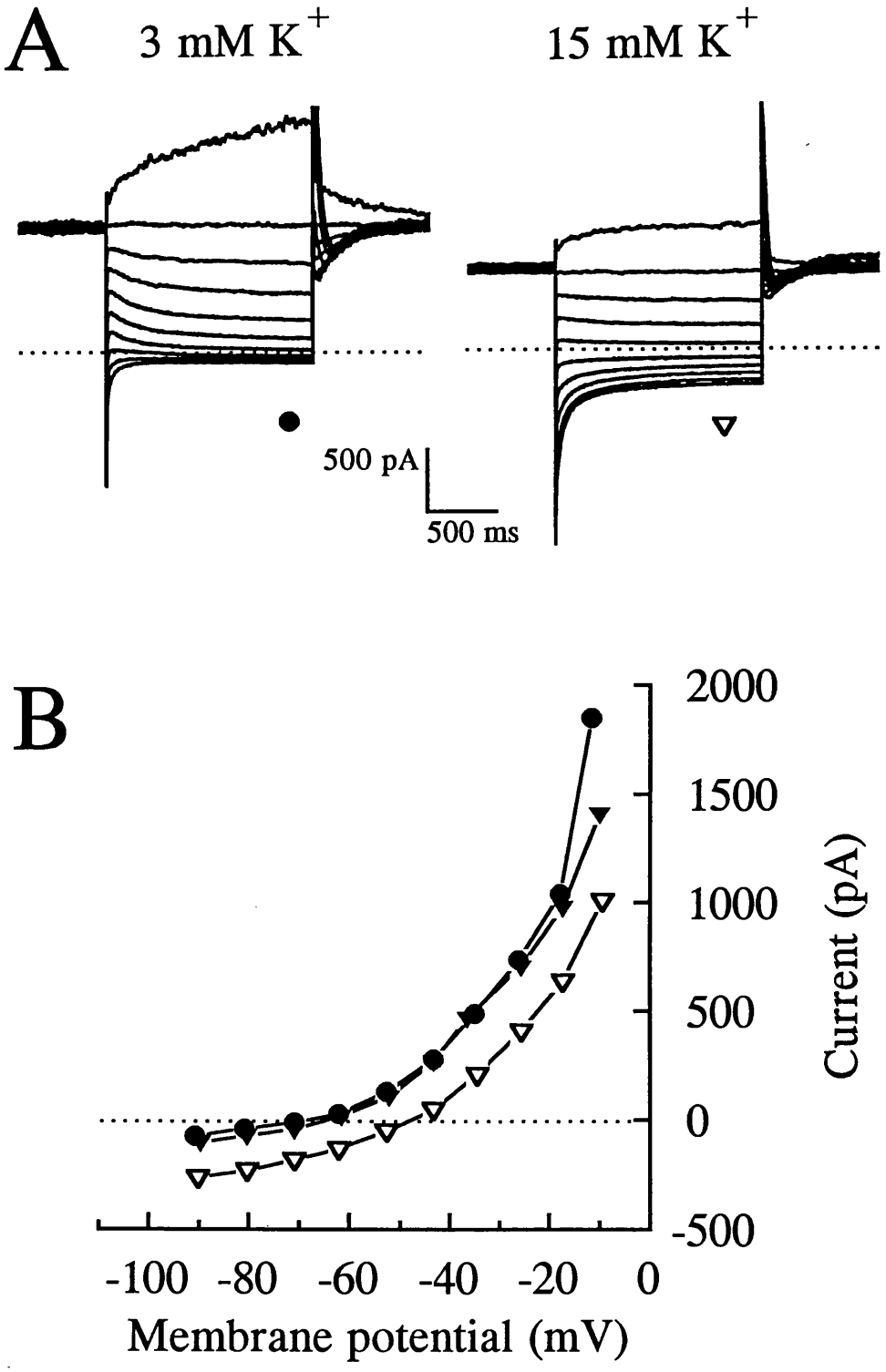

Figure 6. Steady-state current-voltage relationship (perforated patch recording: amphotericin). A. Current records obtained from one cell using an identical voltage protocol to the whole-cell recording in figure 5, but from -11 to -91 mV (V_H -18 mV). Recordings were made using 3 mM and 15 mM extracellular KCl. The dotted line indicates the zero current level, and the scale bar applies to both sets of traces. In the records made in 3 mM KCl, the positive-going capacity transients are off of the current scale. B. Graph of steady-state current (pA) against membrane potential (mV) measured from the records in A in the presence of 3 mM (filled circles), 15 mM (open triangles) and then 3 mM (filled triangles) extracellular KCl.

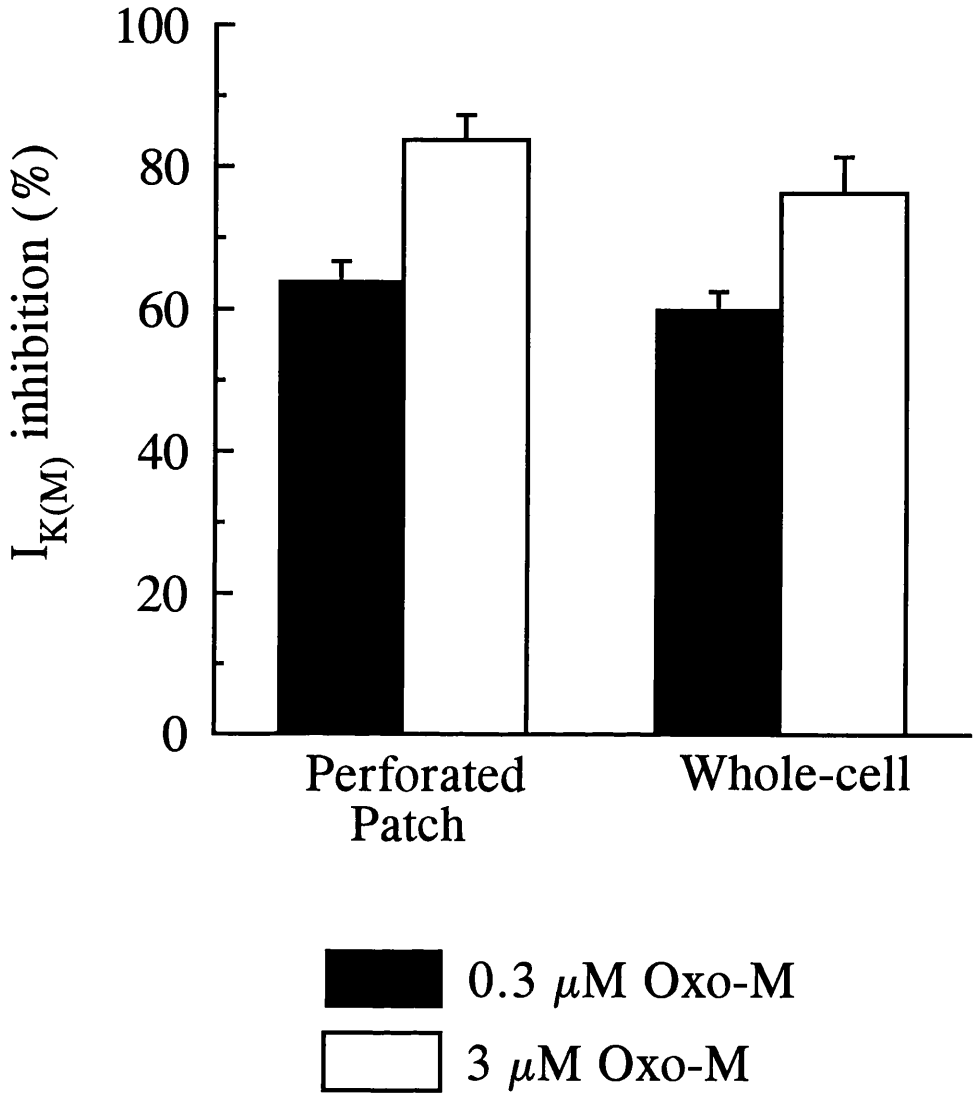

Figure 7. Bar graph showing inhibition of $I_{K(M)}$ deactivation relaxations (%, mean ± SEM, measured as described in Chapter 2) in response to perfusion with 300 nM (solid bar) or 3 μM (open bar) oxo-M when using either perforated patch (nystatin; n = 17 and 9 respectively) or whole-cell (K acetate + ATP/ GTP; n = 7 and 6 respectively) recording methods. Data are from the same cells as the data in figure 4.

Table 1: Properties of $I_{K(M)}$ deactivation relaxations recorded using either whole-cell or perforated patch methods.

Intracellular solution	Deactivation $\tau_{(fast)}$ (ms)	% of total amplitude	Deactivation $\tau_{(slow)}$ (ms)	n	Deactivation amplitude (pA; initial)	Deactivation amplitude (pA; end).	n	Zero current potential (mV; #)	n
Perforated patch	77 ± 4	54 ± 4.2	426 ± 47	6	173 ± 18	147 ± 11	6	-61 ± 3	5
K acetate-based	63 ± 10	39 ± 4.1	408 ± 107	5	103 ± 7*a	33 ± 5	6/ 3	-61 ± 1.5	4
K acetate + ATP/GTP	78 ± 22	48 ± 12.7	566 ± 204	4	160 ± 15	60 ± 8	6/ 3	-54 ± 3.5	4
K gluconate-based	45 ± 15	31 ± 11.9	272 ± 82	3	120 ± 5	40 ± 8	4/ 3	-50, -58	2
K gluconate + ATP/GTP	50 ± 6	43 ± 11.3	414 ± 137	5	120 ± 22	50 ± 13	4/ 3	-70 ± 2*b	3

#: zero current potential recorded at the end of the experiment.

* $p < 0.05$: a, compared with perforated patch; b, compared with K Acetate + ATP/ GTP.

3.3. DISCUSSION.

The purpose of the experiments outlined in this chapter was to determine whether the perforated patch recording method would offer significant improvement for recording $I_{K(M)}$ in cultured sympathetic neurones from the rat SCG compared with the conventional whole-cell method. The experiments were designed to ascertain whether certain disadvantageous features encountered with whole-cell recording could be avoided with the perforated patch technique, and to ensure that the properties of $I_{K(M)}$, and its modulation by agonists, were not altered by the different recording method.

3.3.1. Properties of $I_{K(M)}$ recorded using the perforated patch method.

3.3.1.1. "Run-down" of $I_{K(M)}$.

Initial experiments using the whole-cell voltage-clamp method to record $I_{K(M)}$ from cultured SCG neurones, using a K acetate-based solution similar to that used to record stable $I_{K(M)}$ deactivations in NG108-15 cells (Robbins *et al.*, 1992), revealed a severe and rapid decline in the amplitude of $I_{K(M)}$ deactivation relaxations in SCG neurones. $I_{K(M)}$ "run-down" was surprising in view of the fact that $I_{K(M)}$ is a non-inactivating K^+ current in rat sympathetic ganglia (Constanti and Brown, 1981), and therefore should remain at a constant amplitude once activated. However, this phenomenon has previously been described during whole-cell recordings from cultured SCG neurones (Marrion *et al.*, 1987); moreover, it is not unique to $I_{K(M)}$, and has been described for current through both voltage- and ligand-gated channels (see Horn and Korn, 1992; Kay, 1992 for reviews).

"Run-down" of other ionic conductances has often been overcome by including ATP and GTP in the intracellular solution (reviewed by Horn and Korn, 1992, Kay, 1992), indicating that phosphorylation reactions are required to maintain channel integrity. In the present experiments, inclusion of ATP and GTP in the pipette solution did not prevent the decline in amplitude of $I_{K(M)}$ deactivation records over a 10 minute

recording period. This suggests that the "run-down" of $I_{K(M)}$ under these recording conditions is not due to the loss of an ATP/ GTP-dependent process, such as phosphorylation. Changing the major anion of the intracellular solution is another strategy for improving the stability of recordings for some conductances (Kay, 1992). In this study, when the intracellular solution used to record whole-cell $I_{K(M)}$ was changed to a K gluconate-based solution, there was no relief from the dramatic loss of $I_{K(M)}$ deactivation amplitude. This suggests that the "run-down" of $I_{K(M)}$ was not dependent on the intracellular anion used in the patch pipette, and so the possible benefits of other anions were not investigated although a comprehensive test may have revealed one or more which offered some improvement. The possibility that voltage-clamping the cell to a potential where $I_{K(M)}$ was permanently activated may cause "run-down" was also considered, although this would be inconsistent with the previously reported characteristic property of no inactivation of $I_{K(M)}$ (Constanti and Brown, 1981). During experiments in which the membrane potential was voltage-clamped to the zero current potential, and $I_{K(M)}$ only activated every 5 minutes, there was no benefit to the stability of the $I_{K(M)}$ deactivation recordings. This could have been investigated in further detail, for example by measuring the loss of $I_{K(M)}$ using a range of different holding potentials and voltage protocols. However, the impression from the experiments performed was that $I_{K(M)}$ "run-down" did not depend on the membrane potential and therefore does not appear to be associated with the activation of the current.

A question that was not addressed in this study was whether changing the concentration of free Ca^{2+} in the (whole-cell) pipette solution would affect the stability of $I_{K(M)}$ recordings. In the present experiments, the free Ca^{2+} concentration was buffered to zero (see Chapter 2). As previous whole-cell recordings of $I_{K(M)}$ from rat sympathetic neurones, in which the free Ca^{2+} was buffered to 135 nM, still exhibited rundown (Brown *et al.*, 1989), it was considered unlikely that this was the source of the problem. Furthermore, although a critical level of Ca^{2+} was found to be necessary for $I_{K(M)}$ inhibition in rat sympathetic neurones, there was no indication of $I_{K(M)}$ rundown when intracellular Ca^{2+} was tightly buffered (Beech *et al.*, 1991)

3.3.1.2. Overcoming "rundown" with perforated patch recording.

Changing the recording configuration from conventional whole-cell to perforated patch considerably improved to the stability of $I_{K(M)}$ recordings. By using either nystatin (Horn and Marty, 1988) or amphotericin B (Rae *et al.*, 1991) to permeabilize the cell-attached patch configuration and allow whole-cell currents to be recorded *via* the perforated patch, it became possible to record $I_{K(M)}$ deactivations which exhibited no, or very minor decreases in amplitude over long recording periods (sometimes up to 60-90 minutes). The perforated patch recording method was considered to offer greater advantages than alternative methods for minimizing "run-down". For example, compared with using patch pipettes with reduced tip diameter, perforated patch has the benefit of minimal disturbance of the cell interior caused by forming the whole-cell configuration. Additionally, even small decreases in pipette diameter (for example, from 4 to 7 MΩ tip resistance) caused more frequent blocking of the electrode tip during whole-cell experiments (as indicated by changes in access resistance); this problem was encountered very rarely with perforated patch experiments. Changing the pH of the intracellular solution was the approach of Brown *et al.* (1989), and this was effective in *reducing* the "run-down" of $I_{K(M)}$, but not in preventing it. Changing the pH, and other components of the intracellular solution may have yielded a more ideal internal recording medium, however, the appeal of causing minimal disruption to the cell interior made perforated patch recording a favourable option.

In summary, the perforated patch method first described by Horn and Marty (1988) can be used to record $I_{K(M)}$ deactivation relaxations from rat cultured sympathetic neurones which remain stable in amplitude. This contrasts with whole-cell recordings of $I_{K(M)}$ deactivations in these cells under the same conditions, which "rundown" severely over a 10 minute recording period. The process underlying this current "rundown" has not been investigated, and may involve either diffusion of a factor that is essential for channel integrity into the patch pipette, or diffusion of a component of the intracellular solutions that is/ are detrimental to M-channels into the cell. Unpublished observations of Dr. M. P. Caulfield indicate that the Ca^{2+}-sensitive dye, indo-1, can diffuse into SCG cells, from patch pipettes with access resistances less

than 10 MΩ, with a time constant of 11.9 ± 1.9 minutes

(n = 6 cells). Thus, simple diffusion of a critical factor out of, or into the cell could account for a substantial component of $I_{K(M)}$ rundown in a 10 minute period. Interestingly, anomalous M-channel behaviour has been reported in excised patches from rat sympathetic neurones, with the appearance of faster activation/ deactivation kinetics and a slow, partial inactivation, and these phenomena may be due to the loss or disturbance of a regulatory GTP-binding moiety (Stansfeld *et al.*, 1993). Whether these observations at the single channel level might explain the present observations remains to be determined; however, one difference is that the M-channel inactivation phenomenon was voltage-dependent, increasing with depolarization, whereas whole-cell $I_{K(M)}$ "rundown" was not attenuated by voltage-clamping cells to more hyperpolarized potentials in this study.

3.3.1.3. Amplitude, time constants and voltage- and potassium-dependence of $I_{K(M)}$ deactivations.

Clearly, $I_{K(M)}$ deactivation relaxations recorded using the perforated patch method showed greater stability, with "run-down" virtually absent. Other properties of $I_{K(M)}$ which were measured in this study using the perforated patch method showed no obvious difference to those observed during whole-cell recordings. In the present experiments, the initial amplitudes of $I_{K(M)}$ deactivation currents (at around -55 mV) were not different when using either recording method, other than when using the K acetate-based intracellular solution in the whole-cell configuration, which suggests that, with this solution, there may be a more rapid decline in $I_{K(M)}$ amplitude than with the other whole-cell solutions. This indicates that the perforated patch recording technique has not unmasked an additional component of $I_{K(M)}$ or other voltage-dependent current that can be detected under these conditions. When the deactivation relaxations were fitted with a two exponential function, mean fast and slow time constants of around 45 to 78 ms and 270 to 560 ms respectively were measured, with no significant differences between the different recording methods. These time constants for $I_{K(M)}$ deactivation (at around -55 mV) are similar to those previously reported for a fit of a two exponential function to whole-cell $I_{K(M)}$ deactivations at -50 mV in rat cultured SCG neurones (Stansfeld *et al.*, 1993: see Chapter 2). This, taken in conjunction with the present experiments, suggests that the slightly higher access resistance has not

compromised the detection of the rate of $I_{K(M)}$ deactivation. Furthermore, the voltage range over which $I_{K(M)}$ was activated was qualitatively identical (between -70 and -20 mV) when using either recording method, and $I_{K(M)}$ deactivation relaxations exhibited the phenomenon of increased rate of deactivation with hyperpolarization previously described in rat SCG neurones by Constanti and Brown (1981), as determined by eye from the current records obtained during 1 s, incremental -10 mV steps. Because of the voltage-sensitivity of the deactivation relaxation time course, any change in the time constant would provide an indication of a shift in the activation range for $I_{K(M)}$ (Adams *et al.*, 1982b); the similar time constant values for whole-cell and perforated patch recordings further support a similar $I_{K(M)}$ activation range being detected with each recording method.

Changing the extracellular K^+ concentration had an almost identical effect on whole-cell and perforated patch $I_{K(M)}$ deactivation recordings. In 3 mM $[K^+]_{ec}$, deactivation currents reversed in polarity at around -74 mV in whole-cell recordings and -76 mV in perforated patch recordings. When the liquid junction potential is taken into account for whole-cell recordings (see Chapter 2), this would give a reversal potential of -80 mV, which is 10-15 mV more positive than the equilibrium potential for potassium ions (E_K) of -94 mV (calculated from the Nernst equation; Chapter 2). In frog sympathetic neurones, the reversal potential for M-current was also around 10 mV more positive than E_K (Jones, 1989). The liquid junction potential across a perforated patch is not known, but may very close to the liquid junction potential in whole-cell mode, as the measured reversal potentials for $I_{K(M)}$ deactivation relaxations are similar with both methods. On changing to 15 mM $[K^+]_{ec}$, the reversal potential for $I_{K(M)}$ deactivation relaxations was very close to the calculated E_K of -53 mV in both whole-cell (-51 mV) and perforated patch (-48 mV) recordings. The deviation from the predicted Nernst equilibrium potential at lower $[K^+]_{ec}$ could be explained by a very low permeability of the M-channel to Na^+ ions (P_{Na}/ P_K of 0.02, calculated from a simplified form of the Goldman-Hodgkin-Katz equation: $E_{REV.} = 58.\log_{10} (([K^+]_{ec} + P_{Na}/ P_K.[Na^+]_{ec})/ ([K^+]_{ic}))$ at 20 °C). Na^+ permeability of 2% would give a reversal potential of -75 mV in 3 mM extracellular K^+ and -48 mV in 15 mM extracellular K^+. This would account for the smaller shift in reversal potential than predicted from the

Nernst equation (41 mV) with this increase in $[K^+]_{ec}$. The important finding for the present study is that the sensitivity of the reversal potential for $I_{K(M)}$ to $[K^+]_{ec}$ was the same when using either whole-cell or perforated patch methods.

The zero current potential was also sensitive to extracellular K^+ ions in both whole-cell and perforated patch recordings. In Krebs' solution containing the usual 3 mM $[K^+]_{ec}$, steady-state membrane current was zero at around -60 mV, which tends towards the estimated equilibrium potential for K^+ ions of -94 mV, suggesting that K^+ conductances may contribute partially but not solely to the zero current potential in rat cultured SCG cells. On increasing the concentration of extracellular potassium to 15 mM, the zero current potential shifted during both methods of recording by around 15 mV (and therefore was not dependent on the recording method used), which is not as great as the shift predicted by the Nernst equation (41 mV) if the zero current potential was only determined by K^+ ions. Additionally, there was no significant difference between end-of-experiment zero current potentials during recordings made using whole-cell or perforated patch methods (although there was a difference between the K acetate and the K gluconate solutions containing ATP/ GTP: the reason for this is not known). This indicates that $I_{K(M)}$ may not contribute significantly to the "resting" potential ($I_{K(M)}$ runs down in whole-cell, but not perforated patch recordings), which is not entirely surprising, as in isolated frog sympathetic neurones, a K^+ current with little voltage-dependence and an electrogenic Na^+/ K^+ ATPase pump contribute to the resting potential (Jones, 1989). In NG108-15 cells, $I_{K(M)}$ also appears not to contribute to the zero current potential in whole-cell recording conditions (Robbins *et al.*, 1992).

3.3.2. Properties of $I_{K(M)}$ modulation.

An interesting observation during the whole-cell recordings was that although cells responded to agonists, with oxo-M producing a substantial inhibition of $I_{K(M)}$, the recovery of inhibited $I_{K(M)}$ was very poor, and often non-existent, even during prolonged washing (>20 minutes). Moreover, this was observed at the two concentrations of oxo-M assayed using this recording configuration (submaximally effective (300 nM) and maximally effective (3 μM) concentrations). Therefore, lack of

recovery was evidently not related to the concentration of agonist and the extent to which $I_{K(M)}$ was inhibited. Because of the poor recoveries from inhibition, it was not possible to determine whether the cells would respond to a second application of agonist in the whole-cell recording mode. However, it is clear that within a relatively short time (see Figure 3: <3 minutes), the cell interior is adjusted in such a way that although the cell is capable of responding to the agonist, it is not capable of recovering from this effect.

This failure to recover from agonist effects was not observed in perforated patch recordings, during which cells exhibited responses to oxo-M that were not different in magnitude to responses to two concentrations of oxo-M in whole-cell recordings (indicating that there was no shift in the concentration-response relationship), but which showed rapid and often complete recovery of the inhibited $I_{K(M)}$. This raises the intriguing possibility that, during whole-cell recording, the diffusible messengers required to transduce muscarinic receptor-mediated inhibition of $I_{K(M)}$ (Selyanko *et al.*, 1992) remain intact, whereas an element of the cellular machinery required for recovery of inhibited $I_{K(M)}$ is either lost by diffusion into the patch pipette, or damaged by the diffusion of a component of the pipette solution into the cell. This implies that the process of $I_{K(M)}$ recovery also involves a mechanism, which perhaps inactivates the transduction mechanism for $I_{K(M)}$ inhibition and restores the channel to the conductive state, and which is sensitive to the intracellular environment. Because use of the perforated patch method circumvented the problems encountered, the possible underlying reasons for the lack of recovery of whole-cell $I_{K(M)}$ from inhibition were not investigated.

In summary, the perforated patch method appears to be a useful technique for studying $I_{K(M)}$ inhibition by agonists in rat cultured SCG neurones. The inhibition observed in response to the muscarinic receptor agonist, oxo-M was identical when using either whole-cell or perforated patch methods, and also corresponds well with the inhibitory effect of this agonist on $I_{K(M)}$ previously reported in these cells (Bernheim *et al.*, 1992). However, the poorly reversible effect of the agonist which was encountered in whole-cell recordings in the present experiments was not observed

during perforated patch recordings, which made it feasible to make repeated applications of the same or different concentrations of agonists to the same cell (these experiments are described in subsequent chapters).

3.3.3. Conclusions to Chapter 3.

In this chapter it has been demonstrated that, under the present recording conditions, $I_{K(M)}$ recorded using the conventional whole-cell method shows a marked decline in amplitude over a short recording period, as determined from the amplitude of $I_{K(M)}$ deactivation relaxations. This phenomenon of "rundown" could not be prevented by supplementing the intracellular solution with ATP and GTP. However, it could be circumvented by using pipettes containing either nystatin or amphotericin B in order to achieve the perforated patch recording configuration. In whole-cell recordings, it was possible to obtain at least one response to oxo-M, which caused an inhibition of $I_{K(M)}$ similar to the inhibition observed using the perforated patch recording method. However, in contrast to perforated patch recordings, recovery of the agonist-inhibited $I_{K(M)}$ during whole recordings was very poor, and often absent. Based on these observations, it was concluded that the perforated patch recording method offered significant advantages to the whole-cell method for experiments to study the G proteins transducing inhibition of $I_{K(M)}$ by agonists in rat cultured sympathetic neurones, and this method was therefore adopted for all subsequent experiments.

CHAPTER 4:

The involvement of $G_{\alpha q/11}$ proteins in muscarinic receptor-mediated inhibition of $I_{K(M)}$.

4.1. INTRODUCTION.

In Chapter 1, modulation of the M-type K^+ current ($I_{K(M)}$) by receptors which couple to GTP-binding proteins (G proteins) was described. Thus, in rat sympathetic neurones, M_1 muscarinic acetylcholine receptors couple to a pertussis toxin-insensitive G protein to inhibit $I_{K(M)}$, *via* activation of a diffusible (but unknown) messenger. The experiments described in this chapter were concerned with a specific molecular step in the inhibition of $I_{K(M)}$ by M_1 muscarinic receptors: namely, identification of the G protein(s) that transduce this response in cultured sympathetic neurones from the rat SCG.

4.1.1. Statement of purpose.

The experiments described in this chapter were designed to try and identify the G protein(s) transducing muscarinic receptor mediated $I_{K(M)}$ inhibition in rat sympathetic neurones, by using specific anti-G protein antibodies and antisense DNA. Using the perforated patch recording method, oxotremorine-M (oxo-M) was used as a muscarinic receptor agonist to inhibit $I_{K(M)}$, as this agonist causes reversible and reproducible $I_{K(M)}$ inhibition (Chapter 3) and has no apparent effect at nicotinic receptors at the concentrations used in this study. Although oxo-M has been reported to act as an agonist (at nanomolar concentrations) at *Xenopus* skeletal muscle nicotinic receptors (Reitstetter *et al.*, 1994), concentrations of oxo-M exceeding 10 μM are required to activate nicotinic receptors in coeliac ganglion neurones (Xian *et al.*, 1994). Some of the characteristics of the oxo-M mediated inhibition of $I_{K(M)}$ are also described in this chapter.

4.2. RESULTS.

4.2.1. Properties of muscarinic receptor-mediated inhibition of $I_{K(M)}$.

4.2.1.1. Concentration-dependent inhibition of $I_{K(M)}$ by oxo-M.

The muscarinic receptor agonist, oxotremorine methiodide (oxo-M) caused a concentration-dependent inhibition of $I_{K(M)}$. Figure 8 shows the effect of six different concentrations of oxo-M (30 nM to 10 μM) on $I_{K(M)}$ deactivation relaxations when applied to the same cell using a non-cumulative, random application protocol. Near-complete recovery from inhibition of $I_{K(M)}$ was generally achieved after washing out the agonist for 5 to 10 minutes. The concentration-effect curve for this cell is shown in Figure 9. Individual fits of the logarithmic form of the logistic equation (Chapter 2 and Figure 9, legend) were made to full concentration response curves (using oxo-M concentrations ranging from 30 nM to 10 μM) obtained from a total of 4 cells. The averaged parameters from the four individual fits were: computed maximum response (m), 84.5 ± 5.9%; negative logarithm of the EC_{50} (pK), -6.69 ± 0.04; Hill coefficient (n), 1.07 ± 0.1. The response to a maximally effective concentration of oxo-M (3 μM) did not undergo tachyphylaxis upon repeated application. In 5 cells, the response to two subsequent applications of 3 μM oxo-M (90 to 120 s exposure) was 85.2 ± 3.2% and 84.4 ± 3.1%, with wash intervals of 5 to 10 minutes. An example recording is shown in Figure 10. Additionally, there was no desensitization of the response to a prolonged application of 3 μM oxo-M (up to 6 minutes; Figure 11 (no recovery upon washing)); during this experiment, there was a further slow decrease in outward current during the oxo-M application (seen from the current at the holding potential). This may reflect the slow development of a voltage-insensitive current in response to oxo-M that is distinct from the inhibition of $I_{K(M)}$: this is discussed further in section 4.3.1. Thus, it was possible to obtain reliable $I_{K(M)}$ inhibitions during long applications of agonist (for example, during current-voltage measurements) or repeated applications of agonist (for example, for concentration-response measurements) to the same cell.

The effect of two concentrations of oxo-M on the steady-state current voltage relationship is shown in Figure 12. Steady-state current during 1 s, incremental -10 mV steps from -32 mV to -104 mV was measured in control solution, and this was not different from control current during a voltage ramp across the same voltage range, indicating that the voltage ramp speed was sufficiently slow to detect steady-state current. The subtracted currents (control - oxo-M), representing the oxo-M-sensitive current at each potential, are also shown. Oxo-M (both concentrations) caused a reversible decrease in the outward current at depolarized membrane potentials, and a net inward current between -65 mV and -130 mV in all cells (n = 4) in which voltage ramps were applied in the presence of oxo-M, which ranged in amplitude from -41 to -107 pA (300 nM oxo-M) and -41 to -133 pA (3 μM oxo-M) at -70 mV, although the profound effect of oxo-M was on the voltage range between -70 mV and - 20 mV, the region in which $I_{K(M)}$ is activated. In Figure 12, inhibition of steady-state current between -32 mV and -60 mV was around 50% (300 nM oxo-M) and 75% (3 μM oxo-M); these values are similar to the measurements of inhibition of $I_{K(M)}$ deactivation relaxations with these concentrations of oxo-M (compare with Figure 7).

4.2.1.2. Rate of onset of $I_{K(M)}$ inhibition by oxo-M.

The onset of the $I_{K(M)}$ inhibition in response to a maximally effective concentration of oxo-M (3 μM) had a delay of less than 10 s and in fact was almost fully developed within a 10 s wait between voltage steps in one recording shown in Figure 13A. The recovery from inhibition was almost complete within 60 s of removing oxo-M. During superfusion with oxo-M, the change in current at the holding potential closely followed the change in amplitude of the $I_{K(M)}$ deactivation in both the onset of and the recovery from the effect. Therefore an estimate of the onset latency and the half-time for the development of the response to oxo-M was made by measuring the continuous change in current at the holding potential during superfusion with 3 μM oxo-M (using the rapid perfusion device described in Chapter 2). An example record is shown in Figure 13C. In 5 cells, the estimated onset latency (which includes the time for switching the perfusion system) and half-time was 3.7 ± 0.7 s and 7.5 ± 0.4 s respectively. Compared with the change on switching to high $[K^+]$, which

had a latency of 2.2 s and a half-time of 1.9 s (Chapter 2), this suggests that the latter represents the delay associated with the perfusion system and that the actual onset latency for oxo-M, at 23 °C, is ~~2.5~~ 1·5 s and the half-time for the response development is 5.6 s. Because of the inward current also seen in response to oxo-M in some cells (see above) which would also contribute to these measurements, this is only an approximate measure of the onset latency and development of $I_{K(M)}$ inhibition by oxo-M.

4.2.2. Identification of G proteins mediating inhibition of $I_{K(M)}$ by muscarinic receptors.

4.2.2.1. Visualization of antibody-injected SCG neurones.

In an initial series of experiments to determine the effect of anti-G protein antibodies on $I_{K(M)}$ inhibition by oxo-M, successful microinjection of antibodies was verified, following $I_{K(M)}$ recordings, by the immunostaining method described in Chapter 2. Figure 14 shows a SCG neurone which had been injected with an anti-$G_{\alpha q/11}$ antibody and then incubated with a second, fluorescently-labelled antibody after recordings were completed. The phase contrast photomicrograph (Figure 14A) shows two SCG neurones, but only the neurone on the left has been injected with antibody. The fluorescence photomicrograph (Figure 14B) shows the same neurones after the post-recording immunostaining method to confirm successful injection of antibody. The injected neurone shows bright fluorescence, while the uninjected neurone shows virtually no fluorescence. Only injected neurones which showed bright fluorescence at this stage were included for analysis.

4.2.2.2. Effect of G protein antibodies on $I_{K(M)}$ inhibition by oxo-M.

In SCG neurones injected with an antibody used as a control (raised against glial fibrillary acidic protein, anti-GFAP antibody), oxo-M (300 nM: see Chapter 2) caused an inhibition of $I_{K(M)}$ (56.2 ± 2.5%; n = 9) that was not significantly different to the response in uninjected neurones (64 ± 2.5%; n = 20), indicating that the injection procedure did not affect the response to oxo-M. Responses in neurones injected with anti-G protein antibodies were compared to neurones injected with the anti-GFAP antibody. Figure 15 shows example $I_{K(M)}$ deactivation records from an uninjected

neurone and from neurones injected with anti-GFAP antibody, anti-$G_{\alpha o}$ antibody, or anti-$G_{\alpha q/11}$ antibody. From the scattergram of all the data points for each treatment group, shown in Figure 16, it is clear that there is a difference in the distribution of the anti-$G_{\alpha q/11}$ antibody-injected group data (0 to 59% $I_{K(M)}$ inhibition), compared with the other groups. Bartlett's test for homogeneity of variances indicated that the difference in the standard deviations of the groups was significant ($p<0.05$); thus, a non-parametric analysis of the data was considered more appropriate, as this analysis is not based on assumptions about the group distributions. The anti-$G_{\alpha o}$ antibody had no effect on the response to 300 nM oxo-M (median inhibition, 63%; n = 10; not significantly different to the anti-GFAP injected neurones, 56%: Figure 16). However, in neurones injected with anti-$G_{\alpha q/11}$ antibody the inhibition produced by 300 nM oxo-M ranged from being within the range of control responses to zero inhibition (median inhibition, 32%; n = 17: Figure 16). This was significantly less than responses in control (anti-GFAP antibody-injected) cells ($p<0.05$, Dunn's non-parametric test). The records in Figure 15D show responses in anti-$G_{\alpha q/11}$ antibody injected neurones that are reduced (i) and completely blocked (ii).

The properties of $I_{K(M)}$ deactivation currents were not substantially altered in antibody-injected cells compared with uninjected cells. Table 2 gives estimates of the amplitude and time constants (from the fit of a two exponential function) of the $I_{K(M)}$ deactivation relaxations recorded from uninjected and antibody-injected cells. The amplitude of $I_{K(M)}$ deactivations (in the absence of oxo-M) was not significantly different in the different treatment groups compared with uninjected control cells. The fast time constant ($\tau_{(fast)}$) was not significantly different in anti-GFAP (range: 40 to 75 ms) or anti-$G_{\alpha o}$ (range: 32 to 82 ms) antibody-injected cells compared with uninjected cells (range: 46 to 109 ms), or in anti-$G_{\alpha q/11}$ antibody-injected cells (26 to 75 ms) when compared with anti-GFAP antibody-injected control cells. However, there was a small but significant difference between the $\tau_{(fast)}$ of $I_{K(M)}$ deactivations in anti-$G_{\alpha q/11}$ antibody-injected cells compared with uninjected cells ($p<0.05$; Tukey-Kramer multiple comparisons test). As there was a considerable range of measured values in all groups it is not clear whether this represents an effect of the anti-$G_{\alpha q/11}$ antibody on

$\tau_{(fast)}$ (which is not seen with the other antibodies), or whether it may reflect small changes in the holding potential (and hence the voltage step) for each cell, as the time constant of the $I_{K(M)}$ deactivation is voltage-sensitive (see Chapter 1). A selective effect of the anti-$G_{\alpha q/11}$ antibody seems unlikely, as in subsequent experiments (see below and Chapter 5), this antibody had no significant effect on the deactivation current time constant. As noted in Chapter 3, the slow time constant ($\tau_{(slow)}$) was highly variable in all groups (note SEM values in Table 2), and was not significantly different in the treatment groups compared with uninjected cells.

4.2.2.3. Co-injection of G protein antibodies with FITC-dextran.

Although microinjection of the anti-$G_{\alpha q/11}$ antibody had a significant effect on the response to 300 nM oxo-M, this effect was variable. The most likely source of this variation was considered to be the microinjection procedure and therefore, in a second series of experiments (and using a different anti-$G_{\alpha q/11}$ antibody: see Chapter 2), antibody was co-injected with a fluorescently labelled dextran (FITC-dextran, 0.1%) in order to monitor the success of the injection on-line, with the objective of achieving bright fluorescence in all cells with this low percent solution of FITC-dextran. As the anti-$G_{\alpha o}$ antibody had been shown to have no effect on the inhibition of $I_{K(M)}$ by oxo-M, this was used as the control antibody in this series of experiments. Example $I_{K(M)}$ deactivation records from neurones co-injected with 0.1% FITC-dextran and either anti-$G_{\alpha o}$ or anti-$G_{\alpha q/11}$ antibody are shown in Figure 17. Anti-$G_{\alpha o}$ antibody, co-injected with 0.1% FITC-dextran had no effect on the response to 300 nM oxo-M (range, 50 to 70% inhibition; mean inhibition ± SEM, 60.2 ± 4.8%; n = 7) compared with uninjected cells. Injection of anti-$G_{\alpha q/11}$ antibody again caused a variable reduction of the response to 300 nM oxo-M (range, 0 to 50% $I_{K(M)}$ inhibition; mean inhibition ± SEM, 22.2 ± 6.6%; n = 8). However, the standard deviations for the two groups were not significantly different (Bartlett's test for homogeneity of variances), and parametric analysis revealed a significant difference ($p < 0.001$, Tukey-Kramer test) between the responses to oxo-M in anti-$G_{\alpha q/11}$ antibody- and anti-$G_{\alpha o}$ antibody-injected neurones in this series. Data are summarized in the bar graph in Figure 18. In this series of experiments, neither antibody had any significant effect on the amplitude or

the time constants (from a fit of a two exponential function) of the $I_{K(M)}$ deactivation relaxation compared with data from uninjected cells (Table 3). However, there was a significant decrease in the percentage of $I_{K(M)}$ that deactivated with the faster time constant of 60 to 70 ms in cells injected with anti-$G_{\alpha q/11}$ antibody, compared with anti-$G_{\alpha o}$ antibody-injected cells ($p < 0.05$, Tukey-Kramer multiple comparisons test), although this percentage was not different to that in uninjected cells. The zero current potential, recorded at the end of experiments, did not differ significantly between the three groups.

partial
4.2.2.4. Surmountable reduction of muscarinic $I_{K(M)}$ inhibition by anti-$G_{\alpha q/11}$ antibody.

The effect of the anti-$G_{\alpha q/11}$ antibody on the $I_{K(M)}$ inhibition by oxo-M could be overcome by increasing the concentration of the agonist; thus, the effect of the antibody was surmountable. In 6 neurones which had been injected with the anti-$G_{\alpha q/11}$ antibody (and which showed good recoveries following responses to 300 nM oxo-M), application of a maximally effective concentration of oxo-M (3 μM) caused an increase in the inhibition of $I_{K(M)}$ compared with that seen in response to 300 nM oxo-M. The extent of the recovery of the response depended on the extent to which the response to 300 nM had been reduced by the antibody; there was less recovery in neurones showing *blocked* responses to 300 nM (for example, Figure 19B) than in those showing *reduced* responses (for example, Figure 19A). Although it was possible to partially overcome the effect of the antibody by increasing the concentration of oxo-M, it was not always possible to recover the maximum response normally seen with 3 μM oxo-M: in one recording, illustrated in Figure 19A, the concentration of oxo-M was further increased and the maximum inhibition (with 10-30 μM oxo-M) was greatly reduced to around 50%. Data from 5 antibody-injected cells are compared to the control concentration-response data (from the 4 cells described in section 4.2.1.1.) in Figure 19C. The remaining antibody-injected cell was more atypical, in that the response to 300 nM oxo-M was strongly reduced (9% inhibition), while the response to 3 μM oxo-M almost recovered the maximum effect (68% inhibition; this data has been omitted from the graph, as it obscures the other data points).

4.2.2.5. Effect of specific antisense DNA sequences on $I_{K(M)}$ inhibition by oxo-M.

In order to determine whether $G_{\alpha q}$, $G_{\alpha 11}$ or both of these G proteins specifically couple to muscarinic receptors in mediating inhibition of $I_{K(M)}$, neurones were incubated with phosphorothioate-modified antisense oligodeoxynucleotide (ODN) sequences against $G_{\alpha q}$ or $G_{\alpha 11}$. In an initial series of experiments, $G_{\alpha 11}$ ODN (605a) caused a reduction in the response to 300 nM oxo-M between 10 and 30 hours, with a peak effect at 15 to 20 hours (significantly different to responses in untreated neurones, $p<0.001$; Tukey-Kramer multiple comparisons test) while $G_{\alpha q}$ ODN (485a) caused a small but significant reduction in $I_{K(M)}$ inhibition between 10 and 15 hours incubation ($p<0.001$, test as before; Figure 20A). However, in a second series of experiments using a different $G_{\alpha 11}$ ODN (499a) there was no effect on $I_{K(M)}$ inhibition by oxo-M following incubation for 15 to 25 hours: responses were not significantly different from those seen in untreated cells or cells incubated with a $G_{\alpha 11}$ sense ODN sequence (499s) for the same time period. During this series of experiments, incubation with the first, initially effective, $G_{\alpha 11}$ ODN (605a) was also found to be ineffective in reducing the response to oxo-M. The data from this series are compared with the original ODN data described above (between 15 and 25h incubation) in the bar graph in Figure 20B; the only significant effect, compared with the $G_{\alpha 11}$ sense ODN (499s), was the effect of the first series of incubations with $G_{\alpha 11}$ ODN (605a). Attempts were made to inject the antisense sequences, in order to overcome possible problems of access to the interior of the cell. Difficulties with this approach included the changing morphology and location of SCG neurones over the long incubation times, making it difficult to identify injected neurones. Occasionally, infection of neurones removed from, and then replaced in the sterile environment was encountered; thus, antisense DNA injection experiments did not prove to be successful. Details of all ODN sequences are given in Chapter 2.

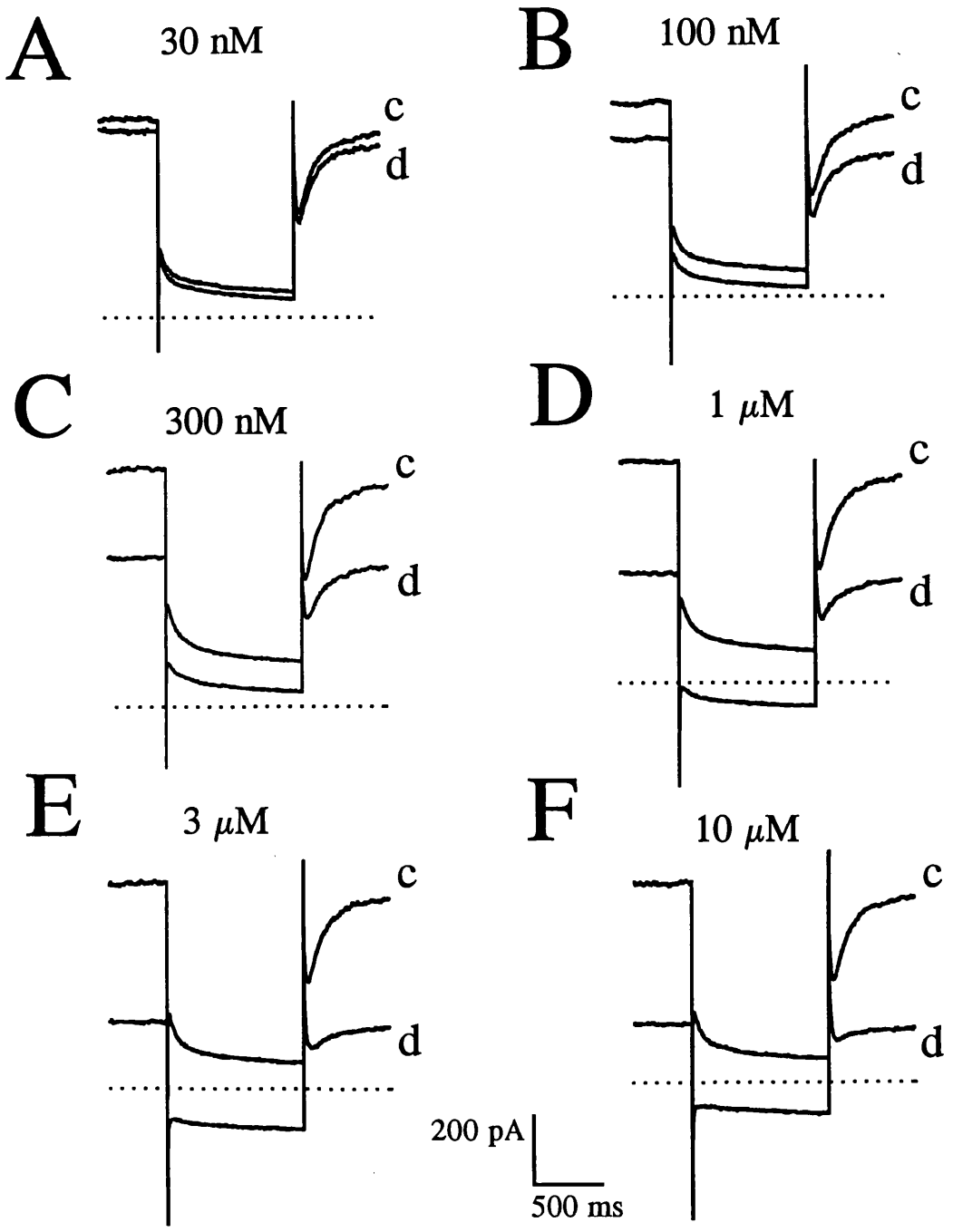

Figure 8. Inhibition of $I_{K(M)}$ by different concentrations of oxotremorine-M.
Example $I_{K(M)}$ deactivation records from one cell (1 s, -30 mV step (see Chapter 2) from V_H -27 mV) showing the effect of non-cumulative addition of oxo-M: A. 30 nM (8% inhibition), B. 100 nM (25%), C. 300 nM (50%), D. 1 μM (67%), E. 3 μM (79%) and F. 10 μM (85%), applied in the order C, D, E, F, A, B. Records show $I_{K(M)}$ deactivation relaxations recorded in control solution (c) immediately prior to perfusion with each concentration of oxo-M, then in the presence of agonist (d). The dotted line in each example represents the zero current level, and the scale bar applies to all records. The recovery from inhibition at each concentration of oxo-M was 90-100%. Deactivation amplitudes, % inhibition and % recovery were measured as described in Chapter 2.

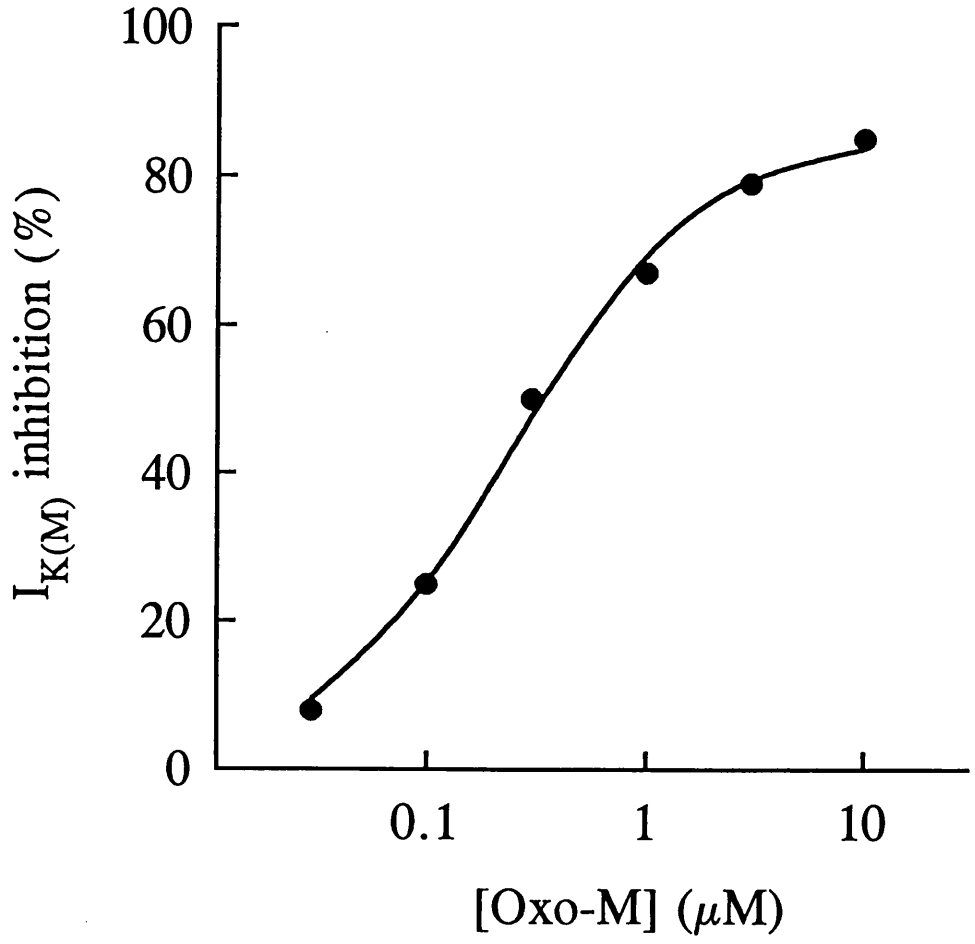

Figure 9. Concentration-response curve for inhibition of $I_{K(M)}$ by oxotremorine-M.
Percent inhibition of $I_{K(M)}$ (y) at each concentration of oxo-M (A; plotted on a logarithmic scale) measured from the deactivation records shown in figure 8. The solid line is the best fit to the data of the function $y = m.10^{n.\log(A)} / (10^{n.\log(A)} + 10^{n.\log(K)})$ where, for this cell, the computed maximum response (m) = 86%, the logarithm of the EC_{50} (K) = -6.62, and the Hill coefficient (n) = 1.

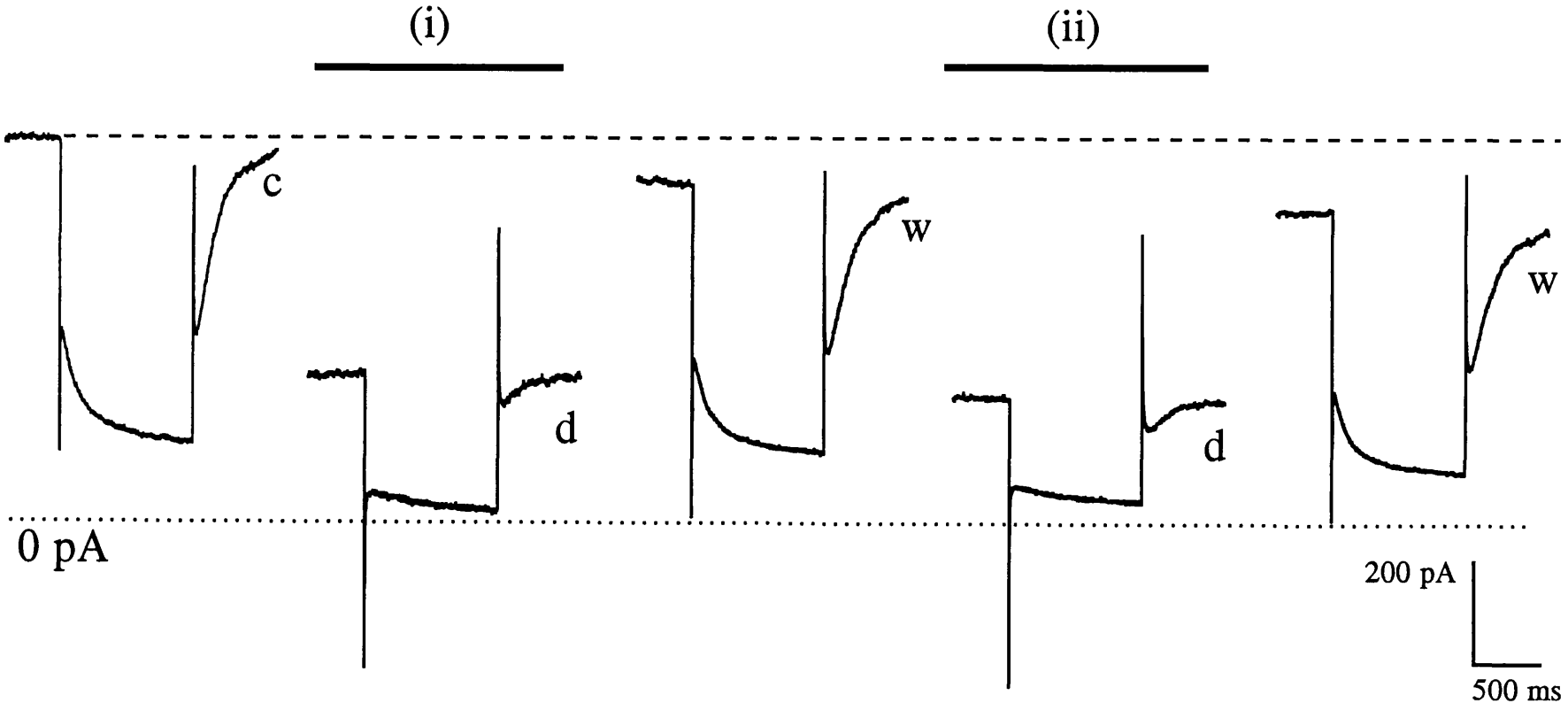

Figure 10. The response to oxotremorine-M does not exhibit tachyphylaxis.
Example $I_{K(M)}$ deactivation records from one cell (1 s, -30 mV steps from V_H -20 mV: see Chapter 2). Deactivation relaxations were recorded in control solution (c), then the cell was superfused with 3 μM oxo-M (d, (i); 86% inhibition). The center record (w) shows the recovery from inhibition 5 minutes after washing out the agonist. A second application of oxo-M was then made (d, (ii); 83% inhibition). Recovery after 10 minutes from the second response to oxo-M is shown in the right-hand record (w). The dashed line represents the level of holding current at the start of the experiment, and the dotted line represents the zero current level.

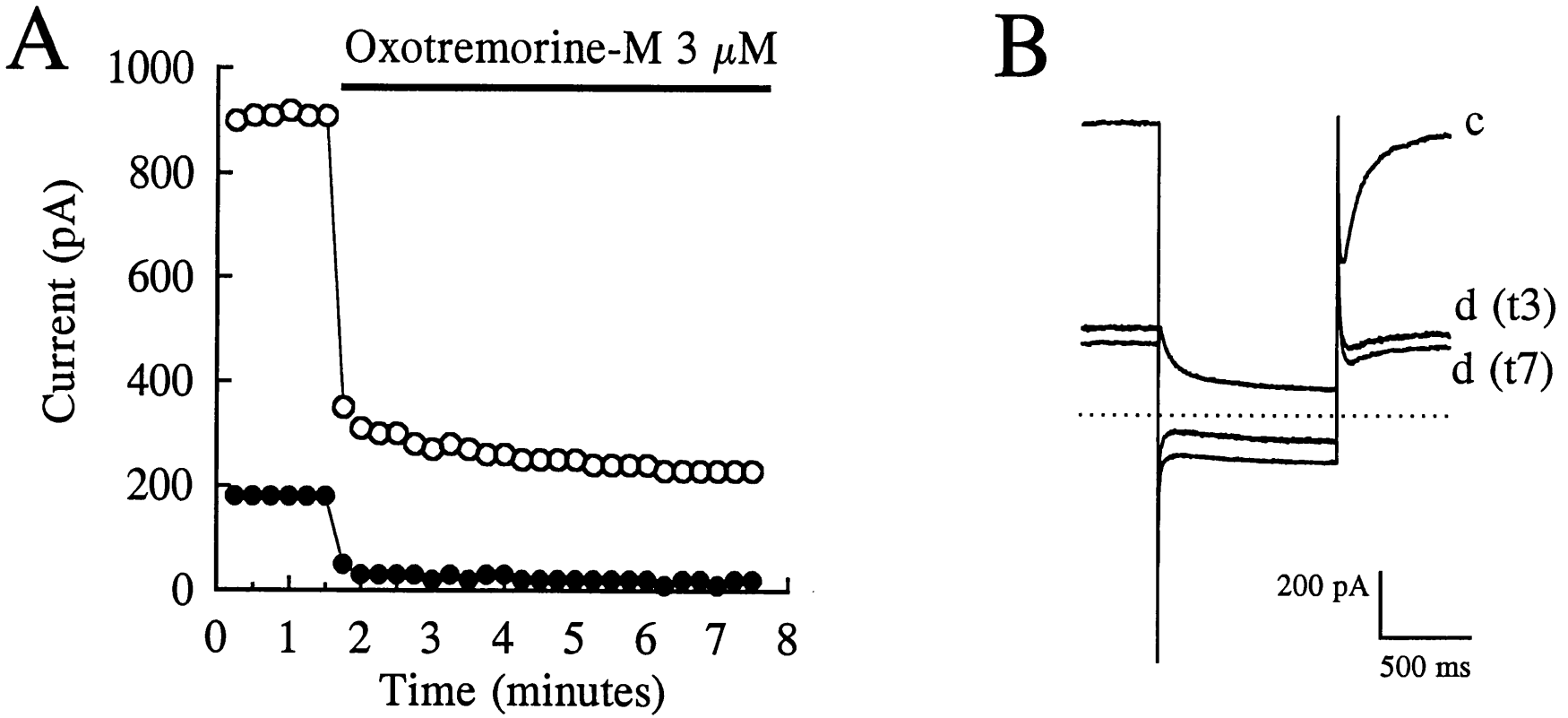

Figure 11. The response to oxotremorine-M does not desensitize.
A. Data from one experiment showing current (pA) at the holding potential (-28 mV, open circles) and $I_{K(M)}$ deactivation relaxation amplitude (pA) at the command potential (-58 mV, filled circles) plotted against time (minutes). Voltage steps were applied every 15 s. After obtaining six stable $I_{K(M)}$ records in control solution, the cell was superfused with 3 μM oxo-M for 6 minutes (bar). B. Example $I_{K(M)}$ deactivation records from the cell in A, recorded in control solution (c) and, after perfusion with oxo-M, at time 3 minutes (d (t3)) and time 7 minutes (d (t7)). The dotted line represents the zero current level.

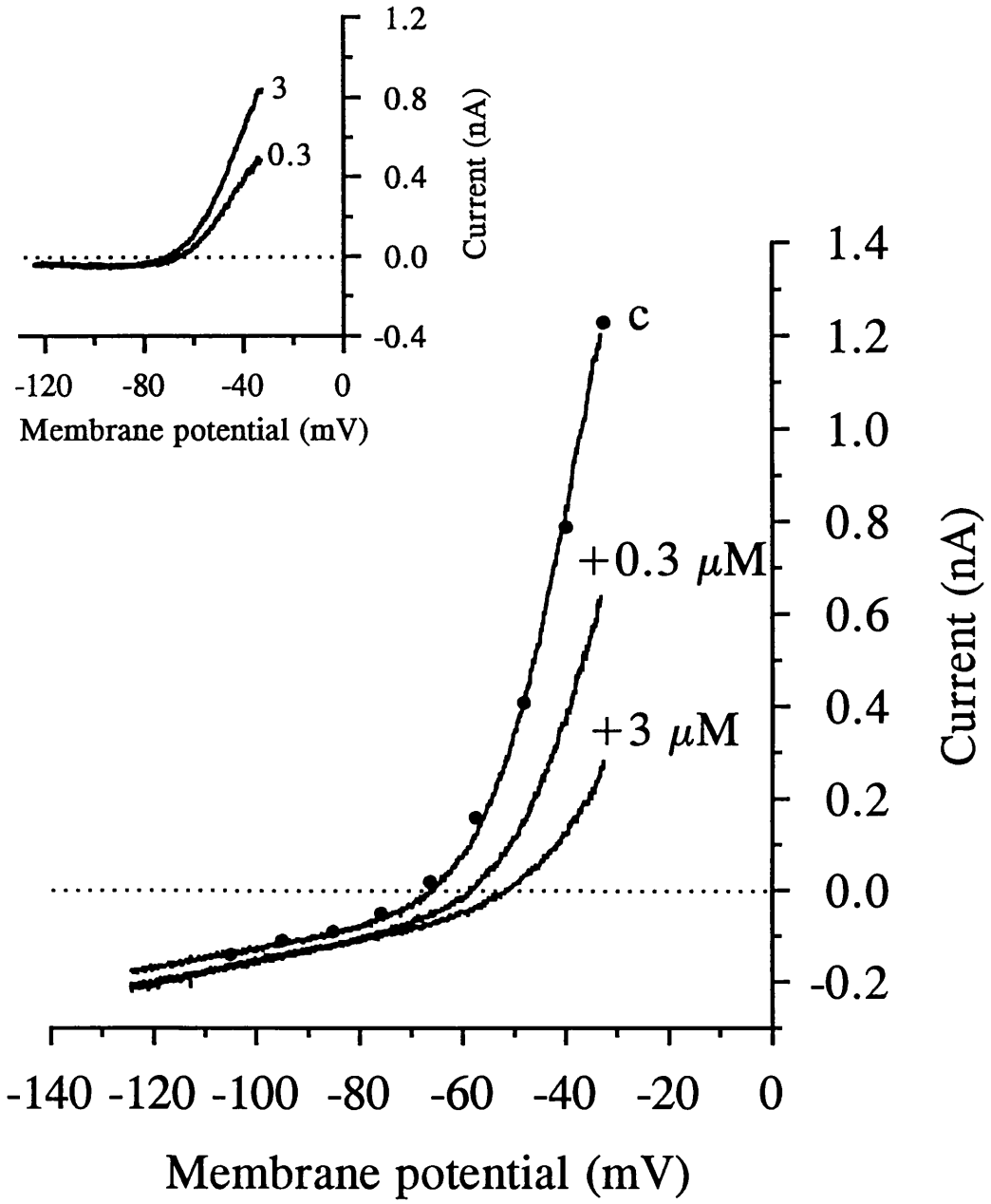

Figure 12. Effect of oxotremorine-M on the steady-state current-voltage relationship.
Main figure. Solid lines represent current during voltage ramps from -32 mV to -124 mV (-10 mV/ s; V_H -32 mV) applied in control solution (c), in the presence of 300 nM oxo-M (+0.3 μM), then in the presence of 3 μM oxo-M (+3 μM). Filled circles represent current at the end of 1 s, -10 mV steps from -32 mV to -104 mV (V_H -32 mV). Inset. Oxo-M-sensitive current across the range of the voltage ramp (0.3: c - oxo-M 0.3 μM; 3: c - oxo-M 3 μM). Ramp currents were graphically reversed for convention.

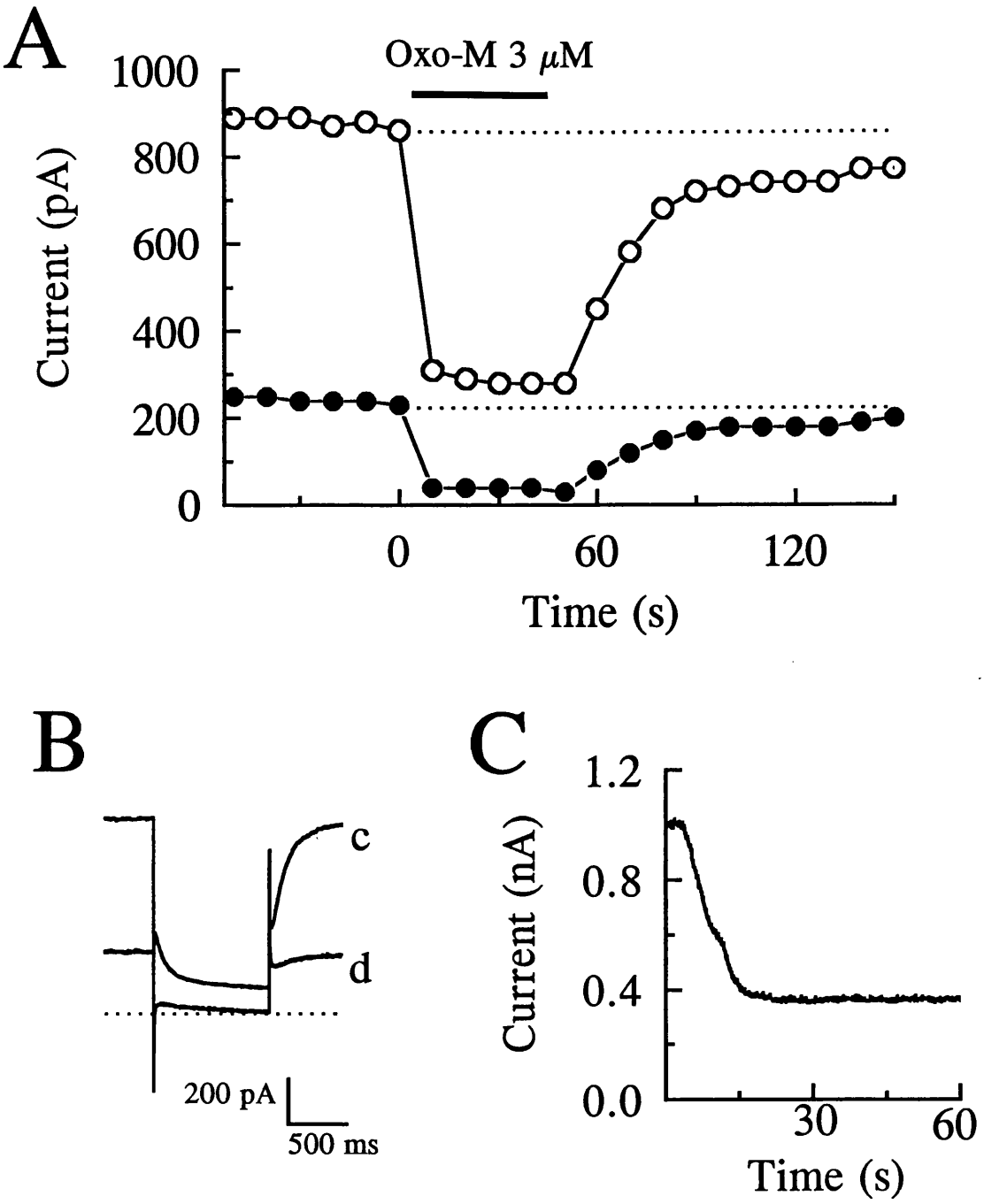

Figure 13. Onset of the response to oxotremorine-M.
A. Data from one experiment showing current at the holding potential (-28 mV, open circles) and $I_{K(M)}$ deactivation relaxation amplitude at the command potential (-58 mV, filled circles) plotted (pA) against time (seconds). After obtaining six stable records in control solution, 3 μM oxo-M was applied (time 0 s) *via* a rapid perfusion system for approximately 40 s (bar; 83% inhibition), then the current was allowed to recover (85% recovery). B. Example $I_{K(M)}$ deactivation records from the cell in A, recorded in control solution (c) and at the peak of the response to oxo-M (d). The dotted line indicates the zero current level. C. Data from a different cell to A showing the continuous change in current (nA) at the holding potential (-26 mV) as a function of time during superfusion with 3 μM oxo-M. The rapid perfusion was manually switched immediately after starting this recording.

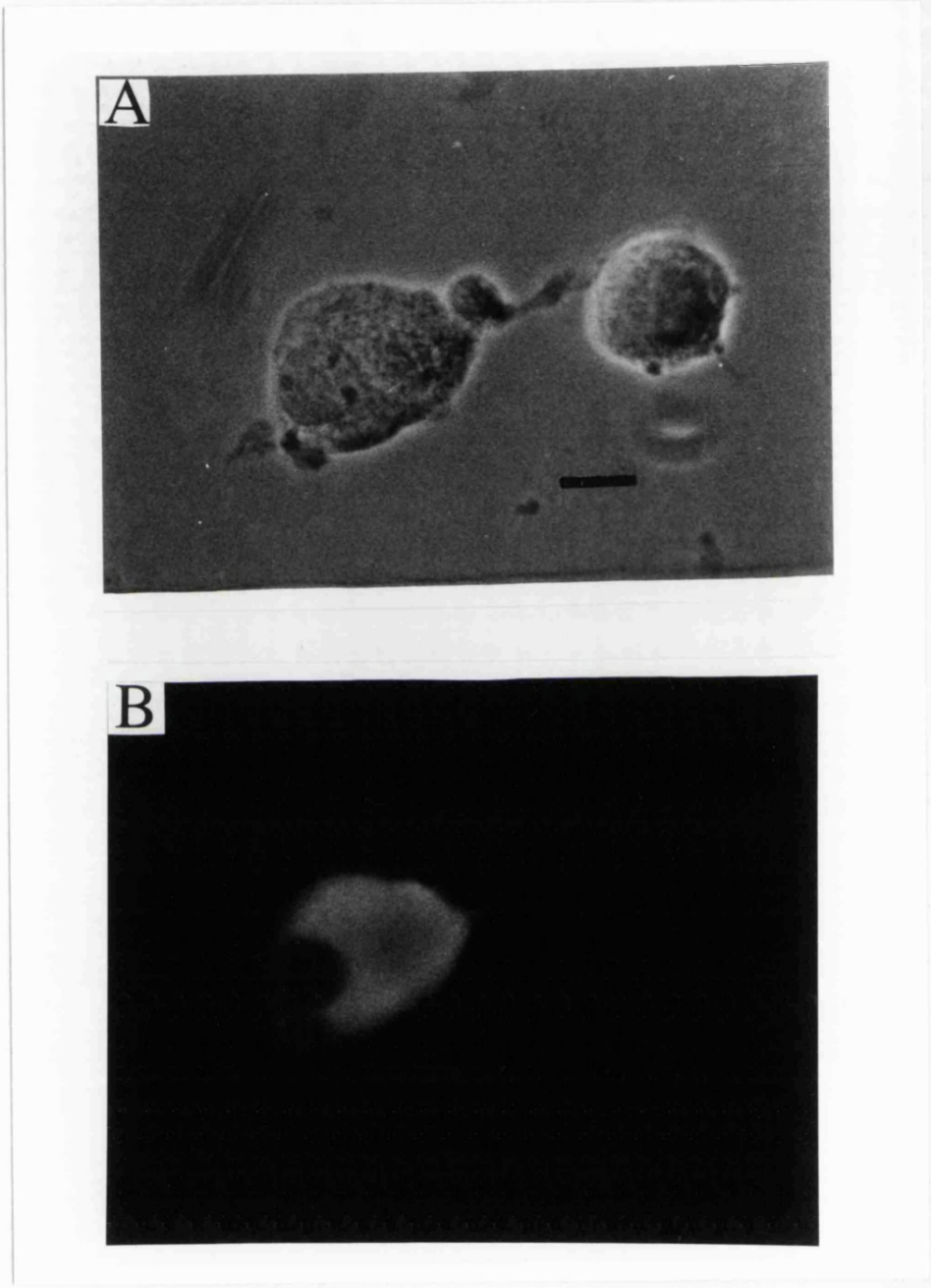

Figure 14. Photomicrographs of SCG neurones injected with anti-$G_{\alpha q/11}$ antibody.
A. Phase contrast photomicrograph of two SCG neurones following the post-recording immunostaining procedure described in Chapter 2. The neurone on the left was injected with anti-$G_{\alpha q/11}$ antibody, the neurone on the right was uninjected. B. Fluorescence photomicrograph of the same cells in A. Photomicrographs were taken by Y. Vallis.

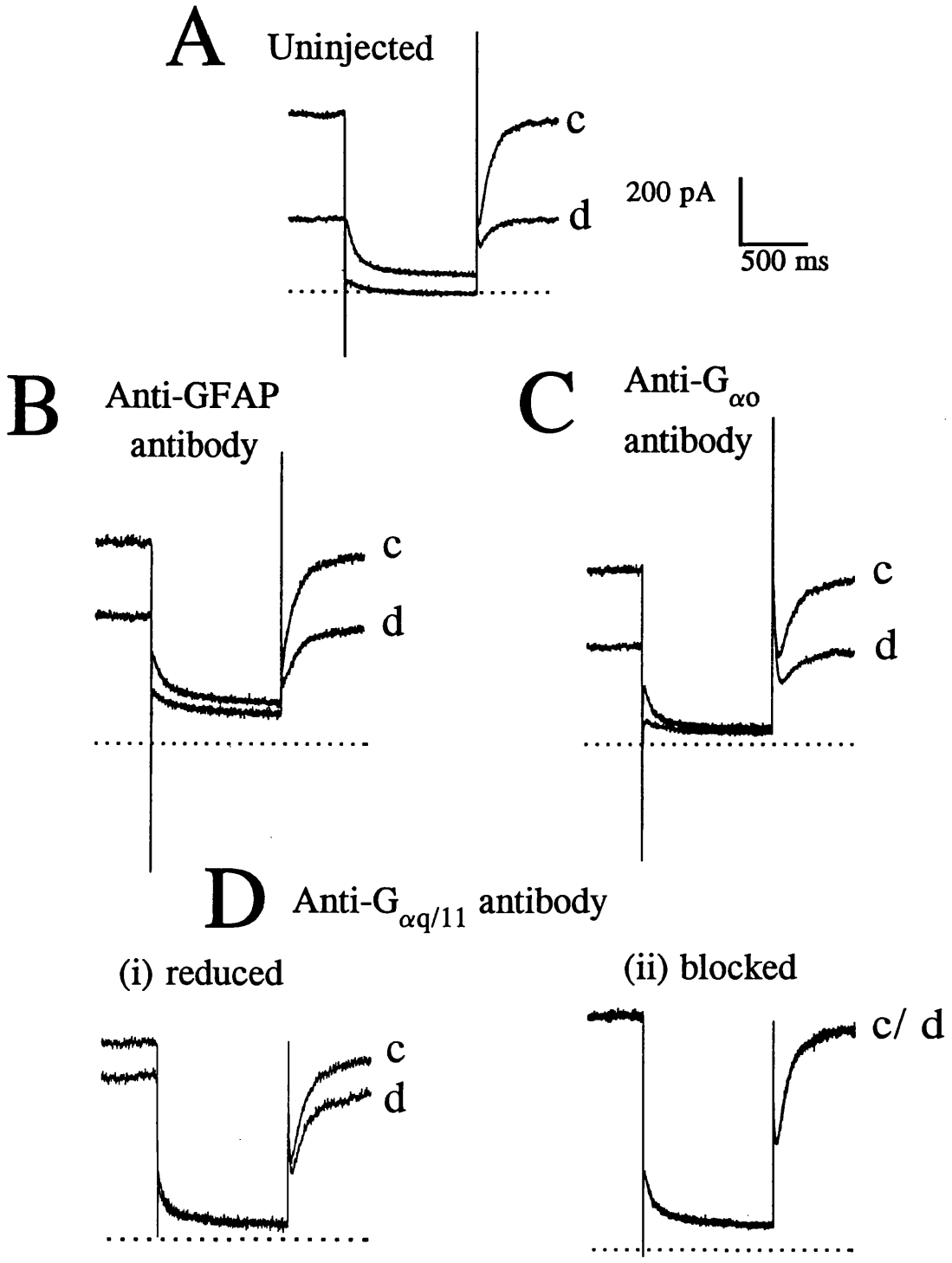

Figure 15. Anti-$G_{\alpha q/11}$ antibody can reduce or block inhibition of $I_{K(M)}$ by oxotremorine-M. Example $I_{K(M)}$ deactivation records (during 1 s, -30 mV steps) in control solution (c) and in the presence of 300 nM oxo-M (d). Recordings shown are from A. an uninjected cell (75% inhibition; V_H -22 mV), and cells injected with B. anti-GFAP antibody (57% inhibition; V_H -23 mV), C. anti-$G_{\alpha o}$ antibody (67% inhibition; V_H -27 mV), and D. anti-$G_{\alpha q/11}$ antibody, showing either a reduced response ((i), 22% inhibition; V_H -27 mV) or a complete block of the response ((ii), 0% inhibition; V_H -27 mV) to oxo-M. The dotted lines indicate zero current, and the scale bar applies to all records.

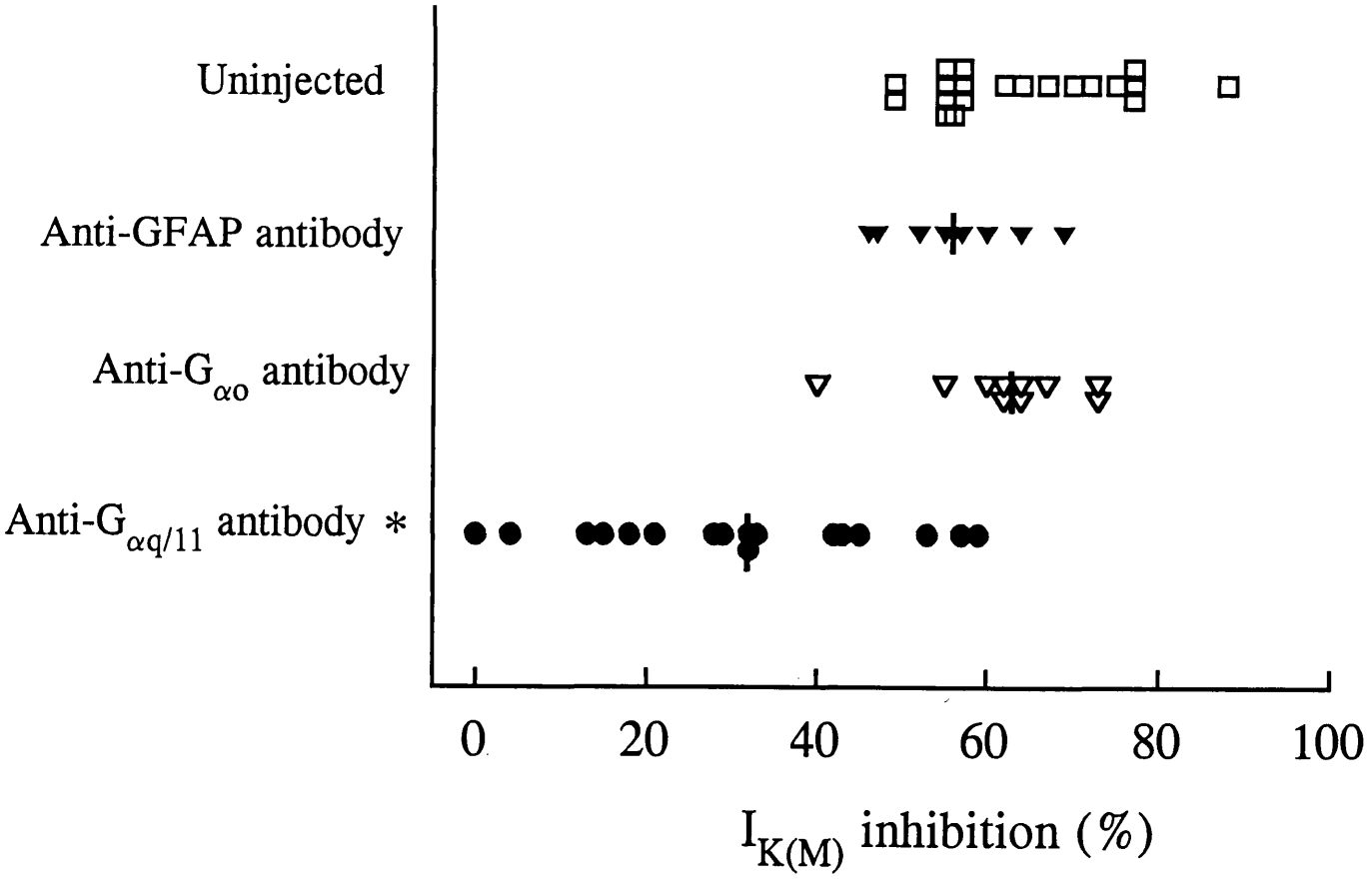

Figure 16. Scattergram showing the effect of anti-G protein antibodies on $I_{K(M)}$ inhibition by 300 nM oxotremorine-M.
$I_{K(M)}$ inhibition (%) in response to 300 nM oxo-M in uninjected cells (n = 20), and cells injected with anti-GFAP antibody (n = 9), anti-$G_{\alpha o}$ antibody (n = 10) and anti-$G_{\alpha q/11}$ antibody (n = 17). Solid bars represent median inhibition. Asterisk indicates a significant difference ($p<0.05$, Dunn's test) between control cells (anti-GFAP antibody injected) and anti-$G_{\alpha q/11}$ antibody-injected cells. The data for this figure were generated in collaboration with Dr. M. P. Caulfield

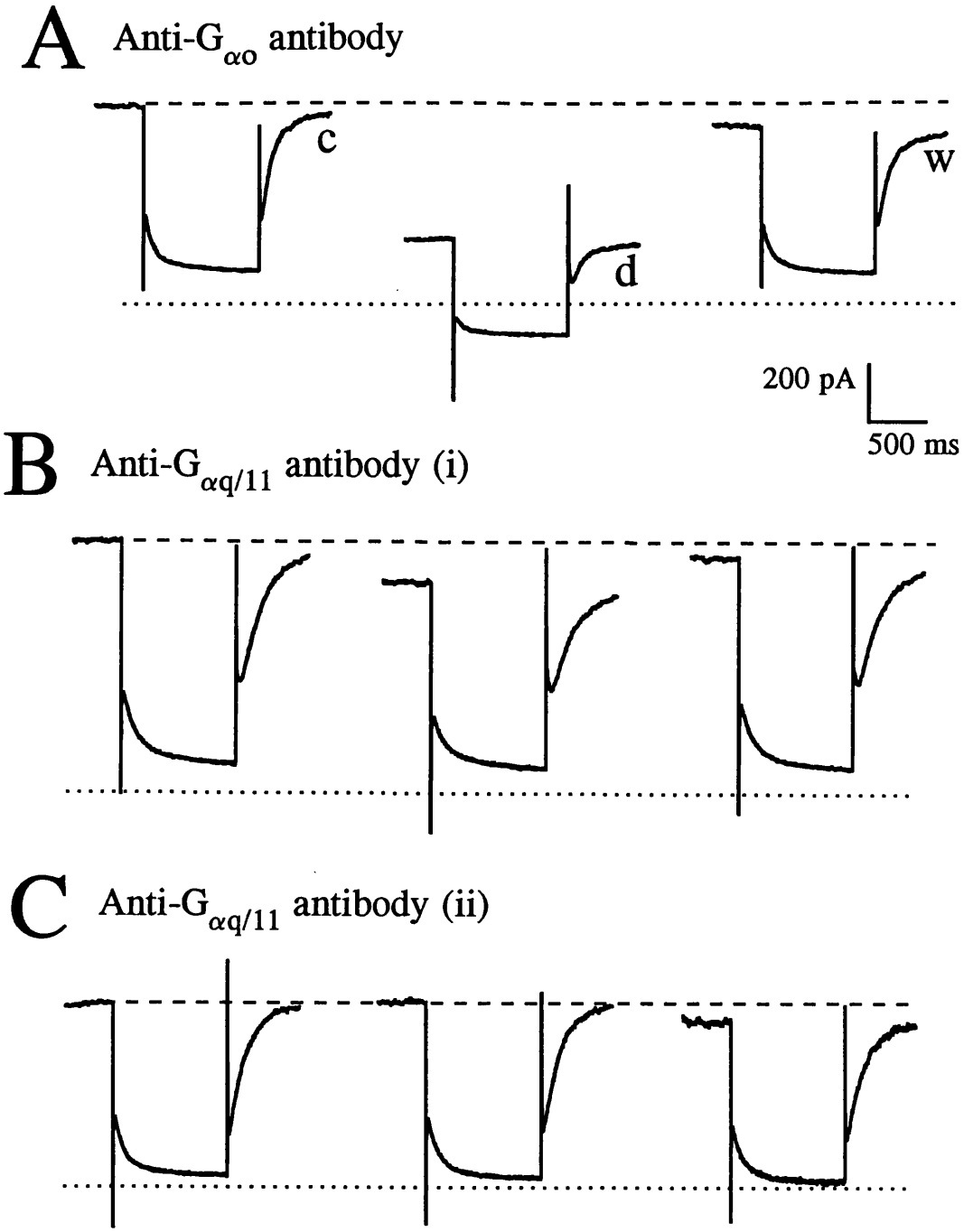

Figure 17. Reduction and block of $I_{K(M)}$ inhibition by anti-$G_{\alpha q/11}$ antibody (co-injection method). Example $I_{K(M)}$ deactivation records (during 1 s, -30 mV steps) in control solution (c), in the presence of 300 nM oxo-M (d) and after washing out the agonist (w). Recordings are from cells co-injected with 0.1% FITC-dextran and either anti-$G_{\alpha o}$ antibody (A; V_H -25 mV; 64% inhibition) or anti-$G_{\alpha q/11}$ antibody showing a reduced response (B; V_H -25 mV; 25% inhibition) or a blocked response (C; V_H -26 mV; 0% inhibition) to oxo-M. The dotted lines represent the zero current level, and the scale bar applies to all records. In these experiments, a different anti-$G_{\alpha q/11}$ antibody was used to the one in figures 15 and 16 (see Chapter 2).

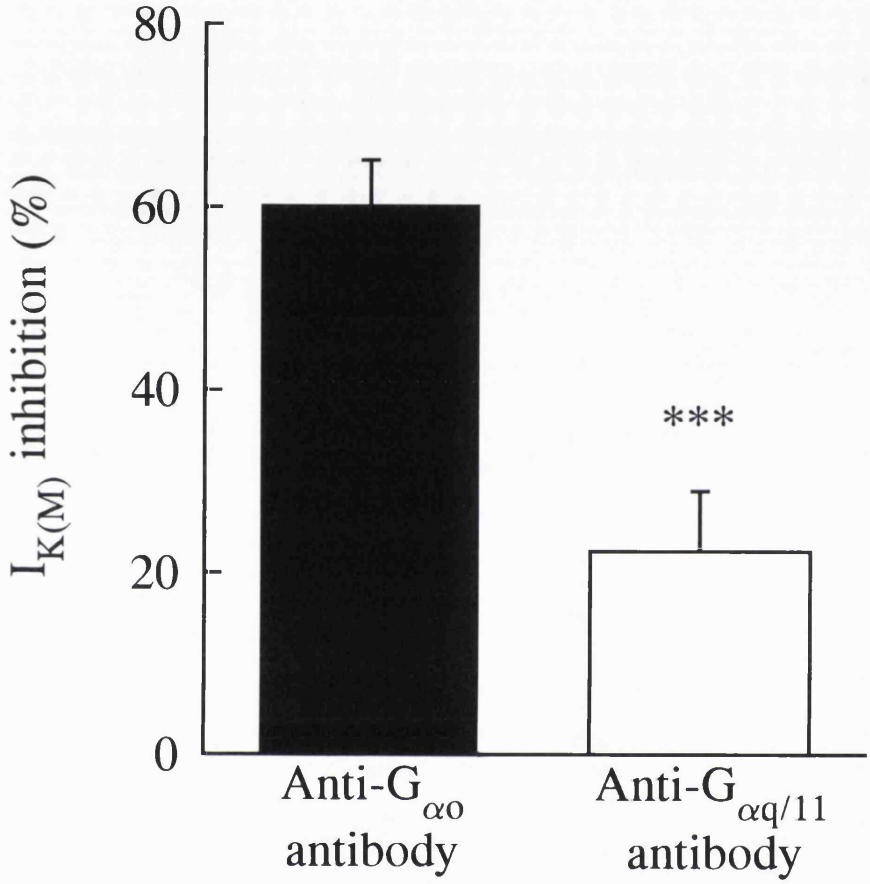

Figure 18. Bar graph showing $I_{K(M)}$ inhibition (%, mean ± SEM) in response to 300 nM oxotremorine-M in cells co-injected 0.1% FITC-dextran and either anti-$G_{\alpha o}$ antibody (n = 7) or anti-$G_{\alpha q/11}$ antibody (n = 8). Asterisks indicate a significant difference ($p < 0.001$, Tukey-Kramer test) from anti-$G_{\alpha o}$ antibody-injected cells.

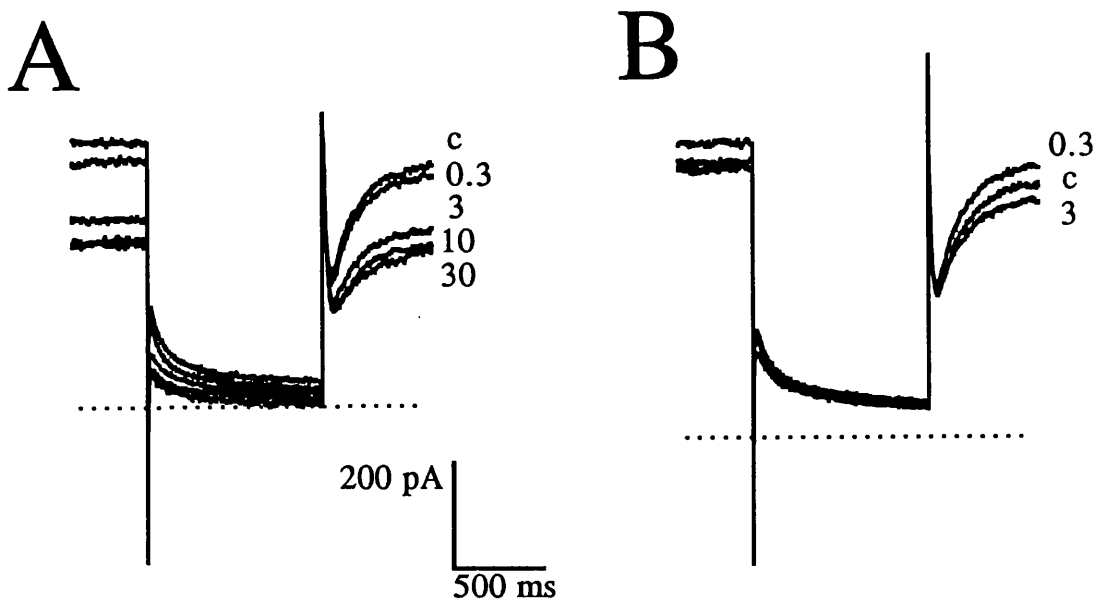

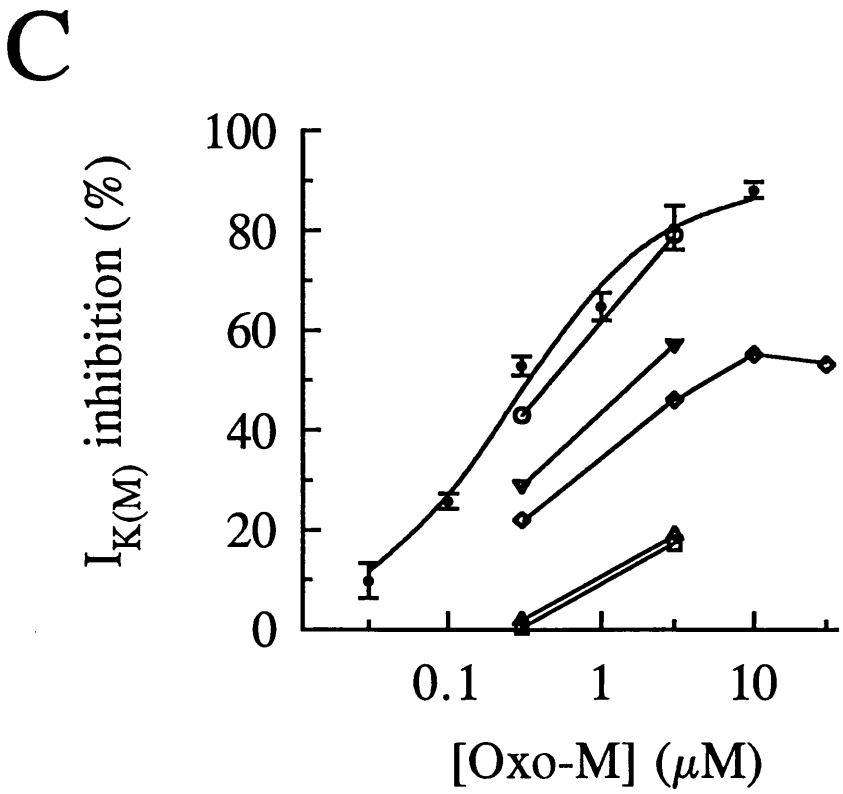

partially

Figure 19. The effect of the anti-$G_{\alpha q/11}$ antibody is surmountable.
Example $I_{K(M)}$ deactivation records (during 1 s, -30 mV steps) showing the effect of increasing the concentration of oxo-M applied to cells injected with anti-$G_{\alpha q/11}$ antibody, and giving responses to 300 nM oxo-M that are A. reduced (V_H -25 mV) or B. completely blocked (V_H -28 mV). Concentrations of oxo-M are given in μM, and c = control recordings. Dotted lines indicate the zero current level. C. Concentration-response graph, showing percent $I_{K(M)}$ inhibition in response to oxo-M (logarithmic scale) in uninjected cells (closed circles, mean ± SEM; solid line is the best fit to the data from 4 cells (see 4.2.1.1.) of the function given in Figure 9) and cells co-injected with anti-$G_{\alpha q/11}$ antibody and 0.1% FITC-dextran (open symbols).

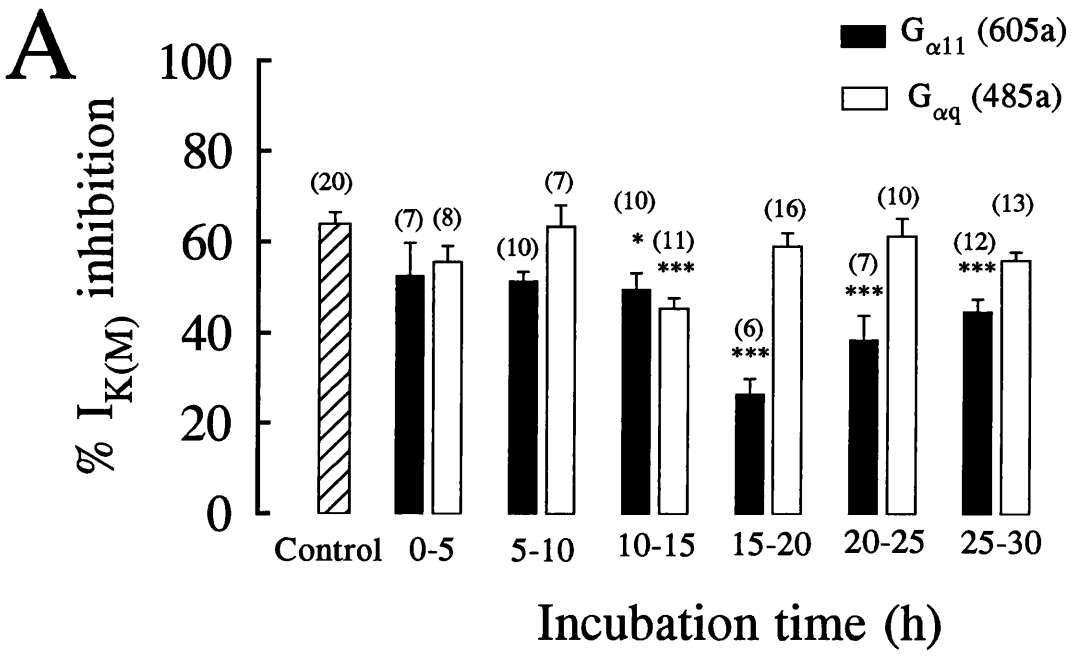

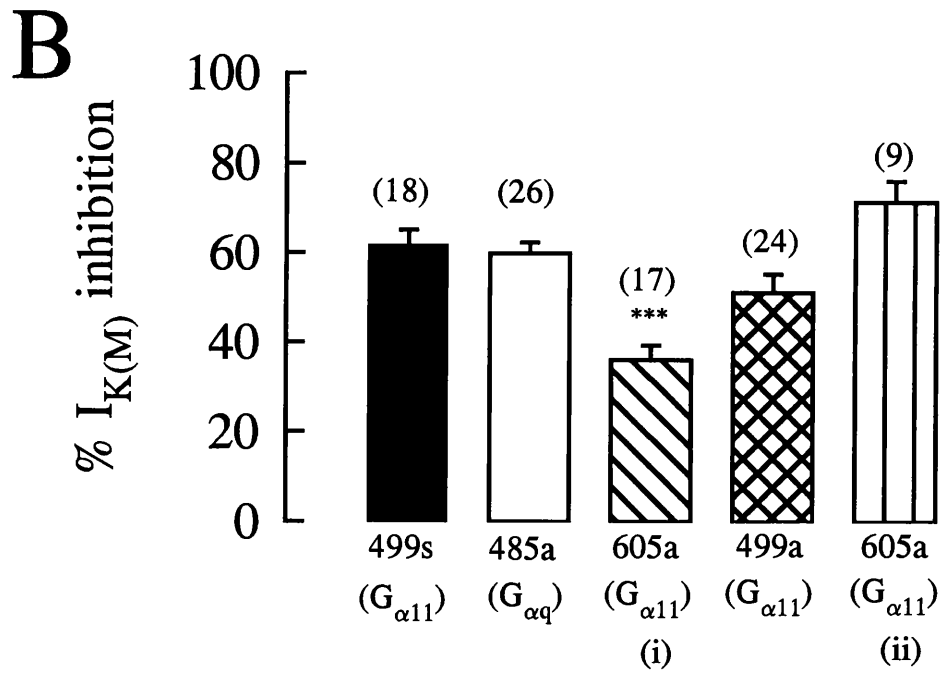

Figure 20. Effect of $G_{\alpha q}$ and $G_{\alpha 11}$ antisense oligodeoxynucleotides on $I_{K(M)}$ inhibition by 300 nM oxotremorine-M.

A. Bar graph showing the effect of incubation of SCG neurones with either $G_{\alpha q}$ (485a; open bars) or $G_{\alpha 11}$ (605a; solid bars) ODNs for 3 to 30 h (data divided into 5 h time bins, each bar is %, mean ± SEM) on $I_{K(M)}$ inhibition by 300 nM oxo-M (*$p<0.05$ and ***$p<0.001$ compared with untreated control cells, diagonal bar). B. Effect of incubation with different $G_{\alpha 11}$ and $G_{\alpha q}$ ODNs (between 15 to 25 h; %, mean ± SEM) on $I_{K(M)}$ inhibition by 300 nM oxo-M. Bars represent: $G_{\alpha 11}$ 499s (solid), $G_{\alpha q}$ 485a (open), $G_{\alpha 11}$ 605a (first series, diagonal; ***$p<0.001$ compared with 499s), $G_{\alpha 11}$ 499a (cross), and $G_{\alpha 11}$ 605a (second series, vertical). Number of cells indicated in parentheses. The data for this figure were generated in collaboration with Dr. M. P. Caulfield.

Table 2: Properties of $I_{K(M)}$ deactivation relaxations in antibody-injected cells.

	Deactivation $\tau_{(fast)}$ (ms)	% of total amplitude	Deactivation $\tau_{(slow)}$ (ms)	n	Deactivation amplitude (pA; control)	n
Uninjected	64 ± 4.4	63 ± 3.5	344 ± 33	14	159 ± 17	20
Anti-GFAP antibody-injected	57 ± 4	63 ± 3	406 ± 47	9	174 ± 23	9
Anti-G_{α_o} antibody-injected	61 ± 5.4	65 ± 5.4	514 ± 123	10	133 ± 6	10
Anti-$G_{\alpha q/11}$ antibody-injected	49 ± 3*	60 ± 4.5	382 ± 51	17	188 ± 19	17

* $p < 0.05$: compared with uninjected neurones.

Table 3: Properties of $I_{K(M)}$ deactivation relaxations in cells co-injected with antibody and FITC-labelled dextran (oxotremorine-M series).

	Deactivation $\tau_{(fast)}$ (ms)	% of total amplitude	Deactivation $\tau_{(slow)}$ (ms)	n	Deactivation amplitude (pA; control)	n	Zero current potential (mV; end-of-experiment)	n
Uninjected*	64 ± 4.4	63 ± 3.5	344 ± 33	14	159 ± 17	20	-55 ± 1.5	17
Anti-$G_{\alpha o}$ antibody-injected	71.5 ± 17	68 ± 5.3	449 ± 74	6	234 ± 17	7	-59 ± 1.9	4
Anti-$G_{\alpha q/11}$ antibody-injected	64 ± 11	47 ± 6.3**	350 ± 73	8	233 ± 30	8	-60.5 ± 2.5	8

* Same data as in Table 3.

** significantly different from % of total amplitude in anti-$G_{\alpha o}$ antibody-injected cells ($p < 0.05$, Tukey-Kramer multiple comparisons test).

4.3. DISCUSSION.

4.3.1. Inhibition of $I_{K(M)}$ by oxo-M.

4.3.1.1. Concentration dependence.

The experiments presented in this chapter agree with previous reports that the muscarinic receptor agonist, oxo-M, can inhibit $I_{K(M)}$ in sympathetic neurones of the rat (Bernheim *et al.*, 1992). Inhibition of $I_{K(M)}$ by oxo-M was not susceptible either to desensitization during prolonged applications of agonist, or tachyphylaxis following a repeated application of agonist, even at maximally effective concentrations of oxo-M. This made it possible to construct full concentration-response curves from a single SCG cell. The EC_{50} for this response was 204 nM, and maximally effective concentrations of oxo-M (3 to 10 μM) caused substantial but incomplete inhibition of $I_{K(M)}$, similar to the findings of Bernheim *et al.* (1992). Oxo-M has been reported to act as an agonist at ganglion nicotinic acetylcholine receptors at concentrations greater than 10 μM (Xian *et al.*, 1994). In the present study, even the highest concentrations of oxo-M used caused a decrease in standing outward current (at depolarized membrane potentials) that followed the same time course in onset and offset as the inhibition of $I_{K(M)}$ deactivation relaxations, suggesting that inhibition of $I_{K(M)}$ is the main source of the effect of oxo-M. However, higher concentrations of oxo-M (0.3 to 10 μM: see Figure 8) did cause a *net* inward current (at potentials where $I_{K(M)}$ was deactivated) which suggests that oxo-M affects another membrane conductance, although this effect is rather slower than that expected for activation of nicotinic receptors (a ligand-gated cation channel), and there was no obvious increase in current noise during the inward current. Possible sources of this inward current are discussed below. Increasing the concentration of oxo-M from 3 μM to 10 μM did not cause a significantly greater inhibition of $I_{K(M)}$, which suggests that $I_{K(M)}$ cannot be fully inhibited by this agonist. This has also been observed in rat sympathetic neurones for a number of other muscarinic receptor agonists including muscarine (60% inhibition), oxotremorine (40%) and methacholine (60 %; Marrion *et al.*, 1989), and peptide receptor agonists such as bradykinin (see Chapter 5), which suggests that a component of $I_{K(M)}$ may be insensitive to inhibition.

Reports of complete inhibition of $I_{K(M)}$ by muscarinic receptor agonists are unusual, even in frog sympathetic neurones (for example, Adams *et al.*, 1982b (Figure 6); Jones, 1985). Although there was no apparent desensitization of the response to oxo-M in the present study, suggesting that this phenomenon does not underlie the incomplete inhibition with maximally effective concentrations of oxo-M, it is possible that a very rapid desensitization process occurred which was beyond the resolution of the experiment described in Figure 11. For example, desensitization of the β_2-adrenergic receptor due to the uncoupling effect of β-adrenergic receptor kinase can occur with a half-time of less than 1 minute (reviewed by Lohse, 1993).

Other muscarinic receptor agonists (such as muscarine) which inhibit $I_{K(M)}$ deactivation relaxations also cause a reduction in the steady-state outward current between -70 mV and -20 mV, the membrane potential range over which $I_{K(M)}$ is activated (Constanti and Brown, 1981; Marrion *et al.*, 1989). In this study, oxo-M caused a concentration-dependent reduction in the outward current during voltage-ramps at depolarized potentials, although a component of outward current at potentials positive to -70 mV remained unaffected even in the presence of 3 μM oxo-M (after accounting for the leak conductance by extrapolating a straight line from the linear conductance at more hyperpolarized potentials). However, percent reduction of steady-state current between -32 mV and -60 mV by 300 nM and 3 μM oxo-M accorded well with inhibition of $I_{K(M)}$ deactivation currents (at around -55 mV), suggesting that the main effect of oxo-M on steady-state current, between -70 and -20 mV, is due to inhibition of $I_{K(M)}$. Although current at potentials more depolarized than -70 mV was more sensitive to oxo-M, smaller effects were observed at potentials more hyperpolarized than the activation threshold for $I_{K(M)}$. Thus, at between -65 mV and -130 mV, oxo-M (300 nM and 3 μM) caused inward currents of variable amplitude, ranging from -41 to -133 pA (measured at -70 mV). A similar effect of muscarinic receptor agonists at these membrane potentials has previously been reported in frog sympathetic neurones (Jones, 1985): in addition to inhibiting M-current, muscarine and peptides evoked an apparently voltage-insensitive inward current (associated with an increase in conductance) having an extrapolated null potential close to 0 mV, and which may be a Na^+ conductance. In frog neurones, this inward current was slower in onset

and offset than M-current inhibition, generally required higher concentrations of agonist than those required for M-current inhibition (although this was somewhat unpredictable), and could be evoked during the slow EPSP. In rat sympathetic neurones, muscarine caused an apparent *outward* current in addition to the apparent inward current resulting from $I_{K(M)}$ inhibition (Brown and Selyanko, 1985a). This outward current was attributed to the reduction of an inward Cl^- current, and inhibition of this current by muscarine led to hyperpolarization and decreased neuronal excitability (the opposite to the inward current activated by muscarine in frog neurones). Also in rat sympathetic neurones, an inward current resulting from a voltage-independent conductance increase, with a reversal potential close to 0 mV, was occasionally observed by Marrion *et al.* (1987). In the present experiments using rat sympathetic neurones, the additional component of current activated by muscarine and seen at hyperpolarized potentials is also inward. Typically, these inward currents are less than 100 pA in amplitude, and so this may have less impact on SCG cell excitability than $I_{K(M)}$ inhibition, as has been observed for the inward current in frog sympathetic neurones (Jones, 1985), where these inward currents are in fact larger than the inward currents seen in rat sympathetic neurones. Concurrent activation of inward current and inhibition of the Cl^- current (Brown and Selyanko, 1985a) may underlie the small size and variable properties of the response to oxo-M at more hyperpolarized potentials.

The small (10-15 mV) shift in the zero current potential by 3 μM oxo-M suggests that M-channels may be open at the zero current potential in rat sympathetic neurones, in contrast to the situation in frog sympathetic neurones (Jones, 1989) and NG108-15 cells (Robbins *et al.*, 1992), although the shift may be due to activation of the voltage-insensitive inward current described above. Concerning this, it is notable that estimates of the zero current potential of cells following whole-cell recordings, during which $I_{K(M)}$ considerably declined, were not significantly different from estimates from those cells in which $I_{K(M)}$ was maintained (perforated patch recordings; see Chapter 3), suggesting that $I_{K(M)}$ does not make a significant contribution to the zero current potential.

4.3.1.2. Rate of response.

Inhibition of $I_{K(M)}$ by muscarinic receptor agonists involves G protein activation (Brown, 1988a) and a diffusible messenger (Selyanko *et al.*, 1992; Marrion, 1993) which, however, may be the G protein α-subunit, as no other candidate has yet been assigned this role without reserve. Using a rapid delivery perfusion system, the onset latency and half-time to maximum effect in response to 3 μM oxo-M has been determined from the decrease in the standing outward current at depolarized potentials (using high $[K^+]_{ec}$ for an estimate of the efficiency of the perfusion system). In initial experiments, the decrease in outward current at the depolarized holding potential and the decrease in amplitude of $I_{K(M)}$ deactivation relaxations during the voltage step were measured every 10 s during application of oxo-M. There was a good correlation in the onset and development of both of these events, with a latency in onset of under 10 s and both events reaching full development within 10 s to 30 s. Subsequently, the continuous change in current at the holding potential in response to oxo-M was monitored in order to provide estimates of these parameters. From these experiments, the response to oxo-M showed an onset latency of 3.7 s (the response to a switch to high $[K^+]_{ec}$ showed a latency of 2.2 s; this probably represents the lag time in the perfusion system). The half-time for the development of the response to oxo-M was 7.5 s (1.9 s for high $[K^+]_{ec}$). Thus, the actual times for latency and development, at 23 °C, were probably close to 1.5 s and 5.5 s respectively. This estimate of onset latency is very close to that obtained for the latency of $I_{K(M)}$ inhibition by ACh in NG108-15 cells (around 1.7 s at 23 °C, after accounting for the latency of $I_{K(M)}$ inhibition in response to Ba^{2+} ions: Robbins *et al.*, 1993). However, the onset latency is much longer than the latency of slow excitatory postsynaptic currents in the rat SCG in response to preganglionic stimulation, which attain peak amplitude within 2 s (Brown and Selyanko, 1985b). A likely explanation for the slow onset of the response in the present study is the dependence of $I_{K(M)}$ inhibition on temperature: Brown and Selyanko (1985b) performed their experiments at 30 °C. Furthermore, Robbins *et al.* (1993) found that increasing the temperature from 23 °C to 35 °C shortened the onset latency of $I_{K(M)}$ inhibition by ACh from around 1.7 s to 270 ms in NG108-15 cells. An additional consideration is that, in the present study, a maximally effective concentration of oxo-M was used (rather than supramaximal, such as might be expected

at the synapse following neurotransmitter release); thus, assuming a receptor reserve, the rate of $I_{K(M)}$ inhibition is probably less than maximum under these conditions (this has also been considered by Jones, 1991), with respect to the rate of $I_{K(M)}$ inhibition by agonists in frog sympathetic neurones). The estimates of onset latency and development in the present study are approximate because, as described above, oxo-M also activates an additional component of inward current at high concentrations in some cells, and this has not been isolated from the $I_{K(M)}$ inhibition for these experiments.

4.3.2. G proteins mediating inhibition of $I_{K(M)}$ by oxo-M.

It is established that muscarinic receptor-mediated inhibition of $I_{K(M)}$ in sympathetic neurones is mediated by a G protein belonging to the PTX-insensitive class (reviewed by Brown, 1988a and Bosma *et al.*, 1990). Therefore, possible G protein candidates for transducing this effect include α or $\beta\gamma$ subunits of the G_q or G_{12} families of PTX-insensitive G proteins, or G_z (Simon *et al.*, 1991).

4.3.2.1. $G_{\alpha q/11}$ involvement: studies with anti-G protein antibodies.

The PTX-insensitive G proteins $G_{\alpha q}$ and $G_{\alpha 11}$ mediate a number of functional responses including PLC stimulation in endogenous (Gutowski *et al.*, 1991; Aragay *et al.*, 1992), transfected/ transiently expressed (Lee *et al.*, 1992; Wu *et al.*, 1992; Lipinsky *et al.*, 1992), and reconstituted (Taylor *et al.*, 1991; Berstein *et al.*, 1992) systems, and modulation of membrane conductance leading to excitatory (ffrench-Mullen *et al.*, 1994: inhibition of I_K) and inhibitory (Wilk-Blaszczak *et al.*, 1994: activation of $I_{K(Ca)}$) effects. Other members of the class of PTX-insensitive G proteins ($G_{\alpha 12}$ through $G_{\alpha 16}$ and $G_{\alpha z}$) have less commonly been implicated in mediating functional responses, but probably do, including activation of certain isozymes of PLC ($G_{\alpha 14}$ and $G_{\alpha 16}$: Lee *et al.*, 1992; constitutively activated mutant α16: Schnabel *et al.*, 1992), and activation of Na^+/ H^+ exchanger (constitutively active mutant $G_{\alpha 12}$ (PKC-dependent) and $G_{\alpha 13}$ (PKC-independent): Dhanasekaran *et al.*, 1994). Likewise, the significance of the $\beta\gamma$-subunit as opposed to the α-subunit of the G protein trimer in transducing receptor-mediated effects is less widely established, but possibly has a

functional role (Clapham and Neer, 1993: see Chapter 1). In the present experiments, anti-$G_{\alpha q/11}$ antibody has been used to identify another functional role for one or both of these homologous G protein α-subunits, in transducing inhibition of $I_{K(M)}$ following muscarinic receptor activation. The submaximal inhibition of $I_{K(M)}$ by 300 nM oxo-M was significantly reduced by microinjection of anti-$G_{\alpha q/11}$ antibody in two experimental series (and using antibodies raised in two different rabbits). In contrast to this effect, an antibody recognizing the $G_{\alpha o}$ subunit did not affect muscarinic $I_{K(M)}$ inhibition. This cannot be attributed to functional inactivity of the anti-$G_{\alpha o}$ antibody, as this antibody does significantly reduce inhibition of voltage-gated Ca^{2+} current by noradrenaline in rat sympathetic neurones cultured under the same conditions; conversely, the anti-$G_{\alpha q/11}$ antibody has no effect on this latter response (Caulfield *et al.*, 1994). As both antibodies recognize the C-terminal decapeptide sequence of the G protein α-subunits, believed to be the site of receptor-G protein interaction (Weiss *et al.*, 1988), this suggests that the anti-$G_{\alpha q/11}$ antibody selectively uncouples muscarinic receptors from the G protein (presumably $G_{\alpha q}$, $G_{\alpha 11}$ or both) transducing $I_{K(M)}$ inhibition, while the anti-$G_{\alpha o}$ antibody selectively uncouples adrenergic receptors from the G protein (presumably $G_{\alpha o}$) transducing inhibition of voltage-gated Ca^{2+} current. It is unlikely that the injection procedure itself caused this effect on agonist-evoked changes in membrane conductance, as injection of a control antibody, anti-GFAP antibody, had no significant effect on either response.

Anti-$G_{\alpha q/11}$ antibody had no effect on the amplitude of control $I_{K(M)}$ deactivation relaxations (recorded prior to agonist application) during the voltage step (see Chapter 2), indicating that there is no substantial basal modulation of $I_{K(M)}$ by unoccupied receptor-$G_{\alpha q/11}$ interaction. However, this does not exclude the possibilities that G protein alone, or unoccupied receptor interacting with an alternative G protein exert a tonic influence on $I_{K(M)}$ (although such an effect is unlikely to come from unoccupied receptor interacting with $G_{\alpha o}$, as the antibody to this G protein was also without effect on $I_{K(M)}$ deactivation amplitude). Moreover, antibody injections *per se* had no consistent effect on the time constants for $I_{K(M)}$ deactivation relaxations, although a significant difference in the fast time constant was detected in the first series of anti-

$G_{\alpha q/11}$ antibody injections, when compared with uninjected (but not with anti-GFAP antibody-injected) controls.

These data suggest that a substantial proportion (and in some cells, all) of the effect of oxo-M on $I_{K(M)}$ is transduced by either $G_{\alpha q}$, $G_{\alpha 11}$ or a combination of these closely related G proteins. However, due to the variable effect observed with the anti-$G_{\alpha q/11}$ antibody, the involvement of additional G proteins in transducing this response cannot be excluded. Possible candidates include other PTX-insensitive G protein α-subunits such as $G_{\alpha z}$, which is found in neurones, $G_{\alpha 12}$ or $G_{\alpha 13}$, which are ubiquitous (Simon *et al.*, 1991), and βγ-subunits, as has been implicated in the muscarinic receptor-activation of $I_{K(ACh)}$ in atrial cells, and inhibition of voltage-gated Ca^{2+} currents by muscarinic and somatostatin receptors in GH_3 pituitary cells (Clapham and Neer, 1993). It should be noted that muscarinic receptor-mediated inhibition of $I_{K(M)}$ is completely PTX-insensitive (Brown *et al.*, 1989); therefore, as PTX locks both the α- and the βγ-subunits into their inactive states (Clapham and Neer, 1993), any involved βγ-subunits must be supplied by another PTX-insensitive G protein. However, the possibility that muscarinic receptors may alter their coupling preference when levels of the (preferred) functional G protein are reduced, and switch to using a PTX-sensitive G protein (either α- or βγ-subunits, or both) to inhibit $I_{K(M)}$ cannot be ignored. This could have been tested by incubating cells in PTX prior to injections of anti-$G_{\alpha q/11}$ antibody. Other explanations for this variable effect of the antibody are discussed below.

4.3.2.2. Variable effect of anti-$G_{\alpha q/11}$ antibody.

A striking observation during the first series of experiments with anti-G protein antibodies (in which injection was verified by post-immunostaining) was the variability of the effect of the anti-$G_{\alpha q/11}$ antibody. Thus, in some anti-$G_{\alpha q/11}$ antibody-injected cells, the $I_{K(M)}$ inhibition in response to 300 nM oxo-M was within control limits, in other cells the response to oxo-M was strongly reduced, and in yet other cells the response was completely blocked. All SCG cells injected with antibody were left for approximately 2 h: the variability of effect showed no dependence on the time of

recording after this 2 h incubation period. Nor was there any correlation of the variability with a given culture: variable antibody effects were observed in all cultures tested, and by both experimenters (SJ and MPC). It was considered that the most likely source of this variation was the injection procedure, with variable amounts of antibody being injected, as the success of the injection was monitored after, rather than during the procedure. In a subsequent series of experiments (carried out by SJ only), antibodies were co-injected with a fluorescent marker (a high molecular weight dextran linked to fluorescein isothiocyanate) so that the injection could be monitored on-line by injecting the cells with the aid of a fluorescence microscope, and aiming to achieve approximately the same intensity of fluorescence in each cell. In these experiments, the variability was reduced (for example, the group distributions were not significantly different in these experiments, allowing parametric statistical tests to be used), but was not entirely abolished: responses still ranged from small reductions to complete block. The co-injection method is not a quantitative method for determining the amount of antibody injected per cell and it is likely that only a quantitative method, for example using a fluorescently-labelled antibody, quantifying the fluorescent signal and relating this to the reduction in response, will reveal the true nature of the variability of the antibody effect: that is, whether it stems from the methodological procedure, or whether it is a genuine phenomenon. A possible source of the incomplete blocking effect of the antibody in many cells is a low titre of anti-$G_{\alpha q/11}$ antibody in the antiserum. Using more purified preparations (such as IgG fractions or affinity purified $G_{\alpha q/11}$ antibody) may have overcome this; however, the purification process can itself introduce problems due to the loss of the active component of the antiserum on affinity columns. Different dilutions of antiserum were not tested, as it would have been difficult to distinguish a genuine effect of increasing dilution from the variability of the effect of the anti-$G_{\alpha q/11}$ antibody. However, this may have provided useful information in determining whether the maximum effect of the antibody had been achieved when using the antiserum: for example, if a small dilution had produced a substantial decrease in the effect of the antibody, then it would suggest that the maximum effect was not attained with the undiluted antiserum.

A genuine variability of antibody effect would not be entirely inexplicable. It is possible that different populations of SCG neurones utilize different PTX-insensitive G proteins to transduce $I_{K(M)}$ inhibition (such as other members of the G_q family or members of the G_{12} family: Simon *et al.*, 1991). Alternatively, differing levels of $G_{\alpha q}$ and $G_{\alpha 11}$ may be expressed in different SCG cells. These possibilities are discussed further in Chapter 6. It is notable that in initial experiments using antisense DNA, the anti-$G_{\alpha 11}$ sequence also had a variable effect on $I_{K(M)}$ inhibition by 300 nM oxo-M, although these data are less reliable for the reasons discussed below.

partial
4.3.2.3. Surmountable effect of anti-$G_{\alpha q/11}$ antibody.

Oxo-M, at a concentration of 300 nM, caused a submaximal inhibition of $I_{K(M)}$ in uninjected SCG neurones. As described above, this effect of oxo-M was reduced or blocked, to varying degrees, by anti-$G_{\alpha q/11}$ antibody. In some cells injected with this antibody, and exhibiting reduced responses to oxo-M, higher concentrations (maximally effective in uninjected cells) of oxo-M were applied to determine whether the effect of the antibody on the response to oxo-M was surmountable on increasing the concentration of agonist. In all anti-$G_{\alpha q/11}$ antibody-injected cells tested, increasing the concentration to 3 μM or higher produced more inhibition of $I_{K(M)}$ than that seen with 300 nM. The inhibition of $I_{K(M)}$ in response to 3 μM was dependent on the extent to which the response to 300 nM oxo-M was reduced. Thus, in antibody-injected cells showing a completely *blocked* response to 300 nM oxo-M, only a small recovery of the inhibition was observed in response to 3 μM. However, in antibody-injected cells showing *reduced* responses to 300 nM oxo-M, more substantial inhibitions were obtained on increasing the concentration to 3 μM.

These observations suggest that surmountability may depend on the extent of loss of G protein from the system, which is consistent with the theoretical proposals of Kenakin and Morgan (1989) on the effects of reducing the levels of G protein transducing a response in which one type of receptor (in this case, M_1) couples to one type of G protein (in this case, $G_{\alpha q/11}$). Surmountability can be explained in the following scheme, where agonist-occupied (active) receptor interacts with G protein to

reduce the frequency of M-channel opening ($\downarrow f_{open}$: by increasing the shut time; Selyanko and Brown, 1993):

$$A + R \rightleftharpoons AR \rightleftharpoons AR^* + G \rightleftharpoons AR^*G \rightarrow G^* \rightarrow \text{M-channel} \rightarrow \downarrow f_{open}$$

Thus, an increase in AR* (active, agonist-occupied receptor) will lead to an increase in AR*G (receptor-G protein complexes) and therefore G* (active G protein), leading to a decrease in the frequency of channel opening. In rat sympathetic neurones, the interaction between AR* and G was decreased by using antibody to uncouple these components of the reaction scheme, and the measured result of this was less inhibition of $I_{K(M)}$ for a given concentration of agonist (300 nM oxo-M). The observation that addition of more agonist-occupied receptor to the equilibrium increased the inhibition of $I_{K(M)}$ suggests that there is a spare G protein capacity available for transducing this response (thus, in the above scheme [G] > > [M-channel], if G can interact directly with the channel, and assuming that all of the G protein population has access to the channels, or that G inhibits M-channel *via* a second messenger, which provides access for all of the G protein population to the channel). Therefore, a small decrease in G protein would cause a rightward shift of the concentration-response curve, but no decrease in the maximum response, in accord with the predictions of Kenakin and Morgan (1989). However, the G protein reserve is finite (possibly to different extents in different SCG neurones), and can be exhausted with sufficient amounts of antibody so that further increases in AR* are ineffective, and the antibody effect becomes insurmountable: the maximum response is now depressed. Of course, the incomplete blocking effect of the antibody may, in this model, be attributed to a reduction of the affinity of AR* for G rather than a total block of this interaction. Although obtaining full concentration-response curves in cells injected with variable amounts of antibody would be the true test of this model, the limited data certainly support these theoretical proposals. However, for a "promiscuous" receptor (one that couples to more than one G protein to produce a given response, proposed as a possibility for muscarinic-inhibition of $I_{K(M)}$ in section 4.3.2.1. as one explanation for the variable effect of the anti-$G_{\alpha q/11}$ antibody), the model of Kenakin and Morgan predicts that reducing the level of one G protein would cause a rightward shift in the concentration response curve with

no decrease in the maximum response. The application of this model to the present data would therefore require that in at least some SCG cells tested, M_1 receptors can couple only to $G_{\alpha q/11}$, and that the variability of the effect of the anti-$G_{\alpha q/11}$ antibody is due to either different amounts of antibody being injected, or different levels of expression of $G_{\alpha q/11}$ in different cells, rather than to the ability of muscarinic receptors to couple to alternative G proteins.

A considerable disadvantage of studies using antibodies to probe G protein function is the limited selectivity which (for example) in the present experiments precludes the definition of the precise G protein ($G_{\alpha q}$ or $G_{\alpha 11}$) mediating muscarinic-inhibition of $I_{K(M)}$. An alternative approach (and one adopted in this study) is to use antisense oligodeoxynucleotides (ODNs) to suppress expression of specific G protein subunits at the nucleic acid level.

4.3.2.4. Studies with G protein antisense DNA

A number of studies have now successfully utilized antisense oligodeoxynucleotides (ODNs) to remove specific elements of neurotransmitter activated pathways: at the level of the receptor for ligand-gated (Listerud *et al.*, 1991) and G protein-linked (Standifer *et al.*, 1994) responses, and at the level of the G protein (Kleuss *et al.*, 1991, 1992 and 1993; Campbell *et al.*, 1993; ffrench-Mullen *et al.*, 1994; Shapira *et al.*, 1994: see Chapter 1). In the present experiments, anti-G protein ODNs were used in an attempt to selectively suppress expression of $G_{\alpha q}$ or $G_{\alpha 11}$. The $G_{\alpha 11}$ ODN (605a) caused a significant reduction in $I_{K(M)}$ inhibition by 300 nM oxo-M between 10 and 30 h, with a peak reduction at 15 to 20 h. In contrast with this, parallel experiments with $G_{\alpha q}$ ODN (485a) showed a smaller but significant reduction in $I_{K(M)}$ inhibition by oxo-M between 10 to 15 h. These data suggested that $G_{\alpha 11}$ antisense DNA caused a decrease in the synthesis of this protein, and subsequent loss of responses transduced by $G_{\alpha 11}$, which includes $I_{K(M)}$ inhibition, whereas a decrease in the synthesis of $G_{\alpha q}$ had only a small and short-lasting effect on $I_{K(M)}$ inhibition. Unfortunately, it was not possible to measure changes in the level of proteins following incubation with anti-G protein antisense DNA, as the antibodies used

in functional experiments exhibited non-specific binding in immunohistochemistry studies, and this could not be reduced to give a signal/ noise ratio sufficiently sensitive for detecting changes in G protein expression (Y. Vallis, personal communication). Therefore it is possible that under our conditions, $G_{\alpha q}$ ODN (485a) caused only small changes in G protein levels, or that $G_{\alpha q}$ and $G_{\alpha 11}$ exhibit differences in their rates of turnover, making them differentially sensitive to incubation times (incubation times of up to 30 h only were investigated in these experiments).

Before further investigating different incubation times for the two antisense sequences, a different $G_{\alpha 11}$ ODN (499a) was used to confirm that this was a selective effect of the $G_{\alpha 11}$ antisense sequence. However, in this second series of experiments, $G_{\alpha 11}$ ODN (499a) had no effect on $I_{K(M)}$ inhibition by 300 nM oxo-M after 15 to 25 h incubation compared with the corresponding $G_{\alpha 11}$ sense ODN used in parallel. When cells were incubated in the original (effective) anti-$G_{\alpha 11}$ ODN (605a), it was also without effect. The reason for this loss of effectiveness is unknown. It is possible that a small change in tissue culture conditions (or in the condition of the animals) could have radically changed the uptake of antisense ODNs into the cells, the removal of ODNs from the cell, sequestration to the nucleus, binding with target nucleic acid, metabolism of ODNs (see Chapter 1) or rate of synthesis and metabolism of the G proteins themselves. All of these possibilities require careful investigation at the molecular level. It seems less likely that the original effect of the $G_{\alpha 11}$ ODN was non-selective or artefactual, as the experiments were tightly controlled (performed and analyzed "blind", in paired experiments), and because the same sequences have also been shown to reduce the muscarinic receptor-inhibition of delayed rectifier K^+ current in ventromedial hypothalamus neurones (ffrench-Mullen *et al.*, 1994). However, despite an initial indication in favour of $G_{\alpha 11}$, rather than $G_{\alpha q}$ being the principal G protein mediating muscarinic-inhibition of $I_{K(M)}$, it is at present unwise to place any emphasis on these data.

4.3.3. Putative second messenger pathways.

The identity of the G protein transducing a response can provide some clue as to the nature of any second messengers involved. In rat sympathetic neurones, cell attached patch single channel recordings have implicated the involvement of a diffusible messenger in mediating inhibition of M-channel activity by muscarine (Selyanko *et al.*, 1992). This suggests that activation of G protein by muscarinic receptors may lead to the generation of a second messenger, and therefore raises the question of the identity of this putative messenger (although the diffusible messenger could be the G protein α-subunit). G proteins which are insensitive to PTX-pretreatment, including $G_{\alpha q}$ and $G_{\alpha 11}$, are established activators of phospholipase C (reviewed by Sternweis and Smrcka, 1992; and see Chapter 1), which leads to the production of a number of signalling messengers including inositol 1,4,5-trisphosphate (IP_3) and diacylglycerol (DAG) followed by increased intracellular levels of Ca^{2+} and activation of protein kinase C (PKC), thereby initiating Ca^{2+}-dependent enzyme and ion channel activity and phosphorylation reactions. Of particular significance to the present observations is the demonstration by Berstein *et al.* (1992) that $G_{\alpha q/11}$ can couple m1 muscarinic receptors (which mediate muscarinic $I_{K(M)}$ inhibition in SCG neurones) to PLC in a reconstituted system. Additionally, different isoforms of PLC can be activated by different members of the PTX-insensitive class of G proteins (Lee *et al.*, 1992: αq and α11 compared with α16 in activating PLCβ isozymes; Wu *et al.*, 1992: αq and α11 compared with αz in activating PLCβ1; see Chapter 1), as well as by βγ-subunits (Camps *et al.*, 1992; Katz *et al.*, 1992). Thus, M_1 receptors could conceivably couple to more than one PTX-insensitive G protein in some SCG neurones and activate more than one isoform of PLC, leading to $I_{K(M)}$ inhibition and possibly other cellular effects, such as inhibition of voltage-gated Ca^{2+} current, which can also be evoked by M_1 receptor activation (Bernheim *et al.*, 1992).

Further inferential evidence that a PLC product may be the intracellular messenger produced by $G_{\alpha q/11}$ activation comes from reports that muscarinic receptors trigger phosphoinositol turnover in the rat SCG (Bone *et al.*, 1984; Patterson and

Volle, 1984; Horwitz *et al.*, 1985) and therefore these receptors are clearly capable of activating PLC. Moreover, in the neuroblastoma cell line, NG108-15 cells, which also express M-type K^+ currents, transfection of muscarinic receptor subtypes which mediate IP_3 production (m1 and m3, but not m2 and m4) also couple preferentially to inhibit $I_{K(M)}$ (Fukuda *et al.*, 1988; Robbins *et al.*, 1991).

Studies which have directly tested the hypothesis that a product of PLC activation mediates muscarinic-inhibition of $I_{K(M)}$ have been numerous, and carried out in a range of preparations of central and peripheral neurones (see Chapter 1). In rat sympathetic neurones, as in others, there is no convincing evidence for any of the known second messengers mediating this effect, including either pathway triggered by PLC activity. There is no positive evidence in favour of IP_3 in mediating $I_{K(M)}$ inhibition (Brown *et al.*, 1989), although a critical level of Ca^{2+} is a requirement for $I_{K(M)}$ inhibition in rat sympathetic neurones (Beech *et al.*, 1991). The other pathway, involving DAG-PKC activation, also remains equivocal. Many studies, employing many different recording conditions have now contributed to the wealth of information on the transduction mechanism for $I_{K(M)}$ inhibition. Unfortunately, this can sometimes provide a rather bewildering array of possibilities (and contradictions) so that it is often difficult to know if the second messenger really is a hitherto unknown species, or whether a more obvious candidate has remained elusive in the conditions used for electrophysiological studies. A re-evaluation of the methods used to identify the diffusible messenger utilized (Selyanko *et al.*, 1992), either as a second messenger or a G protein subunit (and with the present information regarding the identity of G proteins transducing this response), may be required. With the availability of improved techniques for raising concentrations of intracellular messengers (such as Ca^{2+} and IP_3 from "caged" precursors), along with the perforated patch recording method (this would therefore require that such agents be introduced into cells by microinjection, rather than patch loading, which is now clearly feasible), which allows minimum disturbance of the cell interior during whole-cell recordings, it may still be possible to pin-point the elusive messenger.

4.3.4. Conclusions to Chapter 4.

The muscarinic agonist, oxotremorine-M inhibits $I_{K(M)}$ in rat cultured sympathetic neurones. This effect is reproducible, readily reversible and develops with a half-time of around 5 s. Oxo-M has an additional effect on membrane conductance in rat SCG neurones which has not been characterized in this study. Oxo-M inhibits $I_{K(M)}$ by activating $G_{\alpha q}$ and/ or $G_{\alpha 11}$ (although other G protein subunits may be activated and participate in this response in addition to either or both of these). Antibody raised against these G protein α-subunits caused a variable and surmountable attenuation of the muscarinic response. Experiments with antisense DNA were less successful than experiments with antibodies, although initial data implicated $G_{\alpha 11}$, rather than $G_{\alpha q}$ in transducing muscarinic receptor mediated $I_{K(M)}$ inhibition. These findings provide information about a further step in the mechanism by which muscarinic receptors inhibit $I_{K(M)}$ (and excite SCG neurones), and it is hoped that they will provide some clues as to the identity of subsequent signalling messengers involved in $I_{K(M)}$ inhibition.

CHAPTER 5:

A novel effect of bradykinin on sympathetic ganglion neurones: inhibition of $I_{K(M)}$ *via* $G_{\alpha q/11}$ proteins.

5.1. INTRODUCTION.

The properties of the M-type K^+ current ($I_{K(M)}$) and its modulation in various neuronal preparations, including cultured sympathetic neurones of the rat SCG, by receptors which couple to G proteins have been described in the preceding chapters. Muscarinic receptor agonists and angiotensin II have previously been shown to inhibit $I_{K(M)}$ in rat sympathetic neurones (Constanti and Brown, 1981; Shapiro *et al.*, 1994); no other receptor-G protein activated pathways for $I_{K(M)}$ inhibition have been demonstrated in rat sympathetic neurones. In this chapter, a new pathway for inhibition of $I_{K(M)}$ by the peptide bradykinin is described.

5.1.1. Synthesis and metabolism of BK.

Kinins, including bradykinin (BK), are peptides with potent biological activity. The synthesis and metabolism of kinins has been reviewed in detail by Bhoola *et al.* (1992). Kinins are released from large precursor proteins, kininogens, by kininogenases such as plasma and tissue kallikreins. Plasma kallikrein circulates in an inactive form, prekallikrein, which is bound to high molecular weight kininogen, and plasma kinin levels are low in normal states. Formation of kallikrein is associated with activation of the blood clotting cascade, leading to the release of BK from the high molecular weight kininogen. A low molecular weight kininogen is found in various tissues and is the substrate for tissue kallikrein, leading to release of kallidin. The actions of BK are limited by proteolytic enzymes, including peptidases, kininases and converting enzymes (Regoli, 1987) and so BK acts locally, close to the site of release (Dray and Perkins, 1993). However, enzymes acting at the N-terminal do not efficiently quench kinin activity, as they generate the BK metabolite, [des-Arg^9]-BK, which itself has biological activity.

5.1.2. BK receptors.

Two major BK receptor subtypes (B_1 and B_2) were first characterized by Regoli and colleagues in the 1970s on the basis of BK receptor agonist potency in a range of tissues (reviewed by Regoli and Barabé, 1980). The development of selective antagonists has substantiated this classification (reviewed by Hall, 1992). The functional importance of the B_2 subtype in mediating effects of BK on many tissues including sensory neurones is well established, although the role of the B_1 receptor is less well understood as it has a restricted distribution (Hall, 1992; Dray and Perkins, 1993). Both subtypes have now been cloned (McEachern *et al.*, 1991; Hess *et al.*, 1992; Menke *et al.*, 1994), and both have the characteristic structure of receptors that couple to G proteins.

5.1.3. BK and sympathetic nerves.

5.1.3.1. Sympathetic nerves and pain.

BK has a well-established role in inflammation (Lewis, 1970; Regoli, 1987) and pain (Armstrong, 1970; Hall, 1992), and there has been substantial interest in the interaction of BK with sensory nerves, particularly the significance of this interaction in inflammatory pain (see Hall, 1992 for a comprehensive review). There is now evidence that BK can also interact with sympathetic nerves, and that the sympathetic nervous system has a significant role in both pain and inflammation. For example, while in normal states sympathetic postganglionic nerve activity does not stimulate nociceptor activity or produce pain, "sympathetically maintained pain" (SMP) has been diagnosed in some states of chronic pain in humans. In such conditions, sympathetic nervous function is abnormal (for example, irregular vascular control), and alteration of sympathetic activity, for example using adrenergic drugs or by sympathectomy, modifies the pain of the patient (McMahon, 1991). Hypotheses for the underlying mechanisms of SMP have mainly arisen from animal models, which probably do not accurately reproduce the clinical state. The general concept that has been proposed is that SMP is a cycle of events starting with injury to sensory neurones which is then detected by spinal neurones, causing an alteration in neuronal function in the CNS,

which in turn modifies sympathetic nerve responses. This whole cycle is believed to enter a positive feedback system, amplifying the original sensory abnormality. Explanations as to how this cycle is initiated and maintained include the concept that nociceptive sensory neurones upregulate their expression of adrenergic receptors, thus suggesting a *direct* interaction between sympathetic and sensory neurones *via* noradrenaline release; and an *indirect* coupling between these nerves *via* the production of intermediary agents such as prostaglandins. All hypotheses proposing a peripheral site of initiation fail to explain many of the features of SMP, and for this reason there has also been interest in possible CNS changes which may contribute to this condition. So far, no single hypothesis has adequately explained all of the symptoms experienced by SMP patients (see McMahon, 1991 for a review of SMP).

The possible involvement of BK in sympathetic nerve-dependent pain has been highlighted by studies on the interaction between sympathetic and sensory neurones. Levine *et al.* (1986) demonstrated that BK-induced hyperalgesia (represented by changes in pressure nociceptive thresholds) in the rat was abolished by sympathectomy, indicating that BK sensitizes sensory neurones to pressure stimulation by acting on sympathetic nerve terminals. In a subsequent study, Levine and colleagues reported that BK could release prostaglandins from sympathetic nerve terminals (measured by a BK-induced, indomethacin-sensitive increase in plasma extravasation into the knee joint) as this response was abolished by sympathectomy (Coderre *et al.*, 1989), suggesting an *indirect* interaction between sympathetic and sensory nerves *via* the release of inflammatory mediators. However, this has been challenged following the observations of Cambridge and Brain (1994), who reported that chemical sympathectomy in rats led to an *increase* in BK-induced plasma extravasation in the knee joint. Interestingly, BK has also been reported to release noradrenaline from postganglionic sympathetic nerves in the rat knee joint (Green *et al.*, 1993) and in the rat vas deferens (Llona *et al.*, 1991), and from noradrenergic terminals in the spinal cord (which in fact has an antinociceptive effect; Laneuville *et al.*, 1989), and hypothalamic slices (Tsuda *et al.*, 1993). The ability of BK to release noradrenaline would support a role for BK in triggering *direct* interaction between sympathetic and sensory neurones expressing upregulated adrenergic receptors (see above). However,

not all models of BK-induced hyperalgesia are sympathetic nerve-dependent: sympathectomy had no effect on BK-sensitization of cutaneous thermal nociceptors in a rat *in vitro* preparation (Koltzenburg *et al.*, 1991); similarly, in a human subject who underwent sympathectomy, there was no effect on bradykinin-induced cutaneous pain and hyperalgesia to heat stimuli (Meyer *et al.*, 1992). It should also be noted that BK has been shown to *inhibit* nerve-stimulated noradrenaline release from sympathetic nerves innervating pulmonary artery and heart tissue in *in vitro* assays (Starke *et al.*, 1977).

Interaction between BK and sympathetic nerves in inflammatory states has also been proposed. In addition to releasing prostaglandins, sympathetic neurones can respond to immunological stimuli to produce cytokines such as interleukin-1 (Miller Jonakait, 1993); the same stimuli can also induce expression of B_1 BK receptors in some tissues (see Hall, 1992). It has been proposed that B_1 receptors become functionally significant during pathological states, such as chronic inflammation, and the possibility of interactions between sympathetic nerves, B_1 receptors, cytokines, and inflammatory cells in such conditions have been considered by Dray and Perkins (1993), although further information is required to substantiate these proposals.

In summary, there is now evidence that sympathetic nerves can contribute to inflammation and pain perception, although this is by no means a universal finding. There is potential for an interaction between BK and sympathetic nerves in both of these conditions, although the details and significance of such an interaction *in situ* require further clarification.

5.1.3.2. BK-induced excitation of sympathetic nerves.

Using electrophysiological recording methods, BK has been demonstrated to cause excitation of sympathetic neurones. Excitation of the cat superior cervical ganglion (SCG) by BK was first reported by Lewis and Reit (1965), who used the spinal cat preparation to demonstrate that BK-induced contractions of the nictitating membrane depended on the presence of the intact SCG, particularly the postganglionic trunk. They subsequently demonstrated a weaker ganglion-stimulating action of BK on

SCG in the dog and the rabbit (Lewis and Reit, 1966). Extracellular recording from the cat SCG revealed small and inconsistent depolarizing responses to BK (Haefely, 1970), although BK did evoke postganglionic firing in sensitive animals. When the action of BK on rabbit SCG was further investigated using an excised, intact ganglion preparation and extracellular recording (Wallis and Woodward, 1974), small and variable depolarizations were again observed, although BK did increase the amplitude of the postsynaptic action potential in response to a single stimulus. Thus, electrophysiological studies show that BK is certainly capable of stimulating sympathetic nerves *in vivo* and *in vitro*, although whether (and how) these effects relate to the role of sympathetic nerves in inflammation and pain is not yet known.

5.1.3.3. Mechanism of excitation of sympathetic nerves.

In sensory neurones, where the obvious relationship to pain and hyperalgesia has provoked great interest, much attention has been given to the mechanisms of BK-excitation of sensory nerves. The introduction of cultured neurones from the dorsal root ganglion by Baccaglini and Hogan (1983) has aided studies on sensory mechanisms which underlie pain processing. In DRG neuronal cultures, mechanisms of BK-induced excitation have been investigated using voltage-clamp techniques, and BK-evoked depolarization has been attributed to activation of an inward Na^+ (or cation) current (Burgess *et al.*, 1989; Dunn and Rang, 1990). There is some evidence for inhibition of K^+ conductances by BK in cultured DRG neurones, which would also contribute to neuronal excitation (Lindsay and Rang, 1987). All of the excitatory actions of BK on ionic conductances in sensory neurones appear to involve activation of second messenger systems, notably PKC (Burgess *et al.*, 1989; Dray *et al.*, 1988; McGuirk and Dolphin, 1992). On the whole, available data suggests that BK receptors can couple to pertussis toxin-insensitive and -sensitive G proteins (Millar, 1987; Hall, 1992 for reviews) to modulate ion channels in sensory neurones.

Unlike the situation in sensory neurones, the mechanism by which BK excites sympathetic neurones has not been investigated, although the recent demonstration that BK augments a PKC-regulated, depolarizing Cl^- current in rat sympathetic neurones (Marsh *et al.*, 1994) is one possible mechanism. The lack of information is perhaps

surprising in view of the fact that the effects of BK have been researched in considerable detail in certain cell lines exhibiting many similar characteristics to sympathetic neurones. Thus in NG108-15 cells, BK causes a biphasic change in membrane potential, with slow depolarization following an initial hyperpolarization (Reiser and Hamprecht, 1982; Yano *et al.*, 1984). Higashida and Brown (1986) demonstrated that the depolarizing action of BK is due to inhibition of the M-type K^+ current, and that this effect of BK on $I_{K(M)}$ could be mimicked by activators of PKC, suggesting that in NG108-15 cells, as well as in sensory neurones, BK receptors can activate PLC to bring about changes in membrane conductance. A partial role for PKC in mediating BK inhibition of $I_{K(M)}$ has also been inferred using whole-cell recording (Schäfer *et al.*, 1991), although this does not appear to be the whole story. The only definitive studies showing BK receptor coupling to specific G protein α-subunits in neuronal cells have utilized anti-G protein antibodies to show that $G_{\alpha q/11}$ transduces PLC activation and activation of the Ca^{2+}-dependent K^+ current by BK in NG108-15 cells (Gutowski *et al.*, 1991; Wilk-Blaszczak *et al.*, 1994). Specific G proteins mediating excitatory effects of BK, such as $I_{K(M)}$ inhibition, have not been identified. BK also inhibits $I_{K(M)}$ in PC12 cells, although the second messenger system for this effect of BK has not been identified, but does not appear to be a product of PLC activation (Villarroel *et al.*, 1989).

Given the fact that sympathetic neurones express $I_{K(M)}$, and that a modulatory pathway for $I_{K(M)}$ in rat sympathetic neurones involving the PTX-insensitive G proteins $G_{\alpha q}$ and/ or $G_{\alpha 11}$ has now been described, a possible mechanism for BK-induced excitation of SCG neurones is the inhibition of $I_{K(M)}$ *via* a pathway involving a PTX-insensitive G protein, similar to that described for muscarinic receptors. Such a mechanism of action would be consistent with the effects of BK on intact ganglia: excitation in the absence of membrane depolarization could be explained by the inhibition of a membrane conductance that does not substantially contribute to the resting potential of the cell, but activates on depolarization and serves to control neuronal excitability; for example, $I_{K(M)}$ (Brown, 1988b). Excitation of sympathetic neurones by BK *via* inhibition of $I_{K(M)}$ could possibly provide the link between BK/ sympathetic nerve interaction in inflammatory reactions and pain perception, although

this would probably require the expression of $I_{K(M)}$ at sympathetic nerve terminals, unless BK release could be demonstrated within the ganglion.

5.1.4. Statement of purpose.

The purpose of the experiments described in this chapter was initially to investigate the possible inhibition of $I_{K(M)}$ by BK and, having identified this response to BK, to investigate the characteristics of this inhibition and identify the G protein involved. A similar approach to that used to study inhibition of $I_{K(M)}$ by muscarinic receptors (outlined in Chapter 4) has been adopted, to enable comparisons of the two modulatory mechanisms to be made.

5.2. RESULTS.

5.2.1. Properties of BK-induced inhibition of $I_{K(M)}$.

5.2.1.1. Concentration-dependent inhibition of $I_{K(M)}$ by BK.

Figure 21 shows the effect of different concentrations of BK on $I_{K(M)}$ deactivation relaxations. BK caused a very potent inhibition of $I_{K(M)}$, with inhibition observed at sub-nanomolar concentrations. With increasing concentrations of BK, there was a greater decrease in the standing outward current at the depolarized holding potential and a greater reduction in the amplitude of the $I_{K(M)}$ deactivation relaxation. At high concentrations of BK (> 1 nM) it became difficult to obtain a full recovery from inhibition, and often washing times of more than 15 minutes were required to achieve even partial recovery.

Repeated applications of 1 nM BK at intervals of 5 to 15 minutes, with a 2-3 minute exposure each time, caused reproducible inhibitions of $I_{K(M)}$. Figure 22A shows the effect of exposing a cell to two subsequent applications of 1 nM BK at intervals of 5 minutes. The inhibition of $I_{K(M)}$ in response to each application is identical. In three cells, the inhibition of $I_{K(M)}$ in response to two exposures to 1 nM BK was 34.7 ± 3.3% and 33 ± 1.2%. However, at concentrations of 3 nM or higher, there was pronounced tachyphylaxis of the response to BK; for example, in three cells, the response to two subsequent applications (1-2 minute exposures) of 10 nM BK, with intervals of 10-20 minutes, was 52.7 ± 3.7% and 18.3 ± 0.3%. An example of response tachyphylaxis to 10 nM BK is shown in Figure 22B (an interval of 10 minutes was allowed between applications).

Because of the waning responses to repeated applications of high concentrations of BK, it was not possible to obtain a full concentration-response relationship from a single cell. Data for the concentration-response curve shown in Figure 23 were acquired by exposing different cells to a single concentration of BK; for concentrations of BK less than 3 nM, more than one response could be obtained from a given dish of

cells, but following exposure to 3 nM or higher concentrations of BK, the dish was replaced (see Figure 22). BK caused a concentration-dependent inhibition of $I_{K(M)}$, with an estimated negative logarithm of the EC_{50} of -9.02 ± 0.1, a Hill coefficient of 0.8 ± 0.14 and producing a fitted maximum inhibition of 65.5 ± 5.5% (mean ± SEM; calculated from the fit of the logarithmic form of the logistic equation (see Chapter 2 and Figure 23 legend) to the mean data points). Like the muscarinic receptor agonist, oxo-M, BK did not produce complete inhibition of $I_{K(M)}$, and the maximum inhibition was significantly less than that seen in response to oxo-M ($p < 0.05$, unpaired t-test; compare with Figure 9).

Although the response to BK was susceptible to tachyphylaxis, there was no desensitization of the $I_{K(M)}$ inhibition during prolonged exposure to high concentrations of the agonist. Figure 24 shows current recorded at the holding potential and the amplitude of $I_{K(M)}$ deactivation relaxations during a 6 minute application of BK. There is a small (about 50 pA) recovery of current at the holding potential, but the inhibition of $I_{K(M)}$ remains relatively constant throughout the exposure to BK. Thus, it was feasible to apply BK for prolonged periods of time; for example, to obtain current-voltage relationships. Figure 25 shows the effect of two concentrations of BK on the current-voltage relationship between -18 mV and -102 mV, using a voltage ramp protocol. When the cell was initially voltage-clamped to -18 mV, a very large outward current was recorded which decreased to a steady amplitude within about a 2 minute period. This was assumed to be the delayed rectifier K^+ current which activates at potentials more depolarized than -20 mV (although it may also have included a component of Ca^{2+}-dependent K^+ current), and current voltage records were not acquired until the standing outward current approached a steady level, presumably after inactivation of other K^+ channels, leaving $I_{K(M)}$ as the remaining standing outward K^+ current. After first obtaining a steady-state current-voltage relationship from 1 s, 10 mV steps from -18 mV to -92 mV in control solution, a voltage ramp was applied. The current measured at each potential using the two protocols is shown in Figure 25 (main figure), and the two plots are virtually indistinguishable, although at the holding potential there was a decrease in the standing outward current during the steady-state current-voltage relationship, which may reflect continuing inactivation of other K^+

currents. Voltage ramps were next applied in the presence of 1 nM and then 10 nM BK. The subtracted currents (control - BK) are shown in Figure 25 (inset), representing the current that is inhibited by 1 nM and 10 nM BK across the voltage range. The profound effect of BK on this cell was on the voltage range between -60 mV and -20 mV, which encompasses the activation range for $I_{K(M)}$; the reduction in steady-state current between -20 mV and -50 mV was around 30% (1 nM BK) and 60% (10 nM BK), in close agreement with the inhibition of $I_{K(M)}$ deactivation relaxations (for example, see Figure 23). As with the muscarinic receptor agonist, oxotremorine-M, effects of BK were observed between -65 and -100 mV, although these effects of BK were less consistent. In 3 out of 5 cells, 1 nM BK caused inward currents of between 40 and 100 pA (measured at -70 mV), while in 2 cells, there was no effect on steady-state current at -70 mV, but small outward currents (about 50 pA) were seen at between -90 and -100 mV. In 3 cells exposed to 10 nM BK during the voltage ramp, inward currents of 80 to 150 pA were seen at -60 mV; in 1 of the 3 cells, this reduced to no net effect at between -80 and -100 mV.

5.2.1.2. Slow inhibition of $I_{K(M)}$ by BK.

Inhibition of $I_{K(M)}$ by BK was very slow to develop, showing a delay in onset of the response of approximately 10 s following perfusion with a maximally effective concentration (10 nM). Figure 26A shows the effect of 10 nM BK on the current at the holding potential and $I_{K(M)}$ deactivation current amplitude at the command potential. In this experiment there is a delay in onset of at least 10 s; thus, the effect of BK is not apparent until the voltage step applied 20 s after the application of BK. Example current records from this cell are shown in Figure 26B. Because the change in holding current mirrors the change in $I_{K(M)}$ amplitude, an estimate of the rate of development of the response to BK, in comparison with oxo-M, was obtained by monitoring the continuous change in current at the holding potential. Recordings were obtained from cells (n=5) to which both BK and oxo-M were applied. An example recording is shown in Figure 26C. There is clearly a greater delay in onset and a slower development of the response to BK compared with oxo-M (although a BK-induced small outward current develops at the same time as the response to oxo-M: this was seen in 4 of the 5 cells. This outward current has not been studied; however, it may

represent activation of a Ca^{2+}-dependent K^+ current, similar to that described in NG108-15 cells (Higashida and Brown, 1986)). Estimates of the latency of response onset and the half-time for the development of the response to 10 nM BK, compared with 3 μM oxo-M, are given in Table 4. Values for the onset latency and development of zero current on switching to 45 mM $[K^+]_{ec}$ (see Chapter 2) are also given, to indicate the efficiency of the perfusion system. The data show that in 5 cells, the delay in onset of the response to BK is more than twice as long as that for oxo-M; the rate of development of the response to BK is three times slower.

5.2.1.3. Effects of BK and oxo-M on $I_{K(M)}$ when applied to the same cell.

Figure 27A shows the result of an experiment to determine whether there was heterologous tachyphylaxis between the responses to BK and oxo-M. An initial application of 10 nM BK produced a 65% inhibition of $I_{K(M)}$ (BK 1). After allowing the current to recover, BK was applied a second time and, consistent with the observations described in Figure 22, the response was much reduced (BK 2; 19% inhibition). The cell was washed again, then exposed to 3 μM oxo-M (Oxo-M 1): the muscarinic $I_{K(M)}$ inhibition (88%) was not different to that seen in naive cells (see Chapter 4). After washing to recover oxo-M-inhibited $I_{K(M)}$, the cell was exposed to a second application of oxo-M (Oxo-M 2), and once again, a maximum inhibition of $I_{K(M)}$ was observed (88%). To check that the maximum response to oxo-M was not simply a result of the longer recovery time following the initial response to BK, BK was applied again after oxo-M (BK 3). At this time, although the response to BK has shown a small recovery (31% inhibition), it was not as fully developed as the maximum response observed on the first application of BK. Subsequent application of oxo-M (Oxo-M 3) produced an almost identical muscarinic inhibition (79%). The percent inhibition of $I_{K(M)}$ at each agonist application is shown in the bar graph in Figure 27B.

The effects of oxo-M (3 μM) and BK (10 nM) on $I_{K(M)}$ were not additive. In one experiment, 3 μM oxo-M caused inhibition of $I_{K(M)}$ similar to that calculated in Figure 7 (88% compared with 84 ± 3.5%, n = 9). After washing to recover inhibited $I_{K(M)}$, application of 10 nM BK caused a 67% inhibition, similar to that calculated in

Figure 23 (55 ± 4.3% n = 7). At the peak of the response to 10 nM BK, the cell was superfused with 10 nM BK plus 3 μM oxo-M: this resulted in a 90% inhibition of $I_{K(M)}$, similar to that seen when oxo-M alone was applied to this cell. Thus, maximally effective concentrations of both agonists, when applied together, cannot produce a complete (100%) inhibition of $I_{K(M)}$. The example $I_{K(M)}$ deactivation records from this experiment are shown in Figure 28. There was a noticeable large net inward current in response to BK, which reversed on washing. This was barely seen in response to oxo-M, and may have been due to activation of the inward current (see sections 4.3.1.1. and 5.2.1.1.) which (as observed during the present experiments and noted by Jones, 1985) is unpredictable.

5.2.2. Identification of G proteins mediating inhibition of $I_{K(M)}$ by BK.

5.2.2.1. Effect of pertussis toxin on $I_{K(M)}$ inhibition by BK.

Pretreatment of SCG neurones with pertussis toxin (500 ng/ml for 15-20 h) had no effect on $I_{K(M)}$ inhibition in response to BK. Figure 29 shows example $I_{K(M)}$ recordings from one untreated cell (Figure 29A) and one cell treated with pertussis toxin (29B): both cells exhibit similar responses to 1 nM BK. Mean $I_{K(M)}$ inhibition by 1 nM BK in 6 cells treated with pertussis toxin was 39.7 ± 3.6%, compared with control responses in untreated neurones, 37 ± 3.6% (n = 14).

5.2.2.2. Effect of G protein antibodies on $I_{K(M)}$ inhibition by BK.

Microinjection of anti-G_{α_o} antibody had no effect on the $I_{K(M)}$ inhibition in response to 1 nM BK (31.4 ± 3.2%; n = 8), whereas anti-$G_{\alpha q/11}$ antibody virtually abolished the response (6.6 ± 2.4% inhibition; n = 8; significantly different to anti-G_{α_o} antibody-injected cells, $p<0.01$, Tukey-Kramer multiple comparisons test). Example recordings are shown in Figure 30 (B and D) and data are summarized in Figure 31. The synthetic C-terminal decapeptide, against which the anti-$G_{\alpha q/11}$ antibody was raised, was used to preabsorb the antibody and prevent the blocking effect on the response to BK. The peptide, when injected alone, had no effect on $I_{K(M)}$ inhibition by 1 nM BK (40.1 ± 5%; n = 9), as shown in Figure 30C. However, when the peptide

was mixed with the anti-$G_{\alpha q/11}$ antibody and this mixture was injected, the profound blocking action of the antibody on the response to 1 nM BK was significantly reduced ($25.4 \pm 5.2\%$ inhibition of $I_{K(M)}$; $n = 8$; $p<0.05$, Tukey-Kramer test; Figure 30E). All antibodies were co-injected with 0.1% FITC-dextran, and injections were verified as described in Chapter 2. The injection procedure itself, and the co-injected dextran, had no effect on the response to BK, as evidenced by the lack of effect of the anti-$G_{\alpha o}$ antibody and peptide injections on the response to BK.

Table 5 gives the mean amplitudes and time constants (from a fit of a two exponential function) of control $I_{K(M)}$ deactivation relaxations recorded in control solution, prior to application of 1 nM BK, in uninjected cells and in cells injected with the indicated substances. The amplitudes, and both the fast and slow time constants (and their relative contributions) of $I_{K(M)}$ deactivation relaxations recorded from the different treatment groups were not significantly different from measurements in uninjected cells. These data suggest that the injection procedure, the co-injected dextran, and the individual injectates do not affect either the amplitude or the kinetics of $I_{K(M)}$ recorded in these experiments. Furthermore, the cells appear to remain healthy following injections, as indicated by the zero current potentials recorded at the end of each experiment (Table 5) which were not significantly different from the zero current potentials of uninjected cells.

5.2.2.3. Effect of anti-$G_{\alpha q/11}$ antibody on $I_{K(M)}$ inhibition by BK and oxo-M.

Inhibition of $I_{K(M)}$ by 1 nM BK was more effectively reduced, and exhibited a less variable sensitivity to block by the anti-$G_{\alpha q/11}$ antibody than the inhibition of $I_{K(M)}$ by 300 nM oxo-M (compare with Figures 15 and 17). To eliminate the possibility that during the BK series of experiments, cells were more successfully loaded with antibody than during the oxo-M experiments, resulting in more effective and consistent effects of the antibody, some of the anti-$G_{\alpha q/11}$ antibody-injected cells exposed to 1 nM BK (see Figure 31) were also exposed to 300 nM oxo-M. Figure 32 shows example $I_{K(M)}$ deactivation records from three cells exposed to both of the agonists. In all three examples, the response to 1 nM BK was either completely blocked or profoundly

reduced (0%, 0% and 3% inhibition of $I_{K(M)}$). However, in each cell the response to 300 nM oxo-M was different, being completely blocked in one cell and reduced by varying amounts in the other two cells (0%, 22% and 43% inhibition of $I_{K(M)}$).

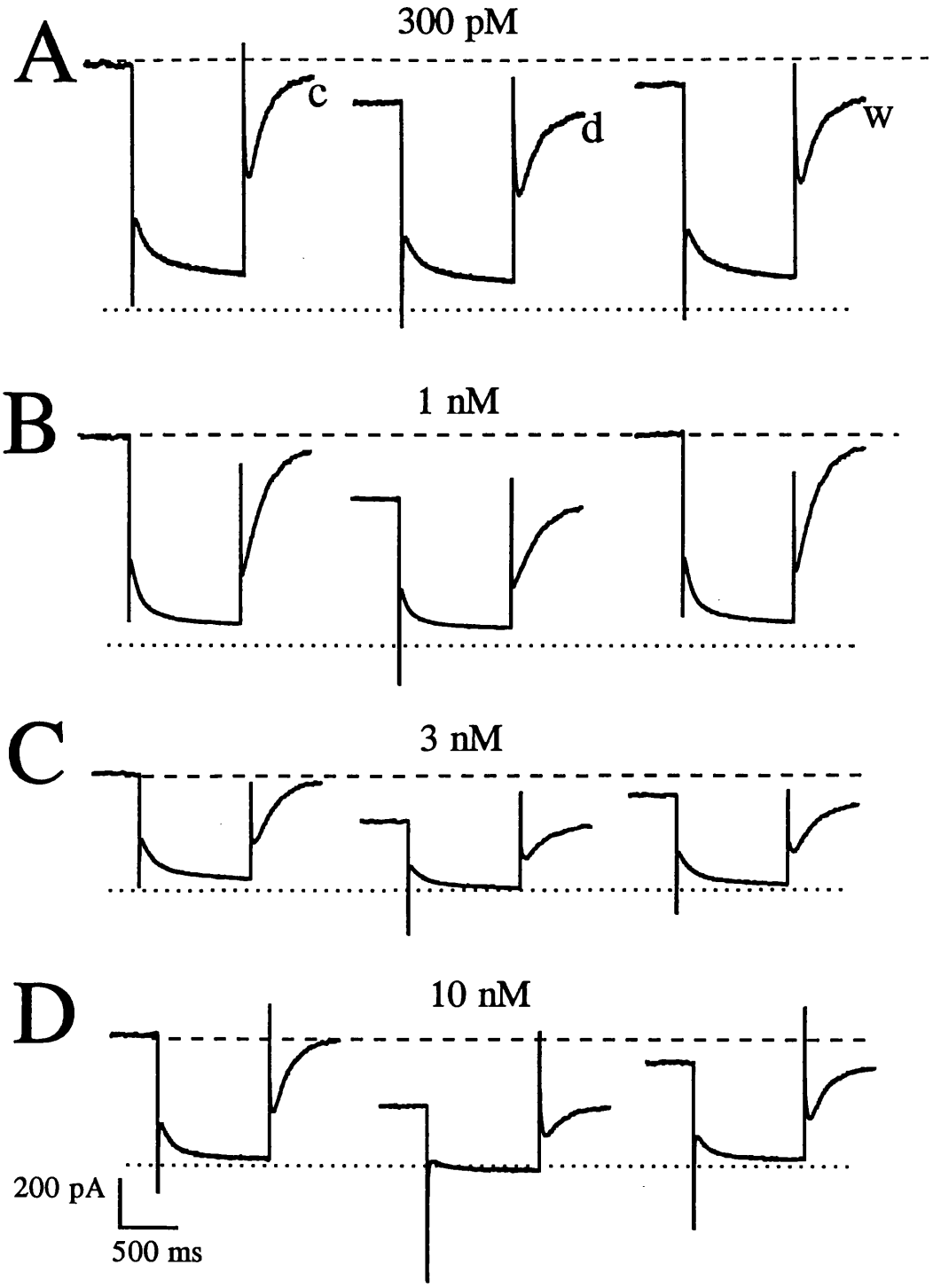

Figure 21. Inhibition of $I_{K(M)}$ by different concentrations of bradykinin.
Example $I_{K(M)}$ deactivation records from 4 different cells showing the effect of BK on $I_{K(M)}$. $I_{K(M)}$ was recorded (during a 1 s, -30 mV step, as described in Chapter 2) in control solution (c), after superfusion with BK (d): A. 300 pM (V_H -29 mV; 19% inhibition), B. 1 nM (V_H -27 mV; 41% inhibition), C. 3 nM (V_H -26 mV; 50 % inhibition) and D. 10 nM (V_H -28 mV; 71% inhibition), then after washing out the agonist for 10-20 minutes (w). The dashed lines represent control current at the holding potential for each cell, and the dotted lines indicate the zero current level. The scale bar applies to all 4 cells. Deactivation amplitudes, % inhibition and % recovery were calculated as described in Chapter 2.

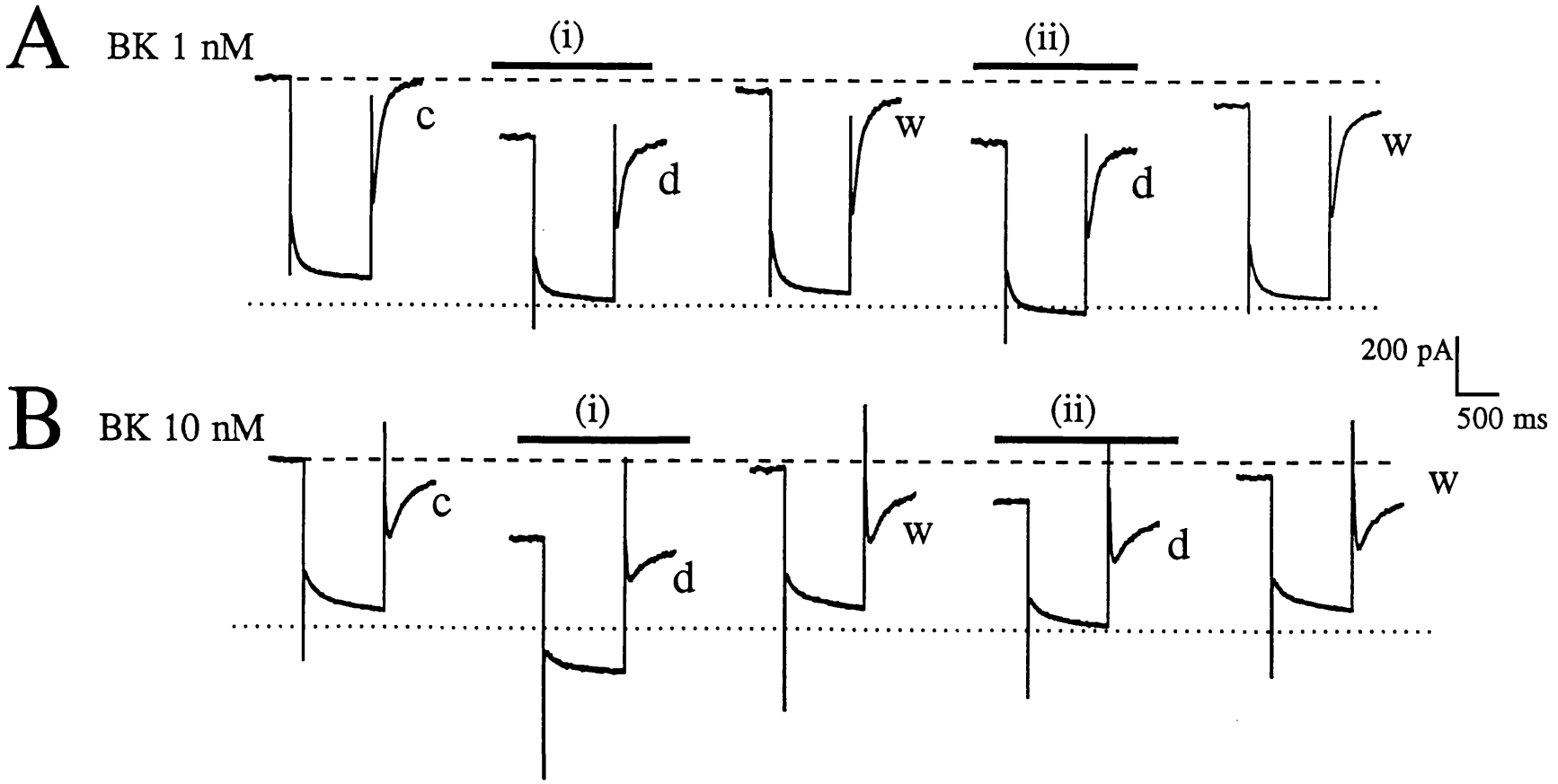

Figure 22. Tachyphylaxis of the response to high concentrations of bradykinin.
A. Example $I_{K(M)}$ deactivation records from one cell (1 s, -30 mV steps from V_H -26 mV). $I_{K(M)}$ was recorded in control solution (c), then after superfusion with 1 nM BK (d (i); 33% inhibition). After washing out the agonist for 5 minutes (w), 1 nM BK was applied again (d (ii); 33% inhibition). B. Example $I_{K(M)}$ deactivation records from a different cell (V_H -26 mV), showing a repeated application of 10 nM BK with a 10 minute wash interval (d (i) and (ii); 50% and 18% inhibition respectively). The dotted lines represent the zero current level, and dashed lines represent the current at the holding potential in control solution.

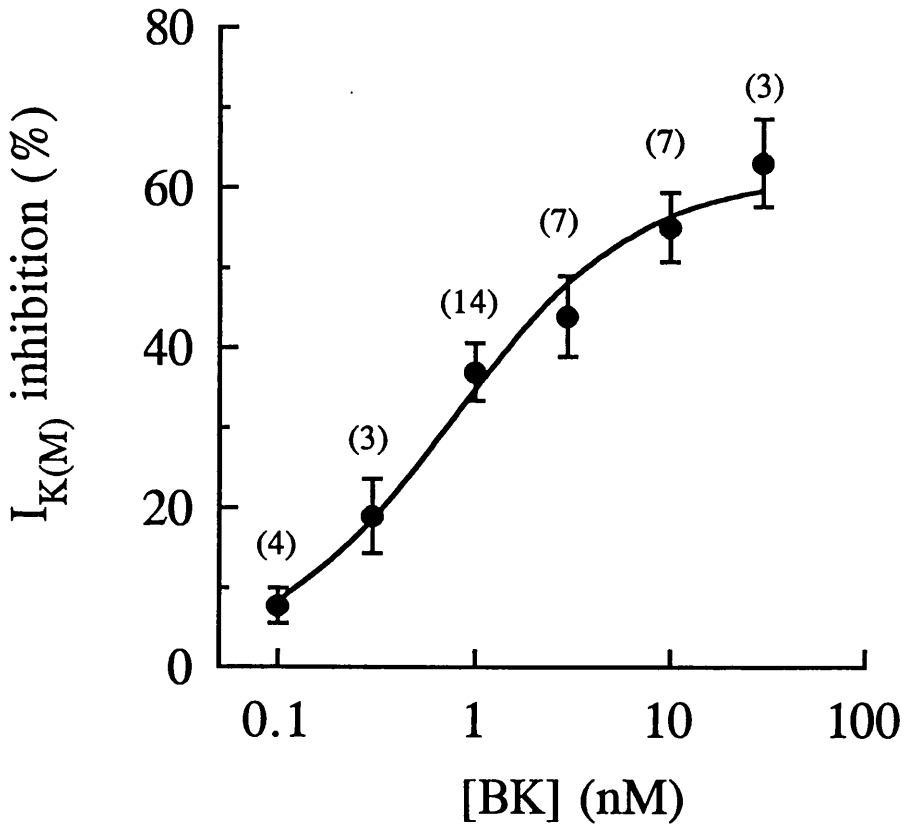

Figure 23. Concentration-response curve for $I_{K(M)}$ inhibition by bradykinin.
Percent inhibition of $I_{K(M)}$ (y; mean ± SEM) by increasing concentrations of BK (A; plotted on a logarithmic scale), obtained from single applications of BK to different cells. The solid line is the best fit to the data of the function $y = m.10^{n.\log(A)}/(10^{n.\log(A)} + 10^{n.\log(K)})$ with weight ($1/SEM^2$). The fitted maximum response (m) is 65.5 ± 5.5%, the logarithm of the EC_{50} (K) is -9.02 ± 0.1, and the Hill coefficient (n) is 0.8 ± 0.14. Number of cells given in parentheses.

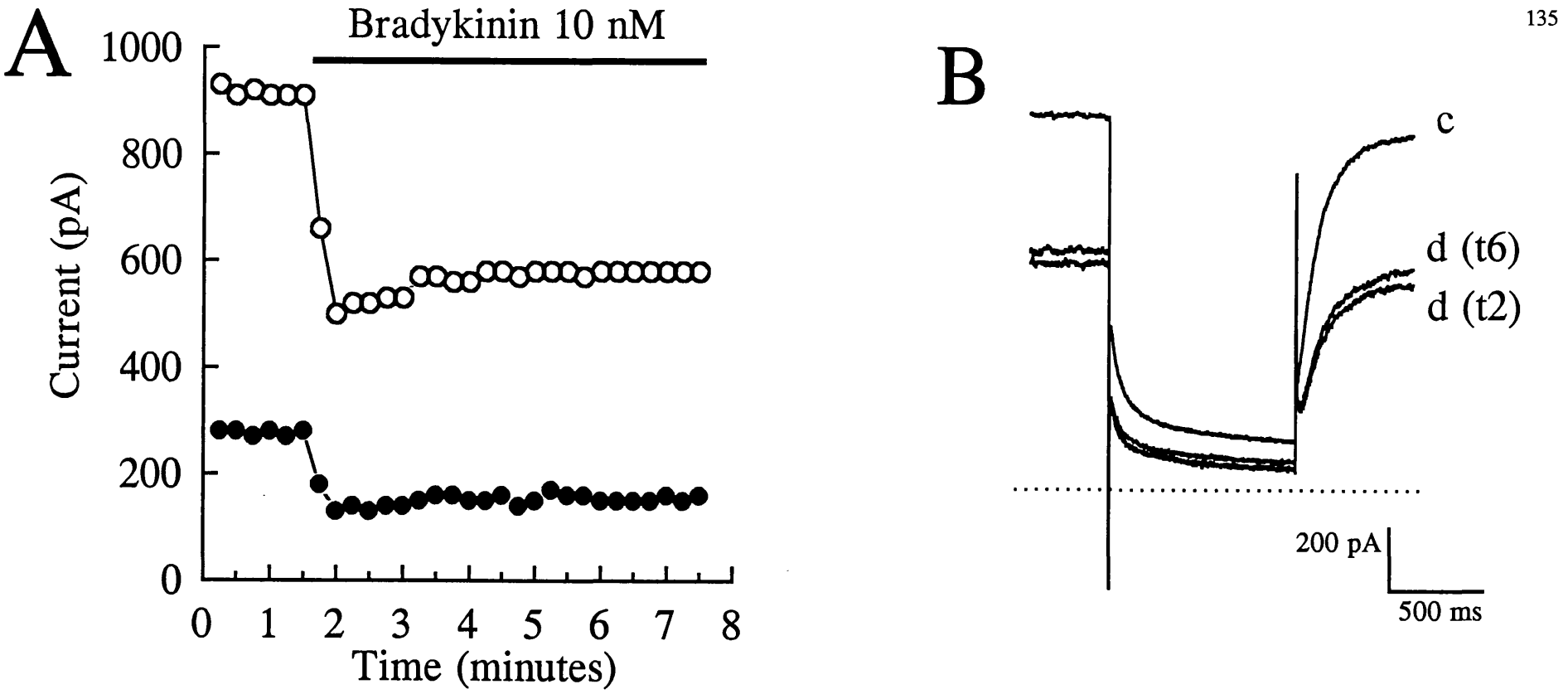

Figure 24. The response to bradykinin does not desensitize.
A. Current (pA) at the holding potential (-27 mV; open circles) and amplitude of $I_{K(M)}$ deactivation relaxations (pA) at the command potential (-57 mV; filled circles) plotted against time (minutes). Voltage steps were applied every 15 s. After obtaining 6 control records, BK (10 nM) was applied continuously for 6 minutes (indicated by the bar). B. Example $I_{K(M)}$ deactivation records from the same cell as A. $I_{K(M)}$ recorded in control solution (c; average of six traces), immediately after superfusion with BK (d (t2)), and after superfusion of BK at time 6 minutes (d (t6)). The dotted line indicates the zero current level.

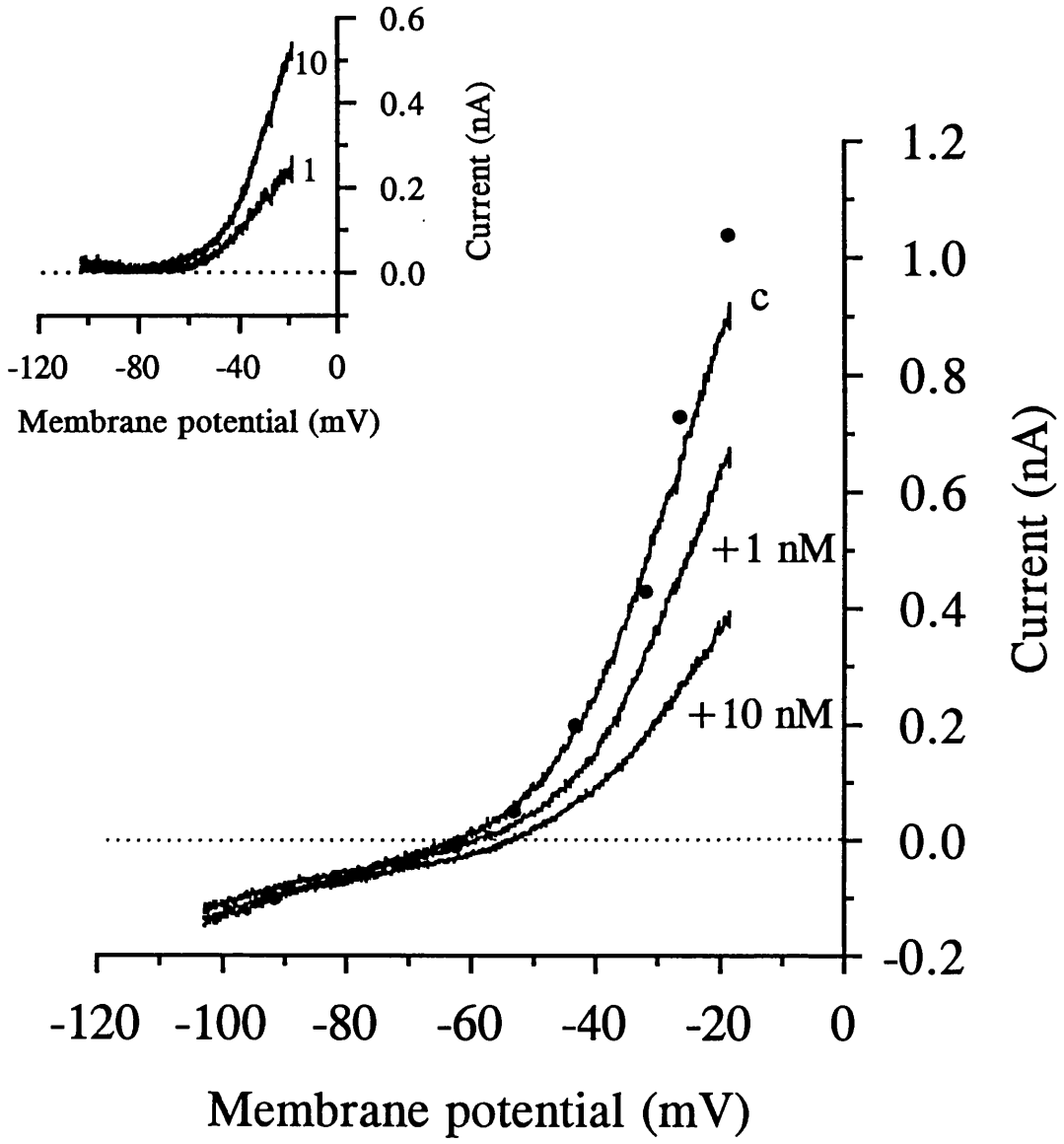

Figure 25. Effect of bradykinin on the steady-state current-voltage relationship.
Main figure. Solid lines represent current (nA) during voltage ramps from -18 mV to -102 mV (-10 mV/s; V_H -18 mV) applied in control solution (c), and in the presence of 1 nM BK (+1 nM) and 10 nM BK (+10 nM). Filled circles represent current at the end of 1 s, -10 mV steps from -18 mV to -92 mV (applied every 15 s from the holding potential, -18 mV). Inset. BK-sensitive current during the voltage ramp (1: c - BK 1 nM; 10: c - BK 10 nM). The ramp currents have been graphically reversed for convention.

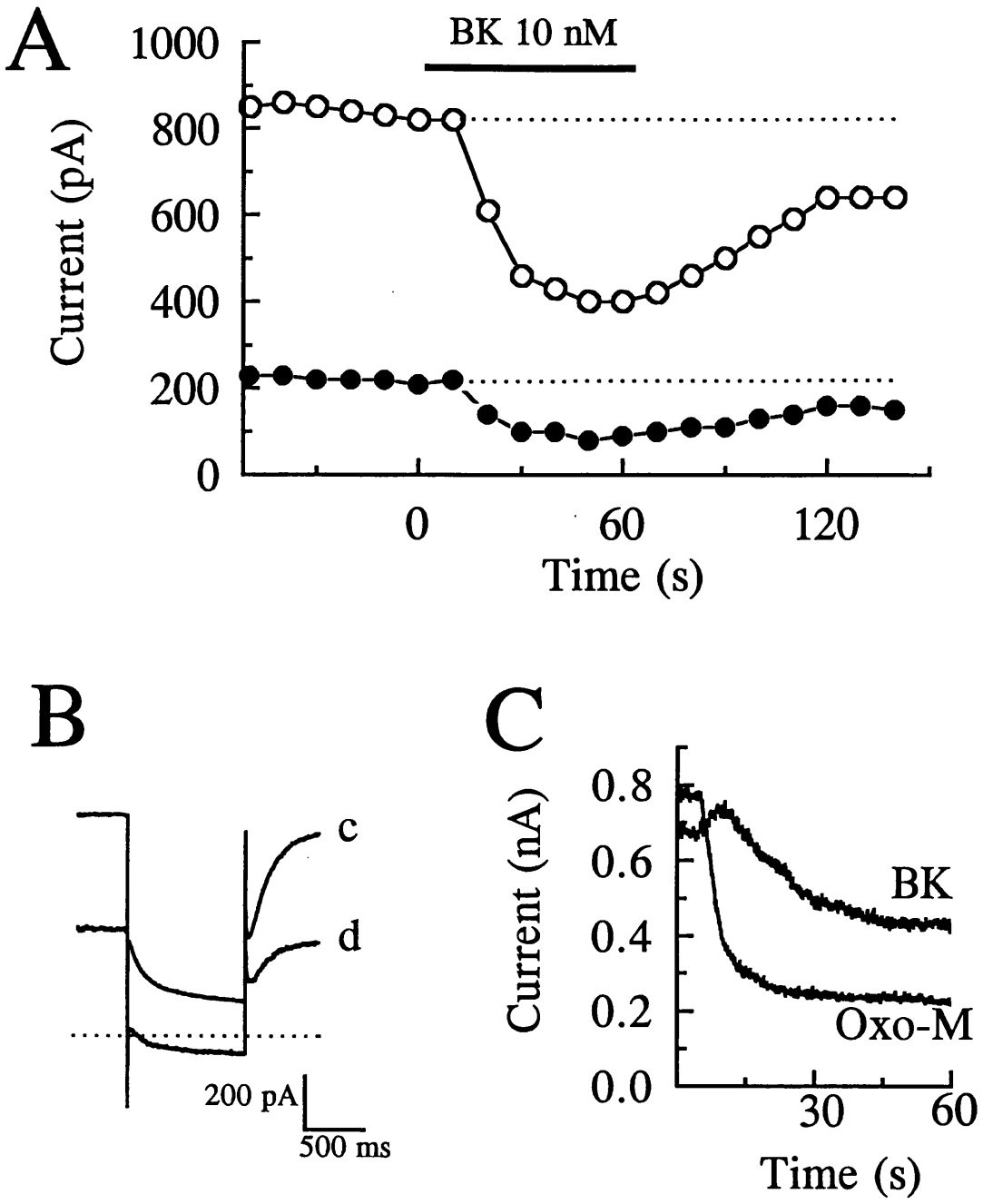

Figure 26. Slow inhibition of $I_{K(M)}$ by bradykinin.
A. Current (pA) at the holding potential (-24 mV; open circles) and amplitude of $I_{K(M)}$ deactivation relaxations at the command potential (-54 mV; filled circles) plotted against time (s). Voltage steps were applied every 10 s. BK (10 nM) was applied at time 0 s, indicated by the bar (65% inhibition, 54% recovery). B. Example $I_{K(M)}$ deactivation records from the same cell as A. $I_{K(M)}$ recorded in control solution (c) and at the peak of the response to 10 nM BK (d). The dotted line indicates the zero current level. C. Continuous current record (nA) from a different cell, plotted against time (s) during perfusion with 3 μM oxo-M (Oxo-M), then 10 nM BK (BK).

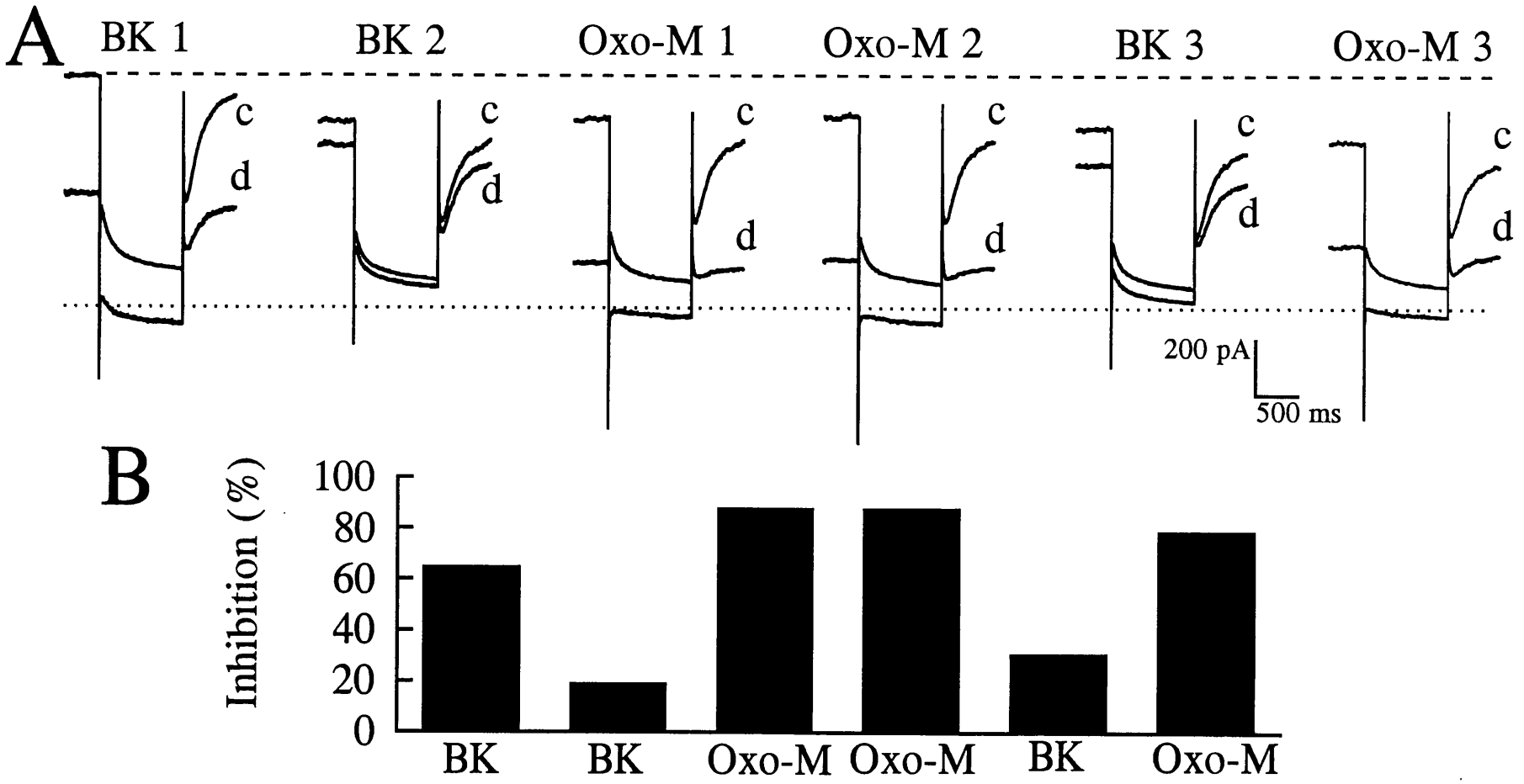

Figure 27. The response to bradykinin does not cause heterologous tachyphylaxis.

A. Example $I_{K(M)}$ deactivation records from one cell (1 s, -30 mV steps from V_H -24 mV) showing the effect of sequential applications of 10 nM BK (BK) and 3 μM oxo-M (Oxo-M). $I_{K(M)}$ deactivation relaxations were recorded in control solution (c) and in the presence of each agonist as indicated (d: BK 1-3 and Oxo-M 1-3). The dotted line indicates the zero current level, and the dashed line indicates the current at the holding potential in control solution. B. Bar graph showing inhibition of $I_{K(M)}$ (%) at each application of the two agonists. (This data is from the same cell as figure 26).

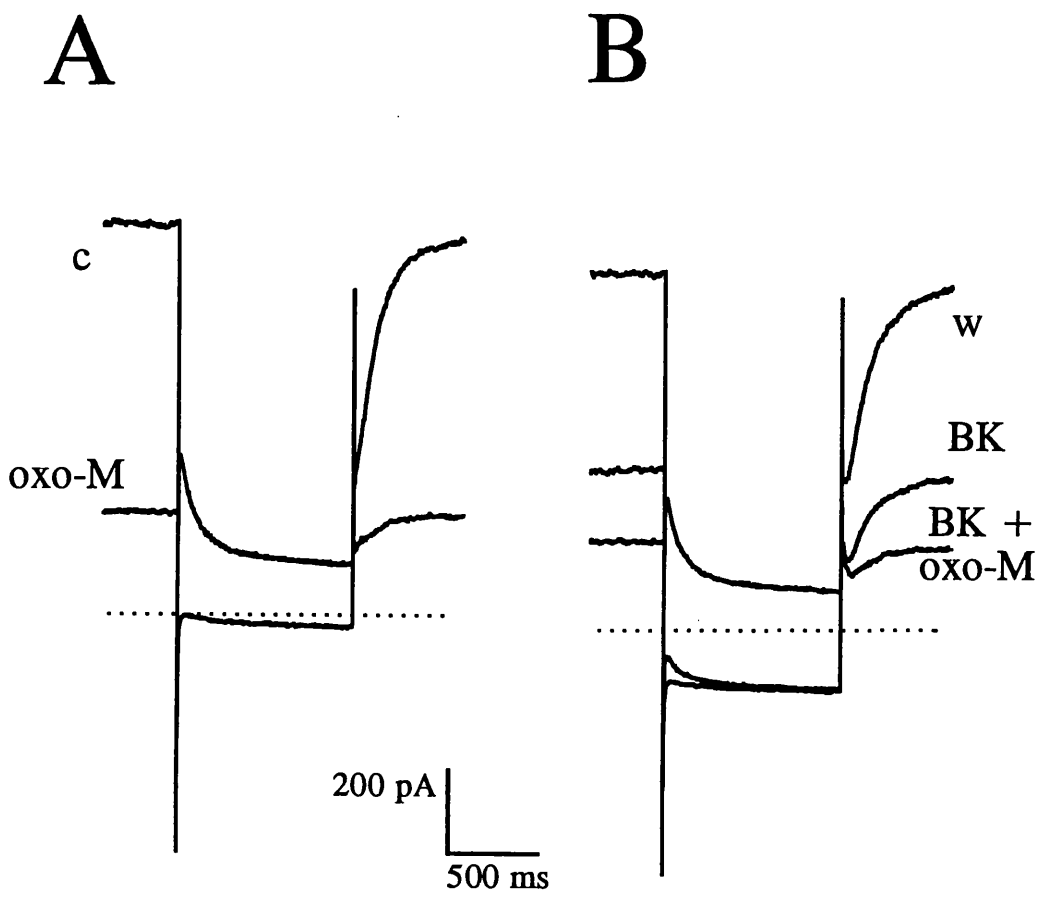

Figure 28. The responses to bradykinin and oxotremorine-M are not additive.
A. Example $I_{K(M)}$ deactivation relaxations (during 1 s, -30 mV steps from V_H -26 mV) recorded in control solution (c) and then after superfusion with 3 μM oxo-M (oxo-M, 88% inhibition). B. $I_{K(M)}$ deactivation records from the same cell, recorded after washing to recover $I_{K(M)}$ (w; 86% recovery), after superfusion with 10 nM BK (BK; 67% inhibition), and then (at the peak of the response to BK) with 10 nM BK plus 3 μM oxo-M (BK + oxo-M; 90% inhibition). The dotted lines indicate zero current.

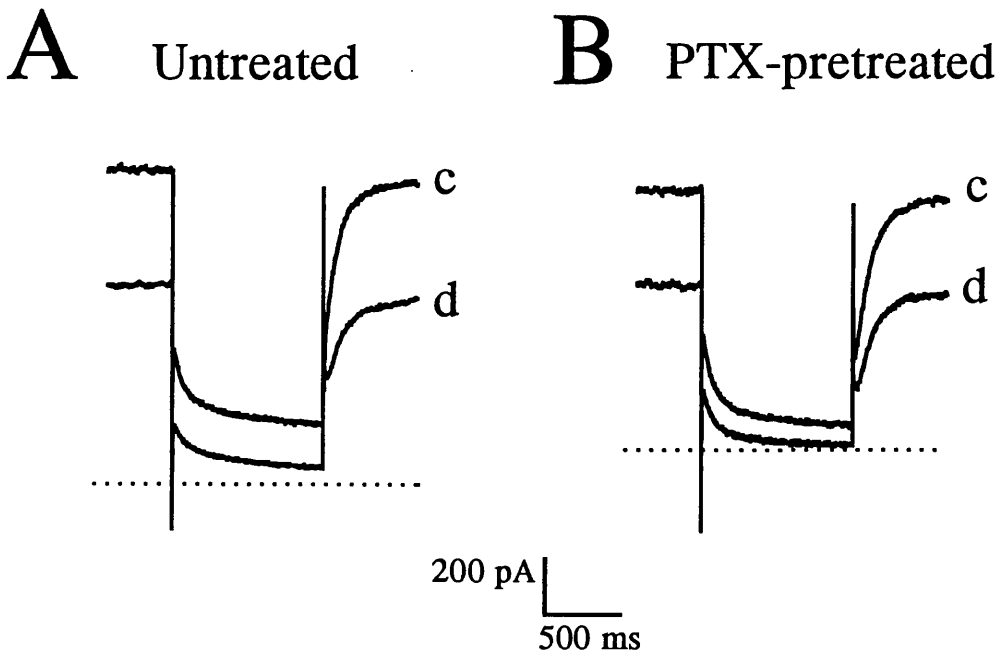

Figure 29. The response to bradykinin is insensitive to pertussis toxin-pretreatment.
A. Example $I_{K(M)}$ deactivation relaxations (during 1 s, -30 mV steps) recorded from an untreated neurone (V_H -33 mV; 44% inhibition) and B. from a PTX-pretreated neurone (V_H -26 mV; 40% inhibition). $I_{K(M)}$ deactivation recordings were made in control solution (c) then after superfusion with 1 nM BK (d). The dotted lines indicate the zero current level.

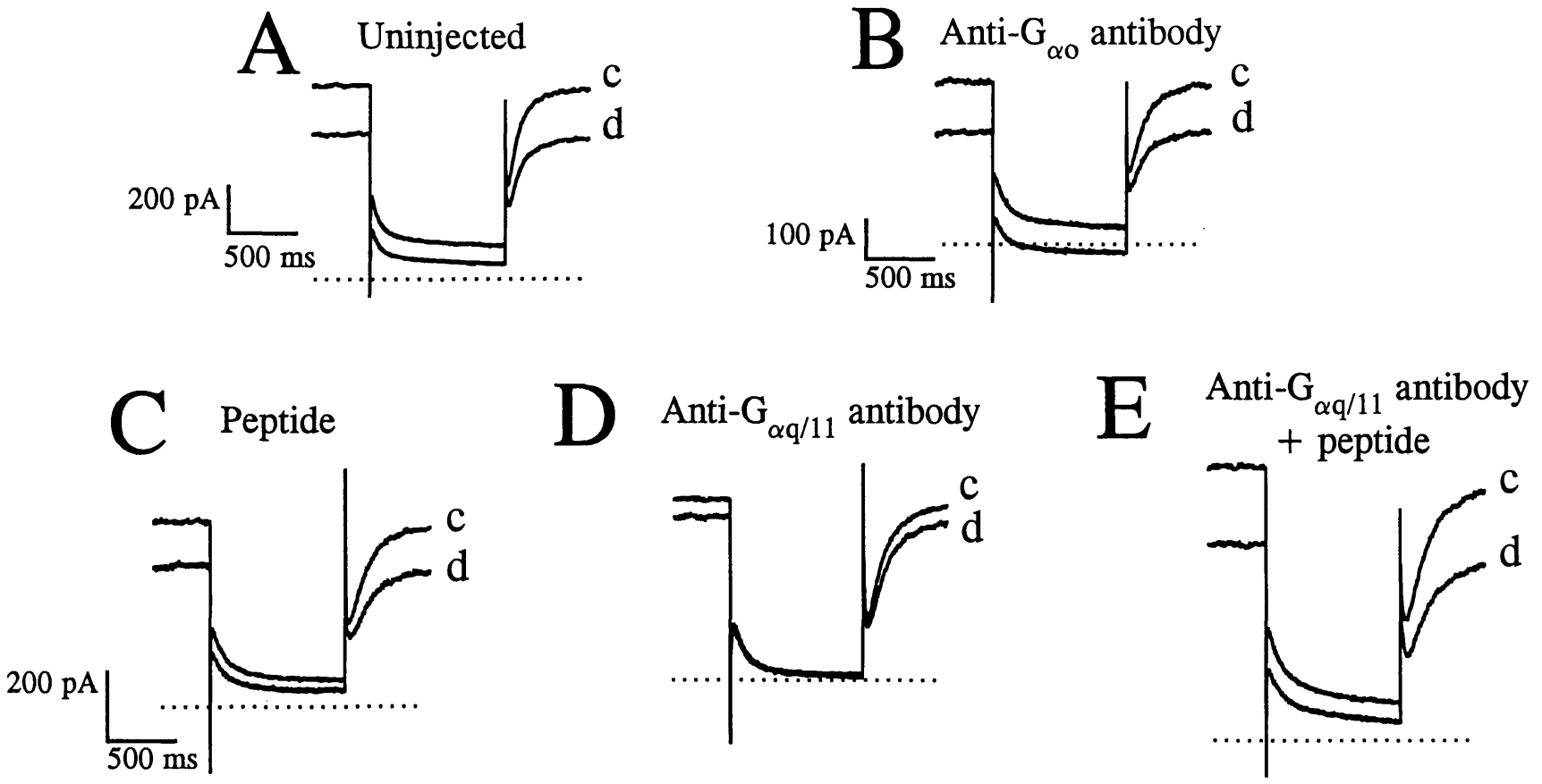

Figure 30. Anti-$G_{\alpha q/11}$ antibody reduces the inhibition of $I_{K(M)}$ by bradykinin.
Example $I_{K(M)}$ deactivation relaxations (during 1 s, -30 mV steps) recorded in control solution (c) and in the presence of 1 nM BK (d). Recordings are from A. an uninjected cell (V_H -26 mV; 38% inhibition), and cells injected with B. anti-$G_{\alpha o}$ antibody (V_H -21 mV; 39% inhibition), C. synthetic C-terminal peptide (V_H -29 mV; 36% inhibition), D. anti-$G_{\alpha q/11}$ antibody (V_H -28 mV; 9% inhibition) and E. a mixture of anti-$G_{\alpha q/11}$ antibody and synthetic peptide (V_H -25 mV; 33% inhibition). Bottom scale bar applies to C, D and E. The dotted lines indicate the zero current level. In these experiments, antibodies and decapeptide were co-injected with 0.1% FITC-dextran, and the anti-$G_{\alpha q/11}$ antibody used was the same as that in Figures 17, 18 and 19.

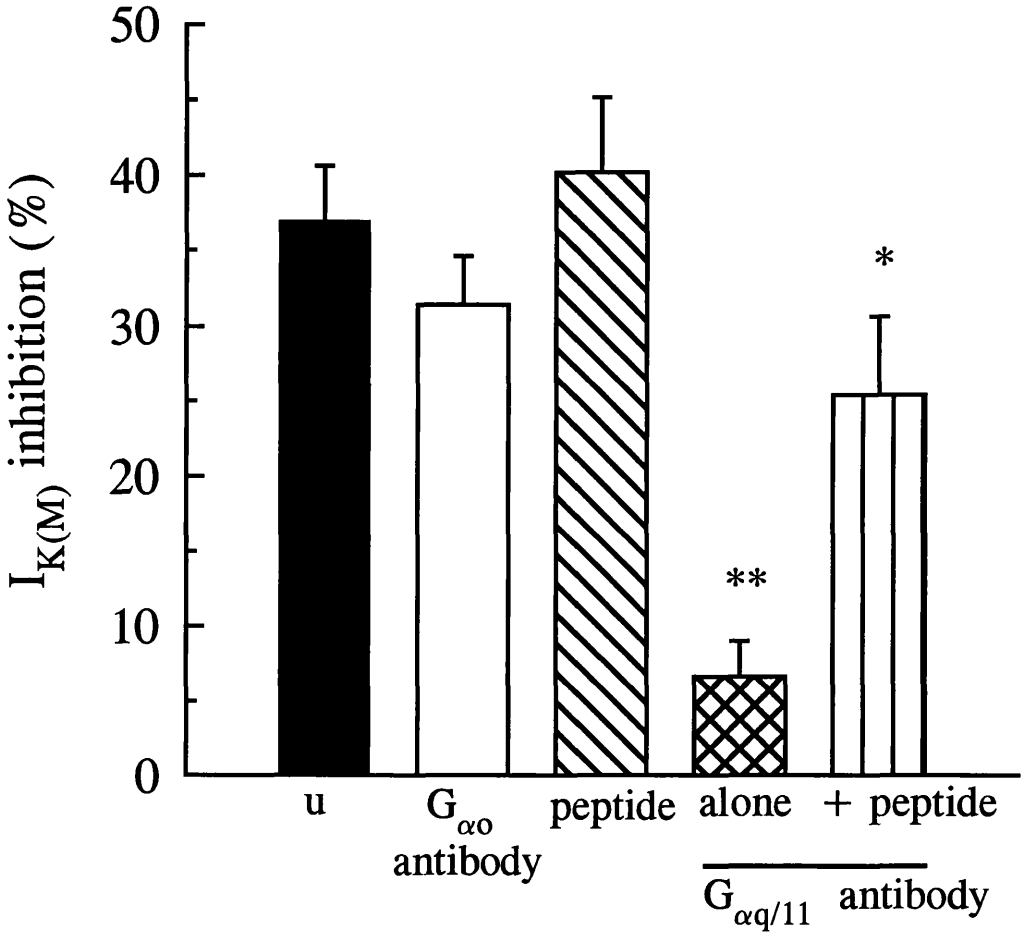

Figure 31. Bar graph of the effect of anti-G protein antibodies on the response to 1 nM bradykinin. $I_{K(M)}$ inhibition (%, mean ± SEM) in uninjected cells (solid bar; n = 14), and cells injected with anti-$G_{\alpha o}$ antibody (open bar; n = 8), synthetic C-terminal peptide (diagonal bar; n = 9), anti-$G_{\alpha q/11}$ antibody (cross bar; n = 8) and a mixture of synthetic peptide and anti-$G_{\alpha q/11}$ antibody (vertical bar; n = 8). Asterisks indicate significant difference (**$p < 0.01$ from anti-$G_{\alpha o}$ antibody injected cells; *$p < 0.05$ from anti-$G_{\alpha q/11}$ antibody (alone) injected cells).

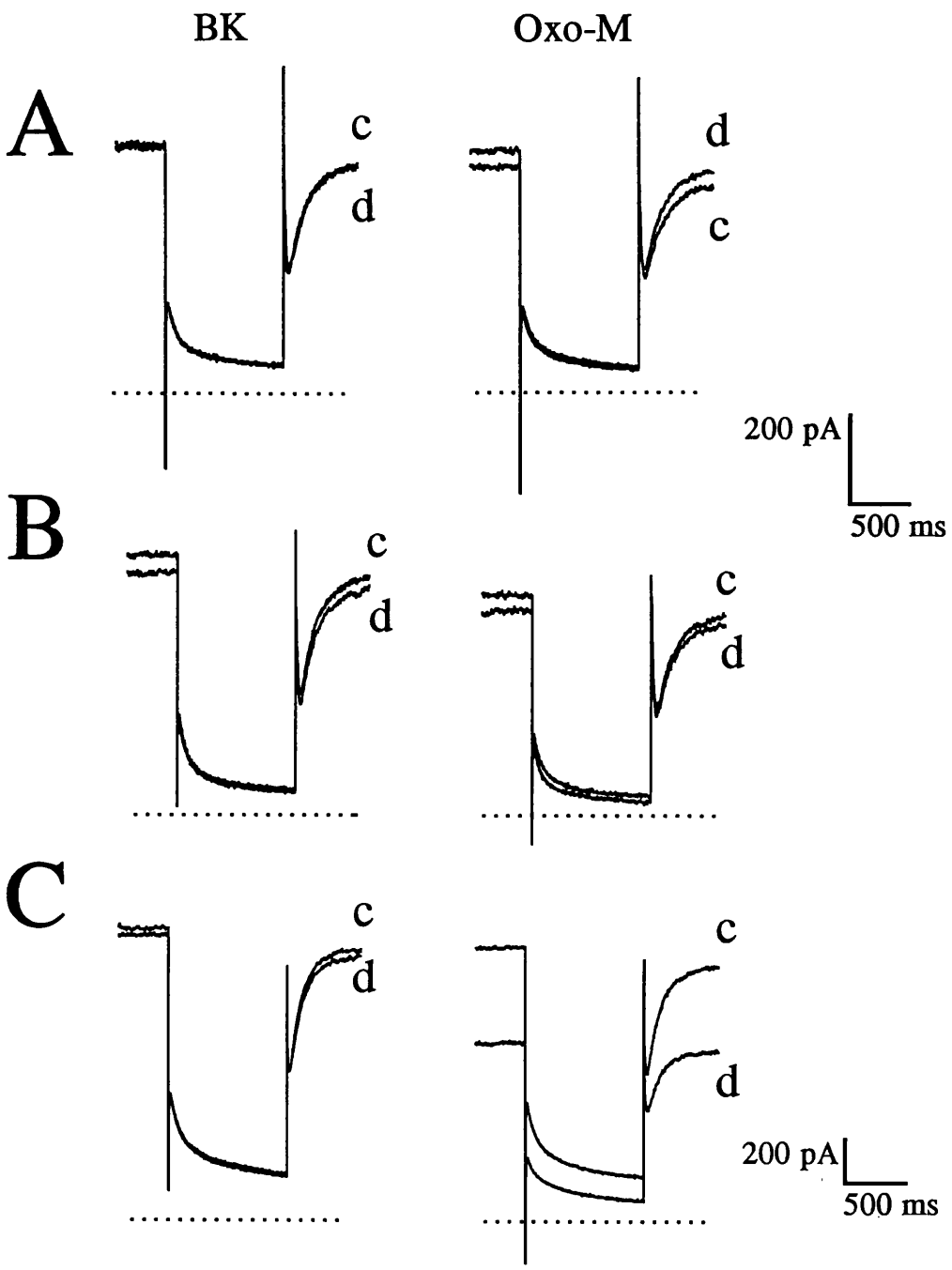

Figure 32. Comparison of $I_{K(M)}$ inhibition by bradykinin and oxotremorine-M in anti-$G_{\alpha q/11}$ antibody-injected cells.
Example $I_{K(M)}$ deactivation relaxations (during 1 s, -30 mV steps) from three cells injected with anti-$G_{\alpha q/11}$ antibody (A, B, and C) recorded in control solution (c) and in the presence of 1 nM BK (d; left-hand traces) or 300 nM oxo-M (d; right-hand traces). A. Recordings from one cell in which the response to both agonists was completely blocked (0% inhibition). B. Recordings from a different cell in which the response to BK was completely blocked (0% inhibition) and the response to oxo-M was greatly reduced (22% inhibition). C. Recordings from a third cell in which the response to BK was almost blocked (3% inhibition), but the response to oxo-M was only slightly reduced (43% inhibition). Dotted lines indicate zero current. Top scale bar applies to A and B, bottom scale bar applies to C. V_H: -28 mV, -25 mV and -25 mV for cells A, B and C respectively.

Table 4: Latency and development of $I_{K(M)}$ inhibition by maximally effective concentrations of oxotremorine-M and bradykinin.

	Onset latency (s)	Onset half-time (s)	n
High $[K^+]_{ec}$	2.2 ± 0.2	1.9 ± 0.4	4#a
Oxo-M (3 μM)	I_{Inward}: 3.7 ± 0.7	7.5 ± 0.4	5
BK (10 nM)	$I_{Outward}$: 2.6 ± 0.7 I_{Inward}#b: 9.8 ± 1.8	(nd) 22 ± 2.5	5

#a: 4 determinations from one cell.

#b: Measured at the peak of the preceding outward current (in 4 out of 5 cells).

nd: not determined.

Table 5: Properties of $I_{K(M)}$ deactivation relaxations in cells co-injected with antibody and FITC-labelled dextran (bradykinin series).

	Deactivation $\tau_{(fast)}$ (ms)	% of total amplitude	Deactivation $\tau_{(slow)}$ (ms)	n	Deactivation amplitude (pA; control)	n	Zero current potential (mV; end-of-experiment)	n
Uninjected	65 ± 6	58 ± 2.6	580 ± 138	12	204 ± 17	14	-55 ± 1.5	14
Anti-$G_{\alpha o}$ antibody-injected	66 ± 5.5	54 ± 6.4	396 ± 95	8	193 ± 16	12	-59 ± 1.5	10
Anti-$G_{\alpha q/11}$ antibody-injected	67 ± 4	53 ± 4.4	326 ± 59	7	230 ± 22	8	-62 ± 1.7	8
Peptide-injected (1 μg/ ml)	75 ± 4	63 ± 3.9	503 ± 144	8	156 ± 11	11	-62 ± 2	9
Peptide plus anti-$G_{\alpha q/11}$ antibody-injected	68 ± 3	60 ± 2.8	401 ± 44	8	207 ± 27	9	-58 ± 3	9

5.3. DISCUSSION.

5.3.1. Inhibition of $I_{K(M)}$ by BK.

5.3.1.1 Concentration dependence.

Bradykinin caused a potent inhibition of $I_{K(M)}$ in rat cultured SCG neurones. BK inhibited $I_{K(M)}$ at sub-nanomolar concentrations, with an EC_{50} of around 1 nM and a maximum, but incomplete, inhibition being observed at 10 to 30 nM. This effect of BK on $I_{K(M)}$ is more potent than that of the muscarinic receptor agonist, oxo-M (Chapter 4), and the peptide angiotensin II, which at 500 nM caused around a 50% inhibition of $I_{K(M)}$ (Shapiro *et al.*, 1994). Moreover, this excitatory effect of BK on sympathetic neurones is also more potent than BK-induced excitation of some sensory neurones. For example, depolarizations recorded from the spinal cord following application of BK to afferent neurones revealed EC_{50} values of BK between 30 nM and 200 nM (Dunn and Rang, 1990; Dray *et al.*, 1988; Dray *et al.*, 1992). Concentrations of BK in excess of 1 μM were used to modulate ionic currents in cultured DRG neurones (Lindsay and Rang, 1987; Burgess *et al.*, 1989), although McGehee *et al.* (1992) reported an EC_{50} of 21 nM for BK-induced activation of the cation current in DRG neurones, and much lower concentrations could evoke increases in IP_3 and intracellular Ca^{2+}, the half maximum effective concentration of BK in each case being 6 nM (Burgess *et al.*, 1989). However, in rabbit nodose ganglion neurones, BK had a very potent excitatory action, suppressing the slow AHP with an EC_{50} of around 0.4 nM (Weinreich, 1986). Inhibition of $I_{K(M)}$ by BK has been reported in other neuronal preparations. In PC12 cells, $I_{K(M)}$ is inhibited by concentrations of BK between 50 and 1000 nM (Villaroel *et al.*, 1989); in NG108-15 cells, Schäfer *et al.* (1991) used a focal application method to study BK inhibition of $I_{K(M)}$ and calculated an EC_{50} of 1.7 nM, with a maximum inhibition of around 60% at 100 nM, a similar concentration dependence to that seen in the present study. Experiments with BK on intact sympathetic ganglia have indicated that BK and angiotensin may be the most potent naturally occurring ganglion-stimulating substances in the cat (Lewis and Reit, 1965), with angiotensin being more potent than BK, which differs from our observations in the

rat SCG (compared with Shapiro *et al.*, 1994). However, there is evidence for species differences, as Lewis and Reit (1966) also found that BK had a much less potent effect on the SCG of rabbits and dogs, and angiotensin was actually inactive in the dog SCG. The inability of maximally effective concentrations of BK to produce complete inhibition of $I_{K(M)}$ parallels observations with the muscarinic receptor agonist, oxo-M (Chapter 4), and with BK in other neuronal cells, for example NG108-15 cells (Schäfer *et al.*, 1991). It is possible that a component of current recorded using the present voltage protocol does represent another voltage-dependent current which is insensitive to muscarinic and BK receptor agonists, or that a component of $I_{K(M)}$ itself is resistant to agonist inhibition. However, it is not clear why BK inhibits a significantly smaller component of $I_{K(M)}$ than oxo-M at maximally effective concentrations. A possible explanation is that at concentrations of BK exceeding 10 nM, a rapid desensitization occurs, which is manifest as a reduced inhibition of $I_{K(M)}$ compared with that which may be expected at the increased concentration: this was discussed in Chapter 4 (section 4.3.1.1) in relation to muscarinic receptor-mediated inhibition of $I_{K(M)}$. Alternatively, BK receptors may couple less efficiently to the G protein(s) than muscarinic receptors: this possibility is discussed further in Chapter 6.

BK caused a concentration-dependent decrease in the steady-state outward current between membrane potentials of -70 mV and -20 mV, the voltage range over which $I_{K(M)}$ is steeply activated. The effect of BK on the steady-state current-voltage relationship suggests that concentrations of BK that inhibit $I_{K(M)}$ can cause a small depolarization of SCG neurones, as 10 nM BK caused around a 10 mV rightward shift in the zero current potential (similar to that seen with the muscarinic receptor agonist, oxo-M). As the threshold for $I_{K(M)}$ activation in rat SCG neurones is close to the zero current potential, around -70 mV (Constanti and Brown, 1981), it might be expected that BK would have a minor action on SCG neurones at rest, and that the excitatory effect of the peptide would become more apparent during depolarization to membrane potentials just positive to resting potential, when $I_{K(M)}$ activation is steep (see Chapter 3), and when the effect of BK on steady-state current is marked. This is consistent with observations in the intact SCG demonstrating BK-induced excitation of the ganglion (Lewis and Reit, 1965), but only small and inconsistent depolarizations (cat

SCG: Haefely, 1970; rabbit SCG: Wallis and Woodward, 1974). These early observations on intact SCG support the idea that this excitatory effect of BK is not restricted to cultured SCG neurones, and indeed that inhibition of $I_{K(M)}$ may be an underlying mechanism of BK-induced excitation, possibly in conjunction with the augmentation of a Cl^- current in these cells (Marsh *et al.*, 1994). The effects of BK at potentials subthreshold to $I_{K(M)}$ activation were less pronounced and more variable than the effects of oxo-M at these potentials during current-voltage measurements (see Chapter 4). In some cells, BK caused an inward current (between -65 and -100 mV) similar to that seen with oxo-M, which may accord with the muscarine and peptide evoked inward current described by Jones (1985) in frog sympathetic neurones. In other cells, BK caused a small outward current (between -90 and -100 mV), which may represent inhibition of a Cl^- current in a similar manner to muscarine, which has been described in rat sympathetic neurones (Brown and Selyanko, 1985b). Simultaneous activation of inward current and inhibition of inward Cl^- current may explain the inconsistent effects of BK at hyperpolarized potentials.

5.3.1.2. Slow rate of response.

The onset of the inhibition of $I_{K(M)}$ was slow, even when a rapid-delivery perfusion system was used. Compared with the muscarinic receptor-G protein-diffusible second messenger-mediated inhibition of $I_{K(M)}$ in these cells (proposed by Selyanko *et al.*, 1992), the delay in onset of the response to BK was 5 times longer (after accounting for the switching time for high K^+): it is unlikely that this was due to poor access of BK to the receptors, as a BK-evoked outward current was seen in 4 out of 5 cells which developed with a latency of 2.6 s (less than that for the oxo-M-induced decrease in standing outward current). The decrease in outward current in response to BK was also about three to four times slower than in response to oxo-M. A slow rate of response has also been observed for inhibition of the voltage-gated Ca^{2+} current in these cells by the peptide angiotensin II (Shapiro *et al.*, 1994). The slower response to BK might be explained by a less efficient coupling of BK receptors with G protein (a low affinity constant for this reaction: this is discussed further in Chapter 6), compared with M_1 receptors. Also like the effect of angiotensin II (on both voltage-gated Ca^{2+} current and $I_{K(M)}$) on SCG neurones, the effect of BK was very slow to reverse, often

showing incomplete recovery from inhibition. In the cat SCG, long latencies to response onset were also noted during experiments with these peptides (with the delay being shorter in response to BK than to angiotensin; Lewis and Reit, 1965).

5.3.1.3. Tachyphylaxis of the response.

An interesting observation was that although there was no waning of the response to BK during a prolonged (6 minute) exposure to maximally effective concentrations of the peptide (no "desensitization"; in contrast to desensitization of BK-inhibition of $I_{K(M)}$ in NG108-15 cells during a 6 minute application: Robbins *et al.*, 1993), there was a waning of the response to repeated, shorter (1-2 minute) applications of maximally effective concentrations of BK (defined here as "tachyphylaxis"). This was not encountered with concentrations of BK at the lower range of the concentration-response curve. In other preparations, "desensitization" or "tachyphylaxis" of the response to BK has frequently been reported; for example, in sympathetic ganglia (Lewis and Reit, 1965), and in sensory neurones (Burgess *et al.*, 1989; Dray *et al.*, 1992). However, it is often unclear whether the phenomenon described is really desensitization or tachyphylaxis, or if both occur concomitantly: for example, Lewis and Reit (1965) described quite clearly tachyphylaxis in response to both BK and angiotensin, but did not indicate whether desensitization during long exposures to the peptide was also encountered.

If tachyphylaxis can occur without desensitization, this would imply that in order to functionally remove its own receptor from biological activity, BK must itself first dissociate from the receptor. This would suggest that it is the unoccupied, inactive form of the receptor (R), rather than the active form (AR*) which is sensitive to a mechanism of tachyphylaxis that is perhaps initiated during occupation of the receptor with BK, but only takes effect when BK dissociates. The mechanism of tachyphylaxis in SCG cells has not been investigated. However, in sensory neurones (cultured DRG cells), "desensitization" of the BK-activation of the cation current (waning of repeated responses to BK, and therefore equivalent to the phenomenon described in the present study) involves a nitric oxide-cGMP pathway: desensitization was reduced by nitric oxide synthase inhibitors, and this effect was overcome using 8Bromo-cGMP

(McGehee *et al.*, 1992). By analogy, it is possible that tachyphylaxis involves receptor (or G protein) phosphorylation, for example, by cGMP-dependent-protein kinase. If such a mechanism can only target unoccupied receptor, then it should be possible to induce tachyphylaxis, using agents which stimulate this pathway (for example, 8Bromo-cGMP), without prior exposure to BK. Conversely, if AR* is the target, then application of BK would be required for tachyphylaxis to occur. Of course, the involvement of such a mechanism must first be demonstrated, by using inhibitors of NO synthase and protein kinases. The lack of cross-tachyphylaxis between BK and oxo-M mediated $I_{K(M)}$ inhibition would suggest that any common transduction mechanism shared by these receptors cannot be affected (see Chapter 6 for further discussion): this is supported by observations in NG108-15 cells, where desensitization of BK-inhibition of $I_{K(M)}$ (see above) had no effect on $I_{K(M)}$ inhibition by acetylcholine (Robbins *et al.*, 1993). Thus, it appears more likely that the BK receptor, rather than the G protein, would be the target for the putative phosphorylation-induced tachyphylaxis.

It is possible that during the present experiments, slow dissociation from the receptor caused BK to remain bound long after the cell was washed with BK-free solution, sufficient to cause classical desensitization, because wash times of 15 to 20 minutes were often necessary to reverse the $I_{K(M)}$ inhibition. If the BK-receptor interaction was maintained throughout this time, then the apparent phenomenon of tachyphylaxis may in fact reflect an on-going desensitization. To investigate whether this was the case, it would be necessary to expose cells to BK for a period in excess of the usual wash times. However, the phenomenon of tachyphylaxis in the absence of desensitization has also been reported for angiotensin II-inhibition of voltage-gated Ca^{2+} current in SCG neurones (Shapiro *et al.*, 1994), and therefore may represent a real process which enables the peptides to have potent and prolonged actions on sympathetic neurones, but which ensures a period of refractoriness following these potent effects; it is also possible that the short life of BK, due to enzymatic degradation, limits the activity of the peptide on sympathetic neurones and precludes the need for a desensitization mechanism.

The effects of maximally effective concentrations of both agonists applied together were not additive, as a component of $I_{K(M)}$ remained insensitive to agonist-inhibition. This suggests that both agonists may utilize the same transduction pathway, although information about the transduction mechanisms for these two receptor-mediated effects on $I_{K(M)}$ must ultimately be obtained by direct experiments; for example, by using anti-G protein antibodies.

5.3.2. G proteins mediating inhibition of $I_{K(M)}$ by BK.

5.3.2.1. Pertussis toxin-insensitivity.

Like the muscarinic inhibition of $I_{K(M)}$ (Brown *et al.*, 1989), the response to BK was found not to involve a pertussis toxin (PTX)-sensitive G protein. The lack of effect of PTX on $I_{K(M)}$ inhibition by BK is unlikely to be due to inactivity of the toxin, as the same batch of toxin has been used to reduce noradrenaline-inhibition of voltage-gated Ca^{2+} current in SCG neurones, and has been shown to completely ADP-ribosylate susceptible G proteins (Caulfield *et al.*, 1994). This substantiated the possibility that BK utilizes the same, or a closely related G protein to the G protein(s) transducing muscarinic receptor-mediated inhibition of $I_{K(M)}$ (Chapter 4).

Previous studies suggest that BK receptors can couple to G proteins belonging to the categories of PTX-sensitive and PTX-insensitive, in different cell types (Hall, 1992 for review). In DRG neurones, inhibition of voltage-gated Ca^{2+} current by BK was PTX-sensitive; after functionally removing the endogenous G protein transducing this effect of BK using PTX, the response could be completely reconstituted with a combination of αo and $\alpha i2$, implicating these G protein subunits in transducing this response (Ewald *et al.*, 1989). In NG108-15 cells, anti-G protein antibodies have been used to demonstrate the involvement of $G_{\alpha q/11}$ in transducing BK-induced activation of PLC (Gutowski *et al.*, 1991) and activation of a Ca^{2+}-dependent K^+ current, but not inhibition of voltage-gated Ca^{2+} current by BK (the latter response does, however, use a PTX-insensitive G protein; Wilk-Blaszczak *et al.*, 1994). In the present experiments, anti-G protein antibodies were used to investigate whether the PTX-insensitive

transduction mechanism for $I_{K(M)}$ inhibition by BK in SCG neurones also involves $G_{\alpha q/11}$.

5.3.2.2. $G_{\alpha q/11}$ involvement.

Experiments with anti-G protein antibodies revealed a powerful blocking action of the anti-$G_{\alpha q/11}$ antibody, with no effect of the anti-$G_{\alpha o}$ antibody on $I_{K(M)}$ inhibition by BK. The response to 1 nM BK was almost completely blocked by injection of anti-$G_{\alpha q/11}$ antibody, with the variation in sensitivity to the antibody action that was observed with the muscarinic receptor inhibition of $I_{K(M)}$ almost absent. The lack of effect of the anti-$G_{\alpha o}$ antibody cannot be attributed to functional inactivity, as this antibody has previously been shown to reduce noradrenaline-inhibition of the voltage-gated Ca^{2+} current in rat cultured SCG cells (Caulfield *et al.*, 1994). This suggests a selective blocking action for the anti-$G_{\alpha q/11}$ antibody that is not seen with the anti-$G_{\alpha o}$ antibody. Additionally, mixing the anti-$G_{\alpha q/11}$ antibody with the synthetic C-terminal peptide (to which the antibody was raised) significantly reduced the blocking effect of the antibody, further supporting a specific interaction of the antibody with the C-terminal decapeptide sequence of the $G_{\alpha q/11}$ subunit, rather than a non-specific effect of another component of the antiserum.

These experiments confirm that the G protein(s) transducing a significant portion of the inhibition of $I_{K(M)}$ by BK is/ are either $G_{\alpha q}$, $G_{\alpha 11}$, or both. However, in 4 out of 8 cells injected with anti-$G_{\alpha q/11}$ antibody, there was a residual (although considerably reduced) response to 1 nM BK, indicating that another G protein may participate in transducing this response to BK. Possible candidates for transducing this residual inhibition include another PTX-insensitive G protein from the known families outlined by Simon *et al.*, 1991, a PTX-sensitive G protein, which may become significant when levels of functional $G_{\alpha q/11}$ are reduced, or $\beta\gamma$ subunits, such as has been proposed for $I_{K(ACh)}$ activation, PLA_2 activation and, interestingly, PLC activation (reviewed by Clapham and Neer, 1993). These possibilities were considered for muscarinic receptor-mediated inhibition of $I_{K(M)}$ in Chapter 4.

As discussed above, the $G_{q/11}$ α-subunits have previously been found to mediate hyperpolarizing effects of BK on NG108-15 cells (activation of $I_{K(Ca)}$; Wilk-Blaszczak *et al.*, 1994), and BK receptors may also couple to the PTX-sensitive G protein α-subunits of G_o and G_i in cultured DRG neurones (Ewald *et al.*, 1989). The demonstration here that BK can activate $G_{\alpha q/11}$ to produce excitatory effects on SCG neurones adds to the diverse repertoire of transduction pathways triggered by BK receptors. This effect of BK on SCG neurones is mediated by the B_2 receptor, as the response was antagonized by 100 nM HOE140, the B_2-selective antagonist (Jones *et al.*, 1995). It would be interesting to determine whether all of these G protein-linked pathways activated by BK are controlled by the same receptor subtype, or whether there is a case for further BK receptor heterogeneity, with different subtypes coupling to different transduction mechanisms, for example in comparison with muscarinic receptor subtypes (see Chapter 1).

5.3.3. Putative second messenger pathways.

As with the muscarinic receptor-mediated inhibition of $I_{K(M)}$, information regarding the identity of the G protein(s) transducing the response to BK can provide some clues to a putative diffusible messenger (although the involvement of such a messenger has not yet been confirmed by single M-channel recordings, similar to those carried out for the muscarinic inhibition of M-channels (Selyanko *et al.*, 1992)). The involvement of $G_{\alpha q}$ and/ or $G_{\alpha 11}$ once more implicates the PLC pathway in $I_{K(M)}$ inhibition (see Chapter 1). Unlike muscarinic receptor-mediated transduction mechanisms in $I_{K(M)}$ modulation , there has been relatively more success in identifying potential signalling pathways for BK receptor-mediated effects. In NG108-15 cells, microelectrode voltage-clamp recordings demonstrated that two products of PLC activation, IP_3 and DAG, could sequentially regulate two ionic conductances, the latter being $I_{K(M)}$, and implicated this pathway in BK receptor-mediated inhibition of $I_{K(M)}$ (Higashida and Brown, 1986). Experiments with whole-cell voltage-clamp recording substantiated a partial role for the DAG-PKC involvement in $I_{K(M)}$ inhibition by BK (Schäfer *et al.*, 1991). There is evidence too that excitatory effects of BK on sensory neurones also involve DAG and PKC activation (for example, Dray *et al.*, 1988;

Burgess *et al.*, 1989; McGuirk and Dolphin, 1992). However, the involvement of PLA_2 products, cyclic nucleotides and even nitric oxide in mediating the effects of BK would not be totally unexpected (see Hall, 1992 for a review of the full repertoire of BK receptor-effector coupling mechanisms).

5.3.4. BK-inhibition of $I_{K(M)}$: possible significance to sympathetic nerve function.

The experiments outlined in this chapter have demonstrated a mechanism by which BK could excite SCG neurones. Thus, BK produces a slow inhibition of $I_{K(M)}$ *via* activation of the G protein α-subunit(s), $G_{\alpha q/11}$ (although this may not be the only pathway by which BK inhibits $I_{K(M)}$). These data complement previous observations *in vivo*, demonstrating a ganglion-stimulating action of BK (Lewis and Reit, 1965). Moreover, this excitatory action of BK provides a potential mechanism by which BK can evoke release of the sympathetic neurotransmitter, noradrenaline (Laneuville *et al.*, 1989; Llona *et al.*, 1991; Green *et al.*, 1993; Tsuda *et al.*, 1993: see Introduction), and inflammatory mediators such as prostaglandins (Dray and Perkins, 1993 for review). Thus, by inhibiting $I_{K(M)}$ BK could effectively recruit sympathetic nerves in inflammatory reactions and in pain. Additionally, by evoking noradrenaline release, BK could also influence vascular tone in blood vessels that are sympathetically innervated. The question therefore arises of whether an interaction between BK and sympathetic nerves, involving inhibition of $I_{K(M)}$, is feasible *in situ*. There have been no reports of BK, or the synthetic and degradative enzymes for BK, within sympathetic ganglia, although the present data, as well as previous experiments on sympathetic ganglia clearly show that sympathetic neurones can express functional BK receptors, and in fact mRNA encoding the B_2 receptor has been detected in SCG from 17 day old rats, and B_2 receptors mediate this effect of BK (Jones *et al.*, 1995), which is interesting considering that B_1 (rather than B_2) receptors have been thought to have greater significance in the interaction between BK and sympathetic nerves during inflammation and pain (Dray and Perkins, 1993). B_1 receptor expression may be induced in various tissues in response to inflammatory and immunological stimuli (Hall, 1992), and so may become more significant in pathological states. While the possibility cannot be excluded at present that tissue kallikrein is present in the rat SCG,

and can act on kininogen to release either BK or kallidin within the ganglion, a more likely target for BK action is at the sympathetic nerve terminal. At this site, BK released by plasma kallikrein or by tissue kallikrein in the target organ for the sympathetic nerve (in response to tissue injury) could act locally before it is enzymatically inactivated. BK is at least as potent in its effect on rat cultured SCG neurones in comparison with effects on cultured sensory neurones, and so concentrations of BK that influence sensory neurones during inflammatory reactions to tissue injury could have a powerful effect on $I_{K(M)}$. Containing the elements of the inflammatory / pain response within a local region would be more consistent with the role of BK as a local hormone, than a situation involving release of kinins within the SCG (where multiple effects on different ganglion cells might also be expected), leading to effects at the distant presynaptic terminals. It would, of course, require that M channels are expressed at the sympathetic nerve terminal, and that inhibition of $I_{K(M)}$ at this site could provide a trigger for release of neurotransmitter and inflammatory mediators: this has not been demonstrated. In order for this possibility to be tested, a selective M-channel blocker is required, which would functionally remove (putative) M-channels from the terminal without affecting neurotransmitter release. One further point of interest is the finding of Shapiro *et al.* (1994) that the peptide angiotensin II also inhibits $I_{K(M)}$ in rat cultured SCG neurones. Again, this parallels *in vivo* findings in the cat SCG, and raises the possibility that $I_{K(M)}$ may be regulated by two potent biological peptides, in addition to acetylcholine acting at muscarinic receptors.

5.3.5. Conclusions to Chapter 5.

The peptide hormone bradykinin (BK) can potently inhibit $I_{K(M)}$ in rat sympathetic neurones. The effect of BK is slow in onset and is poorly reversible. Although this response to BK does not undergo desensitization, it is sensitive to tachyphylaxis at high concentrations of the peptide. BK inhibits $I_{K(M)}$ *via* activation of a PTX-insensitive G protein, either $G_{\alpha q}$ or $G_{\alpha 11}$, or both. As this effect of BK shares some similarities with the inhibition of $I_{K(M)}$ by oxo-M, the response to these two agonists will be compared in Chapter 6. Inhibition of $I_{K(M)}$ by BK may represent the (or one) mechanism by which BK excites sympathetic ganglia (for example, in the cat

and the rabbit). The physiological significance of these findings is not yet known; however, as sympathetic nerves are thought to be important in pain and inflammation, inhibition of $I_{K(M)}$ is a potential mechanism by which BK could stimulate sympathetic nerve involvement in inflammatory reactions.

CHAPTER 6:

Discussion.

In this thesis, inhibition of the M-type K^+ current ($I_{K(M)}$) by two G protein-coupled receptors has been described. The muscarinic agonist oxotremorine-M (oxo-M) acts at M_1 muscarinic receptors (Marrion *et al.*, 1989; Bernheim *et al.*, 1992), and the peptide hormone bradykinin (BK) acts at B_2 receptors (Jones *et al.*, 1995), to inhibit $I_{K(M)}$. The pertussis toxin-insensitive G protein(s), $G_{\alpha q}$ and/ or $G_{\alpha 11}$ transduce at least part of both receptor-mediated effects. While these two pathways for $I_{K(M)}$ inhibition share common features, there are also important distinctions. The similarities and the differences between these G protein-transduced effects on $I_{K(M)}$ will be considered in this chapter.

6.1. Characteristics of $I_{K(M)}$ inhibition by oxo-M and BK.

Table 6 summarizes the key features of the $I_{K(M)}$ inhibition in response to each agonist. From this information, certain observations regarding the two pathways can be discussed: (1) concentration-response curves; (2) rate of response; (3) efficacy; (4) recovery from agonist effect; (5) tachyphylaxis; and (6) effect of G protein antibodies. An extension of the G protein cycling scheme illustrated in Box 1 (Chapter 1) has been made (Box 2) in order to attempt to explain some of these observations.

6.1.1. Concentration-response curves.

BK was around 200 fold more potent in inhibiting $I_{K(M)}$ than oxo-M (EC_{50} values are given in Table 6). Inspection of the receptor-G protein cycle scheme in Box 2 indicates that the difference in potency between the two agonists in inhibiting $I_{K(M)}$ may result either from differences in agonist-receptor interaction (with the affinity constants K_{A2} and/ or $K_{I(R2)}$ being higher than K_{A1} and/ or $K_{I(R1)}$), or from the interaction of occupied, active receptors with G protein (with K_{G2} being higher than K_{G1}). The possibility that the higher potency of BK compared with oxo-M in inhibiting $I_{K(M)}$ is determined by K_A is more consistent with the data in a number of ways: this is discussed under the following sections.

Table 6: Comparison of $I_{K(M)}$ inhibition by oxotremorine-M and bradykinin.

	Oxotremorine-M	Bradykinin
Concentration range	30 nM to 10 μM	100 pM to 30 nM
EC_{50}	c. 200 nM	c. 1 nM
Maximum $I_{K(M)}$ inhibition	c. 85%	c. 65%
Onset latency	c. 1.5 s	c. 7.5 s
Response half-time	c. 5.5 s	c. 20 s
Reversibility	fast: 5 to 10 minutes	slow, often incomplete
Reproducibility	yes	concentration-dependent
G protein identity	$G_{\alpha q/11}$ (and other?)	$G_{\alpha q/11}$
Sensitivity to antibody	Variable, from low to complete	fairly uniform, very sensitive
Surmountability	yes partial	not tested

6.1.2. Rate of response.

The development of the response to BK was almost four times slower than the response to oxo-M (half-times, after accounting for the response on switching to high K^+, are given in Table 6). Because of the higher potency of BK compared with oxo-M in inhibiting $I_{K(M)}$, a lower concentration of BK (10 nM) than oxo-M (3 μM) was used for these experiments. As the rate of formation of [A.R] depends on the concentration of [A] used ($\tau = 1/(k_{+1}.[A] + k_{-1})$), the difference in [A] for each agonist might be expected to underlie the difference in the rates of $I_{K(M)}$ inhibition. For the purpose

Box 2

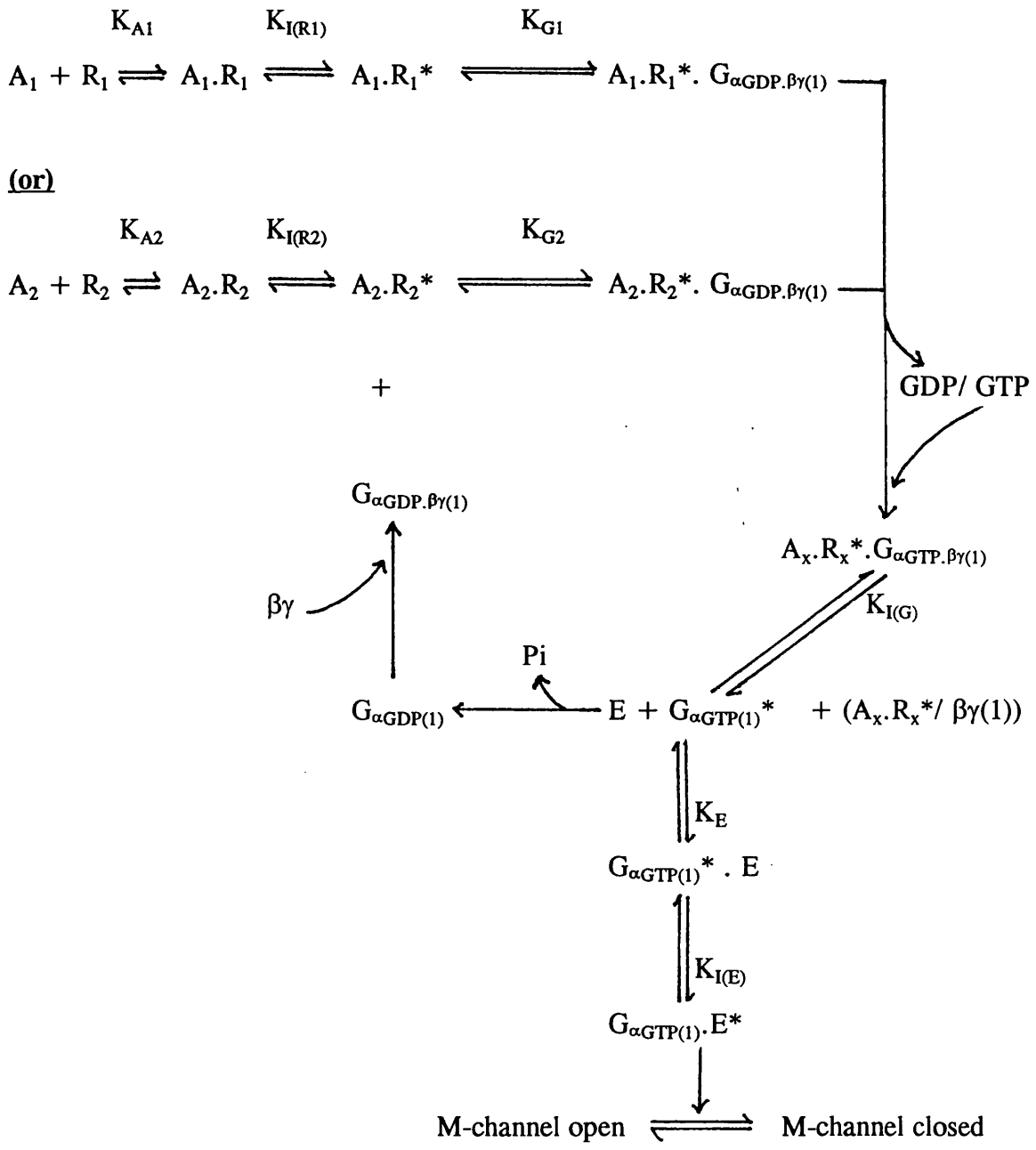

A_1/ A_2 = agonists oxo-M and BK; R_1/ R_2 = M_1/ B_2 receptor; G = G protein; E= effector (assuming a second messenger); $K_{A/ G/ E}$ = affinity constants for agonist-receptor, receptor-G protein and G protein-effector interactions respectively; K_I = affinity constant for isomerization from inactive to active forms (* denotes active forms). This scheme assumes that R_1^* and R_2^* couple to the same G protein.

of calculating this, a value for the association rate constant (k_{+1}) of 10^7 $M^{-1}.s^{-1}$ (which assumes that the rate-limiting step for formation of [A.R] is the collision of [A] with the receptor binding site: see Birdsall and Hulme, 1992) has been assumed for both agonists; the dissociation rate constant (k_{-1}) can be calculated from $K = k_{-1}/ k_{+1}$. The equilibrium dissociation constants (K) are not known, and so the EC_{50} values have been used as approximate estimates of K, giving k_{-1} values of 2 s^{-1} for oxo-M and 0.01 s^{-1} for BK. Thus, the rate of formation of [oxo-M.M_1], using 3 μM oxo-M, has a calculated time constant of around ~~0.5 s~~ 0·03s, while the rate of formation of [BK.B_2], using 10 nM BK, has a calculated time constant of around 10 s.

As the development of the response to 3 μM oxo-M has a half-time of 5.5 s, this suggests that, as [A.R] formation occurs very rapidly (τ = ~~0.5 s~~ 0·03s), subsequent events (formation of [A.R*], [G*], or putative second messenger) develop with a half-time of around ~~5~~ 5·5s s (τ = ~~7.2 s~~ 7·9s) and determine the rate of response to 3 μM oxo-M. For BK, the slower rate of formation of [BK.B_2] (τ = 10 s) at the lower concentration of BK used may partly account for the slower rate of response (half-time = 20 s, τ = 29 s), but this does not provide a full explanation. As this calculation relies on assumptions (notably, that the rate of association, limited by collision, is the same for both agonists, and that K = EC_{50}), it is possible that the calculated differences in rates of formation of [A.R] are incorrect due to inaccurate estimates of these parameters, and that the true rate constant values would explain the observed, experimental differences in the rates of response to the two agonists. However, and with these assumptions in mind, the calculation suggests that approximately 20 s of the time constant for development of the response to BK may also be due to events subsequent to formation of [BK.B_2], and therefore that formation of active G protein (and putative second messenger) is approximately ~~three~~ 2·5 times as slow in response to BK than in response to 3 μM oxo-M, even after accounting for the slower rate of formation of [BK.B_2]. Thus, it would not be unreasonable to suppose that active, occupied M_1 receptor interacts with the G protein with higher affinity than active, occupied B_2 receptor, leading to active G protein (and hence the response) being produced more rapidly. One further assumption is that M_1* and B_2* receptors activate the same G protein, and therefore the affinity

constant for the interaction of active G protein with effector (subsequent to receptor-G protein interaction) is the same for both receptor systems. Therefore (referring back to Box 2), the explanation that is more consistent with the estimates of potency and rate of response is that K_{A2} (for BK-B_2 receptor interaction) is higher than K_{A1} (oxo-M-M_1 receptor interaction), determining the higher potency of BK, while K_{G1} (M_1*-G protein interaction) is higher than K_{G2} (B_2*-G protein interaction), partially determining the shorter latency and faster rate of response to oxo-M, due to more rapid generation of active G protein (although the slow rate of response to BK is in part due to the lower concentration used).

6.1.3. Efficacy.

The observation that the maximum $I_{K(M)}$ inhibition in response to BK is significantly less than the maximum response to oxo-M (see Chapter 5 and Table 6) further implies that the affinity of the B_2*-G protein interaction may be lower than for M_1*-G protein interaction, with the lower affinity coupling underlying the lower efficacy of BK in inhibiting $I_{K(M)}$.

6.1.4. Recovery from inhibition.

The response to BK was slowly (and usually poorly) reversible, in contrast to the response to oxo-M, which frequently showed near-complete recovery within 5 to 10 minutes. The simplest explanation for this, in the scheme outlined in Box 2, is a higher K_{A2} value (for BK-B_2 interaction) compared with K_{A1} (oxo-M-M_1 interaction), due to a slower rate of dissociation of BK from its receptor (τ = 100 s, from the estimate of k_{-1} given above), compared with oxo-M (τ = 0.5 s). The time constant estimates for dissociation are faster than expected from the observed time for recovery from $I_{K(M)}$ inhibition with each agonist; this may be due to re-association of dissociated but unremoved agonist with receptor. For BK (which exhibits a slower dissociation rate), this could have been tested by using a competitive B_2 receptor antagonist, which would reduce re-association of BK with the receptor and therefore increase the observed rate of recovery: this approach was used by Jan and Jan (1992) to show that the long duration of the late, slow EPSP in bullfrog sympathetic ganglia was due to the prolonged presence of the peptide transmitter, LHRH, at the ganglion cell.

6.1.5. Tachyphylaxis.

Unlike the response to oxo-M, inhibition of $I_{K(M)}$ by high concentrations of BK was susceptible to tachyphylaxis (diminishing responses with repeated applications of agonist). This phenomenon was homologous: BK-induced tachyphylaxis of the response to BK did not cause tachyphylaxis of the response to oxo-M (Figure 27). In some experiments where oxo-M was applied prior to BK (for example, Figure 26C), there was no indication that oxo-M caused tachyphylaxis of the response to BK. The lack of cross-tachyphylaxis makes it unlikely that any putative common step in the transduction pathway used by these two agonists to inhibit $I_{K(M)}$ (for example, the G protein) is the target for the mechanism of tachyphylaxis of the BK response. Thus, either the two agonists use distinct transduction mechanisms, or tachyphylaxis is a B_2 receptor-related event. In the case of the latter possibility, this would suggest that the B_2 receptor is regulated by an additional component or pathway which cannot simultaneously regulate the M_1 receptor. By analogy with B_2 receptors in sensory neurones, this may be an intracellular mechanism involving a nitric oxide-cGMP (-protein kinase-phosphorylation) pathway to the B_2 receptor (McGehee *et al.*, 1992: see Chapter 5), although this requires investigation. As discussed in Chapter 5, it appears to be the unoccupied receptor that is the target for the tachyphylaxis mechanism, as this phenomenon is seen only after washing out BK. Differences in the amino acid sequences of B_2 and M_1 receptors (around 20% homology; McEachern *et al.*, 1991) may explain why unoccupied M_1 receptors are not susceptible for any tachyphylaxis mechanism initiated by BK receptor activation. The observation that oxo-M cannot induce tachyphylaxis of the response to BK indicates that either activated B_2 receptors can couple to a different, or an additional G protein to activated M_1 receptors to induce tachyphylaxis, unless BK-induced tachyphylaxis occurs *via* a G protein-independent mechanism.

6.1.6. G proteins.

Both receptor-mediated effects on $I_{K(M)}$ were significantly reduced by antibodies raised against the C-terminal decapeptide sequence common to the α-subunits of G_q and G_{11}, suggesting that both receptors couple to the same or a closely related G protein to inhibit $I_{K(M)}$. However, there was a notable difference in the effect of the anti-$G_{\alpha q/11}$

antibody on the response to the two agonists (Table 6). The effect of BK was more sensitive to the antibody, showing a profound reduction in all neurones tested, compared with the variable reduction of the response to oxo-M. This was not due to greater amounts of antibody being injected during the series of BK experiments; when BK and oxo-M were applied to the same anti-$G_{\alpha q/11}$ antibody-injected cells, the variability in the oxo-M (but not the BK) response was still apparent (Figure 32). There are several possible explanations for this observation. In accord with the proposals outlined above (and refer to Box 2), the observations with the anti-$G_{\alpha q/11}$ antibody may support the concept that M_1 receptors couple to $G_{\alpha q/11}$ with higher affinity (higher K_{G1}) than BK receptors, with each agonist-bound receptor interacting with more G protein and initiating more GTP/ GDP exchange. With a spare capacity of G protein, more would have to be functionally removed to affect the response to oxo-M compared with the response to BK. Thus, a higher K_A value for BK-B_2 interaction, with a lower K_G value for B_2*-$G_{\alpha q/11}$ interaction is consistent with the higher potency of BK, the slower rate of, and recovery from, the response to BK, the lower efficacy of BK, and the greater sensitivity of the response to BK to the anti-$G_{\alpha q/11}$ antibody.

However, alternative explanations for the differing sensitivity of the two responses to the antibody warrant consideration. The variable effect of the antibody on the response to oxo-M may be due to M_1 receptors using an additional PTX-insensitive G protein, or a $\beta\gamma$-subunit, as well as $G_{\alpha q}$ and/ or $G_{\alpha 11}$, with the amounts of each G protein subunit used being different in different SCG neurones. Thus in Box 2, in addition to $G_{\alpha\beta\gamma(1)}$ (representing $G_{\alpha q/11}$), another G protein, $G_{\alpha\beta\gamma(2)}$ (unidentified) would also be available to M_1 receptors, but not B_2 receptors in some SCG neurones. Hence, the response to BK would be more consistently sensitive to the anti-$G_{\alpha q/11}$ ($G_{\alpha\beta\gamma(1)}$) antibody. Antibodies to other G protein α and $\beta\gamma$ subunits (particularly α12 and α13, which are ubiquitously expressed: see Simon *et al.*, 1991) are necessary to test this latter hypothesis: however, it should be noted that the theoretical models of Kenakin and Morgan (1989) predict that for a receptor interaction with more than one G protein to produce a given response, a reduction in the level of one of the G proteins will cause

a rightward shift in the concentration-response curve with no decrease in the maximum response: in the present experiments, a reduction in the maximum response was apparent in some antibody-injected cells (see Figure 19, Chapter 4).

Interestingly, the sequence differences between $G_{\alpha q}$ and $G_{\alpha 11}$ are all in the N-terminal region (Simon *et al.*, 1991), which is proposed to determine $\beta\gamma$ interaction (Weiss *et al.*, 1988). As $\beta\gamma$ subunits regulate GTP/ GDP exchange, the rate of exchange may differ for the two α subunits depending on their interaction with (possibly different) $\beta\gamma$-subunits, and Simon *et al.* (1991) have suggested that $G_{\alpha q}$ and $G_{\alpha 11}$, being found in the same cells, may regulate signals having different time courses. Considering the difference in the time course of the $I_{K(M)}$ inhibition in response to oxo-M and BK, this raises the possibility that one agonist utilizes $G_{\alpha q}$ while the other couples to $G_{\alpha 11}$ to inhibit $I_{K(M)}$, with possible intrinsic differences in the nucleotide cycling kinetics of these two G proteins (or different levels of each being expressed in different SCG neurones) underlying the different sensitivities of the two agonist responses to antibody. Thus, in the scenario outlined in the previous paragraph (and see Box 2), $G_{\alpha\beta\gamma(1)}$ could in fact represent $G_{\alpha 11}$ and $G_{\alpha\beta\gamma(2)}$ could represent $G_{\alpha q}$ (or *vice versa*). If M_1* receptors and B_2* receptors generate different active G proteins, then differences in potency and rate of response/ recovery of response (as well as homologous tachyphylaxis of the BK response) could well be explained by different properties of the active G protein subunits or any (putative) second messenger with which they interact to reduce M-channel opening; for example, differences in K_E or $K_{I(E)}$. It should be noted that although M_1 receptors inhibit $I_{K(M)}$ by a diffusible messenger (Selyanko *et al.*, 1992), this has not yet been tested for B_2 receptors. Furthermore, the experiments of Lopez (1992) on the kinetics of G protein-induced inhibition of M-current in frog sympathetic neurones indicate that the G protein activation-deactivation cycle determines the kinetics of the M-current transduction pathway; therefore, these observations do not exclude the possibility that a G protein subunit acts as the diffusible messenger and interacts directly with the M-channel. Experiments with antisense oligodeoxynucleotides, which suppress the expression of selective G proteins (for example, either $G_{\alpha q}$ or $G_{\alpha 11}$), are required to test the

hypothesis that M_1 and B_2 receptors couple differentially to these highly homologous G proteins. However, this would in turn raise the question of whether the C-terminus of the α-subunit solely determines receptor-G protein coupling, as the C-terminal sequences of $G_{\alpha q}$ and $G_{\alpha 11}$ are identical. If two different receptors can each couple to one, but not the other, then other regions of the α-subunit (for example, the N-terminus, where the sequence differences are found) may regulate receptor-G protein coupling, perhaps due to different conformations of the α-subunits. Alternatively, additional regulatory components may be critical, such as the βγ-subunits. For example, experiments using G protein antisense DNA indicate that, in GH_3 cells, muscarinic receptors couple to $G_{\alpha o1}$ and somatostatin receptors couple to $G_{\alpha o2}$ to inhibit voltage-gated Ca^{2+} current (Kleuss *et al.*, 1991). As the C-terminal sequences of the two $G_{\alpha o}$ subunits are identical, then it might be expected that both receptors would couple to both α-subunits. In this example, the two receptors depend on the availability of different β- and γ-subunits in order to inhibit Ca^{2+} current (Kleuss *et al.*, 1992; 1993): if the β- and γ-subunits can determine the receptor-G_α protein interaction, this would explain the preference of the two receptors for different α-subunits. This would not be surprising, as βγ-subunits are required for receptor-catalyzed nucleotide exchange (Weiss *et al.*, 1988).

The interesting finding that the effect of the antibody on the response to oxo-M was surmountable was not tested for BK. This was because problems with tachyphylaxis at higher concentrations of BK would have made these experiments difficult to control. However, it would have been interesting to see if this feature is common to both transduction mechanisms, particularly with regard to speculation on the efficiency of coupling of the two systems. Thus, if the effect of antibody on the BK response was surmountable, this would indicate a G protein reserve for this response also, and would also have challenged the hypothesis that BK receptors couple less efficiently to the G protein transducing this response.

6.2. Future directions.

Many questions relating to this work remain unanswered. The explanations put forward for differences in the inhibition of $I_{K(M)}$ by the two G protein-coupled receptors are speculative, and require further experiments to test them. A significant step would be to correlate the loss of G protein function in inhibiting $I_{K(M)}$ with the decrease in levels of G protein, and to determine this relationship for the two pathways for $I_{K(M)}$ inhibition. Additionally, it is hoped that G protein antisense DNA sequences will eventually prove more useful in determining which of the two G proteins, $G_{\alpha q}$ and/ or $G_{\alpha 11}$, are used by M_1 and B_2 receptors. The development of antibodies and antisense DNA to target other PTX-insensitive G protein α-subunits as well as different $\beta\gamma$-subunits may also be instructive. Based on the information regarding the G proteins transducing at least part of the $I_{K(M)}$ inhibition by these receptors, it is also hoped that this will provide new impetus in determining the identity of the diffusible messenger mediating $I_{K(M)}$ inhibition, particularly whether it is a G protein subunit that directly regulates the M-channel, or whether an intermediate messenger is required. Now that M-channels have been isolated in cell-attached and excised patches from rat sympathetic neurones, it should be possible to determine whether BK also inhibits $I_{K(M)}$ *via* a diffusible messenger and, ultimately, whether the diffusible messenger is the same for the two receptor systems. It should eventually be possible to develop antibodies to uncouple the G protein from the effector, and determine which part of the G protein participates in this interaction. The cloning of the M-channel is eagerly awaited, as this will provide further opportunities to study receptor-G protein-(messenger)-channel interactions at the molecular level.

References.

Adams, P.R., Brown, D.A., and Constanti, A. (1982a). M-currents and other potassium currents in bullfrog sympathetic neurones. *Journal of Physiology*. **330**, 537-572.

Adams, P.R., Brown, D.A., and Constanti, A. (1982b). Pharmacological inhibition of the M-current. *Journal of Physiology*. **332**, 223-262.

Adams, P.R. and Brown, D.A. (1982). Synaptic inhibition of the M-current. Slow excitatory post-synaptic potential mechanism in bullfrog sympathetic neurones. *Journal of Physiology*. **332**, 263-272.

Akhtar, S. and Juliano, R.L. (1992). Cellular uptake and intracellular fate of antisense oligonucleotides. *Trends in Cell Biology*. **2**, 139-144.

Aragay, A.M., Katz, A., and Simon, M.I. (1992). The $G_{\alpha q}$ and $G_{\alpha 11}$ proteins couple the thyrotropin-releasing hormone receptor to phospholipase C in GH_3 rat pituitary cells. *Journal of Biological Chemistry*. **267**, 24983-24988.

Armstrong, D. (1970). Pain. In Bradykinin, kallidin and kallikrein. E.G. Erdos, ed. *Handbook of Experimental Pharmacology* (Berlin, Heidleberg, New York: Springer-Verlag). **25**, pp. 434-481.

Baccaglini, P.I. and Hogan, P.G. (1983). Some rat sensory neurons in culture express characteristics of differentiated pain sensory cells. *Proceedings of the National Academy of Sciences USA*. **80**, 594-598.

Barry, E.L.R., Gesek, F.A., and Friedman, P.A. (1993). Introduction of antisense oligonucleotides into cells by permeabilization with streptolysin O. *BioTechniques*. **15**, 1016-1020.

Beech, D.J., Bernheim, L., Mathie, A., and Hille, B. (1991). Intracellular Ca^{2+} buffers disrupt muscarinic suppression of Ca^{2+} current and M current in rat sympathetic neurons. *Proceedings of the National Academy of Sciences USA.* **88**, 652-656.

Béhé, P., Sandmeier, K., and Meves, H. (1992). The effect of arachidonic acid on the M current of NG108-15 neuroblastoma x glioma hybrid cells. *Pflügers Archiv.* **422**, 120-128.

Bernheim, L., Mathie, A., and Hille, B. (1992). Characterization of muscarinic receptor subtypes inhibiting Ca^{2+} current and M current in rat sympathetic neurons. *Proceedings of the National Academy of Sciences USA.* **89**, 9544-9548.

Berstein, G., Blank, J.L., Smrcka, A.V., Higashijima, T., Sternweis, P.C., Exton, J.H., and Ross, E.M. (1992). Reconstitution of agonist-stimulated phosphatidylinositol 4,5-bisphosphate hydrolysis using purified m1 muscarinic receptor, $G_{q/11}$, and phospholipase C-β1. *Journal of Biological Chemistry.* **267**, 8081-8088.

Bhoola, K.D., Figueroa, C.D., and Worthy, K. (1992). Bioregulation of kinins: kallikreins, kininogens, and kininases. *Pharmacological Reviews.* **44**, 1-80.

Bone, E.A., Fretten, P., Palmer, S., Kirk, C.J., and Michell, R.H. (1984). Rapid accumulation of inositol phosphates in isolated rat superior cervical sympathetic ganglia exposed to V_1-vasopressin and muscarinic cholinergic stimuli. *Biochemical Journal.* **221**, 803-811.

Bosma, M.M., Bernheim, L., Leibowitz, M.D., Pfaffinger, P.J., and Hille, B. (1990). Modulation of M current in frog sympathetic ganglion cells. In G proteins and signal transduction. N.M. Nathanson and T.K. Harden, eds. (New York: Rockefeller University Press), Chapter 4, pp. 43-59.

Bosma, M.M. and Hille, B. (1989). Protein kinase C is not necessary for peptide-induced suppression of M current or for desensitization of the peptide receptors. *Proceedings of the National Academy of Sciences USA.* **86**, 2943-2947.

Brown, A.M. and Birnbaumer, L. (1990). Ionic channels and their regulation by G protein subunits. *Annual Reviews in Physiology.* **52**, 197-213.

Brown, D.A., Forward, A., and Marsh, S. (1980). Antagonist discrimination between ganglionic and ileal muscarinic receptors. *British Journal of Pharmacology.* **71**, 362-364.

Brown, D.A. (1988a). M-currents: an update. *Trends in Neurosciences.* **11**, 294-299.

Brown, D.A. (1988b). M Currents. In Ion channels. T. Narahashi, ed. (New York: Plenum Press), Chapter 2, pp. 55-94.

Brown, D.A., Marrion, N.V., and Smart, T.G. (1989). On the transduction mechanism for muscarine-induced inhibition of M-current in cultured rat sympathetic neurones. *Journal of Physiology.* **413**, 469-488.

Brown, D.A. (1990). G-proteins and potassium currents in neurons. *Annual Reviews in Physiology.* **52**, 215-242.

Brown, D.A., Higashida, H., Noda, M., Ishizaka, N., Hashii, M., Hoshi, N., Yokoyama, S., Fukuda, K., Katayama, M., Nukuda, T., Kameyama, K., Robbins, J., Marsh, S.J., and Selyanko, A.A. (1993). Coupling of muscarinic receptor subtypes to ion channels: experiments on neuroblastoma hybrid cells. *Annals of the New York Academy of Sciences.* **707**, 237-258.

Brown, D.A. and Adams, P.R. (1980). Muscarinic suppression of a novel voltage-sensitive K^+ current in a vertebrate neurone. *Nature.* **283**, 673-676.

Brown, D.A. and Adams, P.R. (1987). Effects of phorbol dibutyrate on M currents and M current inhibition in bullfrog sympathetic neurons. *Cellular and Molecular Neurobiology*. **7**, 255-269.

Brown, D.A. and Selyanko, A.A. (1985a). Two components of muscarine-sensitive membrane current in rat sympathetic neurones. *Journal of Physiology*. **358**, 335-363.

Brown, D.A. and Selyanko, A.A. (1985b). Membrane currents underlying the cholinergic slow excitatory post-synaptic potential in the rat sympathetic ganglion. *Journal of Physiology*. **365**, 365-387.

Burgess, G.M., Mullaney, I., McNeill, M., Dunn, P.M., and Rang, H.P. (1989). Second messengers involved in the mechanism of action of bradykinin in sensory neurons in culture. *Journal of Neuroscience*. **9**, 3314-3325.

Cambridge, H. and Brain, S.D. (1994). The role of sympathetic nerves in bradykinin (BK)-induced plasma extravasation in the rat knee joint. *Neuropeptides*. **26**, 64 (Abstract).

Campbell, V., Berrow, N., and Dolphin, A.C. (1993). $GABA_B$ receptor modulation of calcium channels by the G protein G_o: evidence from antisense oligonucleotide studies. *Journal of Physiology*. **470**, 1-11.

Camps, M., Carozzi, A., Schnabel, P., Scheer, A., Parker, P., and Gierschik, P. (1992). Isozyme-selective stimulation of phospholipase C-β2 by G protein βγ-subunits. *Nature*. **360**, 684-686.

Caulfield, M.P. (1993). Muscarinic receptors-characterization, coupling and function. *Pharmacology and Therapeutics*. **58**, 319-379.

Caulfield, M.P., Vallis, Y., Mullaney, I., Milligan, G., and Brown, D.A. (1993). α-Adrenoceptor inhibition of voltage-gated calcium current (I_{Ca}) in cultured rat sympathetic neurones is reduced by antibodies to the α-subunit of the G protein G_o. *Journal of Physiology*. **473**, 41P (Abstract).

Caulfield, M.P., Jones, S., Vallis, Y., Buckley, N.J., Kim, G.D., Milligan, G., and Brown, D.A. (1994). Muscarinic M-current inhibition *via* $G_{\alpha q/11}$ and α-adrenoceptor inhibition of Ca^{2+} current *via* $G_{\alpha o}$ in rat sympathetic neurones. *Journal of Physiology*. **477**, 415-422.

Chen, H. and Smith, P.A. (1992). M-currents in frog sympathetic ganglion cells: manipulation of membrane phosphorylation. *British Journal of Pharmacology*. **105**, 329-334.

Clapham, D.E. and Neer, E.J. (1993). New roles for G-protein βγ-dimers in transmembrane signalling. *Nature*. **365**, 403-406.

Cockcroft, S. and Thomas, G.M.H. (1992). Inositol-lipid-specific phospholipase C isoenzymes and their differential regulation by receptors. *Biochemical Journal*. **288**, 1-14.

Coderre, T.J., Basbaum, A.I., and Levine, J.D. (1989). Neural control of vascular permeability: interactions between primary afferents, mast cells, and sympathetic efferents. *Journal of Neurophysiology*. **62**, 48-58.

Constanti, A. and Brown, D.A. (1981). M-currents in voltage-clamped mammalian sympathetic neurones. *Neuroscience Letters*. **24**, 289-294.

Constanti, A. and Galvan, M. (1983). M-current in voltage-clamped olfactory cortex neurones. *Neuroscience Letters*. **39**, 65-70.

Dhanasekaran, N., Vara Prasad, M.V.V.S., Wadsworth, S.J., Dermott, J.M., and van Rossum, G. (1994). Protein kinase C-dependent and -independent activation of Na^+/H^+ exchanger by $G_{\alpha 12}$ class of G proteins. *Journal of Biological Chemistry*. **269**, 11802-11806.

Dolphin, A.C. (1987). Nucleotide binding proteins in signal transduction and disease. *Trends in Neurosciences*. **10**, 53-56.

Dray, A., Bettaney, J., Forster, P., and Perkins, M.N. (1988). Bradykinin-induced stimulation of afferent fibres is mediated through protein kinase C. *Neuroscience Letters*. **91**, 301-307.

Dray, A., Patel, I.A., Perkins, M.N., and Rueff, A. (1992). Bradykinin-induced activation of nociceptors: receptor and mechanistic studies on the neonatal rat spinal cord-tail preparation *in vitro*. *British Journal of Pharmacology*. **107**, 1129-1134.

Dray, A. and Perkins, M. (1993). Bradykinin and inflammatory pain. *Trends in Neurosciences*. **16**, 99-104.

Dunn, P.M. and Rang, H.P. (1990). Bradykinin-induced depolarization of primary afferent nerve terminals in the neonatal rat spinal cord *in vitro*. *British Journal of Pharmacology*. **100**, 656-660.

Dutar, P. and Nicoll, R.A. (1988). Classification of muscarinic responses in hippocampus in terms of receptor subtypes and second-messenger systems: electrophysiological studies *in vitro*. *Journal of Neuroscience*. **8**, 4214-4224.

Ewald, D.A., Pang, I.H., Sternweis, P.C., and Miller, R.J. (1989). Differential G protein-mediated coupling of neurotransmitter receptors to Ca^{2+} channels in rat dorsal root ganglion neurons *in vitro*. *Neuron*. **2**, 1185-1193.

ffrench-Mullen, J.M.H., Plata-Salamán, C.R., Buckley, N.J., and Danks, P. (1994). Muscarinic modulation by a G protein α-subunit of delayed rectifier K^+ current in rat ventromedial hypothalamic neurones. *Journal of Physiology*. **474**, 21-26.

Field, J.L. and Newberry, N.R. (1989). Methoctramine and hexahydrodifenidol antagonise two muscarinic responses on the rat superior cervical ganglion with opposite selectivity. *Neuroscience Letters*. **100**, 254-258.

Finkel, A.S. and Redman, S. (1984). Theory and operation of a single microelectrode voltage clamp. *Journal of Neuroscience Methods*. **11**, 101-127.

Fisher, S.K., Klinger, P.D., and Agranoff, B.W. (1983). Muscarinic agonist binding and phospholipid turnover in brain. *Journal of Biological Chemistry*. **258**, 7358-7363.

Fisher, S.K., Figueiredo, J.C., and Bartus, R.T. (1984). Differential stimulation of inositol phospholipid turnover in brain by analogs of oxotremorine. *Journal of Neurochemistry*. **43**, 1171-1179.

Fleming, W.W., Westfall, D.P., de la Lande, I.S., and Jellett, L.B. (1972). Log-normal distributions of equieffective doses of norepinephrine and acetylcholine in several tissues. *Journal of Pharmacology and Experimental Therapeutics*. **181**, 339-345.

Fukuda, K., Higashida, H., Kubo, T., Maeda, A., Akiba, I., Bujo, H., Mishina, M., and Numa, S. (1988). Selective coupling with K^+ currents of muscarinic acetylcholine receptor subtypes in NG108-15 cells. *Nature*. **335**, 355-358.

Gähwiler, B.H. and Brown, D.A. (1985). Functional innervation of cultured hippocampal neurones by cholinergic afferents from co-cultured septal explants. *Nature*. **313**, 577-579.

Georgoussi, Z., Carr, C., and Milligan, G. (1993). Direct measurement of *in situ* interactions of rat brain opioid receptors with the guanine nucleotide-binding protein G_o. *Molecular Pharmacology*. **44**, 62-69.

Goldsmith, P., Gierschik, P., Milligan, G., Unson, C.G., Vinitsky, R., Malech, H., and Spiegel, A.M. (1987). Antibodies directed against synthetic peptides distinguish between GTP-binding proteins in neutrophil and brain. *Journal of Biological Chemistry*. **262**, 14683-14688.

Green, P.G., Luo, J., Heller, P.H., and Levine, J.D. (1993). Further substantiation of a significant role for the sympathetic nervous system in inflammation. *Neuroscience*. **55**, 1037-1043.

Grove, E.A., Caulfield, M.P., and Evans, F.J. (1990). Inhibition of protein kinase C prevents phorbol ester- but not muscarine-induced depolarizations in the rat superior cervical ganglion. *Neuroscience Letters*. **110**, 162-166.

Gutowski, S., Smrcka, A., Nowak, L., Wu, D., Simon, M.I., and Sternweis, P.C. (1991). Antibodies to the α_q subfamily of guanine nucleotide-binding regulatory protein α-subunits attenuate activation of phosphatidylinositol 4,5-bisphosphate hydrolysis by hormones. *Journal of Biological Chemistry*. **266**, 20519-20524.

Haefely, W.E. (1970). Some actions of bradykinin and related peptides on autonomic ganglion cells. In Bradykinin and related kinins: cardiovascular, biochemical, and neural actions. F. Sicuteri, M. Rocha e Silva, and N. Black, eds. *Advances in Experimental Medicine and Biology* (New York: Plenum Press). **8**, pp. 591-599.

Hall, J.M. (1992). Bradykinin receptors: pharmacological properties and biological roles. *Pharmacology and Therapeutics*. **56**, 131-190.

Halliwell, J.V. and Adams, P.R. (1982). Voltage-clamp analysis of muscarinic excitation in hippocampal neurons. *Brain Research*. **250**, 71-92.

Hamill, O.P., Marty, A., Neher, E., Sakmann, B., and Sigworth, F.J. (1981). Improved patch-clamp techniques for high-resolution current recording from cells and cell-free membrane patches. *Pflügers Archiv.* **391**, 85-100.

Harris-Warrick, R.M., Hammond, C., Paupardin-Tritsch, D., Homburger, V., Rouot, B., Bockaert, J., and Gerschenfeld, H.M. (1988). An α_{40} subunit of a GTP-binding protein immunologically related to G_o mediates a dopamine-induced decrease of Ca^{2+} current in snail neurons. *Neuron.* **1**, 27-32.

Hélène, C. and Toulmé, J.-J. (1990). Specific regulation of gene expression by antisense, sense and antigene nucleic acids. *Biochimica et Biophysica Acta.* **1049**, 99-125.

Hepler, J.R. and Gilman, A.G. (1992). G proteins. *Trends in Biochemical Sciences.* **17**, 383-387.

Hess, J.F., Borkowski, J.A., Young, G.S., Strader, C.D., and Ransom, R.W. (1992). Cloning and pharmacological characterization of a human bradykinin ($BK\text{-}B_2$) receptor. *Biochemical and Biophysical Research Communications.* **184**, 260-268.

Higashida, H. and Brown, D.A. (1986). Two polyphosphatidylinositide metabolites control two K^+ currents in a neuronal cell. *Nature.* **323**, 333-335.

Hille, B. (1992). Potassium channels and chloride channels. In Ionic channels of excitable membranes. (Sunderland, MA: Sinauer Associates), pp. 115-139.

Horn, R. and Korn, S.J. (1992). Prevention of rundown in electrophysiological recording. In Ion channels. B. Rudy and L. Iverson, eds. *Methods in Enzymology* (San Diego, CA: Academic press). **207**, pp. 149-155.

Horn, R. and Marty, A. (1988). Muscarinic activation of ionic currents measured by a new whole-cell recording method. *Journal of General Physiology.* **92**, 145-159.

Horwitz, J., Tsymbalov, S., and Perlman, R.L. (1985). Muscarine stimulates the hydrolysis of inositol-containing phospholipids in the superior cervical ganglion. *Journal of Pharmacology and Experimental Therapeutics*. **233**, 235-241.

Hulme, E.C., Birdsall, N.J.M., and Buckley, N.J. (1990). Muscarinic receptor subtypes. *Annual Reviews in Pharmacology and Toxicology*. **30**, 633-673.

Hulme, E.C. and Birdsall, N.J.M. (1992). Strategy and tactics in receptor-binding studies. In Receptor-ligand interactions. A practical approach. E.C. Hulme, ed. (Oxford, New York, Tokyo: IRL Press, Oxford University Press), pp. 63-176.

Jacquin, T., Champagnat, J., Madamba, S., Denavit-Saubie, M., and Siggins, G.R. (1988). Somatostatin depresses excitability in neurons of the solitary tract complex through hyperpolarization and augmentation of I_M, a non-inactivating voltage-dependent outward current blocked by muscarinic agonists. *Proceedings of the National Academy of Sciences USA*. **85**, 948-952.

Jan, L.Y. and Jan, Y.N. (1982). Peptidergic transmission in sympathetic ganglia of the frog. *Journal of Physiology*. **327**, 219-246.

Jones, S., Brown, D.A., Milligan, G., Willer, E., Buckley, N.J., and Caulfield, M.P. (1995). Bradykinin excites rat sympathetic neurons by inhibition of M-current through a mechanism involving B_2 receptors and $G_{\alpha q/11}$. *Neuron* (in press).

Jones, S.W. (1985). Muscarinic and peptidergic excitation of bullfrog sympathetic neurones. *Journal of Physiology*. **366**, 63-87.

Jones, S.W. (1989). On the resting potential of isolated frog sympathetic neurons. *Neuron*. **3**, 153-161.

Jones, S.W. (1991). Time course of receptor-channel coupling in frog sympathetic neurons. *Biophysical Journal*. **60**, 502-507.

Katz, A., Wu, D., and Simon, M.I. (1992). Subunits βγ of heterotrimeric G protein activate β2 isoform of phospholipase C. *Nature*. **360**, 686-689.

Kay, A.R. (1992). An intracellular medium formulary. *Journal of Neuroscience Methods*. **44**, 91-100.

Kenakin, T.P. and Morgan, P.H. (1989). Theoretical effects of single and multiple transducer receptor coupling proteins on estimates of the relative potency of agonists. *Molecular Pharmacology*. **35**, 214-222.

Kennedy, M.B. (1992). Second messengers and neuronal function. In An introduction to molecular neurobiology. Z.W. Hall, ed. (Sunderland, MA: Sinauer Associates), pp. 207-246.

Kirkwood, A., Simmons, M.A., Mather, R.J., and Lisman, J. (1991). Muscarinic suppression of the M-current is mediated by a rise in internal Ca^{2+} concentration. *Neuron*. **6**, 1009-1014.

Kleuss, C., Hescheler, J., Ewel, C., Rosenthal, W., Schultz, G., and Wittig, B. (1991). Assignment of G-protein subtypes to specific receptors inducing inhibition of calcium currents. *Nature*. **353**, 43-48.

Kleuss, C., Scherubl, H., Hescheler, J., Schultz, G., and Wittig, B. (1992). Different β-subunits determine G-protein interaction with transmembrane receptors. *Nature*. **358**, 424-426.

Kleuss, C., Scherubl, H., Hescheler, J., Schultz, G., and Wittig, B. (1993). Selectivity in signal transduction determined by γ subunits of heterotrimeric G proteins. *Science*. **259**, 832-834.

Koltzenburg, M., Kress, M., and Reeh, P.W. (1991). The nociceptor sensitization by bradykinin does not depend on sympathetic neurons. *Neuroscience*. **46**, 465-473.

Laneuville, O., Reader, T.A., and Couture, R. (1989). Intrathecal bradykinin acts presynaptically on spinal noradrenergic terminals to produce antinociception in the rat. *European Journal of Pharmacology*. **159**, 273-283.

Lee, C.H., Park, D., Wu, D., Rhee, S.G., and Simon, M.I. (1992). Members of the G_q a subunit gene family activate phospholipase Cβ isozymes. *Journal of Biological Chemistry*. **267**, 16044-16047.

Levine, J.D., Taiwo, Y.O., Collins, S.D., and Tam, J.K. (1986). Noradrenaline hyperalgesia is mediated through interaction with sympathetic postganglionic neurone terminals rather than activation of primary afferent nociceptors. *Nature*. **323**, 158-160.

Lewis, G.P. (1970). Kinins in inflammation and tissue injury. In Bradykinin, kallidin and Kallikrein. E.G. Erdos, ed. *Handbook of Experimental Pharmacology* (Berlin: Springer-Verlag). **25**, pp. 516-530.

Lewis, G.P. and Reit, E. (1965). The action of angiotensin and bradykinin on the superior cervical ganglion of the cat. *Journal of Physiology*. **179**, 538-553.

Lewis, G.P. and Reit, E. (1966). Further studies on the actions of peptides on the superior cervical ganglion and the suprarenal medulla. *British Journal of Pharmacology*. **26**, 444-460.

Libet, B. (1970). Generation of slow inhibitory and excitatory postsynaptic potentials. *Federation Proceedings*. **29**, 1945-1956.

Lindau, M. and Fernandez, J.M. (1986). IgE-mediated degranulation of mast cells does not require opening of ion channels. *Nature*. **319**, 150-153.

Lindsay, R.M. and Rang, H.P. (1987). Effects of bradykinin on the membrane currents of rat sensory neurones in tissue culture. *Journal of Physiology*. **309**, 74P (Abstract).

Lipinsky, D., Gershengorn, M.C., and Oron, Y. (1992). $G_{\alpha 11}$ and $G_{\alpha q}$ guanine nucleotide regulatory proteins differentially modulate the response to thyrotropin-releasing hormone in *Xenopus* oocytes. *FEBS Letters*. **307**, 237-240.

Listerud, M., Brussaard, A.B., Devay, P., Colman, D.R., and Role, L.W. (1991). Functional contribution of neuronal AChR subunits revealed by antisense oligonucleotides. *Science*. **254**, 1518-1521.

Lledo, P.M., Homburger, V., Bockaert, J., and Vincent, J.-D. (1992). Differential G protein-mediated coupling of D_2 dopamine receptors to K^+ and Ca^{2+} currents in rat anterior pituitary cells. *Neuron*. **8**, 455-463.

Llona, I., Galleguillos, X., Belmar, J., and Huidobro-Toro, J.P. (1991). Bradykinin modulates the release of noradrenaline from vas deferens nerve terminals. *Life Sciences*. **48**, 2585-2592.

Logothetis, D.E., Kurchi, Y., Galper, J., Neer, E.J., and Clapham, D.E. (1987). The βγ-subunits of GTP-binding proteins activate the muscarinic K^+ channel in heart. *Nature*. **325**, 321-326.

Lohse, M.J. (1993). Molecular mechanisms of membrane receptor desensitization. *Biochimica et Biophysica Acta*. **1179**, 171-188.

Lopez, H.S. (1992). Kinetics of the G protein-mediated modulation of the potassium M-current in bullfrog sympathetic neurons. *Neuron*. **8**, 725-736.

Lopez, H.S. and Adams, P.R. (1989). A G protein mediates the inhibition of the voltage-dependent potassium M current by muscarine, LHRH, substance P and UTP in bullfrog sympathetic neurons. *European Journal of Neuroscience*. **1**, 529-542.

Malenka, R.C., Madison, D.V., Andrade, R., and Nicoll, R.A. (1986). Phorbol esters mimic some cholinergic actions in hippocampal pyramidal neurons. *Journal of Neuroscience*. **6**, 475-480.

Marrion, N.V., Smart, T.G., and Brown, D.A. (1987). Membrane currents in adult rat superior cervical ganglia in dissociated tissue culture. *Neuroscience Letters*. **77**, 55-60.

Marrion, N.V., Smart, T.G., Marsh, S.J., and Brown, D.A. (1989). Muscarinic suppression of the M-current in the rat sympathetic ganglion is mediated by receptors of the M_1-subtype. *British Journal of Pharmacology*. **98**, 557-573.

Marrion, N.V., Zucker, R.S., Marsh, S.J., and Adams, P.R. (1991). Modulation of M-current by intracellular Ca^{2+}. *Neuron*. **6**, 533-545.

Marrion, N.V. (1993). Selective reduction of one mode of M-channel gating by muscarine in sympathetic neurons. *Neuron*. **11**, 77-84.

Marrion, N.V. (1994). M-current suppression by agonist and phorbol esters in bullfrog sympathetic ganglion cells. *Pflügers Archiv*. **426**, 296-303.

Marsh, S.J., Trouslard, J., Vallis, Y., and Browning, B. (1994). Bradykinin augments a PKC-regulated chloride conductance in cultured rat sympathetic neurones. *Neuropeptides*. **26**, 67 (Abstract).

McEachern, A.E., Shelton, E.R., Bhakta, S., Obernolte, R., Bach, C., Zuppan, P., Fujisaki, J., Aldrich, R.W., and Jarnagin, K. (1991). Expression cloning of a rat B_2 bradykinin receptor. *Proceedings of the National Academy of Sciences USA*. **88**, 7724-7728.

McFadzean, I., Mullaney, I., Brown, D.A., and Milligan, G. (1989). Antibodies to the GTP binding protein, Go, antagonize noradrenaline-induced calcium current inhibition in NG108-15 hybrid cells. *Neuron*. **3**, 177-182.

McGehee, D.S., Goy, M.F., and Oxford, G.S. (1992). Involvement of the nitric oxide-cyclic GMP pathway in the desensitization of bradykinin responses of cultured rat sensory neurons. *Neuron*. **9**, 315-324.

McGuirk, S.M. and Dolphin, A.C. (1992). G-protein mediation in nociceptive signal transduction: an investigation into the excitatory action of bradykinin in a subpopulation of cultured rat sensory neurons. *Neuroscience*. **49**, 117-128.

McMahon, S.B. (1991). Mechanisms of sympathetic pain. In Pain. J.C.D. Wells and C.J. Woolf, eds. *British Medical Bulletin* (Edinburgh, London, Melbourne and New York: Churchill Livingstone). **47**, pp. 584-600.

Menke, J.G., Borkowski, J.A., Bierilo, K.K., MacNeil, T., Derrick, A.W., Schneck, K.A., Ransom, R.W., Strader, C.D., Linemeyer, D.L., and Hess, J.F. (1994). Expression cloning of a human B_1 bradykinin receptor. *Journal of Biological Chemistry*. **269**, 21583-21586.

Menon-Johansson, A.S., Berrow, N., and Dolphin, A.C. (1993). G_o transduces $GABA_B$-receptor modulation of N-type calcium channels in cultured dorsal root ganglion neurons. *Pflügers Archiv*. **425**, 1-9.

Meyer, R.A., Davis, K.D., Raja, S.N., and Campbell, J.N. (1992). Sympathectomy does not abolish bradykinin-induced cutaneous hyperalgesia in man. *Pain*. **51**, 323-327.

Millar, R.J. (1987). Bradykinin highlights the role of phospholipid metabolism in the control of nerve excitability. *Trends in Neurosciences*. **10**, 226-228.

Miller Jonakait, G. (1993). Neural-immune interactions in sympathetic ganglia. *Trends in Neurosciences*. **16**, 419-423.

Milligan, G. (1988). Techniques used in the identification and analysis of function of pertussis toxin-sensitive guanine nucleotide binding proteins. *Biochemical Journal.* **255**, 1-13.

Mitchell, F.M., Mullaney, I., Godfrey, P.P., Arkinstall, S.J., Wakelam, M.J.O., and Milligan, G. (1991). Widespread distribution of $G_{q\alpha}/G_{11\alpha}$ detected immunologically by an antipeptide antiserum directed against the predicted C-terminal decapeptide. *FEBS Letters.* **287**, 171-174.

Moises, H.C., Rusin, K.I., and Macdonald, R.L. (1994). μ-opioid receptor-mediated reduction of neuronal calcium current occurs *via* a G_o-type GTP-binding protein. *Journal of Neuroscience.* **14**, 3842-3851.

Neher, E. and Sakmann, B. (1976). Single-channel currents recorded from membrane of denervated frog muscle fibres. *Nature.* **260**, 799-801.

Neher, E. (1992). Correction for liquid junction potentials in patch clamp experiments. In Ion channels. B. Rudy and L. Iverson, eds. *Methods in Enzymology* (San Diego, CA: Academic press). **207**, pp. 123-131.

North, R.A. (1989). Drug receptors and the inhibition of nerve cells. *British Journal of Pharmacology.* **98**, 13-28.

Owen, D.G., Marsh, S.J., and Brown, D.A. (1990). M-current noise and putative M-channels in cultured rat sympathetic ganglion cells. *Journal of Physiology.* **431**, 269-290.

Pang, I.-H. and Sternweis, P.C. (1990). Purification of unique α subunits of GTP-binding regulatory proteins (G proteins) by affinity chromatography with immobilised βγ subunits. *Journal of Biological Chemistry.* **265**, 18707-18712.

Patterson, B.A. and Volle, R.L. (1984). Muscarinic receptors and [^{3}H]inositol incorporation in a rat sympathetic ganglion. *Journal of the Autonomic Nervous System.* **10**, 69-72.

Pennefather, P., Lancaster, B., Adams, P., and Nicoll, R.A. (1985). Two distinct Ca-dependent K currents in bullfrog sympathetic ganglion cells. *Proceedings of the National Academy of Sciences USA.* **82**, 3040-3044.

Pfaffinger, P. (1988). Muscarine and t-LHRH suppress M-current by activating an IAP-insensitive G-protein. *Journal of Neuroscience.* **8**, 3343-3353.

Pfaffinger, P.J., Leibowitz, M.D., Subers, E.M., Nathanson, N.M., Almers, W., and Hille, B. (1988). Agonists that suppress M-current elicit phosphoinositide turnover and Ca^{2+} transients, but these events do not explain M-current suppression. *Neuron.* **1**, 477-484.

Ping Yu, S., O'Malley, D.M., and Adams, P.R. (1994). Regulation of M current by intracellular calcium in bullfrog sympathetic ganglion neurons. *Journal of Neuroscience.* **14**, 3487-3499.

Rae, J., Cooper, K., Gates, P., and Watsky, M. (1991). Low access resistance perforated patch recordings using amphotericin B. *Journal of Neuroscience Methods.* **37**, 15-26.

Regoli, D. (1987). Kinins. In Inflammation-mediators and mechanisms. D.A. Willoughby, ed. *British Medical Bulletin* (Edinburgh, London, Melbourne and New York: Churchill Livingstone). **43**, pp. 270-284.

Regoli, D. and Barabé, J. (1980). Pharmacology of bradykinin and related kinins. *Pharmacological Reviews.* **32**, 1-46.

Reiser, G. and Hamprecht, B. (1982). Bradykinin induces hyperpolarizations in rat glioma cells and in neuroblastoma x glioma hybrid cells. *Brain Research.* **239**, 191-199.

Reitstetter, R., Sheng He, D., and Gruener, R. (1994). Oxotremorine-M activates single nicotinic acetylcholine receptor channels in cultured *Xenopus* myocytes. *European Journal of Pharmacology.* **264**, 27-32.

Reuveny, E., Slesinger, P.A., Inglese, J., Morales, J.M., Iñiguez-Lluhi, J.A., Lefkowitz, R.J., Bourne, H.R., Jan, Y.N., and Jan, L.Y. (1994). Activation of the cloned muscarinic potassium channel by G protein βγ subunits. *Nature.* **370**, 143-146.

Robbins, J., Caulfield, M.P., Higashida, H., and Brown, D.A. (1991). Genotypic m3-muscarinic receptors preferentially inhibit M-currents in DNA-transfected NG108-15 neuroblastoma x glioma hybrid cells. *European Journal of Neuroscience.* **3**, 820-824.

Robbins, J., Trouslard, J., Marsh, S.J., and Brown, D.A. (1992). Kinetic and pharmacological properties of the M-current in rodent neuroblastoma x glioma hybrid cells. *Journal of Physiology.* **451**, 159-185.

Robbins, J., Marsh, S.J., and Brown, D.A. (1993). On the mechanism of M-current inhibition by muscarinic m1 receptors in DNA-transfected rodent neuroblastoma x glioma cells. *Journal of Physiology.* **469**, 153-178.

Ross, E.M. (1992). G proteins and receptors in neuronal signaling. In An introduction to molecular neurobiology. Z.W. Hall, ed. (Sunderland, MA: Sinauer Associates), pp. 181-206.

Schäfer, S., Béhé, P., and Meves, H. (1991). Inhibition of the M current in NG108-15 neuroblastoma x glioma hybrid cells. *Pflügers Archiv.* **418**, 581-591.

Schmitt, H. and Meves, H. (1993). Protein kinase C as mediator of arachidonic acid-induced decrease of neuronal M current. *Pflügers Archiv.* **425**, 134-139.

Schnabel, P., Schreck, R., Schiller, D.L., Camps, M., and Gierschik, P. (1992). Stimulation of phospholipase C by a mutationally activated G protein α_{16} subunit. *Biochemical and Biophysical Research Communications.* **188**, 1018-1023.

Selyanko, A.A., Stansfeld, C.E., and Brown, D.A. (1992). Closure of potassium M-channels by muscarinic acetylcholine-receptor stimulants requires a diffusible messenger. *Proceedings of the Royal Society B.* **250**, 119-125.

Selyanko, A.A. and Brown, D.A. (1993). Effects of membrane potential and muscarine on potassium M-channel kinetics in rat sympathetic neurones. *Journal of Physiology.* **472**, 711-724.

Shapira, H., Way, J., Lipinsky, D., Oron, Y., and Battey, J.F. (1994). Neuromedin B receptor, expressed in *Xenopus laevis* oocytes, selectively couples to $G_{\alpha q}$ and not $G_{\alpha 11}$. *FEBS Letters.* **348**, 89-92.

Shapiro, M.S., Wollmuth, L.P., and Hille, B. (1994). Angiotensin II inhibits Calcium and M current channels in rat sympathetic neurons *via* G proteins. *Neuron.* **12**, 1319-1329.

Sigworth, F.J. and Neher, E. (1980). Single Na^+ channel currents observed in cultured rat muscle cells. *Nature.* **287**, 447-449.

Simon, M.I., Strathmann, M.P., and Gautam, N. (1991). Diversity of G proteins in signal transduction. *Science.* **252**, 802-808.

Spiegel, A.M., Simonds, W.F., Jones, T.L.Z., Goldsmith, P.K., and Unson, C.G. (1990). Antibodies against synthetic peptides as probes of G protein structure and function. In G proteins and signal transduction. N.M. Nathanson and T.K. Harden, eds. (New York: Rockefeller University Press), pp. 185-195.

Standifer, K.M., Chien, C.-C., Wahlestedt, C., Brown, G.P., and Pasternak, G.W. (1994). Selective loss of δ opioid analgesia and binding by antisense oligodeoxynucleotides to a δ opioid receptor. *Neuron.* **12**, 805-810.

Stansfeld, C.E., Marsh, S.J., Gibb, A.J., and Brown, D.A. (1993). Identification of M-channels in outside-out patches excised from sympathetic ganglion cells. *Neuron.* **10**, 639-654.

Starke, K., Peskar, B.A., Schumacher, K.A., and Taube, H.D. (1977). Bradykinin and postganglionic sympathetic transmission. *Naunyn-Schmiedeberg's Archives of Pharmacology.* **299**, 23-32.

Stein, C.A. and Cheng, Y.-C. (1993). Antisense oligonucleotides as therapeutic agents-is the bullet really magical? *Science.* **261**, 1004-1012.

Sternweis, P.C. and Smrcka, A.V. (1992). Regulation of phospholipase C by G proteins. *Trends in Biochemical Sciences.* **17**, 502-506.

Strathmann, M. and Simon, M.I. (1990). G protein diversity: A distinct class of α subunits is present in vertebrates and invertebrates. *Proceedings of the National Academy of Sciences USA.* **87**, 9113-9117.

Taylor, S.J., Smith, J.A., and Exton, J.H. (1990). Purification from bovine liver membranes of a guanine nucleotide-dependent activator of phosphoinositide-specific phospholipase C. Immunologic identification as a novel G protein α subunit. *Journal of Biological Chemistry.* **265**, 17150-17156.

Taylor, S.J., Chae, H.Z., Rhee, S.G., and Exton, J.H. (1991). Activation of the β1 isozyme of the phospholipase C by α subunits of the Gq class of G proteins. *Nature.* **350**, 516-518.

Tsuda, K., Tsuda, S., Goldstein, M., Nishio, I., and Masuyama, Y. (1993). Effects of bradykinin on [^{3}H]-norepinephrine release in rat hypothalamus. *Clinical and Experimental Pharmacology and Physiology.* **20**, 787-791.

Villarroel, A., Marrion, N.V., Lopez, H., and Adams, P.R. (1989). Bradykinin inhibits a potassium M-like current in rat pheochromocytoma PC12 cells. *FEBS Letters.* **255**, 42-46.

Wahlestedt, C. (1994). Antisense oligonucleotide strategies in neuropharmacology. *Trends in Pharmacological Sciences.* **15**, 42-46.

Wallis, D.I. and Woodward, B. (1974). The facilitatory actions of 5-hydroxytryptamine and bradykinin in the superior cervical ganglion of the rabbit. *British Journal of Pharmacology.* **51**, 521-532.

Weight, F.F. and Votava, J. (1970). Slow synaptic excitation in sympathetic ganglion cells: evidence for synaptic inactivation of a potassium conductance. *Science.* **170**, 755-758.

Weinreich, D. (1986). Bradykinin inhibits a slow spike afterhyperpolarization in visceral sensory neurons. *European Journal of Pharmacology.* **132**, 61-63.

Weiss, E.R., Kelleher, D.J., Woon, C.W., Soparkar, S., Osawa, S., Heasley, L.E., and Johnson, G.L. (1988). Receptor activation of G proteins. *FASEB Journal.* **2**, 2841-2848.

Wilk-Blaszczak, M.A., Gutowski, S., Sternweis, P.C., and Belardetti, F. (1994). Bradykinin modulates potassium and calcium currents in neuroblastoma hybrid cells *via* different pertussis toxin-insensitive pathways. *Neuron.* **12**, 109-116.

Womble, M.D. and Moises, H.C. (1992). Muscarinic inhibition of M-current and a potassium leak conductance in neurones of the rat basolateral amygdala. *Journal of Physiology.* **457**, 93-114.

Wu, D., Lee, C.H., Rhee, S.G., and Simon, M.I. (1992). Activation of phospholipase C by the α subunits of the G_q and G_{11} proteins in transfected Cos-7 cells. *Journal of Biological Chemistry.* **267**, 1811-1817.

Xian, H., Coggan, J.S., Knoper, S.R., and Kreulen, D.L. (1994). The muscarinic receptor agonist oxotremorine methiodide evokes a nicotinic response in mammalian sympathetic neurones. *European Journal of Pharmacology.* **259**, 21-25.

Yano, K., Higashida, H., Inoue, R., and Nozawa, Y. (1984). Bradykinin-induced rapid breakdown of phosphatidylinositol 4,5-bisphosphate in neuroblastoma x glioma hybrid NG108-15 cells. *Journal of Biological Chemistry.* **259**, 10201-10207.

Kay, A.R. (1991). An intracellular medium formulary. *J.Neurosci.Meth.* **121** 101-117.

Muscarinic M-current inhibition via $G_{\alpha q/11}$ and α-adrenoceptor inhibition of Ca^{2+} current via $G_{\alpha o}$ in rat sympathetic neurones

Malcolm P. Caulfield, Susan Jones, Yvonne Vallis, Noel J. Buckley, Gun-Do Kim*, Graeme Milligan* and David A. Brown

*Wellcome Laboratory for Molecular Pharmacology, Department of Pharmacology, University College London, Gower Street, London WC1E 6BT and *Molecular Pharmacology Group, Departments of Biochemistry and Pharmacology, University of Glasgow, Glasgow G12 8QQ*

1. Microinjection of selective antibodies into superior cervical ganglion (SCG) neurones has identified the G-protein α-subunits mediating muscarinic receptor inhibition of M-type K^+ current ($I_{K(M)}$) and α-adrenoceptor inhibition of Ca^{2+} current (I_{Ca}).

2. Antibodies specific for $G_{\alpha q/11}$, but not those for $G_{\alpha o}$, reduced M-current inhibition by the muscarinic agonist oxotremorine-M, whereas anti-$G_{\alpha o}$ antibodies, but not anti-$G_{\alpha q/11}$ or anti-$G_{\alpha i1-3}$ antibodies, reduced calcium current inhibition by noradrenaline.

3. Immunoblots with specific anti-G-protein antibodies demonstrated the presence of both $G_{\alpha q}$ and $G_{\alpha 11}$, while $G_{\alpha o1}$ (but virtually no $G_{\alpha o2}$) was present.

4. We conclude that M_1 muscarinic receptor inhibition of $I_{K(M)}$ is transduced by $G_{\alpha q}$ and/or $G_{\alpha 11}$, and that $G_{\alpha o}$ transduces α-adrenoceptor inhibition of I_{Ca}.

In neurones of rat superior cervical ganglion (SCG), muscarinic receptors of the M_1 subtype couple to inhibit the M-type K^+ current ($I_{K(M)}$; Marrion, Smart, Marsh & Brown, 1989), while α_2-adrenoceptor activation inhibits voltage-gated Ca^{2+} currents (I_{Ca}; Galvan & Adams, 1982). The range of G-proteins expressed in these neurones and the precise identity of the G-proteins mediating these responses remains to be determined; however, there is some information about the nature of receptor–G-protein coupling. Muscarinic $I_{K(M)}$ suppression in SCG neurones is mediated by an as yet unidentified pertussis toxin (PTX)-insensitive G-protein (Brown, Marrion & Smart, 1989), probably via the action of a diffusible second messenger (Selyanko, Stansfeld & Brown, 1992). On the other hand, noradrenaline inhibition of I_{Ca} is through a rapid pathway not involving a second messenger (Bernheim, Beech & Hille, 1991) and a PTX-sensitive G-protein plays a major role in transducing this response (Beech, Bernheim & Hille, 1992). This suggests that the G_i or G_o class of G-proteins may be involved. There is evidence from other systems that G_o rather than G_i mediates transmitter inhibition of I_{Ca} (McFadzean, Mullaney, Brown & Milligan, 1989; Kleuss, Hescheler, Ewel, Rosenthal, Schultz & Wittig, 1991; Menon-Johannson, Berrow & Dolphin, 1993), so one or more of the subtypes of G_o seem likely candidates to couple α_2-adrenoceptors to inhibit I_{Ca} channels. For muscarinic receptor inhibition of $I_{K(M)}$, potential PTX-insensitive G-proteins which could transduce the response are the five known members of the G_q family, G_{12} or G_{13} and G_z (see Simon, Strathmann & Gautam, 1991).

Neurotransmitter receptors are thought to couple to the carboxy-terminus of G-protein α-subunits, and polyclonal antibodies raised against C-terminal peptide sequences of different G_α subunits have been shown to functionally antagonize neurotransmitter receptor modulation of ion channel currents (e.g. anti-$G_{\alpha o}$: McFadzean *et al.* 1989; Menon-Johannson *et al.* 1993; anti-$G_{\alpha q/11}$: Wilk-Blaszczak, Gutowski, Sternweis & Belardetti, 1994). In this paper, we show that microinjection into SCG neurones of specific antibodies raised against the C-terminal decapeptide sequence common to $G_{\alpha q}$ and $G_{\alpha 11}$ (but not antibodies against $G_{\alpha o}$) attenuate muscarinic receptor inhibition of $I_{K(M)}$, while antibodies against a similar region of $G_{\alpha o}$ (but not antibodies against $G_{\alpha i1-3}$ or $G_{\alpha q/11}$) reduce α-adrenoceptor inhibition of I_{Ca}. $G_{\alpha q}$, $G_{\alpha 11}$ and $G_{\alpha o1}$ were detected in SCG neurones by immunoblotting with specific antibodies. $G_{\alpha o2}$ was barely detectable. From this, we conclude that $G_{\alpha q}$ and/or $G_{\alpha 11}$ mediates muscarinic $I_{K(M)}$ inhibition, while inhibition of I_{Ca} by noradrenaline involves $G_{\alpha o}$.

METHODS

Cell culture

Superior cervical ganglia were isolated from rats (15–19 days old; killed by CO_2 asphyxiation) and were dissociated and cultured on laminin-coated plastic dishes, as described previously (see Selyanko *et al.* 1992). The dishes were marked on the underside with a grid of 1 × 1 mm squares, to help with localization of antibody-injected cells. For recording I_{Ca}, neurones were cultured for 1 day, after which they were resuspended and replated (to remove processes and thereby improve voltage clamp). Recordings were made at least 5 h after replating. During all recordings, cells were superfused at room temperature (20–26 °C) with a modified Krebs solution containing (mM): NaCl, 120; KCl, 3; $CaCl_2$, 2·5; $MgCl_2$, 1·2; $NaHCO_3$, 23; glucose, 11; Hepes, 5; tetrodotoxin, 0·0005, and bubbled with a 95 % O_2–5 % CO_2 mixture. The pH of this solution was 7·36.

PTX-catalysed ADP ribosylation of G-proteins

Cultured SCG neurones (untreated, or pretreated with 500 ng ml^{-1} PTX for 15–18 h) were washed in phosphate-buffered saline (PBS), suspended in 500 μl of 10 mM Tris-HCl–0·1 mM EDTA, pH 7·5 (Tris–EDTA) and homogenized with fifty strokes with a Teflon–glass homogenizer. The samples were then centrifuged at 150000 *g* for 10 min, the pellet resupended in 50 μl Tris–EDTA and aliquots (20 μl) were then subjected to PTX-catalysed [^{32}P]ADP ribosylation for 2 h (37 °C). The assay mixture contained 2 μCi [^{32}P]nicotinamide adenine dinucleotide, 20 mM thymidine, 0·1 mM GTP, 250 mM sodium phosphate (pH 7·0), 1 mM ATP, 20 mM arginine hydrochloride and 1·5 μg ml^{-1} thiol-activated PTX. The assays were terminated by precipitation with sodium deoxycholate and trichloroethanoic acid. Samples were resolved by sodium dodecyl sulphate–polyacrylamide gel electrophoresis (SDS–PAGE) (10 % w/v acrylamide) and autoradiographs made by exposure for 48 h.

Immunoblots

Antisera were generated in New Zealand White rabbits, as described previously (Goldsmith *et al.* 1987), using conjugates of keyhole limpet haemocyanin and synthetic decapeptides corresponding to the carboxy terminal of G-protein α-subunits. Cultured SCG neurones were washed twice with PBS and pelleted (at 500 *g*), then resuspended in Laemmli's sample buffer for resolution of G_α proteins using the SDS–PAGE system (12·5 % acrylamide, 0·0625 % bis-acrylamide, containing a linear gradient of 4–8 M urea) described by Mullaney, Mitchell, McCallan, Buckley & Milligan (1993). Following transfer to nitrocellulose, the cells were immunoblotted using an anti-$G_{\alpha q/11}$ antiserum (CQ2, 1:200 dilution: Mitchell, Mullaney, Godfrey, Arkinstall, Wakelam & Milligan, 1991), an anti-$G_{\alpha o1/2}$ antiserum (OC2, 1:1000 dilution), or an anti-$G_{\alpha i1/2}$ antiserum (SG1, 1:400).

Injection of antisera

Neurones were injected with either anti-G-protein antiserum or rabbit antiserum raised against human brain glial fibrillary acidic protein (anti-GFAP; Sigma Chemical Co., UK). The anti-G-protein antisera used were those described above, and also an antiserum (I3C) raised against the C-terminal decapeptide sequence of $G_{\alpha i\text{-}3}$ (KNNLKECGLY), as described by Goldsmith *et al.* (1987). Injections were made from high resistance (> 30 MΩ) electrodes, and cell penetration was apparent from the appearance of a standing negative voltage while in 'bridge' recording mode. Antiserum was expelled by application of gentle pressure to the back of the electrode with a syringe. Recordings were made at least 2 h after injection of antiserum.

$I_{K(M)}$ recording

Whole-cell $I_{K(M)}$ currents were recorded using the nystatin perforated patch method (Horn & Marty, 1988) from neurones which had been cultured for 2 days. Patch pipettes (5–8 MΩ) were filled by dipping the tip into a filtered solution containing (mM): potassium acetate, 80; KCl, 30; $MgCl_2$, 3; Hepes, 40 (adjusted to pH 7·4 and 290 mosmol l^{-1}), for 15–60 s, after which the pipette was back-filled with the above solution containing 0·25 mg ml^{-1} nystatin. After achieving high resistance (> 2 GΩ) seals, access resistances after nystatin permeabilization were < 30 MΩ. Neurones were voltage clamped at about −25 mV using a switching amplifier (Axoclamp 2A, Axon Instruments, Foster City, CA, USA; switching frequency 2–4 kHz) and $I_{K(M)}$ was recorded as the slowly developing inward deactivation relaxation during 1 s jumps to a command potential of about −55 mV (Fig. 2). Muscarinic inhibition of $I_{K(M)}$ was measured after perfusion with a solution containing the muscarinic agonist oxotremorine methiodide (Oxo-M, 300 nM; Semat, St Albans, UK). We only analysed data from cells showing recovery of $I_{K(M)}$ of at least 60 % from agonist-inhibited levels (usually within 5 min).

I_{Ca} recording

Voltage-gated Ca^{2+} currents were recorded in whole-cell mode, using patch pipettes filled with a solution containing (mM): CsCl, 13; caesium acetate, 120; Hepes, 10; Cs-EGTA, 3; NaATP, 2; NaGTP, 0·5; $MgCl_2$, 4; adjusted to pH 7·4 with CsOH, and to 290 mosmol l^{-1}. Neurones were voltage clamped (Axoclamp 2A) at −80 mV and I_{Ca} were evoked every 60 s by stepping for 50 ms to +10 mV. A pulse to −40 mV immediately preceding the command step served to reduce capacity transients (Bernheim *et al.* 1991). I_{Ca} amplitude was estimated by digitally subtracting the outward current (using pCLAMP software; Axon Instruments) remaining during the same voltage step in the presence of Krebs solution in which $CaCl_2$ had been replaced with $CoCl_2$. Inhibition of I_{Ca} was measured 1 min after the normal perfusion solution was changed to one containing noradrenaline (which had no effect on the outward current in the presence of Co^{2+}; $n = 3$, data not shown). Data were only included from cells in which recovery from noradrenaline inhibition was to > 90 % of the control current.

Visualization of injected antibody

After a series of injections and recordings, the Krebs solution in the dish was replaced by ice-cold 0·1 M PBS containing 4 % bovine serum albumin (PBS–BSA). After 2 min, the cells were permeabilized and fixed for 15 min at −20 °C in 5 % acetic acid in ethanol. The dish was then washed 3 times with PBS–BSA, and the solution was finally replaced with 1 ml of a 1:100 solution (in PBS–BSA) of fluorescein isothiocyanate-labelled sheep anti-rabbit IgG antibody (Serotec, Oxford, UK). After incubation for 30 min at room temperature, unbound second layer antibody was removed by three washes with PBS–BSA, and the preparation was mounted in Citifluor (Citifluor,

Guildford, UK) under a glass coverslip. The identified injected (and recorded) cells were then checked for antibody loading under a fluorescence microscope.

RESULTS

Expression of G-proteins in SCG neurones

Resolution of membranes of SCG neurones by SDS–PAGE, followed by immunoblotting with specific anti-G-protein antisera showed very strong bands for $G_{\alpha q}$, $G_{\alpha 11}$, (Fig. 1*A*), $G_{\alpha o1}$ (Fig. 1*Ba*) and $G_{\alpha i2}$ (Fig. 1*Bb*). Immunoblots showed very faint bands of $G_{\alpha o2}$ (Fig. 1*Ba*) and $G_{\alpha i1}$ (Fig. 1*Bb*) proteins, indicating that the G_o and G_i subtypes expressed in SCG neurones are almost exclusively $G_{\alpha o1}$ and $G_{\alpha i2}$, respectively. The ability of the immunoblotting procedure to distinguish G_i and G_o isoforms was verified by detection of G_{i1} and G_{i2} (in membranes of rat frontal cortex; Fig. 1*Bb*), and G_{o1}, G_{o2} and G_o* (in membranes of NG108-15 neuroblastoma cells; Fig. 1*Ba*; see Mullaney & Milligan, 1990). Reverse transcription/polymerase chain reaction analysis, using specfic $G_{\alpha i3}$ primers, demonstrated the presence of $G_{\alpha i3}$ transcripts in cultures of SCG neurones (N. J. Buckley, unpublished observations).

PTX pretreatment of SCG neurones (500 ng ml^{-1} for 15–18 h) achieved almost complete ADP ribosylation of susceptible G-proteins, as measured by inhibition of incorporation of [^{32}P]-labelled nicotinamide adenine dinucleotide (Fig. 1*C*).

Anti-$G_{\alpha q/11}$ antibodies reduce muscarinic inhibition of $I_{K(M)}$

To test the effects of antibody injection or PTX pretreatment, we chose to use 300 nM Oxo-M as a test concentration, since any change in efficiency of receptor–G-protein transduction would have been detectable by the submaximal response to this agonist concentration (in five experiments, the mean concentration of Oxo-M producing half-maximal $I_{K(M)}$ inhibition was 166 nM, with a Hill slope of 1·3). In order to ensure that we measured transmitter responses only from neurones which had been successfully injected with antibody, we routinely stained cells to demonstrate antibody loading once electrophysiological experiments were completed. Figure 2 shows a neurone which was injected with anti-$G_{\alpha q/11}$ antibody and then, after recording $I_{K(M)}$ and its inhibition by Oxo-M, stained with a second fluorescein-tagged antibody. The bright fluorescence in the antibody-injected neurone, but not in the uninjected neurone, was taken to indicate loading with anti-G-protein (or control) antibody. About 90 % of anti-

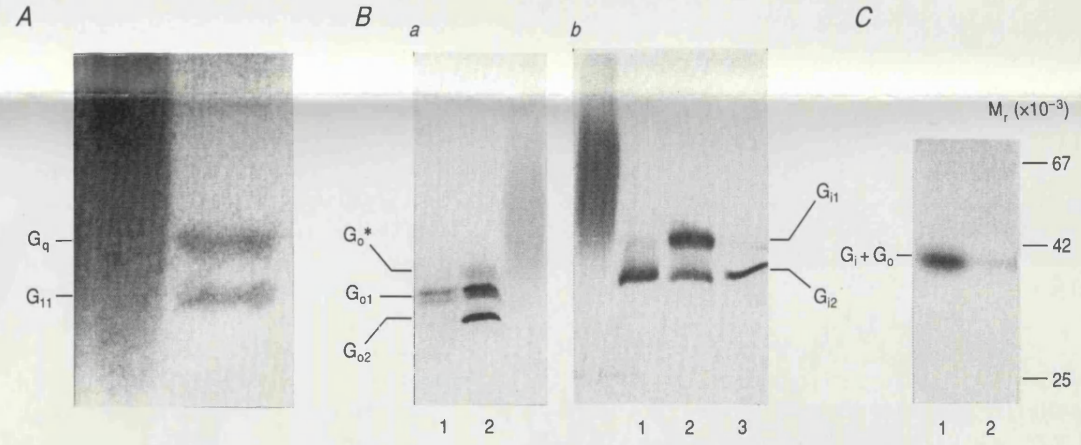

Figure 1. Expression of G-proteins by SCG neurones, and ADP ribosylation of susceptible G-proteins by PTX

A, immunological detection of the co-expression of $G_{\alpha q}$ and $G_{\alpha 11}$ in SCG neurones. The sample in the left-hand lane of the immunoblot is prestained lactic dehydrogenase (LDH; Sigma, UK), which we have noted to migrate in a similar position to $G_{\alpha q}$ and $G_{\alpha 11}$ in such gels, and was used as a marker for the migration of the G-proteins. Bands showing $G_{\alpha q}$ and $G_{\alpha 11}$ are in the right-hand lane. *B*, immunological detection of the co-expression of $G_{\alpha o1}$ and $G_{\alpha i2}$, and barely detectable levels of $G_{\alpha o2}$ or $G_{\alpha i1}$ in SCG neurones. *Ba*, $G_{\alpha o1}$ (but virtually no $G_{\alpha o2}$) in SCG membranes is shown in lane 1 of the immunoblot. Lane 2 shows $G_{\alpha o1}$, $G_{\alpha o2}$ and G_o* in membranes (100 μg) from NG108-15 cells. The LDH size marker was run in the far right lane. *Bb*, $G_{\alpha i2}$ (with barely detectable expression of $G_{\alpha i1}$) in SCG neurones is shown in lane 1 of the immunoblot, while lane 2 shows predominant expression of both $G_{\alpha i1}$ and $G_{\alpha i2}$ in rat brain frontal cortex membranes (25 μg), and lane 3 shows $G_{\alpha i2}$ (but no detectable $G_{\alpha i1}$) in NG108-15 cell membranes (50 μg). The LDH size marker is in the far left lane. *C*, PTX-catalysed [^{32}P]ADP ribosylation of membranes of control and PTX-treated SCG neurones. Autoradiographs show that PTX pretreatment (lane 2) caused virtually complete ADP ribosylation of the available pool of PTX-sensitive G-proteins (G_i and G_o, which cannot be distinguished because they co-migrate in this gel system). Untreated neurones (lane 1) showed good incorporation of radioactivity into these polypeptides.

body-injected neurones survived the experimental protocol and showed bright fluorescence after immunostaining. Since we were concerned that injection of antiserum might itself influence transmitter responses, neurones injected with antibody to glial fibrillary acidic protein (GFAP) were used as antibody-injected controls.

In neurones injected with antibodies raised against $G_{\alpha q/11}$, the standard deviation of Oxo-M inhibition of $I_{K(M)}$ was significantly greater ($P = 0{\cdot}02$; Bartlett's test) than in either uninjected, anti-GFAP- or anti-$G_{\alpha o}$-injected cells (Fig. 3), so statistical analyses were carried out using Dunn's non-parametric test. This showed that median inhibition of $I_{K(M)}$ in anti-$G_{\alpha q/11}$ antibody-treated neurones (32·0 %) was significantly less ($P < 0{\cdot}05$) than in anti-GFAP antibody-injected neurones, (56·0 %), uninjected neurones (59·5 %) or anti-$G_{\alpha o}$ antibody-injected neurones (63 %), respectively. In the anti-$G_{\alpha q/11}$ antibody-treated neurones, the amplitude of $I_{K(M)}$ (188 ± 19·4 pA) was not significantly different from that seen in the anti-GFAP antibody-injected neurones (174 ± 22·8 pA), the anti-$G_{\alpha o}$ antibody-treated neurones (133 ± 6·2 pA), and the uninjected neurones (159 ± 17 pA), showing that antibody injection *per se* did not alter $I_{K(M)}$. We also confirmed the previous observation (Brown *et al.* 1989) that muscarinic inhibition of $I_{K(M)}$ in PTX-treated (500 ng ml^{-1} for 15–18 h) SCG neurones (median inhibition by 300 nM Oxo-M, 56 %) did not differ from that in control cells (Fig. 3*B*).

Anti-G_o antibodies reduce α-adrenoceptor inhibition of I_{Ca}

We also tested the ability of the different G-protein antibodies to suppress α-adrenoceptor inhibition of I_{Ca} in SCG

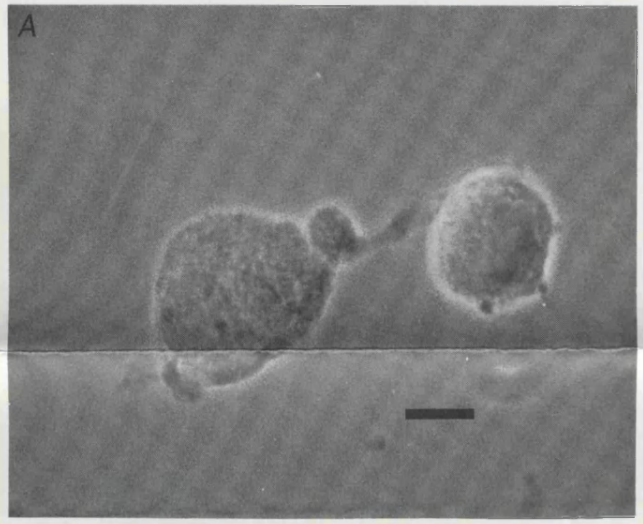

Figure 2. Labelling with a fluorescent second antibody demonstrates successful injection of an SCG neurone with anti-$G_{\alpha q/11}$ antibody
A, phase contrast photomicrograph showing a neurone injected with anti-$G_{\alpha q/11}$ antibody on the left and an uninjected neurone on the right. The scale bar represents 10 μm. *B*, fluorescence photomicrograph of the neurons in *A*. Only the antibody-injected neurone shows significant fluorescence.

neurones. Noradrenaline (1 μM) gave readily measurable, submaximal I_{Ca} inhibition (from three experiments, the mean concentration producing half-maximal response was 140 nM, while the mean Hill slope of the concentration–response relationship was 1·45). This concentration was used in subsequent experiments. In neurones which had been pre-injected with anti-$G_{\alpha o}$ antibody, inhibition of I_{Ca} by 1 μM noradrenaline was 27·0 ± 3·3 % ($n = 12$), significantly less ($P < 0·001$, ANOVA and Dunnet's test) than in uninjected (53·7 ± 2·4 %; $n = 11$) or anti-GFAP-injected cells (46·4 ± 3·1 %; $n = 9$; Fig. 4). In contrast, neurones injected with antibodies recognizing the C-terminus of $G_{\alpha q/11}$, $G_{\alpha 11/2}$ and $G_{\alpha 13}$ exhibited noradrenaline inhibition of I_{Ca} (41·1 ± 4·9 %, $n = 7$; 41·3 ± 5·4 %, $n = 9$; and 34·5 ± 3·1 %, $n = 13$, respectively) which did not differ significantly from that of anti-GFAP-injected cells (Fig. 4). Neurones injected with either control antibody (against GFAP) or anti-G-protein antibodies had mean I_{Ca} amplitudes of 0·89–0·96 nA (standard errors ranged from 0·11 to 0·22 nA). These were not different from I_{Ca} in uninjected neurones (0·96 ± 0·13 nA; ANOVA and Dunnet's test), showing that antibody injection *per se* did not alter I_{Ca}.

Treatment of neurones with PTX (500 ng ml^{-1} for 15–18 h) reduced noradrenaline I_{Ca} inhibition to 13·2 ± 1·7 % ($n = 5$); neurones incubated in a higher concentration of PTX (2·5 μg ml^{-1} for 15–18 h) showed similar responses to noradrenaline (14·8 ± 2·6 %; $n = 4$). Injection of anti-$G_{\alpha o}$ antibodies into PTX-pretreated neurones reduced the noradrenaline inhibition of I_{Ca} almost to zero (6·6 ± 1·8 %, $n = 11$; Fig. 4).

DISCUSSION

Many cells express a wide range of heterotrimeric G-proteins. We have used immunoblots with specific antisera to demonstrate expression of the G-proteins $G_{\alpha q}$, $G_{\alpha 11}$, $G_{\alpha o1}$ and $G_{\alpha i2}$ in SCG neurones. $G_{\alpha o2}$ and $G_{\alpha i1}$ were

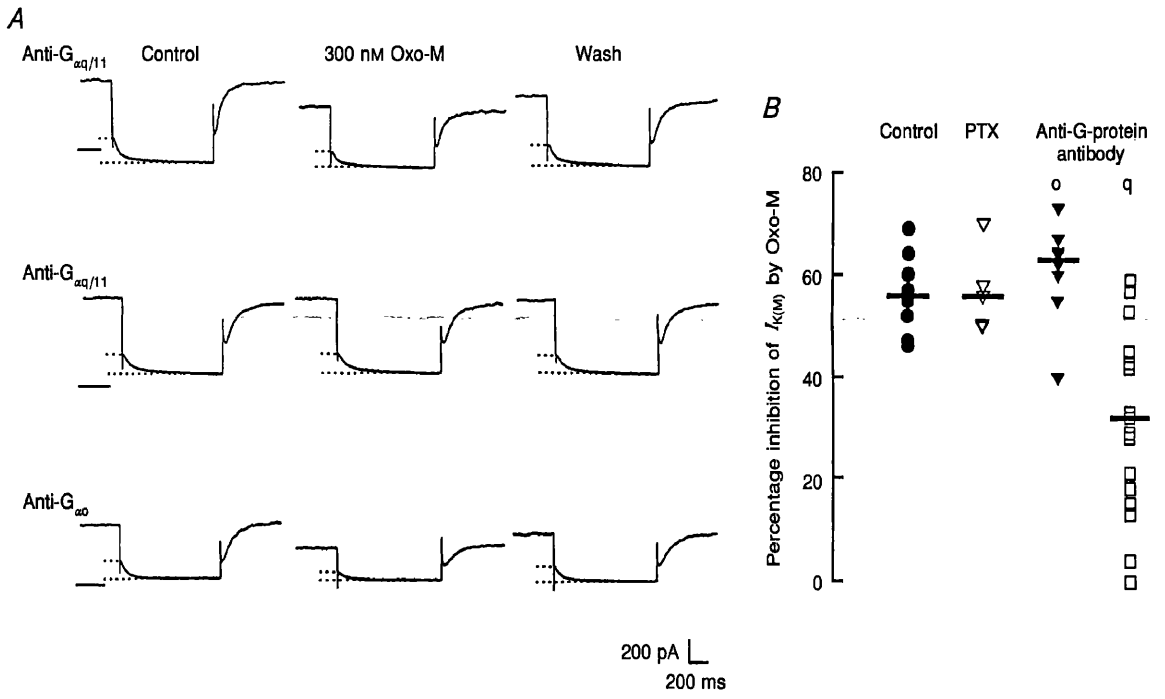

Figure 3. Anti-$G_{\alpha q/11}$ antibody injected in SCG neurones significantly reduces $I_{K(M)}$ inhibition by Oxo-M, while anti-GFAP or anti-$G_{\alpha o}$ antibody injection, or PTX pretreatment were without effect

A, representative traces showing M-current deactivation relaxations (between the dotted lines on each trace) during a 1 s hyperpolarizing step to −55 mV from a holding potential of −25 mV. Control traces are shown on the left, currents in the presence of 300 nM oxotremorine-M (Oxo-M) are in the middle, and the right-hand traces show recovery after removing the agonist. The zero current level is indicated by the continuous line. The top series of traces shows a reduction of muscarinic M-current inhibition in a neurone injected with anti-$G_{\alpha q/11}$ antibody, while the middle traces show almost complete abolition of the muscarinic response in another neurone injected with the same antibody. The bottom traces show a normal inhibition of M-current by Oxo-M in a neurone which had been injected with an anti-$G_{\alpha o}$ antibody. *B*, scatter plot showing $I_{K(M)}$ inhibition by 300 nM Oxo-M in neurones injected with anti-GFAP antibody (control; $n = 9$), neurones treated with 500 ng ml^{-1} PTX (PTX; $n = 5$), neurones injected with anti-$G_{\alpha o}$ antibody (o; $n = 10$) and anti $G_{\alpha q/11}$ antibody (q; $n = 17$). Median values are indicated by the horizontal bars.

virtually undetectable. The strong bands for $G_{\alpha o1}$ and $G_{\alpha i2}$ in the immunoblots clearly show that these are the major isoforms of $G_{\alpha o}$ and $G_{\alpha i}$ in SCG neurones. Injection of SCG neurones with selective anti-G-protein antibodies has demonstrated a divergence in coupling pathways between muscarinic M_1 receptors and inhibition of the M-type K^+ current on the one hand, and between α-adrenoceptors and inhibition of calcium currents on the other. Muscarinic inhibition of $I_{K(M)}$ was significantly reduced in neurones loaded with anti-$G_{\alpha q/11}$ antibodies, while adrenergic inhibition of I_{Ca} was diminished in cells injected with antibodies against $G_{\alpha o}$. Inhibition of either transmitter response by the antibodies was not complete and, in the case of $I_{K(M)}$ and anti-$G_{\alpha q/11}$ antibodies, varied from no inhibition to complete abolition of the response. We feel that this may result from variations in the amount of antibody injected into each cell.

Our finding that $I_{K(M)}$ inhibition is mediated by $G_{\alpha q}$ and/or $G_{\alpha 11}$ (and the lack of effect of anti-$G_{\alpha o}$ antibodies) is consistent with the PTX-insensitive muscarinic inhibition of $I_{K(M)}$ previously demonstrated in rat SCG neurones (Brown *et al.* 1989). There is evidence that muscarinic $I_{K(M)}$ inhibition in SCG neurones is mediated by a diffusible second messenger (Selyanko *et al.* 1992) and our finding that the response is transduced by $G_{\alpha q/11}$ suggests a product of phospholipase C (PLC) as a second messenger. This is because muscarinic receptor activation has been shown to increase inositol 1,4,5-trisphosphate ($InsP_3$) levels

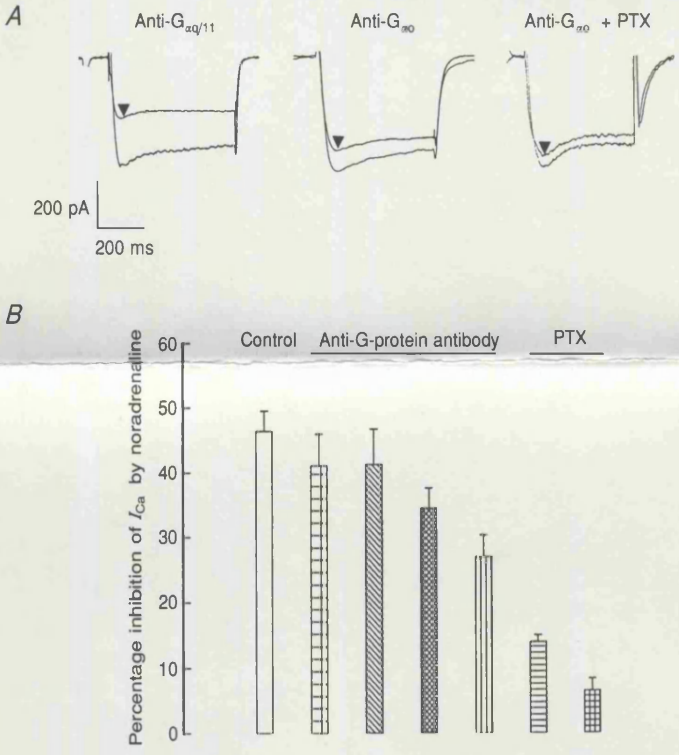

Figure 4. Anti-$G_{\alpha o}$ antibody reduces noradrenaline inhibition of I_{Ca} in SCG neurones, while anti-$G_{\alpha q/11}$, anti-$G_{\alpha i1/2}$ and anti-$G_{\alpha i3}$ antibodies are without effect

A, representative traces showing I_{Ca} (evoked by voltage steps to +10 mV from a holding potential of −80 mV), with control currents superimposed on currents reduced in the presence of 1 μM noradrenaline (▲). The left-hand traces show normal inhibition of I_{Ca} in a cell injected with an anti-$G_{\alpha q/11}$ antibody, while the middle traces show reduction of the noradrenaline response in a cell which had been injected with an anti-$G_{\alpha o}$ antibody. The right-hand traces show further reduction of the noradrenaline I_{Ca} inhibition in an anti-$G_{\alpha o}$ antibody-injected cell which had been pretreated with pertussis toxin. The inward tail current evident in the trace on the right probably results from inadequate space clamp, perhaps due to residual processes which survived the resuspension and replating procedure. *B*, histogram showing I_{Ca} inhibition by 1 μM noradrenaline in anti-GFAP (control, □; $n = 9$), anti-$G_{\alpha q/11}$ (⊞; $n = 7$), anti-$G_{\alpha i1/2}$ (▨; $n = 9$), anti-$G_{\alpha i3}$ (▩; $n = 13$) and anti-$G_{\alpha o}$ (▥; $n = 12$) antibody-injected neurones. Also shown is noradrenaline inhibition of I_{Ca} in PTX-treated neurones either uninjected or injected with anti-GFAP (▤; $n = 9$) or anti-$G_{\alpha o}$ antibody (▦; $n = 11$).

in intact rat SCG (Bone, Fretten, Palmer, Kirk & Michell, 1984) and coupling of M_1 muscarinic receptors to G_q or G_{11} can stimulate phopholipase Cβ (PLCβ) activity (Berstein *et al.* 1992). However, the identity of the second messenger involved remains elusive (see Robbins, Marsh & Brown, 1993).

In contrast to muscarinic inhibition of $I_{K(M)}$, injection of anti-$G_{\alpha q/11}$ antibodies did not affect noradrenaline inhibition of I_{Ca} and antibodies raised against the C-terminus of $G_{\alpha o1/2}$ significantly reduced the inhibitory effect of noradrenaline on I_{Ca}, pointing to $G_{\alpha o1}$ or $G_{\alpha o2}$ as a mediator. However, our finding that the predominant $G_{\alpha o}$ isoform in SCG neurones is $G_{\alpha o1}$ may indicate that this is the G-protein that couples α-adrenoceptors to I_{Ca} channels, although we cannot discount the possibility that even the small amount of $G_{\alpha o2}$ may mediate this response. In contrast, antibodies raised against the C-terminus of $G_{\alpha i1/2}$ and of $G_{\alpha i3}$ did not significantly alter adrenoceptor suppression of I_{Ca}. These negative findings could be attributed to inactivity of the antibodies, or insufficient loading of cells with antibody. However, we feel that these are unlikely explanations and that our results suggest that G_{i1-3} and $G_{q/11}$ do not transduce the noradrenaline response, for the following reasons: (1) our analysis was based solely on data from cells which had been loaded with antibodies, as evidenced by immunocytochemical visualization post-recording; (2) the antibodies raised against $G_{\alpha i1/2}$ and $G_{\alpha i3}$ which we used have been shown to functionally inhibit an action of the target G-proteins (i.e. receptor-mediated stimulation of GTPase: see McClue & Milligan, 1991); and (3) the anti-$G_{\alpha q/11}$ antibody was clearly effective in inhibiting muscarinic modulation of $I_{K(M)}$.

The conclusion that $G_{\alpha o}$, but not $G_{\alpha i}$, couples α-adrenoceptors to I_{Ca} is paralleled by similar findings with selective antibodies in NG108-15 neuroblastoma cells (McFadzean *et al.* 1989). The use by Kleuss *et al.* (1991) of antisense oligonucleotide sequences in a rat pituitary cell line has identified $G_{\alpha o1}$ as the mediator of L-type I_{Ca} inhibition by muscarinic receptors, so it appears that α-adrenergic receptors (our data) may couple to I_{Ca} channels through the same G-protein as muscarinic receptors.

The PTX-insensitive portion of the α-adrenoceptor inhibition of I_{Ca} was also noted in SCG neurones by Beech *et al.* (1992), who concluded that a PTX-insensitive G-protein can inhibit I_{Ca} channels. We felt that the apparent PTX-insensitive response did not result from inadequate ADP ribosylation of $G_{\alpha o1}$ by PTX, as this was nearly total even with 500 ng ml^{-1} PTX. Also, a higher concentration of PTX (2·5 μg ml^{-1}) inhibited the response to the same extent as 500 ng ml^{-1} PTX. Given this, we expected that anti-$G_{\alpha o}$ antibodies should produce no further reduction of α-adrenoceptor response in PTX-treated cells, so we were interested to find that noradrenaline inhibition of I_{Ca} was virtually eliminated by a combination of PTX pretreatment and injection of anti-$G_{\alpha o}$ antibody. It is possible that the residual response in PTX-treated neurones is mediated by a population of G-protein which is not ADP ribosylated, for example, any $G_{\alpha o}$ which remains dissociated from $\beta\gamma$ during the PTX treatment. Another possibility is that agonist-occupied receptors can still partially activate either ADP ribosylated or antibody-bound $G_{\alpha o1}$ subunits, and only a combination of ADP ribosylation by PTX together with antibody can completely prevent receptor activation of $G_{\alpha o}$.

In conclusion, the data we have obtained identify further key elements in the known complex transduction pathways between M_1 muscarinic receptors and M-type K^+ channels, and between α-adrenoceptors and Ca^{2+} channels in SCG neurones. Fast inhibition of I_{Ca} is probably the result of a direct action of activated $G_{\alpha o}$ subunits on 'N-type' Ca^{2+} channels, while muscarinic receptor inhibition of $I_{K(M)}$ operates through a $G_{\alpha q/11}$-mediated indirect mechanism involving a second messenger (Selyanko *et al.* 1992).

REFERENCES

Beech, D. J., Bernheim, L. & Hille, B. (1992). Pertussis toxin and voltage dependence distinguish multiple pathways modulating calcium channels of rat sympathetic neurons. *Neuron* **8**, 97–106.

Bernheim, L., Beech, D. J. & Hille, B. (1991). A diffusible second messenger mediates one of the pathways coupling receptors to calcium channels in rat sympathetic neurons. *Neuron* **6**, 859–867.

Berstein, G., Blank, J., Smrcka, A., Higashijima, T., Sternweis, P., Exton, J. & Ross, E. (1992). Reconstitution of agonist-stimulated phosphatidylinositol 4,5-bisphosphate hydrolysis using purified m1 muscarinic receptor, Gq/11 and phospholipase C-β1. *Journal of Biological Chemistry* **267**, 8081–8088.

Bone, E. A., Fretten, P., Palmer, S., Kirk, C. J. & Michell, R. H. (1984). Rapid accumulation of inositol phosphates in isolated rat superior cervical ganglia exposed to V1 vasopressin and muscarinic cholinergic stimuli. *Biochemical Journal* **22**, 803–811.

Brown, D. A., Marrion, N. V. & Smart, T. G. (1989). On the transduction mechanism for muscarine-induced inhibition of M-current in cultured rat sympathetic neurons. *Journal of Physiology* **413**, 469–488.

Galvan, M. & Adams, P. R. (1982). Control of calcium current in rat sympathetic neurons by noradrenaline. *Brain Research* **244**, 135–144.

Goldsmith, P., Gierschik, P., Milligan, G., Unson, C. G., Vinitsky, R., Malech, H. & Spiegel, A. M. (1987). Antibodies directed against synthetic peptides distinguish between GTP-binding proteins in neutrophil and brain. *Journal of Biological Chemistry* **262**, 14683–14688.

Horn, R. & Marty, A. (1988). Muscarinic activation of ionic currents measured by a new whole-cell recording method. *Journal of General Physiology* **92**, 145–159.

Kleuss, C., Hescheler, J., Ewel, C., Rosenthal, W., Schultz, G. & Wittig, B. (1991). Assignment of G-protein subtypes to specific receptors inducing inhibition of calcium currents. *Nature* **353**, 43–48.

McClue, S. J. & Milligan, G. (1991). Molecular interaction of the human α_2-C10-adrenergic receptor, when expressed in Rat-1 fibroblasts, with multiple pertussis toxin-sensitive guanine nucleotide-binding proteins: studies with site-directed antisera. *Molecular Pharmacology* **40**, 627–632.

McFadzean, I., Mullaney, I., Brown, D. A. & Milligan, G. (1989). Antibodies to the GTP binding protein, G_o, antagonize noradrenaline-induced calcium current inhibition in NG108-15 hybrid cells. *Neuron* **3**, 177–182.

Marrion, N. V., Smart, T. G., Marsh, S. J. & Brown, D. A. (1989). Muscarinic suppression of the M-current in the rat sympathetic ganglion is mediated by receptors of the M_1-subtype. *British Journal of Pharmacology* **98**, 557–573.

Menon-Johansson, A. S., Berrow, N. & Dolphin, A. C. (1993). G_o transduces $GABA_B$ receptor modulation of N-type calcium channels in cultured dorsal root ganglion neurones. *Pflügers Archiv* **193**, 1–9.

Mitchell, F. M., Mullaney, I., Godfrey, P. P., Arkinstall, S. J., Wakelam, M. J. O. & Milligan, G. (1991). Widespread distribution of $G_{q\alpha}/G_{11\alpha}$ detected immunologically by an anti-peptide antiserum directed against the predicted C-terminal decapeptide. *FEBS Letters* **287**, 171–174.

Mullaney, I. & Milligan, G. (1990). Identification of two distinct isoforms of the guanine nucleotide binding protein, G_o in neuroblastoma × glioma hybrid cells: Independent regulation during cyclic AMP-induced differentiation. *Journal of Neurochemistry* **55**, 1890–1898.

Mullaney, I., Mitchell, F. M., McCallan, J. F., Buckley, N. J. & Milligan, G. (1993). The human muscarinic m_1 acetylcholine receptor, when expressed in CHO cells, activates and downregulates both $G_{q\alpha}$ and $G_{11\alpha}$ equally and non-selectively. *FEBS Letters* **324**, 241–245.

Robbins, J., Marsh, S. J. & Brown, D. A. (1993). On the mechanism of M-current inhibition by muscarinic m1 receptors in DNA-transfected rodent neuroblastoma × glioma cells. *Journal of Physiology* **469**, 153–178.

Selyanko, A. A., Stansfeld, C. E. & Brown, D. A. (1992). Closure of potassium M-channels by muscarinic acetylcholine-receptor stimulants requires a diffusible messenger. *Proceedings of the Royal Society* B **250**, 119–125.

Simon, M. I., Strathmann, M. P. & Gautam, N. (1991). Diversity of G proteins in signal transduction. *Science* **252**, 802–808.

Wilk-Blaszczak, M. A., Gutowski, S., Sternweis, P. C. & Belardetti, F. (1994). Bradykinin modulates potassium and calcium currents in neuroblastoma hybrid cells via different pertussis toxin-insensitive pathways. *Neuron* **12**, 119–126.

Acknowledgements

We thank Robin Cloues for helpful criticism of the manuscript and Brenda Browning for help with tissue culture. We are grateful to Professor Ann Warner for assistance with fluorescence microscopy. This work was supported by the UK Medical Research Council.

Received 23 February 1994; accepted 29 March 1994.